

https://dspace.org/

# Cranial morphology of embrithosaurus schwarzi (Parareptilia, Pareiasauria) and a taxonomic and stratigraphic reassessment of the South African Middle Permian Pareiasaurs

**Van den Brandt, Marc Johan**

**2017**

http://hdl.handle.net/10539/22742

Van den Brandt, Marc Johan (2017) Cranial morphology of embrithosaurus schwarzi (Parareptilia, Pareiasauria) and a taxonomic and stratigraphic reassessment of the South African Middle Permian Pareiasaurs, University of the Witwatersrand, Johannesburg, <http://hdl.handle.net/10539/22742>

Downloaded from a DSpace repository. https://dspace.org/




# CRANIAL MORPHOLOGY OF *EMBRITHOSAURUS SCHWARZI* (PARAREPTILIA, PAREIASAURIA) AND A TAXONOMIC AND STRATIGRAPHIC REASSESSMENT OF THE SOUTH AFRICAN MIDDLE PERMIAN PAREIASAURS

Marc Johan Van den Brandt

A Dissertation submitted to the Faculty of Science, University of the Witwatersrand, Johannesburg, in fulfilment of the requirements for the Degree of Master of Science

Johannesburg, 2016

*The financial assistance of the National Research Foundation (NRF) towards this research is hereby acknowledged. Opinions expressed and conclusions arrived at, are those of the author and are not necessarily to be attributed to the NRF.*

## DECLARATION

I declare that this dissertation is my own, unaided work. It is being submitted for the Degree of Master of Science at the University of the Witwatersrand, Johannesburg, South Africa. It has not been submitted before for any degree or examination in any other University.

---

On this _29th_ day of November 2016 in Johannesburg.

## ABSTRACT

Pareiasaurs were abundant, large, herbivorous parareptiles of the middle and late Permian which had a global distribution. The most basal pareiasaurs are found only in the middle Permian of South Africa, suggesting a Gondwanan origin for the group. Despite their relative abundance, most pareiasaurs are poorly known, especially the large middle Permian South African taxa that went extinct at the end of the *Tapinocephalus* Assemblage Zone. Historic taxonomic confusion was reduced with studies by Lee (1995, 1997a) that addressed the alpha-taxonomy of all pareiasaurs. He reduced the middle Permian South African pareiasaurs from 11 to four species: *Bradysaurus baini*, *B. seeleyi*, *Embrithosaurus schwarzi* and *Nochelesaurus alexanderi*. However this revision did not include detailed anatomical descriptions of any of the middle Permian South African *Tapinocephalus* Assemblage Zone taxa.

The first detailed cranial description of *Embrithosaurus schwarzi* is presented in this contribution. Within the middle Permian pareiasaurians, *Embrithosaurus* has unique wide, short and stubby teeth with nine marginal cusps arranged more regularly.

A cranial taxonomic reassessment of all middle Permian pareiasaurs has confirmed the validity of the four taxa identified by Lee and produced updated cranial diagnoses for each species. Diagnostic features noted by Lee and retained include an autapomorphic large distinctive maxillary boss on a strongly buckled or bent maxilla for *B. baini*, distinctive horizontally flat and pointed bosses on the posterior margin of the quadratojugal for *Nochelesaurus* and the smallest cheek flanges for *B. seeleyi*.

Using the updated diagnoses, re-identification of 39 specimens out of 108 studied has produced updated biostratigraphic ranges for the middle Permian species. *B. seeleyi* is the first to make an appearance, in the middle Koornplaats Member of the Abrahamskraal Formation. *B. baini* first appears in the upper

Koornplaats Member, *Nochelesaurus* in the Swaerskraal Member, and *Embrithosaurus* in the lower Moordenaars Member of the Abrahamskraal Formation. All taxa disappear by the top of the Karelskraal Member of the Abrahamskraal Formation, confirming that all the middle Permian pareiasaur species went extinct at the end of the *Tapinocephalus* Assemblage Zone.

## ACKNOWLEDGEMENTS

My supervisors, Professor Bruce Rubidge and Professor Fernando Abdala of the Evolutionary Studies Institute (ESI) at the University of the Witwatersrand (Wits) receive my most sincere thanks for their guidance and generous assistance during this project. Their constructive feedback and comments on all aspects of this project and their open door policy has proved instrumental in enabling project completion.

Financial support was provided by a Centre of Excellence in Palaeosciences (COE) Masters Bursary, the National Research Foundation (NRF) Innovation Masters Bursary, the Paleontological Scientific Trust (PAST) and its Scatterlings of Africa programme support bursary, African Origins Programme (NRF), and the University of the Witwatersrand's Postgraduate Merit Award for Master's Degree tuition.

I thank Luke Norton and Professor Jonah Choiniere (ESI) for advice and assistance with regards to photographic techniques and the use of the drawing software programs of Inkscape, GIMP 2 (GNU Image Manipulation Program) and Adobe Illustrator CC.

Evolutionary Studies Institute staff and students, including Kimmi Chapelle, Sue Dykes, Luke Norton, Maria Combrink, Bongi Zwane, Ashley Kruger, Cameron Penn-Clarke, Pia Viglietti, Julien Beniot, Natasha Barbolini, Aurore Val, Mike Day, Casey Staunten, Katherine Clayton, Cory Dinter, Natasha Phillips, Blair McPhee, Safiyyah Iqbal, Sandra Jasinoski, Micke Engelbrecht, David Groenewald, Simone Kock, Ian Mckay, Amanda Mudau, Marion Bamford, Tea Jashashvili, Kris Carlson , Christine Steininger and Cynthia Kemp are thanked for their part in making the ESI a uniquely pleasant and rewarding institute at Wits.

For additional preparation of the teeth of the holotype cranial specimens of *Embrithosaurus schwarzi* (SAM-PK-8034) and *Nochelesaurus alexanderi* (SAM-PK-6239), I thank Gilbert Mokgethoa and Charlton Dube (ESI).

For assistance with the re-assembly of the cranial fragments of the holotype cranial specimen of *Embrithosaurus schwarzi* (SAM-PK-8034), Sifelani Jirah and Charlton Dube (ESI) are acknowledged.

For access to the material studied, I appreciatively thank Sandra Chapman and Paul Barrett (NHMUK), Zaituna Erasmus, Sibusiso Mtungata, Roger Smith (SAM), Bernhard Zipfel, Sifelani Jirah (ESI), Ellen de Kock, Johann Neveling, and Nonhlanhla Mchunu (CGP), Heidi Fourie (TM), Billy de Klerk and Rose Prevec (AM), Rochelle Vlok (VW), and Tom White (UMZC).

Mike Lee is thanked for his correspondence, photographs of specimens and for general discussions and communications on all aspects of his seminal pareiasaurian taxonomic PhD completed in 1995.

For the funding of transport, logistical support, administration, accommodation, and general expenses incurred during the numerous museum visits required for this project, I thank Professor Bruce Rubidge, Professor Fernando Abdala, Bronwyn Quinn and Tandi Scott-Turner (ESI), my sister Tanya Van den Brandt and my brother-in-law Peter van't Hoogerhuys and good friends Martin Meyer and his wife Helen Meyer in London, and my parents John and Naomi Van den Brandt in Cape Town.

Lastly, I thank Dr Mike Day (ESI) for the use of the stratigraphic range intervals that he determined for the deposits found on different farm localities of the South Western Karoo, conducted as part of his PhD (2013) on the bio- and liothostratigraphy review of the lower Assemblage Zones of the Beaufort Group.

## TABLE OF CONTENTS

## CHAPTER ONE: INTRODUCTION AND LITERATURE REVIEW


1.1 General Introduction 1

1.2 Taxonomic history of middle Permian South African pareiasaurs 6

1.2.1 South African pareiasaurs described between 1856 and 1903 6

1.2.2 Watson (1914b) 12

1.2.3 Haughton and Boonstra (1929a) 14

1.2.4 Boonstra (1934a) 17

1.2.5 Broom (1935) 20

1.2.6 Boonstra (1969) 22

1.2.7 Kuhn (1969) 23

1.2.8 Lee (1995, 1997a) 25

1.3 Project Objectives 28

1.3.1 Descriptive and taxonomical improvements 28

1.3.2 Stratigraphic range improvement 30


## CHAPTER TWO: MATERIAL AND METHODS


2.1 Material 34

2.1.1 Holotype *Embrithosaurus schwarzi* SAM-PK-8034 34

2.1.2 Horizon and Locality 36

2.1.3 Holotype *Nochelesaurus alexanderi* SAM-PK-6239 37

2.1.4 Horizon and Locality 37

2.1.5 Holotype *Bradysaurus baini* NHMUK R1971 38

2.1.6 Horizon and Locality 38

2.1.7 Holotype *Bradysaurus seeleyi* NHMUK 49426 39

2.1.8 Horizon and Locality 39

2.2 Methods 40

2.2.1 Preparation *Embrithosaurus schwarzi* SAM-PK-8034 40

2.2.2 Suture identification methods 40

2.2.3 Distortions 42

2.2.4 Preparation *Nochelesaurus alexanderi* SAM-PK-6239 43

2.2.5 Suture identification 44

2.2.6 Distortions 44

2.2.7 Preparation *Bradysaurus baini* NHMUK R1971 45

2.2.8 Suture identification 45

2.2.9 Distortions 46

2.2.10 Preparation *Bradysaurus seeleyi* NHMUK 49426 46

2.2.11 Suture identification 47

2.2.12 Distortions 47

2.3 Abbreviations 48

2.3.1 Institutional abbreviations 48

2.3.2 Anatomical abbreviations 48

## CHAPTER THREE: RESULTS: DESCRIPTION

3.1 Systematic Palaeontology 50

3.2 Cranial Description 50

3.2.1 Skull Roof 50

3.2.2 Palate 73

3.2.3 Braincase and Occiput 78

3.2.4 Lower Jaw 88

3.2.5 Marginal Dentition 96

## CHAPTER FOUR: RESULTS: TAXONOMIC REVIEW

4.1 Format and introduction 127

4.2 *Embrithosaurus schwarzi* Watson (1914) 130

4.2.1 Diagnosis (Lee 1995, 1997a) 130

4.2.2 Amended Diagnosis 131

4.2.3 Specimens and Comments 137

4.3 *Nochelesaurus alexanderi* Haughton and Boonstra (1929) 138

4.3.1 Diagnosis (Lee 1995, 1997a) 138

4.3.2 Amended Diagnosis 139

4.3.3 Specimens and Comments 140

4.4 *Bradysaurus baini* Watson (1914) 146

4.4.1 Diagnosis (Lee 1995, 1997a) 146

4.4.2 Amended Diagnosis 148

4.4.3 Specimens and Comments 149

4.5 *Bradysaurus seeleyi* Haughton and Boonstra (1929) 158

4.5.1 Diagnosis (Lee 1995, 1997a) 158

4.5.2 Amended Diagnosis 159

4.5.3 Specimens and Comments 159

**CHAPTER FIVE: RESULTS: STRATIGRAPHIC RANGES**

5.1 Determination of stratigraphic ranges for Abrahamskraal

Formation taxa 166

5.2 This study 167

5.3 Stratigraphic ranges of middle Permian pareiasaurs 168

5.3.1 *Bradysaurus* stratigraphic range 168

5.3.2 *Embrithosaurus* stratigraphic range 170

5.3.3 *Nochelesaurus* stratigraphic range 171

**CHAPTER SIX: DISCUSSION**

6.1 Taxonomy 174

6.1.1 *Embrithosaurus schwarzi* 178

6.1.2 *Nochelesaurus alexanderi* 183

6.1.3 *Bradysaurus baini* 186

6.1.4 *Bradysaurus seeleyi* 190

6.2 Stratigraphy 192

**CHAPTER SEVEN: CONCLUSION**

7.1 Project achievements 194

7.2 Opportunities for future improvements 196

**8 REFERENCES** 199

**9 APPENDICES**

9.1 Appendix A: List of measurements (1-33) and ratios (34-39) taken on the fourholotype skulls: SAM-PK-8034 *Embrithosaurus schwarzi*, SAM-PK-6239 *Nochelesaurus alexanderi*, NHMUK R1971 *Bradysaurus baini*, and NHMUK 49426 *B. seeleyi*. 207

9.2 Appendix B: Table of distances (in mm) of the different measurements and ratios presented in Appendix A, for the four holotype skulls: SAM-PK-8034 *Embrithosaurus schwarzi*, SAM-PK-6239 *Nochelesaurus alexanderi*, NHMUK R1971 *Bradysaurus baini*, and NHMUK 49426 *B. seeleyi.* 210

9.3 Appendix C: Table of 108 South African middle Permian cranial pareiasaur specimens studied, showing the original species identifications and the identifications of this study. 211

9.4 Appendix D: Table of the 35 specimens identified during this study to species level, with the stratigraphic range intervals (Member Range) compiled by Day (2013) for individual farm localities. 214

## LIST OF FIGURES


Figure 1.1: The most recent Phylogentic relationships of Pareiasaurians by Turner *et al.* (2015), derived from an analysis of 139 characters; 78 cranial, 61 postcranial. The most basal pareiasaurs are known only from the middle Permian *Tapinocephalus* Assemblage Zone of South Africa and are represented by four species: *Bradysaurus seeleyi, B. baini, Nochelesaurus alexanderi,* and *Embrithosaurus schwarzi.* 3

Figure 1.2: Cladogram showing approximate stratigraphic ranges of pareiasaurs (except for *Bradysaurus baini, Sanchuansaurus*, *Nanoparia*, and the Welgewonden and Kupferschiefer pareiasaurs). The most basal members of the group (*Bradysaurus seeleyi, Nochelesaurus alexanderi,* and *Embrithosaurus schwarzi*) occur in the middle Permian *Tapinocephalus* Assemblage Zone of South Africa. The younger southern African members (*Pareiasuchus peringueyi, Pareiasuchus nasicornis, Pareiasaurus*, *Anthodon and Pumiliopareia*) are from the late Permian *Tropidostoma*, *Cistecephalus* and *Dicynodon* Assemblage Zones (Jalil and Janvier 2005). 5

Figure 1.3: Interpretive drawing of the holotype skull of *Bradysaurus seeleyi* (NHMUK 49426), in (A) left lateral and (B) dorsal views, taken from Seeley (1888). 9

Figure 1.4: Interpretive drawing of the holotype skull of *Bradysaurus baini* (NHMUK R1971), in (A) left lateral and (B) dorsal views, taken from Seeley (1892). 10

Figure 1.5: Photograph of the holotype of *Bradysaurus baini* (NHMUK R1971), currently on display in the Natural History Museum, London (2016). 11

Figure 1.6: Interpretive drawing of the holotype of *Embrithosaurus schwarzi* (SAM-PK-8034), taken from Broom (1903). 11
Figure 1.7: Photograph of the holotype skull of *Embrithosaurus schwarzi* (SAM-PK-8034), in (A) left lateral and (B) occipital views, taken from Boonstra (1934a). Both angular bosses of the lower jaw were present, but are now lost. 18
Figure 1.8: Photograph of the right rami of SAM-PK-8034 (Fragment A), in (A) right medial and (B) right lateral views, taken from Haughton and Boonstra (1930a). Note the presence of the now lost right angular boss of the lower jaw. 19
Figure 1.9: Photograph of the holotype skull of *Nochelesaurus alexanderi* (SAM-PK-6239), in (A) right lateral and (B) dorsal views, taken from Boonstra (1934a). 20
Figure 1.10: Composite stratigraphic ranges of parareptile genera from the middle Permian Beaufort Group, taken from Day 2013. Note the stratigraphic ranges of *Bradysaurus*, *Embrithosaurus* and *Nochelesaurus* are restricted to the top of the Abrahamskraal Formation. Numerals denote meters above the base of the Abrahamskraal Formation. Solid lines indicate well constrained stratigraphic provenances for positively identified specimens of each species. Dotted lines indicate a wide range of possible stratigraphic provenances for positively identified specimens of each species. 33
Figure 3.1: Photograph (A) and interpretive drawing (B) of the skull of the holotype of *Embrithosaurus schwarzi* (SAM-PK-8034), in dorsal view. 102
Figure 3.2: Photograph (A) and interpretive drawing (B) of the skull of the holotype of *Embrithosaurus schwarzi* (SAM-PK-8034), in left lateral view. 103
Figure 3.3: Photograph (A) and interpretive drawing (B) of the skull of 104

the holotype of *Embrithosaurus schwarzi* (SAM-PK-8034), in right lateral view.

Figure 3.4: Photograph (A) and interpretive drawing (B) of the skull of the holotype of *Embrithosaurus schwarzi* (SAM-PK-8034), in ventral view. 105

Figure 3.5: Photograph (A) and interpretive drawing (B) of the skull of the holotype of *Embrithosaurus schwarzi* (SAM-PK-8034), in occipital view (excluding the lower jaw fragment A). 106

Figure 3.6: Photograph (A) and interpretive drawing (B) of the lower jaw and snout (fragment A) of SAM-PK-8034, in dorsal view. 107

Figure 3.7: Photograph (A) and interpretive drawing (B) of the lower jaw and snout (fragment A) of SAM-PK-8034, in ventral view. 107

Figure 3.8: Photograph (A) and interpretive drawing (B) of the left lower jaw (fragment A) of SAM-PK-8034, in lateral view. 108

Figure 3.9: Photograph (A) and interpretive drawing (B) of the left lower jaw (fragment A) of SAM-PK-8034, in medial view. 108

Figure 3.10: Photograph (A) and interpretive drawing (B) of the right lower jaw (fragment A) of SAM-PK-8034, in lateral view. 109

Figure 3.11: Photograph (A) and interpretive drawing (B) of the right lower jaw (fragment A) of SAM-PK-8034, in medial view. 109

Figure 3.12: Photograph (A) and interpretive drawing (B) of the skull table (fragment B) of SAM-PK-8034, in dorsal view. Anterior to the top of the page. 110

Figure 3.13: Photograph (A) and interpretive drawing (B) of the skull table (fragment B) of SAM-PK-8034, in ventral view. Anterior to the top of the page. 110

Figure 3.14: Photograph (A) and interpretive drawing (B) of the left cheek (fragment C) of SAM-PK-8034, in lateral view, with metal plates, screws and putty shown. Dorsal to the top of the page. 111

Figure 3.15 Photograph (A) and interpretive drawing (B) of the left cheek (fragment C) of SAM-PK-8034, in medial view. Dorsal to the top of the page. 111
Figure 3.16 Photograph (A) and interpretive drawing (B) of the left lacrimal (fragment D) of SAM-PK-8034, in lateral view. Dorsal to the top of the page. 112
Figure 3.17 Photograph (A) and interpretive drawing (B) of the left lacrimal (fragment D) of SAM-PK-8034, in medial view. Dorsal to the bottom of the page. 112
Figure 3.18 Photograph (A) and interpretive drawing (B) of the right cheek (fragment E) of SAM-PK-8034, in lateral view. Dorsal to the top of the page. 113
Figure 3.19 Photograph (A) and interpretive drawing (B) of the right cheek (fragment E) of SAM-PK-8034, in medial view. Dorsal to the top of the page. 113
Figure 3.20 Photograph (A) and interpretive drawing (B) of the palate (fragment F) of SAM-PK-8034, in dorsal view. Anterior to the top of the page. 114
Figure 3.21 Photograph (A) and interpretive drawing (B) of the palate (fragment F) of SAM-PK-8034, in ventral view. Anterior to the top of the page. 115
Figure 3.22 Photograph (A) and interpretive drawing (B) of the braincase (fragment G) of SAM-PK-8034, in dorsal view. Anterior to the top of the page. 116
Figure 3.23 Photograph (A) and interpretive drawing (B) of the braincase (fragment G) of SAM-PK-8034, in ventral view. Anterior to the top of the page. 117
Figure 3.24 Photograph (A) and interpretive drawing (B) of the braincase (fragment G) of SAM-PK-8034, in left lateral view. Dorsal to the top of the page. 118

Figure 3.25 Photograph (A) and interpretive drawing (B) of the right quadrate (fragment H) of SAM-PK-8034, in occipital view. Dorsal to the top of the page. 119
Figure 3.26 Photograph (A) and interpretive drawing (B) of the right quadrate (fragment H) of SAM-PK-8034, in anterior view. Dorsal to the top of the page. 119
Figure 3.27 Photograph (A) and interpretive drawing (B) of the left quadrate (fragment I) of SAM-PK-8034, in occipital view. Dorsal to the top of the page. 120
Figure 3.28 Photograph (A) and interpretive drawing (B) of the left quadrate (fragment I) of SAM-PK-8034, in anterior view. Dorsal to the top of the page. 120
Figure 3.29 Photograph of the skull of SAM-PK-8034, in anterior view. 121
Figure 3.30 Photograph of the anterior snout and upper jaw teeth (premaxilla) of SAM-PK-8034, in anterior view. Three damaged premaxillary teeth can be seen either side of the midline. 121
Figure 3.31 Photograph of the upper left tooth row of SAM-PK-8034, in left lateral view, showing all thirteen exposed maxillary teeth (numbered 1-13), including the gap where the missing ninth tooth would be. 122
Figure 3.32 Photograph of the upper left maxillary teeth of SAM-PK-8034, in lateral view, showing the fifth to eighth teeth. Cusp numbers are not easy to discern due to uncleared matrix and the overlapping nature of the teeth. 122
Figure 3.33 Photograph of the upper right tooth row of SAM-PK-8034, in lateral view, showing all three exposed premaxillary teeth (numbered 1-3) and all thirteen exposed maxillary teeth (numbered 1-13). 123
Figure 3.34 Photograph (A) and interpretive drawing (B) of the upper 123

right maxillary teeth of SAM-PK-8034, in lateral view, showing the eighth to eleventh teeth. Nine cusps are easily identifiable on the eighth, tenth and eleventh teeth.

Figure 3.35 Photograph (A) and interpretive drawing (B) of the right maxillary teeth of NHMUK R1970, in lateral view. Cusps number seven on each tooth. Note the elongated tooth shape, with the three central cusps located at the distal end of the long trident. 124

Figure 3.36 Photograph of the upper right tooth row of SAM-PK-9098, in lateral view, showing nine cusps on each tooth on wide, short, stubby maxillary teeth, allowing for positive identification as *Embrithosaurus*. 124

Figure 3.37 Photograph of the lower right mandibular tooth row of SAM-PK-8034, in medial view, showing the fourth to fifteenth dentary teeth. 125

Figure 3.38 Photograph (A) and interpretive drawing (B) of the lower right mandibular tooth row of SAM-PK-8034, in medial view, showing the fourth to ninth teeth. Nine cusps are easily identifiable on the fourth, fifth, seventh and ninth teeth. Note the triangular bulge. 125

Figure 3.39 Photograph (A) and interpretive drawing (B) of lower right mandibular teeth of SAM-PK-6239, in medial view. Note the vertical ridges from cusps four and six, and the non-symmetrically arranged lateral marginal cusps on the anterior margin (cusps one and two) and the posterior margin (cusps eight and nine). 126

Figure 4.1 Photograph of the skull of the holotype of *Nochelesaurus alexanderi* (SAM-PK-6239), in dorsal view. 145

Figure 4.2 Photograph of the skull of the holotype of *Nochelesaurus alexanderi* (SAM-PK-6239), in ventral view. 145

Figure 4.3 Photograph of the skull of the holotype of *Nochelesaurus alexanderi* (SAM-PK-6239), in right lateral view. 146
Figure 4.4 Photograph of the skull of the holotype of *Bradysaurus baini* (NHMUK R1971), in dorsal view. 155
Figure 4.5 Photograph of the skull of the holotype of *Bradysaurus baini* (NHMUK R1971), in ventral view. 155
Figure 4.6 Photograph of the skull of the holotype of *Bradysaurus baini* (NHMUK R1971), in left lateral view. 156
Figure 4.7 Photograph of the skull of the holotype of *Bradysaurus baini* (NHMUK R1971), in right lateral view. 156
Figure 4.8 Photograph of the skull of the holotype of *Bradysaurus baini* (NHMUK R1971), in occipital view. 157
Figure 4.9 Photograph of the skull of the holotype of *Bradysaurus baini* (NHMUK R1971), in anterior view. 157
Figure 4.10 Photograph of the skull of the holotype of *Bradysaurus seeleyi* (NHMUK 49426), in dorsal view. 163
Figure 4.11 Photograph of the skull of the holotype of *Bradysaurus seeleyi* (NHMUK 49426), in ventral view. 163
Figure 4.12 Photograph of the skull of the holotype of *Bradysaurus seeleyi* (NHMUK 49426), in left lateral view. 164
Figure 4.13 Photograph of the skull of the holotype of *Bradysaurus seeleyi* (NHMUK 49426), in right lateral view. 164
Figure 4.14 Photograph of the skull of the holotype of *Bradysaurus seeleyi* (NHMUK 49426), in occipital view. 165
Figure 4.15 Photograph of the skull of the holotype of *Bradysaurus seeleyi* (NHMUK 49426), in anterior view. 165
Figure 5.1 Composite stratigraphic ranges of basal pareiasaur genera in the middle Permian Beaufort Group, Day (2013) and this study. Numerals denote meters above the base of the Abrahamskraal Formation. Solid lines indicate well 173

constrained stratigraphic provenances for positively identified specimens of each species. Dotted lines indicate a wide range of possible stratigraphic provenances for positively identified specimens of each species.

## LIST OF TABLES


| | | |
|---|---|---|
| Table 1.1 | Classification of *Tapinocephalus* Assemblage Zone pareiasaurs (Watson 1914b). | 13 |
| Table 1.2 | Classification of *Tapinocephalus* Assemblage Zone pareiasaurs (Haughton and Boonstra 1929a). | 16 |
| Table 1.3 | Classification of *Tapinocephalus* Assemblage Zone pareiasaurs (Broom 1935). | 21 |
| Table 1.4 | Classification of *Tapinocephalus* Assemblage Zone pareiasaurs (Boonstra 1969). | 23 |
| Table 1.5 | Classification of *Tapinocephalus* Assemblage Zone pareiasaurs (Kuhn 1969). | 24 |
| Table 1.6 | Classification of *Tapinocephalus* Assemblage Zone pareiasaurs (Lee 1995, 1997a). | 27 |
| Table 4.1 | Dental comparison of South African middle Permian pareiasaurs. Normal text indicates when the feature is shared by more than one species. Bold text indicates when the feature is unique to a particular species in the group. | 127 |
| Table 4.2 | Cranial comparison of South African middle Permian pareiasaurs. Bold text indicates when the feature is unique to a particular species, or is shared by more than one species in the group. | 128 |
| Table 5.1 | Specimen identification per institution, for the 108 cranial pareiasaur specimens recovered from the *Tapinocephalus* Assemblage Zone. Thirty nine specimens (36%) were identifiable to species level. Institutional Abbreviations: **BPI**, Evolutionary Studies Institute, University of the Witwatersrand, Johannesburg (formerly the Bernard Price Institute for Palaeontological Research); **CGP**, Council for Geosciences, Pretoria; **NHMUK**, Natural History Museum of | 167 |

London, United Kingdom; **SAM**, Iziko South African Museum, Cape Town.

# CHAPTER ONE: INTRODUCTION AND LITERATURE REVIEW

## 1.1 General Introduction

Pareiasaurs are a monophyletic group of large, heavily built, armoured, herbivorous parareptiles which occurred only in the middle to late Permian (Lee 1993, 1997a, 1997b). The monophyletic clade of Parareptilia includes the well-known and diverse groups of Pareiasauria, Procolophonoidea, Millerettidae, Mesosauridae, Lanthanosuchoidea, Bolosauridae, and "nycteroleters" (Tsuji and Muller 2009). Recent phylogenetic systematic theory has united all members of Parareptilia into a strongly supported clade, defined by the presence of six unequivocal autapomorphies (Tsuji and Muller 2009). The name "Pareiasaur" means "cheek-piece of a helmet-lizard", the group being named by Owen (1876) after their ventrolaterally expanded quadratojugal or "cheek" regions of their skulls.

This group has been known since the discovery of the "Blinkwater Monster" in 1838 by Andrew Geddes Bain, near Blinkwater, in the Eastern Cape Province of South Africa (Owen 1876). The majority of pareiasaur specimens have been found in southern Africa, Russia, and China (Boonstra 1932a, Lee 1997a, 1997b, Benton 2016) with a few specimens also found and described from Zambia (Lee *et al.* 1997), Niger (Sidor *et al.* 2003, Tsuji *et al.* 2013, Turner *et al.* 2015), Morocco (Jalil and Janvier 2005), Brazil (Cisneros *et al.* 2005), Scotland (Newton 1893) and Germany (von Meyer 1857, Tsuji 2010).

Pareiasaurs, which were mostly medium- to large-sized herbivores, made up an important component of middle to late Permian biodiversity and ecosystems. This is borne out by the abundance of pareiasaur remains found in the *Tapinocephalus* Assemblage Zone of the Beaufort Group of the South African Karoo Supergroup (Seeley 1892, Boonstra 1969, Smith and Keyser 1995a, Nicolas 2007, Day 2013). They were the only anapsid reptile group that attained massive size (up to 3m long) and were one of several groups that developed specialized

crenulated teeth for herbivory (Lee 1997a). The relative abundance of their remains prompted Seeley (1892) in his first biostratigraphic subdivision of the Karoo, to propose a Pareiasaurian Zone, close to the base of the Beaufort succession. Watson (1914b) renamed Seeley's *Pareiasaurus* zone to the *Tapinocephalus* Zone, noting that the taxon *Pareiasaurus* occurs in the higher *Cistecephalus* Assemblage Zone.

Although pareiasaurs are known from several Pangaean stratigraphic successions around the world (Rubidge 2005), recent phylogenetic analysis reveals that the pareiasaurs from the *Tapinocephalus* Assemblage Zone of South Africa are the most basal genera and are the earliest pareiasaurs known, suggesting a Gondwanan origin for the group (Fig. 1.1) (Lee 1997a, 1997b, Jalil and Janvier 2005, Tsuji 2010, Tsuji *et al.* 2013, Turner *et al.* 2015). These basal forms are therefore important as they form a baseline from which to understand and investigate the origin and subsequent diversification and distribution of the group throughout Pangea. Four species are currently recognised in this basal group: *Bradysaurus seeleyi, B. baini, Nochelesaurus alexanderi* and *Embrithosaurus schwarzi* (Fig. 1.1).

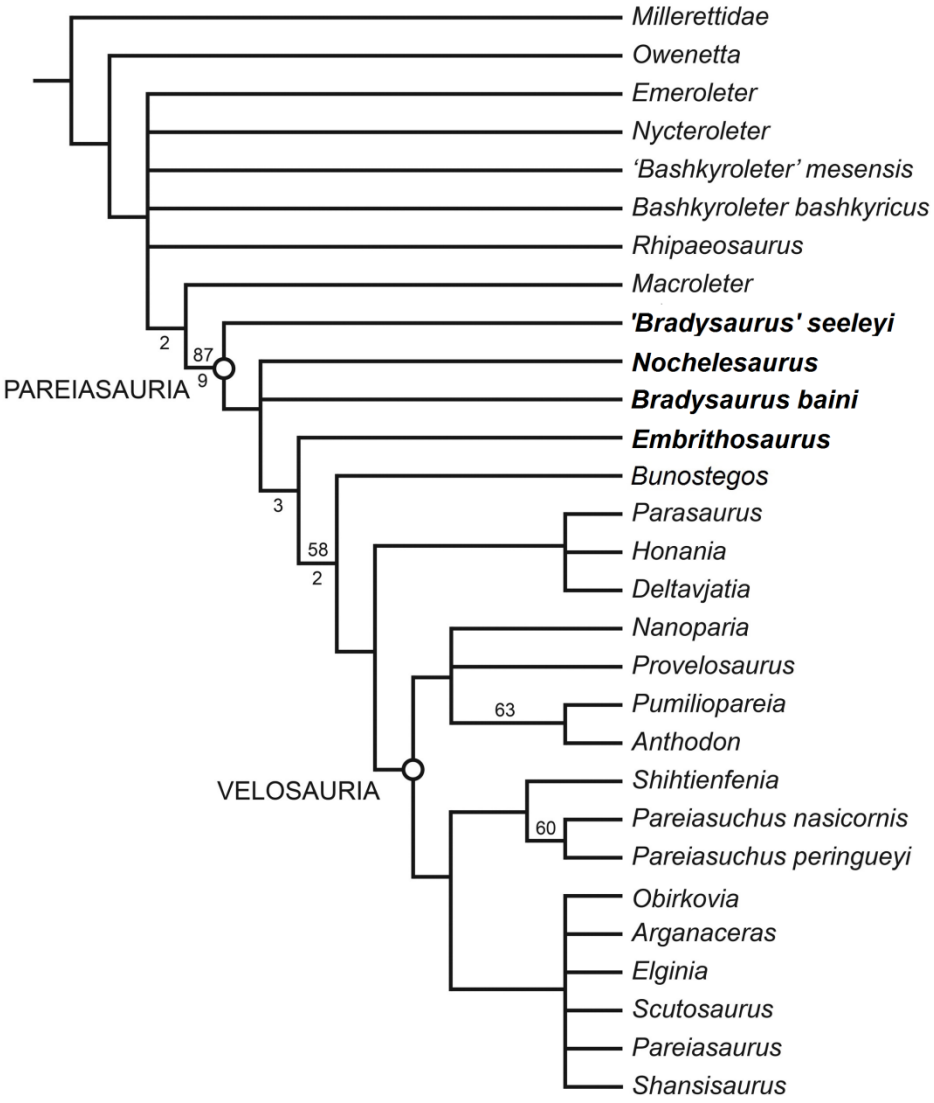


**Figure 1.1:** The most recent Phylogentic relationships of Pareiasaurians by Turner *et al.* (2015), derived from an analysis of 139 characters; 78 cranial, 61 postcranial. The most basal pareiasaurs are known only from the middle Permian *Tapinocephalus* Assemblage Zone of South Africa and are represented by four species: *Bradysaurus seeleyi, B. baini, Nochelesaurus alexanderi,* and *Embrithosaurus schwarzi.*

The southern African pareiasaurs were victim to two extinction events and are therefore distributed in two distinct groups (Fig. 1.2):

1) the large sized basal forms from the middle Permian *Tapinocephalus* Assemblage Zone (Boonstra 1932a, Lee 1997a, Smith and Keyser 1995a), that became extinct at the top of the Abrahamskraal Formation at the end of the Gaudalupian (Day 2013, Day *et al*. 2015, Nicolas 2007), and

2) the medium to small sized younger forms from the late Permian *Tropidostoma*, *Cistecephalus* and *Dicynodon* Assemblage Zones (Smith and Keyser 1995c,1995d, Kitching 1995 ), that became extinct at the end of the Permian (Boonstra 1932a, Lee 1997a, Smith and Botha-Brink 2014, Nicolas 2007).

The basal forms are characterised by their large size of up to 3m in body length, fewer cusps on their teeth, and less extensive armour or dermal osteoderms which are restricted to a narrow band across the vertebral column (Watson 1914b, Boonstra 1932a, Lee 1995, 1997a).

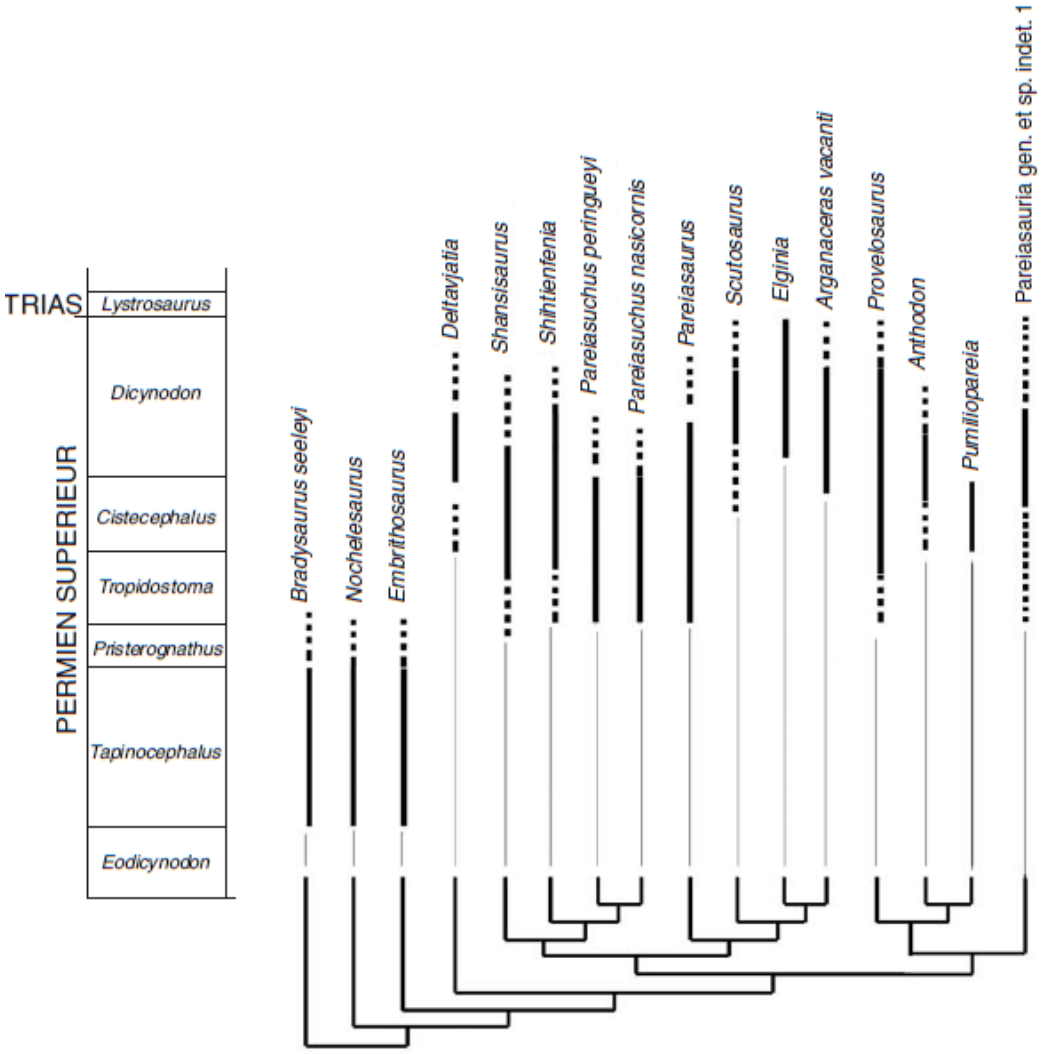


**Figure 1.2:** Cladogram showing approximate stratigraphic ranges of pareiasaurs (except for *Bradysaurus baini, Sanchuansaurus*, *Nanoparia*, *Parasaurus*, and the Welgewonden and Kupferschiefer pareiasaurs). The most basal members of the group (*Bradysaurus seeleyi, Nochelesaurus alexanderi,* and *Embrithosaurus schwarzi*) occur in the middle Permian *Tapinocephalus* Assemblage Zone of South Africa. The younger southern African members (*Pareiasuchus peringueyi, Pareiasuchus nasicornis, Pareiasaurus*, *Anthodon and Pumiliopareia*) are from the late Permian *Tropidostoma*, *Cistecephalus* and *Dicynodon* Assemblage Zones (Jalil and Janvier 2005).

## 1.2 Taxonomic history of middle Permian South African pareiasaurs

Due to the abundance of fossil specimens, pareiasaurian taxonomy became problematic early in the 20th century, through continuous naming of new taxa by various workers (Owen 1876, Seeley 1892, Broom 1912, 1913, 1914, 1915, 1924, Watson 1914b, Haughton and Boonstra 1929a, Boonstra 1934a, Broom 1935). In these early descriptive papers, new diagnoses were often based on minor morphological skull differences, in many cases using very imperfect, distorted or fragmentary specimens.

Initially, in the middle to late nineteenth century, the South African pareiasaurs were studied and named in London by workers such as Owen (1876) and Seeley (1888, 1892). The use of very imperfect, fragmentary or distorted specimens as holotypes, the loss of specimens, and the incorrect referencing and assignment of individual elements from the same specimen, to different specimens and species, created taxonomic problems that have been worked on for several decades .

### 1.2.1 South African pareiasaurs described between 1856 and 1903

It is important to note the early history, specimen numbers and classifications of the first pareiasaurs named from South Africa, in order to better understand the taxonomic history of the group.

The first pareiasaur to be found in the world (NHMUK R4063/R1710/R1710a), consisted of a large skull, lower jaw, and pelvis, from South Africa, and was discovered by A.G. Bain in 1838 and sent to the Natural History Museum in 1853. This specimen (the“Blinkwater Monster”), was not the world’s first pareiasaur described though, as von Meyer (1857) named *Parasaurus geinitzi*, from Germany, in 1857. Parts of the Blinkwater Monster specimen were unfortunately initially mixed with other specimens and later even lost. Owen initially described only the pelvis (1856, 1862) and mistakenly referred it to a dicynodont synapsid,

i.e. *Dicynodon tigriceps*. In 1876 Owen finally described the skull and lower jaw and named the genus and species *Pareiasaurus serridens.* However, the holotype skull was lost sometime after 1876, and by 1888 was represented only by a skull cast and a fragment of the original lower jaw (Seeley 1888, Lydekker 1890).

Also presented by A.G. Bain to the Natural History Museum in 1853 was a small very imperfect skull (NHMUK 47337) from Styl-Krantz, Sneewberg range which was named *Anthodon serrarius* by Owen (1876) and mistakenly classified in the Dinosauria. This locality is attributed to the *Cistecephalus* Assemblage Zone.

Seeley (1888) named one *Cistecephalus* Assemblage Zone pareiasaur, *Propappus omocratus* (NHMUK R4064) based on a right femur found at the Brak River, Fort Beaufort District, presented by A.G. Bain to the Natural History Museum in 1853.

Sent to London in 1872 by Dr W.G. Atherstone*, Pareiasaurus bombidens* was the first *Tapinocephalus* Assemblage Zone pareiasaur described by Owen (1876) but consisted only of a very imperfect snout and vertebral column (NHMUK R1714/43525) from the farm Vers Fontein/Varsfontein, Prince Albert District. Due to the very imperfect nature of the material, after Owen's (1876) initial description this pareiasaurian species was subsequently ignored by Watson (1914b), was rejected in the classification scheme of Haughton and Boonstra (1929a) and was specified as indeterminate in the taxonomic reassessment of Boonstra (1934a). Only Broom (1935) and Kuhn (1969) retained *P. bombidens* (in the form of *Bradysaurus bombidens*) in their pareiasaurian taxonomic work. Lee (1995, 1997a) rejected this species as invalid (*nomen dubium*) due to the holotype material being poorly preserved and indeterminate.

Seeley (1888) described and illustrated, in some detail, the skull and central axial skeleton of a relatively complete pareiasaur specimen (NHMUK 49426, Fig. 1.3) from the farm Palinut/Palmiet Fontein, at the foot of the Nieuwveld mountains, in the Beaufort West district, which was sent to London in 1878 by T. Bain. Of the two large South African pareiasaurian taxa known at the time (i.e. *P. serridens* and *P. bombidens*) this *Tapinocephalus* Assemblage Zone pareiasaur was referred

by Seeley to Owen's *P. bombidens.* Since Haughton and Boonstra (1929a) did not recognise *P. bombidens* as valid, they made this specimen the holotype for a new species, *Bradysaurus seeleyi*, which was retained as valid by Lee (1995, 1997a).

In 1889 Seeley visited South Africa to search for new pareiasaur specimens from *Tapinocephalus* Assemblage Zone localities and collected two new pareiasaurs. In 1892, he described the specimen he collected from the farm Tamboer Fontein, north of Fraserberg Road Station, in the Beaufort West district (NHMUK R1970) consisting primarily of numerous postcrania with a fragmentary skull. The top half of the skull is completely weathered away with only the palate, lower jaw and maxilla with some teeth remaining. Seeley (1892) referred this specimen to Owen's *Pareiasaurus bombidens.*

In the same paper (1892), Seeley described the second pareiasaur specimen (NHMUK R1971, Fig. 1.4) collected by himself, T. Bain, J.S. Marais, and S Marais on 12 August 1889. Found on the farm De Bad in the Beaufort West district, this specimen is very complete and is represented by most of the skull and postcrania and was named a new species, *Pareiasaurus baini* (Seeley 1892). This specimen was later made the holotype of *Bradysaurus baini* by Watson (1914b) and retained as valid by Lee (1995, 1997a). This specimen is currently (2016) on permanent display in the Natural History Museum, London (Fig. 1.5).

Broom (1903) described a very complete new *Tapinocephalus* Assemblage Zone specimen (SAM-PK-8034, Fig. 1.6) found by A.W Rogers and E.H.L Schwarz on the farm Hoogeveld Lot A (270), near Knoflock's Fontein, Van der Byl's Kraal, in the Gouph. He referred this new specimen to *Pareiasaurus serridens,* but it was later made the holotype for *Embrithosaurus schwarzi* by Watson (1914b) and retained as valid by (Lee 1995, 1997a).

*Nochelesaurus alexanderi* (SAM-PK-6239), based on a partial skull and skeleton from the *Tapinocephalus* Assemblage Zone, was described by Haughton and Boonstra (1929a, Fig. 1.9) and retained as a valid species by (Lee 1995, 1997a).

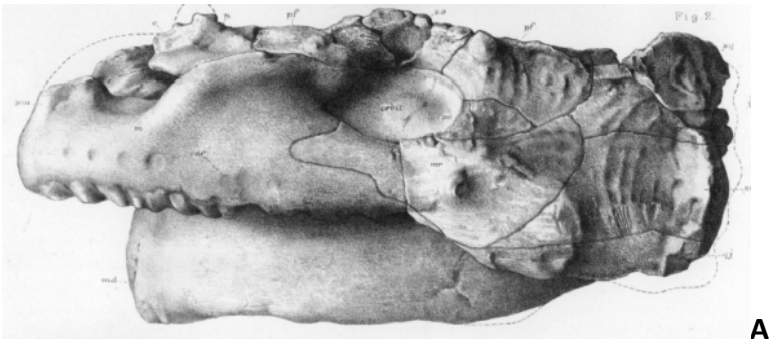

A

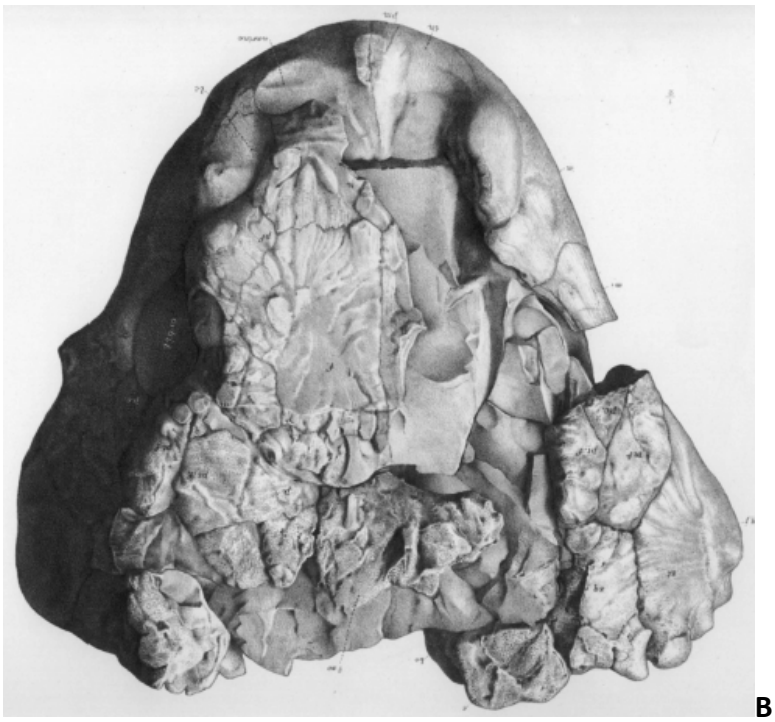

B

**Figure 1.3:** Interpretive drawing of the holotype skull of *Bradysaurus seeleyi* (NHMUK 49426), in (A) left lateral and (B) dorsal views, taken from Seeley (1888).

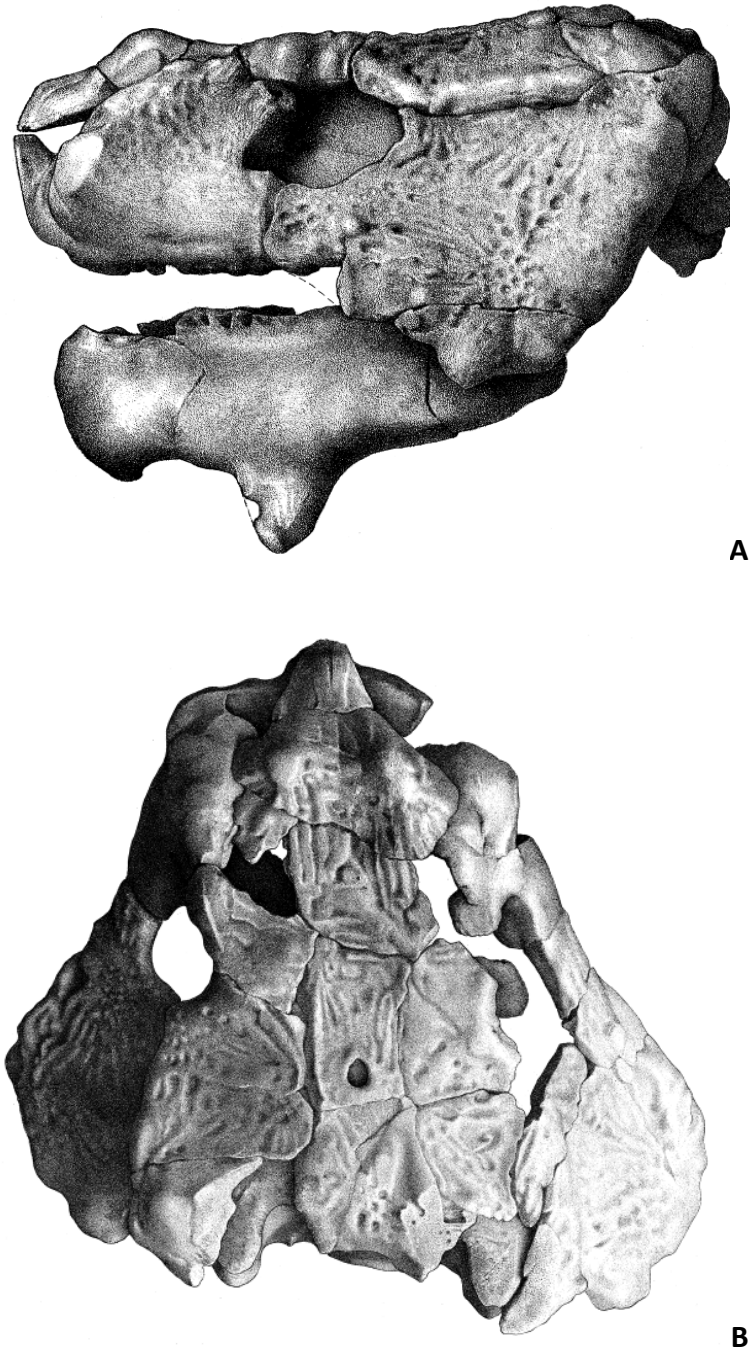


**Figure 1.4:** Interpretive drawing of the holotype skull of *Bradysaurus baini* (NHMUK R1971), in (A) left lateral and (B) dorsal views, taken from Seeley (1892).




**Figure 1.5:** Photograph of the holotype of *Bradysaurus baini* (NHMUK R1971), currently on display in the Natural History Museum, London (2016).

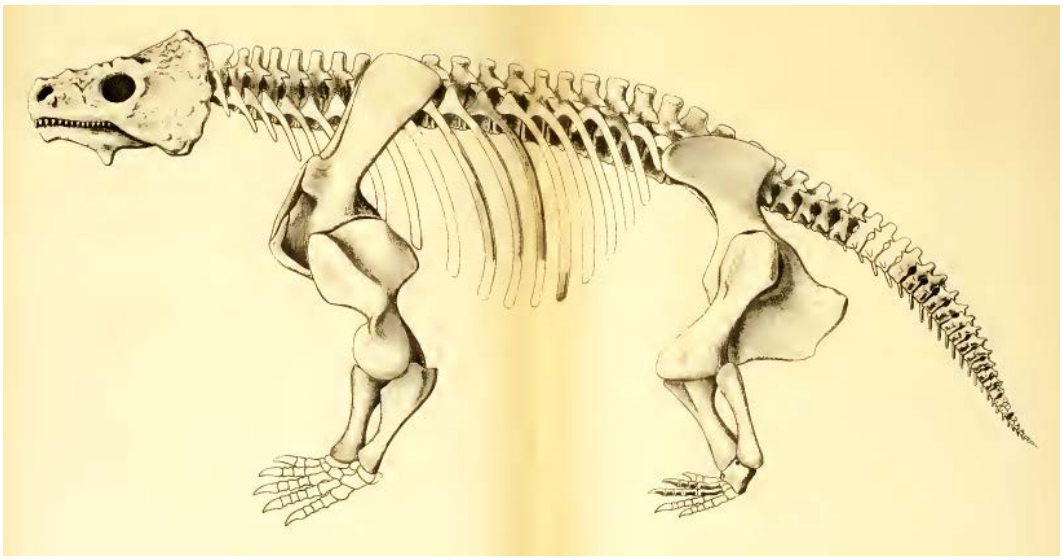

**Figure 1.6:** Interpretive drawing of the holotype of *Embrithosaurus schwarzi* (SAM-PK-8034), taken from Broom (1903).

### 1.2.2 Watson (1914b)

The first attempt to resolve the taxonomic confusion created by earlier workers for the various pareiasaurian species described was performed by Watson (1914b). By re-examining museum catalogues and records and by reassessing the holotypes held at the Natural History Museum, London, he matched misplaced and incorrectly referred elements to their original specimens, including the pelvis of the type of *Pareiasaurs serridens.* In so doing Watson was the first to discover differences in the placement of body scutes between the now restored complete holotype of *P.serridens*, from the *Cistecephalus* Assemblage Zone, and specimens from the *Tapinocephalus* Assemblage Zone referred to the same species. The specimens from the *Cistecephalus* Assemblage Zone possess body armour over most of their dorsal body surface and even their legs, whereas the dermal armour is restricted to a narrow band above the vertebral column in *Tapinocephalus* Assemblage Zone pareiasaurs. Watson (1914b) also realised that the specimen referred to *P. serridens* by Broom in 1903, was in fact very different and did not belong to that species. Based on these findings, Watson deemed it necessary to reconsider the South African pareiasaurian genera and to give new generic names where necessary, which resulting in his recognition of five genera, for which he gave brief generic diagnoses.

For specimens from the *Cistecephalus* Assemblage Zone, Watson (1914b) retained the genera *Pareiasaurus* (Owen 1876), *Anthodon* (Owen 1876) and *Propappus* (Seeley 1888) and updated their diagnoses.

Watson created the new genus of *Bradysaurus,* comprising the type of *Bradysaurus baini* for Seeley's 1892 holotype of *Pareiasaurus baini*, exhibiting minimal body armour, from the *Tapinocephalus* Assemblage Zone. Watson based this decision on his discovery that the holotype of *Pareiasaurus* is characterised by extensive body armour and was not from the *Tapinocephalus* Assemblage Zone, but is from the higher *Cistecephalus* Assemblage Zone.

Watson lastly created the new genus of *Embrithosaurus*, comprising the holotype of *Embrithosaurus schwarzi*, for Broom's 1903 specimen incorrectly referred to *Pareiasaurus serridens*, as Watson noted that the specimen was different from the *Cistecephalus* Assemblage Zone *Pareiasaurus serridens*.

Watson (1914b) mentions Owen's *Pareiasaurus bombidens* (Owen 1876), but appears to omit it from his classification scheme. Broom (1935) suggested that this was probably because the material was represented by a very imperfect partial snout.

This resulted in the following classification of pareiasaurs from the *Tapinocephalus* Assemblage Zone (Watson 1914b):

| **Genus** | **Species** | **Holotype** | **Original Identification** |
|---|---|---|---|
| *Bradysaurus* (Watson 1914) | *Bradysaurus baini* | NHMUK R1971 | *Pareiasaurus baini* Seeley 1892 |
| *Embrithosaurus* (Watson 1914) | *Embrithosaurus schwarzi* | SAM-PK-8034 | *Pareiasaurus serridens* Broom 1903 |

**Table 1.1:** Classification of *Tapinocephalus* Assemblage Zone pareiasaurs (Watson 1914b).

Broom (1916) published a note in which he expressed strong discontent with Watson's 1914 replacement of *Pareiasaurus* with *Bradysaurus* and *Embrithosaurus* for the large pareiasaurs from the *Tapinocephalus* Assemblage Zone that show only minimal body armour. This is because Broom considered all large pareiasaurs, irrespective of differences in their dermal scute arrangement, to be closely related and that they all should remain in the original genus *Pareiasaurus*, with Watson's new generic names being relegated to sub-genera. As a result of his rejection of Watson's classifications, between 1912 and 1924, Broom described three new species of large pareiasaurs from the *Tapinocephalus* Assemblage Zone. He placed them all within *Pareiasaurus*: i.e. *Pareiasaurus acutirostris* (Broom 1913), *Pareiasaurus whaitsi* (Broom 1914, 1915) and *Pareiasaurus strubeni* (Broom 1924). In addition, a new small

specimen from the *Tapinocephalus* Assemblage Zone was named *Propappus rogersi* (Broom 1912).

### 1.2.3 Haughton and Boonstra (1929a)

Between 1929 and 1934, Haughton and Boonstra produced an eleven-part study of all South African pareiasaurs. They published papers focusing on the braincases, manus, pes, mandibles, hind limbs, fore limbs, dermal armour and vertebrae (Boonstra 1929a, 1929b, 1932b, 1932c, 1934b, 1934c, Haughton and Boonstra 1929b, 1930a, 1930b) and included two important taxonomic reassessment papers, focusing on skull features (Haughton and Boonstra 1929a, Boonstra 1934a).

In the first taxonomic contribution (Haughton and Boonstra 1929a) analysed 25 specimens. Most of them are held at the South African Museum in Cape Town (now the Iziko South African Museum, Cape Town) but the sample also included the historic holotype specimens from the Natural History Museum, London. A very brief cranial description, without illustrations, was provided for the group as a whole, and individual cranial elements were not discussed. Haughton and Boonstra (1929a) noted the variability of many of the skulls due to post-mortem deformation and decided to base their classification primarily on features least likely to be affected by compression and deformation, i.e. dentition. They assigned the specimens into three primary divisions; those that have less than, equal to, and more than nine cusps on their teeth. Secondarily, because they recognised that the post-mortem deformation particularly affects the snout and cheek regions, they decided to consider the top of the skull, interpreted as less susceptible to deformation. In their classification, they recognised three secondary divisions; those with interorbital width greater than, equal to, or less than the tabular width.

Haughton and Boonstra (1929a) contributed to the *Tapinocephalus* Assemblage Zone classifications through retaining Watson's classification, naming new taxa based on new material, and assigning specimens recently described by Broom to new genera and species. These three contributions are each described below.

For the *Tapinocephalus* Assemblage Zone forms, Haughton and Boonstra (1929a) accepted Watson's (1914b) taxonomical changes and retained *Embrithosaurus schwarzi* (Watson 1914b) and *Bradysaurus baini* (Seeley 1892).

For new material from the *Tapinocephalus* Assemblage Zone in the Iziko South African Museum, Haughton and Boonstra (1929a) named five new species, which included *Dolichopareia angusta, Platyoropha broomi*, *Bradysaurus vanderbyli, Nochelesaurus alexanderi* and *Brachypareia watsoni.*

Haughton and Boonstra (1929a) did not recognise the four new species from the *Tapinocephalus* Assemblage Zone named by Broom between 1912 and 1924, as Broom had not accepted or used Watson's (1914b) taxonomy. They therefore reassigned all four by creating new genera for them:

- *Bradysuchus whaitsi* (Haughton and Boonstra 1929a) based on an American Museum of Natural History specimen originally described by Broom (1914) as *Pareiasaurus whaitsi* (AMNH 5567).
- *Nochelesaurus strubeni* (Haughton and Boonstra 1929a) based on a very complete skull and skeleton in the American Museum of Natural History, whos lower jaw was originally described by Broom (1924), as *Pareiasaurus strubeni* (AMNH: Broom collection: FR2232).
- *Koalemasaurus acutirostris* (Haughton and Boonstra 1929a) based on an Albany Museum specimen (AM 3748) originally described by Broom (1913) as *Pareiasaurus acutirostris.*
- *Brachypareia rogersi* (Haughton and Boonstra 1929a) based on a Iziko South African Museum specimen (SAM-PK-8953) originally described by Broom (1912) as *Propappus rogersi.* As this specimen consists of only postcrania,

they assigned a new specimen (SAM-PK-5012), comprising of an almost complete skeleton and skull, as a neotype, in order to describe the skull characteristics from it.

Haughton and Boonstra (1929a) considered the very imperfect snout used by Owen (1876) to name *Pareiasaurus bombidens* (NHMUK R1714/43525) an extremely unsatisfactory type that could not be accurately placed in their new classification. They therefore removed *Pareiasaurus bombidens* and created the new species of *Bradysaurus seeleyi*, for the two London specimens (NHMUK 49426 and R1970) referred to *Pareiasaurus bombidens* by Seeley (1888, 1892) and assigned NHMUK 49426 as the holotype.

Their classification resulted in a total of eight genera and twelve species from the *Tapinocephalus* Assemblage Zone. They correctly noted that all forms from this Assemblage zone forms exhibit less than nine cusps per tooth, except for *Embrithosaurus,* which has nine cusps.

This resulted in the following classification of pareiasaurs from the *Tapinocephalus* Assemblage Zone (Haughton and Boonstra 1929a):

| **Genus** | **Species** | **Holotype** | **Original Identification** |
|---|---|---|---|
| *Embrithosaurus* (Watson 1914) | *Embrithosaurus schwarzi* | SAM-PK-8034 | *Pareiasaurus serridens* Broom 1903 |
| *Bradysaurus* (Watson 1914) | *Bradysaurus baini* | NHMUK R1971 | *Pareiasaurus baini* Seeley 1892 |
| | *Bradysaurus seeleyi* | NHMUK 49426 | *Pareiasaurus bombidens* Seeley 1888 |
| | *Bradysaurus vanderbyli* | SAM-PK-3718 | Haughton and Boonstra 1929 |
| *Bradysuchus* (Haughton and Boonstra 1929) | *Bradysuchus whaitsi* | AMNH 5567 | *Pareiasaurus whaitsi* Broom 1914 |
| *Nochelesaurus* (Haughton and Boonstra 1929) | *Nochelesaurus strubeni* | AMNH (Broom collection: FR2232) | *Pareiasaurus strubeni* Broom 1924 |
| | *Nochelesaurus alexanderi* | SAM-PK-6239 | Haughton and Boonstra 1929 |
| *Dolichopareia* (Haughton and Boonstra 1929) | *Dolichopareia angusta* | SAM-PK-6238 | Haughton and Boonstra 1929 |

| | | | |
|---|---|---|---|
| *Platyoropha* (Haughton and Boonstra 1929) | *Platyoropha broomi* | SAM-PK-5002 | Haughton and Boonstra 1929 |
| *Koalemasaurus* (Haughton and Boonstra 1929) | *Koalemasaurus acutirostris* | AM 3748 | *Pareiasaurus acutirostris* Broom 1913 |
| *Brachypareia* (Haughton and Boonstra 1929) | *Brachypareia rogersi* | SAM-PK-8953 | *Propappus rogersi* Broom 1912 |
| | *Brachypareia watsoni* | SAM-PK-6240 | Haughton and Boonstra 1929 |

**Table 1.2:** Classification of *Tapinocephalus* Assemblage Zone pareiasaurs (Haughton and Boonstra 1929a).

### 1.2.4 Boonstra (1934a)

The next major pareiasaurian taxonomic reassessment (Boonstra 1934a) was conducting using 62 specimens, of which 49 were from the *Tapinocephalus* Assemblage Zone, most held at the Iziko South African Museum. A detailed description of a typical pareiasaur skull was provided. This included descriptions of individual cranial elements, but separate cranial descriptions were not provided for the different species. Boonstra produced a comprehensive catalogue of interpretative cranial drawings for all species and in all major views, along with some selected photographs, although the drawings were only rough hand drawn sketches with most sutures being hypothetical (Boonstra 1934a). Cranial diagnoses were provided for each species, although most of the characteristics and conditions mentioned are not unique to each species and are shared across most taxa. Boonstra (1934a) retained the taxonomic classifications proposed by Haughton and Boonstra (1929a) and expanded the diagnosis for each species by including additional cranial proportions and size differences which are susceptible to deformation in his assessment, such as snout and lateral cheek sizes. He also assigned numerous additional specimens to each recognised taxon. The number of valid South African *Tapinocephalus* Assemblage Zone

species was decreased from 12 to 11 as *Platyoropha broomi* was considered as a junior synonym for *Bradysaurus baini.*



**A**



**B**

**Figure 1.7:** Photograph of the holotype skull of *Embrithosaurus schwarzi* (SAM-PK-8034), in (A) left lateral and (B) occipital views, taken from Boonstra (1934a). Both angular bosses of the lower jaw were present, but are now lost.

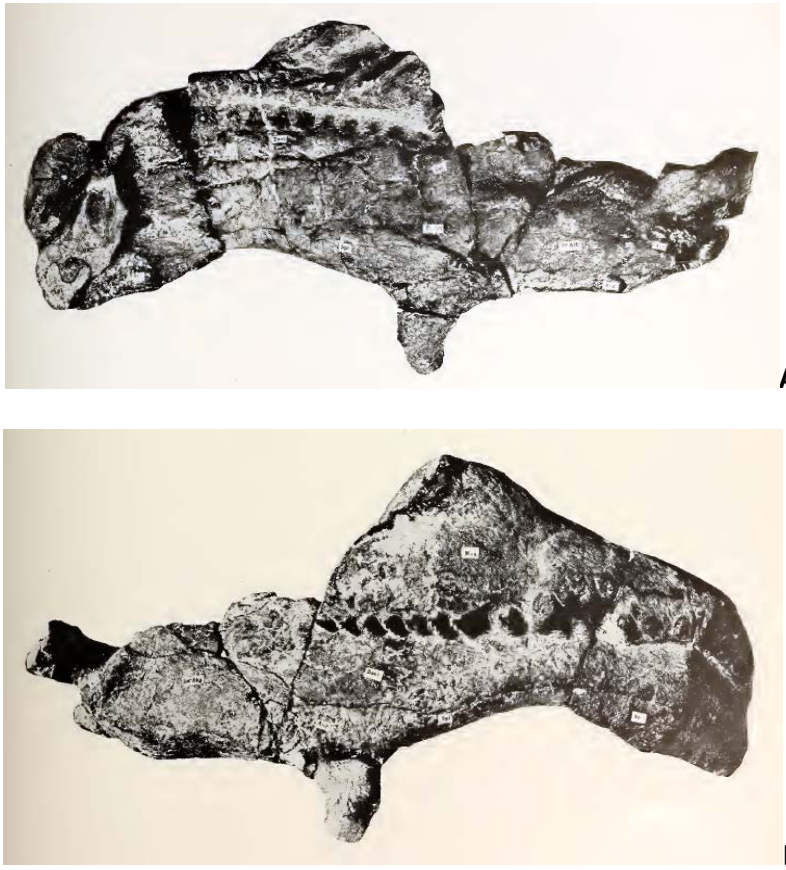


**Figure 1.8:** Photograph of the right rami of SAM-PK-8034 (Fragment A), in (A) right medial and (B) right lateral views, taken from Haughton and Boonstra (1930a). Note the presence of the now lost right angular boss of the lower jaw.



A




B

**Figure 1.9:** Photograph of the holotype skull of *Nochelesaurus alexanderi* (SAM-PK-6239), in (A) right lateral and (B) dorsal views, taken from Boonstra (1934a).

### 1.2.5 Broom (1935)

Broom, by 1935, had come to agree with Watson (1914b) regarding the extensive armour of *Cistecephalus* forms as distinguishing them from the feebly armoured *Tapincephalus* Assemblage Zone forms, which served as the basis for

Watsons's 1914(b) reclassification of *Pareisaurus* specimens to *Bradysaurus* and *Embrithosaurus*. Broom accepted *Bradysaurus* as the most important genus for the majority of species from the *Tapincephalus* Assemblage Zone. He considered *Embrithosaurus* as valid for the very distinct specimen described by him in 1903.

The three new species of large *Pareiasaurus* from the *Tapinocephalus* Assemblage Zone described by Broom between 1913 and 1924, he now placed within *Bradysaurus,* i.e. *P. acutirostris* (Broom 1913), *P. whaitsi* (Broom 1914) and *P. strubeni* (Broom 1924). He admitted that *P. whaitsi* was originally created by himself (Broom 1914) based on the mistaken observation of two angular bosses, one of which was probably a displaced scute or ostederm.

Broom rejected the new genera and species proposed by Haughton and Boonstra (1929a, 1934a), i.e. *Bradysaurus vanderbyli, Nochelesaurus alexanderi, Dolichopareia angusta* and *Brachypareia watsoni*.

Broom (1935) lamented the fact that Watson (1914b) ignored the holotype specimen described by Owen (1876) for *Pareiasaurus bombidens*, and speculated that it was probably due to the fact that it is represented by a very imperfect fragmentary snout. Broom (1935) consequently reinstated Owen's (1876) original specimen as the holotype for *Bradysaurus bombidens*.

This resulted in the following classification of pareiasaurs from the *Tapinocephalus* Assemblage Zone (Broom 1935):

| **Genus** | **Species** | **Holotype** | **Original Identification** |
|---|---|---|---|
| *Embrithosaurus* (Watson 1914) | *Embrithosaurus schwarzi* | SAM-PK-8034 | *Pareiasaurus serridens* Broom 1903 |
| *Bradysaurus* (Watson 1914) | *Bradysaurus baini* | NHMUK R1971 | *Pareiasaurus baini* Seeley 1892 |
| | *Bradysaurus acutirostris* | AM 3748 | *Pareiasaurus acutirostris* Broom 1913 |
| | *Bradysaurus whaitsi* | AMNH 5567 | *Pareiasaurus whaitsi* Broom 1914 |
| | *Bradysaurus strubeni* | AMNH (Broom collection: FR2232) | *Pareiasaurus strubeni* Broom 1924 |

| | | | |
|---|---|---|---|
| | *Bradysaurus bombidens* | BMNH R1714/43525 | *Pareiasaurus bombidens* Owen 1876 |

**Table 1.3:** Classification of *Tapinocephalus* Assemblage Zone pareiasaurs (Broom 1935).

### 1.2.6 Boonstra (1969)

Boonstra (1969), in his comprehensive review of the fauna of the *Tapinocephalus* Assemblage Zone, included a brief section on the Pareiasauridae. He did not accept Broom's (1935) classification and instead used his own (Boonstra 1934a) classification scheme as a starting point. He noted that his 1934 classifications, which recognised seven genera, were primarily based on the nature of the teeth and some proportions of the skull table that were susceptible to deformation. With more material available Boonstra (1969) suggested a reappraisal of this taxonomy, still using the nature of the teeth to distinguish the genera. However this time he also took into account the effects of deformation more specifically. He noted that only two conditions actually exist; *Embrithosaurus* with nine cusps in the teeth and *Bradysaurus* with less than nine cusps into which all other genera were included.

Boonstra (1969) noted that *Bradysuchus whaitsi* (*Pareiasaurs whaitsi* Broom 1914) was mistakenly created by Broom based on a pathological feature, the supposed unique second angular boss, and is therefore a synonym for *Bradysaurus*, but did not assign it a species within *Bradysaurus*. Boonstra (1969) considered the two species of *Brachypareia* to be mistakenly diagnosed on immature specimens and thus invalid.

Boonstra (1969) made no mention of *Bradysaurus vanderbyli, Nochelesaurus alexanderi* and *Koalemasaurus acutirostris* and appears to have ignored these taxa in his new classification. *Dolichopareia angusta* and *Nochelesaurus strubeni*

were assigned their own species within *Bradysaurus*, based on a similar cusp arrangement to *Bradysaurus.*Boonstra (1969) provided no descriptions, but included detailed illustrations of the cranium of *Bradysaurus*, with cranial elements and sutures identified.

Boonstra (1969) recognised the following five species from the *Tapinocephalus* Assemblage Zone as valid:

| Genus | Species | Holotype | Original Identification |
|---|---|---|---|
| *Embrithosaurus* (Watson 1914) | *Embrithosaurus schwarzi* | SAM-PK-8034 | *Pareiasaurus serridens* Broom 1903 |
| *Bradysaurus* (Watson 1914) | *Bradysaurus baini* | NHMUK R1971 | *Pareiasaurus baini* Seeley 1892 |
| | *Bradysaurus seeleyi* | NHMUK 49426 | *Pareiasaurus bombidens* Seeley 1888 |
| | *Bradysaurus strubeni* | AMNH (Broom FR2232) | *Pareiasaurus strubeni* Broom 1924 |
| | *Bradysaurus angusta* | SAM-PK-6238 | *Dolichopareia angusta* Haughton and Boonstra 1929 |

**Table 1.4:** Classification of *Tapinocephalus* Assemblage Zone pareiasaurs (Boonstra 1969).

### 1.2.7 Kuhn (1969)

Kuhn (1969) considered all forms from the *Tapinocephalus* Assemblage Zone in only two genera; *Bradysaurus* having fewer than nine cusps per tooth and *Embrithosaurus* with nine cusps. Kuhn used the 12 species in the scheme of Haughton and Boonstra (1929a) as the basis for in his reassessment and also included *Pareiasaurs bombidens* (Owen 1876). This species and specimen was excluded by Watson (1914b), Haughton and Boonstra (1929a) and Boonstra (1934a) in their classifications. Kuhn thus recognised 13 species: four for *Embrithosaurus* and nine for *Bradysaurus*. This resulted in the following

classification of pareiasaurs from the *Tapinocephalus* Assemblage Zone (Kuhn 1969):

| **Genus** | **Species** | **Holotype** | **Original Identification** |
|---|---|---|---|
| *Embrithosaurus* (Watson 1914) | *Embrithosaurus schwarzi* | SAM-PK-8034 | *Pareiasaurus serridens* Broom 1903 |
| | *Embrithosaurus strubeni* | AMNH (Broom collection: FR2232) | *Pareiasaurus strubeni* Broom 1924 |
| | *Embrithosaurus alexanderi* | SAM-PK-6239 | *Nochelesaurus alexanderi* Haughton and Boonstra 1929 |
| | *Embrithosaurus angusta* | SAM-PK-6238 | *Dolichopareia angusta* Haughton and Boonstra 1929 |
| *Bradysaurus* (Watson 1914) | *Bradysaurus baini* | NHMUK R1971 | *Pareiasaurus baini* Seeley 1892 |
| | *Bradysaurus baini* | NHMUK R1971 | *Pareiasaurus baini* Seeley 1892 |
| | *Bradysaurus bombidens* | BMNH R1714/43525 | *Pareiasaurus bombidens* Owen 1876 |
| | *Bradysaurus vanderbyli* | SAM-PK-3718 | *Bradysaurus vanderbyli* Haughton and Boonstra 1929 |
| | *Bradysaurus seeleyi* | NHMUK 49426 | *Pareiasaurus bombidens* Seeley 1888 |
| | *Bradysaurus whaitsi* | AMNH 5567 | *Pareiasaurus whaitsi* Broom 1914 |
| | *Bradysaurus acutirostris* | AM 3748 | *Pareiasaurus acutirostris* Broom 1913 |
| | *Bradysaurus watsoni* | SAM-PK-6240 | *Brachypareia watsoni* Haughton and Boonstra 1929 |
| | *Bradysaurus rogersi* | SAM-PK-8953 | *Propappus rogersi* Broom 1912 |
| | *Bradysaurus broomi* | SAM-PK-5002 | *Platyoropha broomi* Haughton and Boonstra 1929 |

**Table 1.5:** Classification of *Tapinocephalus* Assemblage Zone pareiasaurs (Kuhn 1969).

### 1.2.8 Lee (1995, 1997a)

In the most recent taxonomic reassessment, Lee (1995, 1997a) undertook a study of all the pareiasaur species held in museum collections around the world. This important work greatly improved understanding of the group and resulted in the reduction of the number of described species from 49 to only 17 with southern African species diversity reduced from 31 to 11. Updated and new diagnoses were erected for all valid taxa. Lee reduced the number of *Tapinocephalus* Assemblage Zone species from eleven to four: *Bradysaurus seeleyi, B.baini, Nochelesaurus alexanderi* and *Embrithosaurus schwarzi*.

Lee considered the early taxonomic assessments by Watson (1914b), Haughton and Boonstra (1929a) and Boonstra (1934a) as most important as they cover the period in which the South African pareiasaur taxa were first described. Lee, though direct personal observations, studied the holotypes of the 12 species of pareiasaurs from the *Tapinocephalus* Assemblage Zone described by Haughton and Boonstra (1929a), as well as the holotype of *Pareiasaurus bombidens* (Owen 1876).

Lee (1997a) noted that the features used by Haughton and Boonstra (1929a) to distinguish species, i.e. variation in dorsal skull shape, were unreliable as they were mostly due to mediolateral and/or dorsoventral distortion. He considered only four of the species reconised by Haughton and Boonstra (1929a) to be valid taxa: *Bradysaurus seeleyi, B.baini, Nochelesaurus alexanderi* and *Embrithosaurus schwarzi*.

Lee synonymised several of the taxa identified by Haughton and Boonstra (1929a) into these four valid taxa:

- *Platoropha broomi* (Haughton and Boonstra 1929a) he found to be a junior synonym *for Bradysaurus baini*, confirming Boonstra's (1934a) earlier synonymising of this taxon into *Bradysaurus baini*,

- *Dolichopareia angusta* (Haughton and Boonstra 1929a) and *Brachypareia watsoni* (Haughton and Boonstra 1929a) Lee concluded to be junior synonyms of *Nochelesaurus alexanderi,*
- *Brachypareia rogersi* (Haughton and Boonstra 1929a) (*Propappus rogersi* Broom 1912*)* Lee considered a junior synonym of *Pareiasaurus serridens,* and
- *Bradysaurus vanderbyli* (Haughton and Boonstra 1929a) Lee found to be a junior synonym of *Bradysaurus seeleyi*.

Lee finally declared four species as *nomen dubium* due to indeterminate holotype material:

- *Nochelesaurus strubeni* (AMNH Broom collection: FR2232) (Haughton and Boonstra 1929a) (*Pareiasaurus strubeni* Broom 1924) a complete juvenile skull and skeleton of one of the large *Tapinocephalus* Assemblage Zone pareiasaurs,
- *Bradysuchus whaitsi* (AMNH 5567) Haughton and Boonstra 1929a) (*Pareiasaurs whaitsi* Broom 1914) a skull of *Bradysaurus,* but of indeterminate species,
- *Pareiasaurus bombidens* (NHMUK R1714/43525) (Owen 1876) a badly preserved snout and jaw fragment only of a large *Tapinocephalus* Assemblage Zone pareiasaur belonging to either *Bradysaurus seeleyi* or *Nochelesaurus alexanderi*, and
- *Koalemasaurus acutirostris* (AM 3748) (*Pareiasaurus acutirostris*) Broom 1913) a poorly preserved juvenile skull of a large *Tapinocephalus* Assemblage Zone pareiasaur of indeterminate placement.

The following species from the *Tapinocephalus* Assemblage Zone are considered to be valid by Lee (1995, 1997a):

| Genus | Species | Holotype | Original Identification |
|---|---|---|---|
| *Embrithosaurus* (Watson 1914) | *Embrithosaurus schwarzi* | SAM-PK-8034 | *Pareiasaurus serridens* Broom 1903 |
| *Bradysaurus* (Watson 1914) | *Bradysaurus baini* | NHMUK R1971 | *Pareiasaurus baini* Seeley 1892 |
| | *Bradysaurus baini* | SAM-PK-5002 | *Platyoropha broomi* Haughton and Boonstra 1929 |
| | *Bradysaurus seeleyi* | NHMUK 49426 | *Pareiasaurus bombidens* Seeley 1888 |
| | *Bradysaurus seeleyi* | SAM-PK-3718 | *Bradysaurus vanderbyli* Haughton and Boonstra 1929 |
| *Nochelesaurus* (Haughton and Boonstra 1929) | *Nochelesaurus alexanderi* | SAM-PK-6239 | *Nochelesaurus alexanderi* Haughton and Boonstra 1929 |
| | *Nochelesaurus alexanderi* | SAM-PK-6238 | *Dolichopareia angusta* Haughton and Boonstra 1929 |
| | *Nochelesaurus alexanderi* | SAM-PK-6240 | *Brachypareia watsoni* Haughton and Boonstra 1929 |

**Table 1.6:** Classification of *Tapinocephalus* Assemblage Zone pareiasaurs (Lee 1995, 1997a).

Lee's taxonomic review was by his own admission not a definitive review of pareiasaurian systematics due to its scope of work being extremely broad and wide. Hundreds of large specimens assigned to 47 species were studied and it is possible that not all anatomical details were discovered or investigated to completion due to time constraints (Lee 1997a: 236). In particular, the pareiasaurs from the *Tapinocephalus* Assemblage Zone of South Africa "pose a major problem" (Lee 1997a: 236). Lee was able to properly examine only a relatively small proportion of this material, due to the large quantity of specimens and the crudely prepared nature of the majority of the specimens. He

did not produce an updated detailed description of any of the southern African middle Permian pareiasaurs. Tsuji (2010) in the phylogenetic chapter of her PhD thesis, also emphasized the need for much more taxonomic and anatomical research on the *Tapinocephalus* Assemblage Zone pareiasaurs, which are notoriously difficult to study due to bad preparation and preservation.

## 1.3 Project Objectives

### 1.3.1 Descriptive and taxonomical improvements

Despite their long history and relative abundance, most pareisaurs have not been properly described at a species level. Notable recent detailed cranial descriptions include *Scutosaurs karpinskii* (Lee 1995), *Pareiasuchus nasicornis* (Lee *et al.* 1997), *Arganaceras vacanti* (Jalil and Janvier 2005), *Deltavjatia vjatkensis* (Tsuji 2010), and *Bunostegos akokanenis* (Tsuji *et al.* 2013, Turner *et al.* 2015). The cranial sutures of most pareiasaurs are difficult to observe, often being obscured by dermal ornamentation and bosses, exacerbated by inadequate preparation of many specimens. The recent updated cranial descriptions were achievable through the use of multiple specimens, which increases the chances of detecting sutures, especially the use of juvenile specimens, which show more clearly the usually obscured cranial sutures of adult specimens. Often the external cranial sutures are visible only in juvenile or half-grown specimens, as the bony elements have not yet fused and the skull ornamentation and bosses are not yet fully developed (Lee 1995, Lee *et al.* 1997). Sutures are usually not visible or only faintly visible in adult specimens. Previous authors have also studied the inner surfaces of cranial bones to reveal sutures (e.g. Lee 1995 in *Scutosaurs karpinskii*, Watson 1914a in *Embrithosaurus schwarzi*).

Despite a recorded descriptive history of nearly 150 years and the large number of specimens available, detailed full cranial descriptions for the middle Permian pareiasaurs *Bradysaurus*, *Embrithosaurus* and *Nochelesaurus* do not exist and

only brief, old and outdated initial descriptions have been completed (Seeley 1888, 1892, Broom 1903, Watson 1914a). In addition their diagnostic cranial features have been only briefly defined (Watson 1914b, Haughton and Boonstra 1929a, Boonstra 1934a, Kuhn 1969, Lee 1997a). Besides for *Bradysaurus*, which was illustrated by Boonstra (1969) and recently re-illustrated in detail by Lee (1995, 1997a), all other *Tapinocephalus* Assemblage Zone pareiasaurs were last illustrated in 1934 (Boonstra 1934a), where only rough initial sketches were produced. These old and rough illustrations (Boonstra 1934a) have been used by most subsequent workers and are in urgent need of being updated and confirmed, particularly for *Embrithosaurus* and *Nochelesaurus*.

- For the holotype of *Bradysaurus baini*, a relatively brief cranial description including cranial interpretive illustrations was produced by Seeley (1892). The specimen is curated at the Natural History Museum in London thereby limiting its availability to South African palaeontologists. Lee (1995, 1997a) produced updated detailed cranial illustrations of all major views, using the holotype and a referred specimen curated at the Iziko South African Museum in Cape Town.
- For the holotype of *Bradysaurus seeleyi*, a reasonably detailed and thorough cranial description including cranial interpretive illustrations was produced by Seeley (1888). The specimen is also curated at the Natural History Museum in London.
- For *Nochelesaurus alexanderi*, a cranial description of the holotype or any of the referred specimens has not been produced. The holotype and referred specimens are part of the Iziko South African Museum in Cape Town.
- For *Embrithosaurus schwarzi*, a detailed cranial description of the holotype has not been produced. Only Broom (1903) briefly described the cranial bosses of the holotype. A reasonably detailed cranial description of a referred specimen of *Embrithosaurus* was produced by Watson

(1914a). This specimen is curated at the Natural History Museum in London. The holotype is at the Iziko South African Museum in Cape Town.

In light of the above considerations, it is practical and prudent to produce a new updated detailed cranial description of *Embrithosaurus*, and at the same time to confirm or add additional reliable characters to diagnose the four taxa from the *Tapinocephalus* Assemblage Zone. Once this has been achieved, all the specimens from the *Tapinocephalus* Assemblage Zone, stored in South African museum collections, and in London, will be re-identified for stratigraphic range determination.

### 1.3.2 Stratigraphic range improvement

#### Introduction

Pareiasaurs comprise a large component of middle Permian biodiversity in the continental realm, and are abundant in the South African middle Permian record. Refining their taxonomy is key to better interpreting the faunal composition of this time and would allow for refinements to their bio stratigraphic distribition.

Rubidge, students and colleagues at the Evolutionary Studies Institute (ESI) at the University of the Witwatersrand, Johannesburg, have for many years been involved in a study to understand middle Permian biodiversity changes in the continental realm (Rubidge 2005, Nicolas 2007, Van der Walt *et al.* 2011, Day 2013, Rubidge *et al.* 2013, Day *et al*. 2015, Rubidge *et al*. 2016). The lower Beaufort Group of South Africa is currently divided into three faunal Assemblage Zones, and preserves the world's most time-extensive and continuous stratigraphic succession of middle Permian deposits. An extensive faunal Assemblage zone was established in 1892 (Seeley), named the *Pareiasaurus* Zone, which Watson (1914b) renamed the *Tapinocephalus* Assemblage Zone. The uppermost section of the *Tapinocephalus* Assemblage Zone, was apportioned into a new Assemblage Zone, the *Pristerognathus* Assemblage Zone (Keyser and

Smith 1977). Rubidge (1987) established the *Eodicynodon* Assemblage Zone below the *Tapinocephalus* Assemblage Zone, immediately above the Ecca-Beaufort contact. The earliest record of pareiasaurs occurs in middle Permian of South Africa (Lee 1995, 1997a). The Lower Beaufort fossil record contains evidence of an extinction event at the end of the Guadalupian, which has been correlated with the end-Guadalupian marine extinction event recognised in China. The main victims of this extinction event on land were the large bodied pareiasaurs and dinocephalian therapsids (Day *et al.* 2015).

**Recent stratigraphic work**

Due to taxonomic chaos and confusion, and a lack of proper diagnoses that only started to surface in the 1930's, pareiasaurian specimens recovered from the *Tapinocephalus* Assemblage Zone have historically been challenging to identify and have been assigned to *Bradysaurus* as a waste-basket taxon in most instances.

For the long-term middle Permian biostratigraphic project of the ESI, the lithostratigaphy has been largely sorted out (Day 2013, Day *et al.* 2015), numerous reliable radiometric dates have been obtained for different stratigraphic levels (Rubidge *et al.* 2013) and the taxonomy of most of the major tetrapod taxonomic groups has recently been revised and updated (i.e. dicynodonts: Angielczyk and Rubidge 2013, therocephalians: Abdala *et al.* 2014, dinocephalians: Guven *et al.* 2013, Kammerer 2011, gorgonopsians: Kammerer *et al.* 2015).

Reliable stratigraphic ranges depend on accurate specimen identifications based on clear taxonomy and reliable unambigious diagnoses. Parieasaurian taxonomy was last revised and updated by Lee (1995, 1997a) reducing the number of valid taxa. However, Lee's updated diagnosis and revised taxonomic classifications, have not been applied to the majority of existing museum-curated specimens in South Africa, with the result that many specimens of pareiasaurs are currently assigned to invalid species on museum catalogues. Lee (1995, 1997a) was only

able to re-identify a minority of museum curated specimens using his updated taxonomy and diagnosis. Consequently, in order to produce updated stratigraphic ranges for the South African middle Permian pareiasaurs, Day (2013) used a combination of data:

1. For *Embrithosaurus* and *Nochelesaurus,* only referred specimens identified by Lee (1995, 1997a) in his taxonomic reassessment were considered by Day. Because Lee substantially altered the diagnoses for these taxa, specimens identified as such using old diagnoses of Watson (1914b) and Haughton and Boonstra (1929a) were excluded.
2. For *Bradysaurus baini* and *B. seeleyi*, existing museum specimen identifications recognised in the Beaufort Fossil Vertebrate database (Nicolas 2007) were used by Day, as Lee (1995, 1997a) did not substantially alter the diagnosis for these taxa. Existing museum catalogue specimen identifications are therefore relatively accurate. However, Day (2013) recognised identities of these taxa to the level of genus only. Lee (1995, 1997a) identified only a few specimens of these taxa and utilization of only these few specimens by Day would have resulted in the exclusion of a large dataset of specimens held in museum collections assigned to *Bradysaurus*.

Day's work resulted in a basic understanding of the stratigraphic ranges of these genera and the group as a whole (Fig. 1.10). However, the stratigraphic ranges produced by Day are compromised by the use of only the few specimens directly studied and re-identified as *Embrithosaurus* and *Nochelesaurus* by Lee. For *Bradysaurus*, Day used existing museum identifications, which may be unreliable as Lee's updated diagnosis (1995, 1997a) was not assessed in these specimens. Also, the stratigraphic ranges were generated at a genus level for *Bradysaurus* and not separated into *B. baini* and *B. seeleyi.*

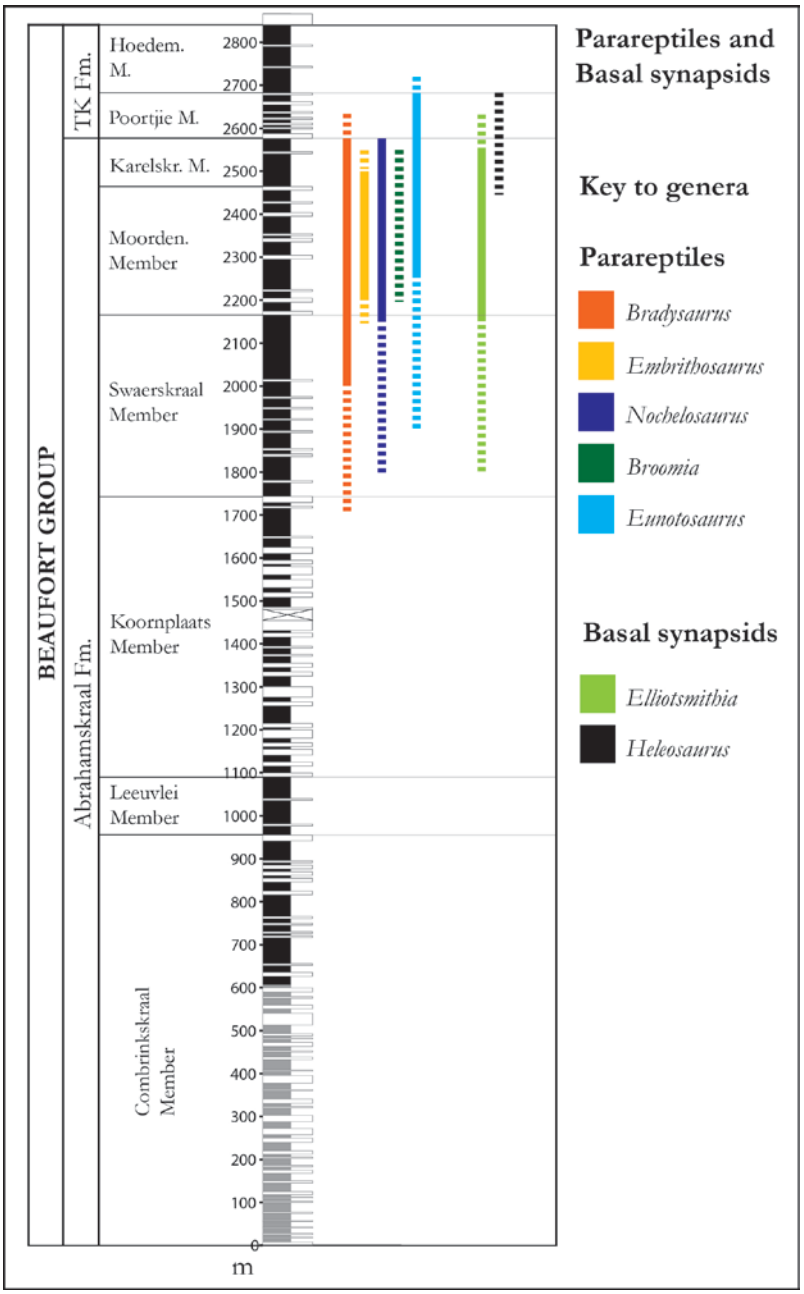


**Figure 1.10:** Composite stratigraphic ranges of parareptile genera from the middle Permian Beaufort Group, taken from Day 2013. Note the stratigraphic ranges of *Bradysaurus*, *Embrithosaurus* and *Nochelesaurus* are restricted to the top of the Abrahamskraal Formation. Numerals denote meters above the base of the Abrahamskraal Formation. Solid lines indicate well constrained stratigraphic provenances for positively identified specimens of each species. Dotted lines indicate a wide range of possible stratigraphic provenances for positively identified specimens of each species.

# .CHAPTER TWO: MATERIAL AND METHODS

## 2.1 Material

### 2.1.1 Holotype *Embrithosaurus schwarzi* SAM-PK-8034

The holotype material of *Embrithosaurus schwarzi* comprises an almost complete skull with tightly occluded lower jaw and an isolated hyoid. Numerous postcranial elements are also preserved, consisting of vertebrae, the scapulo-coracoid, part of the clavicle, humerus, ulna, radius, almost complete pelvis, femora, tibiae, fibulae, and isolated phalanges.

The cranial material is very light in appearance, ranging from nearly white to light grey in colour, and with matrix appearing light green-grey. Dark grey plaster infill and white plaster infill are present on the material.

Boonstra (1934a, Fig. 1.7) includes two cranial photographs of the specimen; the left lateral and the occipital views, confirming that the separate cranial fragments were assembled together. Dark grey plaster and paraloid glue were used to join the fragments together and to fill in sections of the skull not preserved, such as the area below the left orbit (Fig. 1.7). Larger and heavier cranial fragments were held together using three small metal plates with screws used as supporting struts to join fragments, such as in the centre of the left cheek region (Fig. 1.7). Most of the dark grey plaster infill and metal plates and screws had since become dettached, leaving the skull in nine fragments. Only one metal plate remains, visible on the left lateral cheek region.

For this study, the skull was reconstructed from the nine cranial fragments, using two-part Pratley Putty (TM) (standard setting), which appears beige in colour, and very thick B-72 paraloid glue to join the pieces (Figs. 3.1-3.5). It was decided to reconstruct the skull into three large separate sections (i.e. the lower jaw, the skull roof, and the palate and braincase), and not into one unit, to allow for

easier future research access to the inner skull surfaces, and to the palate and braincase.

The nine cranial fragments are here designated A-I:

**A.** The largest fragment comprises both the left and right rami of the entire lower jaw (i.e. dentaries, splenials, coracoids, angulars, articulars, prearticulars, and surangulars, including marginal teeth) which has tightly occluded to upper jaw elements (i.e. premaxillaries, vomers, maxillas, lacrimals, left jugal, palatines, marginal teeth, ectopterygoids, distal quadrate flanges, and a small piece of the right quadratojugal) (Figs. 3.6-3.11).

**B.** Large rectangular fragment comprising complete (i.e. nasals, frontals, right parietal, right prefrontal) and partial (i.e. postparietal, lacrimals, left prefrontal, left postfrontal, right postorbital, left parietal, right supratemporal and right squamosal) elements of the dorsal skull roof (Fig. 3.12). On the inner skull surface, the sphenethmoid and part of the supraoccipital are preserved along with small partial pieces of the right maxilla, jugal and palatine (Fig. 3.13).

**C.** Large fragment consisting of the entire left lateral cheek (i.e. jugal, quadratojugal, squamosal, postorbital, quadrate from the left side), as well as part of the left dorsal skull table (i.e. supratemporal, and partial postparietal, parietal and postfrontal) (Fig. 3.14). On the inner surface, a small piece of the left quadrate is preserved (Fig. 3.15).

**D.** Small triangular fragment consisting of part of the left lateral side of the face (i.e. partial left maxilla, lacrimal and prefrontal) (Figs. 3.16, 3.17).

**E.** Large fragment consisting of most of the right lateral cheek (i.e. jugal, quadratojugal, partial squamosal and partial postorbital from the right side), as well as small part of the right dorsal skull roof consisting of the partial right supratemporal) (Figs. 3.18, 3.19).

**F.** Medium sized fragment consisting of most of the palatal region (i.e. most of the pterygoids, and all the palatal teeth) as well as partial vomers, palatines, epipterygoids and part of the basisphenoid (Figs. 3.20, 3.21).

**G.** Medium sized fragment comprising most of the occipital and braincase region (i.e. basioccipital, opisthotics, exoccipitals, prootics and partial supraoccipital), most of the basisphenoid, large portions of the right squamosal and supratemporal and small pieces of the left squamosal and supratemporal (Figs. 3.22-3.24).

**H.** Medium sized fragment consisting of a small part of the right quadrate ramus of the pterygoid, most of the right quadrate, and thin, tall sections of the right squamosal and quadratojugal medial flanges (Figs. 3.25, 3.26).

**I.** Small fragment consisting of a small part of the left quadrate ramus of the pterygoid and most of the left quadrate (Figs. 3.27, 3.28).

### 2.1.2 Horizon and Locality

Specimen SAM-PK-8034 was collected by Mr A.W. Rogers and Mr E.H.L. Schwarz in 1902 on the farm Hoogeveld Lot A (Hoogeveld 270), in the Gouph region, near Knoflock's Fontein, Van der Byl's Kraal, Price Albert district of the Western Cape Province of South Africa (Broom 1903). Kitching (1977) assigns the farm of Hoogeveld Lot A to the Low Horizon of the *Tapinocephalus* Assemblage Zone, Abrahamskraal Formation, Beaufort Group.

According to Day (2013, Day *et al.* 2015) this locality is high in the *Tapinocephalus* Assemblage Zone and can be constrained to the stratigraphic interval of 2150-2250 m above the base of Abrahamskraal Formation, occurring in the lower part of the Moordenaars Member of the Abrahamskraal Formation and represents the earliest stratigraphic occurrence of *Embrithosaurus*.

### 2.1.3 Holotype *Nochelesaurus alexanderi* SAM-PK-6239:

The holotype cranial material of *Nochelesaurus alexanderi* comprises three fragments: a large flattened skull roof fragment with most of the left side, palate and braincase missing, a small fragment of the right lower jaw, with the angular boss broken off and a small fragment of the right maxilla. Numerous postcranial elements are also preserved. The right side only of the skull is preserved, consisting of the right cheek, along with the dorsal skull table (Fig. 1.9). Internally, the sphenethmoid, a partial left quadrate, partial left paroccipital process of the opisthotic, and small piece of the mid premaxillary flange are all that is preserved of the palate and braincase, preserved on the inside of the skull.

The cranial material of the holotype of *Nochelesaurus* is very light in colour, similar to the holotype of *Embrithosaurus*, also ranging from nearly white to light grey, with uncleared matrix appearing darker grey.

### 2.1.4 Horizon and Locality

Specimen SAM-PK-6239 was collected in 1923 from the farm Boesmanskop (Bushmans Kop 302), Beaufort West district of the Western Cape Province of South Africa and named in honour of Dr. Alexander du Toit (Haughton and Boonstra 1929a). Kitching (1977) assigns the farm of Boesmanskop, to the Low Horizon of the *Tapinocephalus* Assemblage Zone, Abrahamskraal Formation, Beaufort Group.

According to Day (2013, *et al.* 2015) this locality is high in the *Tapinocephalus* Assemblage Zone, is restricted to the uppermost Karelskraal Member of the Abrahamskraal Formation, and represents the highest stratigraphic occurrence of *Nochelesaurus*.

### 2.1.5 Holotype *Bradysaurus baini* NHMUK R1971:

The holotype cranial material of *Bradysaurus baini* comprises a virtually complete skull and postcranium, except for some ribs, are preserved. The cranial material comprises an almost complete skull, with braincase and palate tightly occluded. The left maxilla shows a large, elongated, oval and raised boss which is posterodorsally oriented. The lower jaw is complete and separated from the skull. On the inside of the skull, all of the braincase is preserved, except for a small piece at the distal end of the right paroccipital process of the opisthotic. Most of the palate is preserved, except for a large piece of the right palatal flanges of the palatine and ecotopterygoid.

The external cranial material of the holotype of *Bradysaurus baini* is much darker than the holotypes of *Embrithosaurus* and *Nochelesaurus*, and ranges from a medium shade of grey to dark black, which is "glassy" and shiny in appearance and includes brown areas on the snout and posterior edges of the dorsal skull.

### 2.1.6 Horizon and Locality

Specimen NHMUK R1971 was collected on the farm Die Bad 286 in the Beaufort West district. Kitching (1977) assigns the farm of Die Bad 286, Beaufort West, to the Low Horizon of the *Tapinocephalus* Assemblage Zone, Abrahamskraal Formation, Beaufort Group.

According to Day (2013, *et al.* 2015) this locality is high in the *Tapinocephalus* Assemblage Zone, and can be restricted to the lower to mid Moordenaars Member of the Abrahamskraal Formation.

### 2.1.7 Holotype *Bradysaurus seeleyi* NHMUK 49426:

The holotype cranial material of *Bradysaurus seeleyi* comprises an almost complete skull and lower jaw. Postcranially only the central trunk of the axial body is preserved, with a partial pelvic girdle and a partial shoulder girdle attached.

Most of the right dorsal skull table is not preserved (Fig. 1.3) and the preserved sections are very badly weathered, with the external surface of the bone eroded away. Most of the palate is preserved but poorly prepared. Dorsally, a large section of the right skull roof has been displaced downwards. The lower jaw is complete and separated from the skull.

The cranial material of the holotype of *Bradysaurus seeleyi* is light brown to orange. The skull is heavily ornamented with small to medium sized bosses and many thick rugose long lines and ridges, with small deep circular pits.

### 2.1.8 Horizon and Locality

Specimen NHMUK 49426 was collected on the farm Palmiet Fontein 229, at the foot of the Nieuwveldt range, in the Beaufort West district. Kitching (1977) assigns the farm of Palmiet fontein, Beaufort West, to the High Horizon of the *Tapinocephalus* Assemblage Zone.

According to Day (2013, *et al.* 2015) this locality is high in the *Tapinocephalus* Assemblage Zone, and can be constrained to the upper Karelskraal Member, within 100 m of the top of the Abrahamskraal Formation, and is the highest stratigraphic occurrence of *B.seeleyi.*

## 2.2 Methods:

### 2.2.1 Preparation *Embrithosaurus schwarzi* SAM-PK-8034:

The holotype skull of *Embrithosaurus*, SAM-PK-8034 was originally mechanically prepared in 1902 using hammer and chisel under the supervision of Dr Robert Broom at the South African Museum in Cape Town (Broom 1903). There is no indication that any further preparation was performed after this time. Broom's preparation of the skull was reasonably complete, exposing most of the external bone surface of the right lateral cheek, the lower jaw, and the palatal and occipital regions. However uncleared matrix is still present in most of the pits and furrows in the rugose regions of the external skull roof (i.e. the dorsal skull table, the left cheek and facial and snout regions), obscuring the external cranial sutures.

For the current study, additional preparation was performed by Gilbert Mokgethoa of the Evolutionary Studies Institute (ESI), University of the Witwatersrand, Johannesburg, in 2015, to reveal dental cusps. On the right mandible, the lingual surfaces of the fourth to tenth teeth (counting back from the front) were prepared. On the left maxilla, the labial surfaces of the second to tenth maxillary teeth were prepared. On the right maxilla, the labial surfaces of the fifth to ninth maxillary teeth were prepared.

### 2.2.2 Suture identification methods

A combination of several methods were used to identify cranial sutures for *Embrithosaurus*:

1) Use of microscope and magnification glasses.
2) Use of alcohol to wet the specimen, which momentarily reveals matrix, sutures and cracks.

3) Use of previous workers “drawn on” sutures directly on the bone in black ink, notably on the lower jaw and on the internal surfaces of certain portions of the skull roof. These “drawn on” sutures are clearly visible on the specimen in photographs of the lower jaw from 1930 (Haughton and Boonstra 1930a, Fig. 1.8). In terms of the skull roof, my assessment is in agreement with these “drawn on” internal sutures. However, on the lower jaw, there are differences of interpretation, and this is noted in the description.
4) This study has employed the method used by Watson (1914b), in his cranial description of the second specimen of *Embrithosaurus* (i.e. BMNH R7782), of projecting identified internal cranial sutures perpendicularly through the bone onto the external bone surface. Internal cranial sutures are often more identifiable than the external sutures as the internal bone surface is not obscured with ornamentation. Internal sutures are also indicated by slightly raised ridges of bone, along sutural contacts, or by matrix infill allowed by slightly displaced or slippage of the separate elements. This method is only reliable if it can be confirmed that the sutures pass directly through the bone, perpendicular to the internal and external surface. This condition can be observed in the sutures of the orbital bar (left prefrontal-postfrontal contact), and on certain skull table sutures where both the internal and external sutures are clearly visible.
5) Bones were chemically stained using the dye “Alizarin Red S” and the technique described by and Rubidge and van den Heever (1997). A 10% solution of hydrochloric acid (HCl) was brushed on the bones, and immediately rinsed off with tap water. A small amount of the biological staining agent Alizarin Red S was mixed with 4% solution of potassium hydroxide (KOH). This mixture was then brushed onto the bones, staining them with a deep purple colour. This helped reveal sutures and cracks in the bone. To remove the stain, the 10% solution of HCl was again brushed on the bones and immediately rinsed off very well using tap water.

6) It was possible to identify sutures on the sides of the nine cranial fragments, which matched the corresponding suture on the adjacent fragment, when fitted together.

Due to the difficulty in identifying the cranial sutures, in the description of each element of the skull and lower jaw, special mention is made as to which sutures were clearly identifiable and by which method, and which sutures were not identifiable.

### 2.2.3 Distortions

The skull has been distorted or displaced in five main directions. Firstly, the entire skull roof, consisting of the flat central skull table, and the laterally orientated face and cheeks regions, is displaced downwards. The ventral margin of the face and cheek, consisting of the premaxilla, maxilla, jugal and quadratojugal, has been ventrally displaced to cover over much of the occluded lower jaw, including both mandibular tooth rows (Figs. 3.8, 3.10). The right cheek flange is somewhat dorsoventrally flattened, thereby widening the appearance of the skull on the right, whilst the left cheek is mediolaterally compressed towards the midline, narrowing the appearance on the left (Fig. 3.1). In addition, the left side of the dorsal skull table is twisted laterally to overhang the left cheek edge, obscuring the view of much of the left squamosal in dorsal view (Fig. 3.1).

Secondly, the dorsal skull table has been displaced backwards compared to the anterior tip of the snout, so that in dorsal view the bottom of the external naris on the premaxilla is visible as anterior to the top of the external naris on the nasal (Fig. 3.1). Without this displacement, the bottom and top of the external naris would be vertically aligned. The backwards displacement of the dorsal skull table has given the orbits the appearance of being posterodorsally elongated in lateral view, but they were likely more circular when undistorted.

Thirdly, the skull roof has been displaced towards the right, so that the skull table and lateral cheeks lie to the right of their normal position. The ventral parts (palate, braincase and lower jaw) are positioned to the left (Fig. 3.1).

Fourthly, the midline of the skull, as observed on the anterior tip of the snout and lower jaw, is twisted to the right, resulting in the left side appearing anteriorly pushed forward and shortened, and the right side appearing much extended posteriorly and lengthened. Although this distortion has affected the entire skull, it is particularly apparent on the lower jaw and occluded upper jaw partial elements of the ventral margin of the skull (i.e. the premaxillaries, vomers, maxillas, lacrimals, left jugal, palatines, and ectopterygoids) (Figs. 3.6, 3.7). It has also badly affected the symmetry of the dorsal view of the skull table, such that each paired element is not transversely aligned, instead the left elements are extended unnaturally far forward and the right elements are extended far posteriorly (Figs. 3.1, 3.12, 3.13)**.**

Finally, the skull has been mediolaterally compressed inwards towards the midline (particularly noticeable on the lower jaw and the anterior region of the skull) resulting a somewhat a pointed snout compared to that of other basal South African pareiasaurs. This false impression of a pointed snout is important to note as this character was mistakenly used by several early workers (Watson 1914b, Haughton and Boonstra 1929a, Boonstra 1934a) to distinguish the species from others with wider snout shapes, as noted by Lee (1997a).

### 2.2.4 Preparation *Nochelesaurus alexanderi* SAM-PK-6239:

The holotype skull of *Nochelesaurus*, SAM-PK-6239 was mechanically prepared between 1923 and 1929 in Cape Town. The preparation of the skull is much better than the holotype skull of *Embrithosaurus* SAM-PK-8034 and is very complete, with most dorsal and lateral elements well exposed. Only very small amounts of uncleared matrix are still present in some of the pits and furrows

between the rugose ridges and bosses of the external skull roof, but this matrix does not obscure any sutures or important features.

The majority of the maxillary and mandibular teeth however, are still covered in matrix on most sides and are broken off about half way up their crowns.

For the current study, additional preparation of selected upper jaw and lower jaw teeth was performed by Gilbert Mokgethoa and Charlton Dube of the Evolutionary Studies Institute (ESI), University of the Witwatersrand, Johannesburg, in February and March 2016, to reveal dental marginal cusps and the surfaces of the teeth. On the right upper jaw, the labial and lingual surfaces of the third premaxillary tooth and the first maxillary tooth were prepared. On the right mandible, the labial and lingual surfaces of the fifth and sixth teeth were prepared.

### 2.2.5 Suture identification methods

The cranial sutures are easily visible on this skull, as dark grey interdigitating crisscross or "zig zag" lines. As with the holotype skull of *Embrithosaurus*, previous workers at the Iziko South African museum in Cape Town, have "drawn on" sutures directly on the bone (in white ink) on the external skull surface. My interpretation of the sutural contacts is in agreement with these "drawn on" sutures of previous workers.

### 2.2.6 Distortions

The skull of *Nochelesaurus* is severely dorsoventrally crushed such that the sharp edge between the dorsal skull table and the lateral cheeks has been greatly flattened. This distortion has lowered and widened the snout and skull. It has also flattened the preserved right lateral cheek, decreasing the external angle created between the dorsal skull table and lateral cheek.

This distortion has also bucked the right maxilla, such that it juts out noticeably from the side of the face, giving the false impression of a maxillary boss. On the inside of the skull, this distortion has also flattened and displaced anteriorly the preserved partial right quadrate.

### 2.2.7 Preparation *Bradysaurus baini* NHMUK R1971:

According to Seeley (1892) the fragments of the holotype skull of *Bradysaurus baini*, NHMUK R1971 were transported from South Africa in late 1889 and re-assembled by himself at the Natural History Museum, London, by Christmas of that year. The matrix was removed by Mr Richard Hall, an assistant mason of the Geological department of the museum in January 1890 (Seeley 1892). The preparation of the dorsal and lateral surfaces of the skull is essentially complete, with all elements and cranial bosses very well exposed. Strong, long rugose radiating rows or ridges, parallel ridges and circular pits are clearly visible due to the good preparation, especially on the lateral cheek and dorsal skull roof regions. Very thin and tiny stripes of remaining uncleared matrix appear brown/green in colour.

The palate is generally well prepared, except for the medial and lateral rows of palatal teeth which are still embedded in matrix, creating the appearance of very high raised ridges of bone. This matrix has probably been left in place in order to protect the fragile, long, and thin palatal teeth.

### 2.2.8 Suture identification

Despite the excellent preparation of the skull, external dorsal skull table and lateral cranial sutures are not discernible, as the dark grey to black appearance of the bone and the heavy ornamentation of the skull obscures most sutures, which are also dark coloured. Exceptions include certain of the lateral cheek sutures

between the quadratojugal and jugal, and jugal and postorbital. Internal sutures are relatively easily identifiable, but most are covered by the still tightly occluded palate, braincase, quadrates and paroccipital processes of the opisthotics.

### 2.2.9 Distortions

An obvious posterior displacement affects the right side of the skull, such that the right external naris, orbits and posterior edges of the skull are displaced posteriorly. The right side of the skull also appears to suffer from slight dorsoventral crushing. The skull junction between the flat dorsal skull table and the left lateral cheek is very distinct and forms a large, thick, overhanging swelling. In contrast, the right skull junction forms a smoother curved edge, possibly as a result of the slight dorsoventral downwards distortion of the right side of the skull.

### 2.2.10 Preparation *Bradysaurus seeleyi* NHMUK 49426:

According to Seeley (1888) specimen NHMUK 49426 was prepared by the masons in the British Museum in 1879 or 1880 under the supervision of Mr William Davies. The skull is not very well prepared. The left lateral cheek surface has a thin layer of the light brown/orange concretion covering and obscuring much of the extrenal surface. The right lateral cheek is better exposed, but is badly weathered. The dorsal skull table is also badly weathered where dark brown matrix has not been cleared out of the depressions between the rugose lines.

On the ventral palate, the preparation is also very poor. All palatal teeth are unprepared and deeply encased in light grey coloured uncleared matrix, with the broken off crowns of some of the palatal teeth visibly protruding out of the matrix. The vomer, pterygoid, palatine and ectopterygoids are badly prepared on

the ventral surface. However, the dorsal surface of the vomer, pterygoid, palatine and ectopterygoids are much better prepared and almost completely free of matrix.

### 2.2.11 Suture identification

Due to the weathered and eroded nature of the external surfaces of the bones of the skull, cranial sutures are discernible relatively easily on the dorsal skull table. The dorsal sutures appear as darker-coloured brown filled in “zig zagging” cracks amongst the lighter white/grey bone.

On lateral side of the right cheek dorsoventral compression and weathering have caused individual elements to shift apart along their sutural contacts, leaving long and thin cracks and gaps with some plaster filled in along the sutures. On the left cheek, deposits of brown/orange concretion obscure most sutures. Some sutures are also discernible, on the medial surfaces of the skull. Since the palate and braincase elements are still attached to the inner skull roof, access to this portion of the skull is not possible.

### 2.2.12 Distortions

The skull of *Bradysaurus seeleyi* is severely dorsoventrally crushed, with the dorsal skull table pushed down and positioned well below the tops of each lateral supratemporal boss or supratemporal edges. The right side is more ventrally compressed than the left side. In left lateral view the orbit is flattened and horizontally elongated.

Despite dorsoventral crushing, the lateral cheeks are not flattened outwards, as is usually seen in specimens with this deformation, but are almost vertical when viewed occipitally (Fig. 4.14). It appears that the lateral cheeks have been crushed vertically downwards and flattened, and the bottom of the left cheek is

not straight but is bent inwards. The right cheek is straight, but has been reattached to the skull with plaster and has been attached higher than it should be (as shown by the misalignment and gap between the broken portions of the right squamosal that should fit together). The right cheek has also been oriented too vertically upright.

## 2.3 Abbreviations:

### 2.3.1 Institutional abbreviations

**AM,** Albany Museum, Grahamstown; **BPI**, Evolutionary Studies Institute, University of the Witwatersrand, Johannesburg (formerly the Bernard Price Institute for Palaeontological Research); **CGP,** Council for Geosciences, Pretoria; **NHMUK,** Natural History Museum of London, United Kingdom; **NMQR,** National Museum, Bloemfontein; **SAM,** Iziko South African Museum, Cape Town; **TM,** Ditsong National Museum of Natural History (formerly Transvaal Museum, Northern Flagship Institution), Pretoria; **UMZC,** University Museum of Zoology, Cambridge, United Kingdom; **VW,** Victoria West Regional Museum, Victoria West.

### 2.3.2 Anatomical abbreviations

**aam**, area articularis mandibularis; **ab**, angular boss; **af**, adductor fossa; **Ang**, angular; **Art**, articular; **Bo**, basioccipital; **Bs**, basisphenoid; **bt**, tubera basispheniodales (basal tubera); **btp,** basipterygoid process; **cd**, crista dentalis; **cs**, crista supraoccipitalis; **Cor**, coronoid; **cp**, cultriform process; **D**, dentary; **dnp**, descending nasal process; **Ect**, ectopterygoid; **Ept**, epipterygoid; **Exo**, exoccipital; **F,** frontal; **fdm**, foramen dentofaciale majus; **fic**, foramen intermandibularis caudalis; **fim,** foramen intermandibularis medius; **fm**, foramen magnum; **fo**, fenestra ovalis; **for,** foramen orbitonasale; **fpp**, foramen palatinum posterius

(suborbital vacuity); **itv**, interpterygoid vacuity; **J,** jugal; **jf**, jugular foramen; **Lac**, lacrimal; **mb**, maxillary boss; **mf**, maxillary foramen; **Mx**, maxilla; **N**, nasal; **oc**, occipital condyle; **Op**, opisthotic; **P**, parietal; **Pal**, palatine; **pf,** pineal foramen; **Pm**, premaxilla; **Po**, postorbital; **Pof**, postfrontal; **Pp**, postparietal; **ppf,** prepalatal foramen; **Pra**, prearticular; **Prf**, prefrontal; **Pro**, prootic; **Pt**, pterygoid; **pw,** pterygoid wing; **Q**, quadrate; **qf**, quadrate foramen; **Qj**, quadratojugal; **So,** supraoccipital; **Sph**, sphenethmoid; **Spl**, splenial; **Sq,** squamosal; **St**, supratemporal; **Sur,** surangular; **V**, vomer.

# CHAPTER THREE: RESULTS: DESCRIPTION

The main purpose of this dissertation is to provide a comprehensive description of the cranial morphology of *Embrithosaurus schwarzi* based largely on the holotype which has undergone additional preparation.

## 3.1 Systematic Palaeontology

REPTILIA Linnaeus, 1758

ORDER: PARAREPTILIA Olsen, 1947

SUBORDER: PAREIASAURIA Seeley, 1888

FAMILY: PAREIASAURIDAE Cope, 1896

GENUS: *EMBRITHOSAURUS* Watson, 1914

TYPE SPECIES: *Embrithosaurus schwarzi* Watson, 1914 (SAM-PK-8034)

## 3.2 Cranial Description

### 3.2.1 Skull Roof

**General Comments**

Directional terms used. Wide, broad and narrow indicates the mediolateral or transverse direction. Long and short indicates the anteropostero or longitudinal direction. High, tall and low indicates the dorsoventral direction. The skull is roughly triangular in dorsal view with the circular orbits facing laterally. The snout appears pointed, but this is due to mediolateral compression, and is infact wider than high if undistorted (Appendix A, B). The cheeks appear wider than

they would have been in their natural position due to dorsoventral crushing. Right twisting of the midline of the skull has badly affected the symmetry of the skull in dorsal view. In lateral view, the cheeks extend far below the level of the tooth row and cover the posterior half of the lower jaw.

The pareiasaurian skull roof consists of three distinct regions: a) a dorsally oriented, flat central skull table, b) the laterally oriented facial regions on the front half of the skull, and c) the laterally oriented cheek regions on the back half of the skull. The skull table comprises the nasals, frontals, parietals, postparietal, supratemporals, postfrontals, and the dorsal parts of prefrontals, and postorbitals. The cheek region includes the quadratojugals, squamosals, jugals and the ventral part of the postorbitals. The facial regions house the premaxilla, lacrimals, maxilla, and the ventral part of the prefrontals.

The skull table is bounded laterally by a longitudinal ridge, extending the entire length of the skull, which creates a distinct sharp edge and distinguishes the dorsal skull table from the lateral facial and cheek regions on the side of the skull. Anteriorly, between the external naris and the orbit, the longitudinal ridge is formed by the prominent nasal bosses; two anterodorsal orbital marginal bosses of the prefrontal, and the postfrontal boss. Posteriorly, between the orbit and the back of the skull, the ridge is formed by the postorbital bosses, continuing posteriorly as a thickened ridge with an overhanging ledge, on the most dorsal portion of the squamosal.

Dorsally, a large proportion of the right supratemporal, including the entire large supratemporal boss, is not preserved. Most of the left supratemporal is present, except for a part of the supratemporal boss, which is broken off near its base. The right lateral posterior border boss of the postparietal is not preserved, but the left is. Laterally, on both sides of the skull, large portions of the jugal below the orbit are not preserved.

The external surfaces of the skull roofing elements are heavily ornamented with bosses, rugose ridges, furrows between the ridges and small circular pits. Most

bones house one main boss near the centre of the bone with or without additional smaller bosses present. Most bosses are wide, low, bulbous, and often indistinct, but a few are small, pointed and distinct. In particular, the multiple lateral cheek bosses on the jugals and quadratojugals are very distinct, and dorsally the nasals and prefrontals also carry numerous distinct bosses. Regularly spaced, rugose ridges with associated small circular pits in the furrows between the ridges radiate outwards from the centre of most large central bosses. These rugose ridges are prominent on the nasals, frontals, and parietals, where they radiate out from each central boss, creating a radial pattern of straight, regular rugose lines. Rugose ridges are also prominent on the lateral cheeks, where in lateral view they form three areas of straight, parallel ridges: vertical, horizontal and obliquely directed, crossing the squamosal, jugal and quadratojugal. The small circular pits are more prominent on the lateral cheek regions than on the dorsal skull table. In contrast internal surfaces of the skull roof bones are relatively smooth and lack ornamentation.

External cranial sutures of the skull roof are mostly difficult to trace out due to the heavy ornamentation. Sutural contacts were easier to recognise on internal bone surfaces and these were used for the majority of sutural contact interpretations of the skull roof.

The skull roof features three important openings: the large external naris at the anterior tip of the snout separated medially by the internarial bar, which is mostly not preserved, and surrounded by the nasal, lacrimal and maxilla laterally; the large circular orbits surrounded by the jugal, lacrimal, prefrontal, postfrontal, and postorbital; and the pineal foramen between the parietals.

**Premaxilla** (Figs. 3.1, 3.2, 3.3, 3.6, 3.8, 3.9, 3.29)

The premaxilla is a relatively small bone located at the anterior tip of the snout, and has a midline sutural contact with its contralateral element. It is an

unornamented bone that forms part of the medial and ventral margin of the external naris and includes a thin horizontal palatal flange or ledge on the inside of the skull that forms part of the palate. On the inside of the skull, the palatal flange of the premaxilla sutures with the maxilla laterally, and the vomer posteriorly.

The midline suture and the long oblique suture with the maxilla are clearly visible on the tip of the snout and on both sides of the external skull surface (Figs. 3.1, 3.3, 3.6, 3.10). The internal suture with the vomer on the palatal flange of the premaxilla is identifiable on the right side only (Fig. 3.6) and dorsal contacts with the nasal on the internarial bar, are not preserved (Fig. 3.29).

Most of the internarial bar, and therefore the tip of the snout, is not preserved and a longitudinally expanded oval break (2 x 4 cm) marks the point where the bar was anchored on the premaxilla (Figs. 3.1, 3.3, 3.6, 3.10). In lateral view (Figs. 3.2, 3.3), the orientation of the missing internarial bar and therefore the tip of the snout, is observed as leaning posterodorsally from the anchorage point on the premaxilla to the dorsal descending process of the nasal. This orientation is false and is created by the backwards displacement or distortion of the skull table. The orientation of the internarial bar would be vertical or only slightly posterodorsally if undistorted.

The premaxilla comprises a wide, flat, vertical plate-like structure, with its broadest surface facing anteriorly, which extends posterolaterally to contact the maxilla. The dorsal margin of the premaxilla forms a horizontally oriented border to the ventral portion of the external naris. The posterior margin of the premaxilla forms a sutural contact with the anterior margin of the maxilla. This suture extends posterodorsally from its origin on the alveolar margin (Figs. 3.8, 3.10).

In ventral view, along the midline of the skull and immediately posterior to the internarial bar, a thin horizontal palatal flange of the premaxilla extends posteriorly for a short distance to form part of the anterolateral margin of the

internal naris. This flange is in a plane well above the level of the tooth row, and contacts the vomer posteriorly. The single medial prepalatal foramen is located at the midline contact between the premaxillae and anteriorly to the vomers (Figs. 3.1, 3.6).

Along the tooth row, the sutural contact with the maxilla reveals that the premaxilla carries three marginal teeth. This contradicts Boonstra (1934a) who stated that all pareiasaurs possess two premaxillary teeth, and instead supports Lee's (1997a) contention that all pareiasaurs possess three premaxillary teeth.

**Maxilla** (Figs. 3.1, 3.2, 3.3, 3.4, 3.6, 3.7, 3.8, 3.10, 3.11, 3.13, 3.16, 3.17)

The maxilla is a large bone forming most of the side of the face. It comprises primarily a wide, curved, vertical plate and a smaller, thin, horizontal palatal flange on the inside of the skull that forms part of the palate. The maxilla has sutural contact with the premaxilla anteriorly, the lacrimal dorsally, the jugal posterodorsally, and is precluded from contributing to the orbital margin by the lacrimal and the jugal. The sutural contact with the jugal is most clearly visible on the left external surface (Fig. 3.8). Also on the same side, the sutures between the maxilla and lacrimal are revealed on the internal surface only (Fig. 3.17). Posteriorly, the maxilla extends far beyond the level of the anterior margin of the orbit.

In dorsal view, the anterior margin of the maxilla is strongly convex and the anterior margin is slightly concave just before the level of the anterior margin of the orbit**.** In anterior view, the maxilla sutures with the premaxilla below the external naris and forms the lateral portion of the floor and most of the lateral border of the external naris (Fig. 3.1, 3.6).

In lateral view, the maxilla is highest anteriorly, making up part of the posterior border of the external naris, and tapers posteriorly. A relatively small but distinct maxillary boss is present immediately behind the external naris just below the

sutural contact with the lacrimal (Figs. 3.2, 3.3, 3.16)**.** This is the "maxilla lump" used by Lee (1997a) to distinguish *Bradysaurus baini* from all other *Tapinocephalus* Assemblage Zone pareiasaurs as it is massively developed in *B.baini*. It is weakly developed in SAM-PK-8034, but more identifiable on the left side of the skull (Figs. 3.2, 3.16) as it has been eroded on the right (Fig. 3.3)**.** Some distance below the boss, a single large anterolateral maxillary foramen (mf) is present above and slightly behind the level of the sixth tooth from the front**.** A long, shallow and horizontally oriented groove is present on the maxilla, extending just above the tooth row between the anterolateral maxillary foramen and the anterior margin of the orbit (Figs. 3.2, 3.3, 3.8, 3.10).

In dorsal view, on the internal surface of the skull, the maxillary palatal flange forms part of the anterolateral margin of the internal naris and sutures with the palatal flange of the premaxilla. Posteriorly, the flange sutures with the palatine and ectopterygoid as can be best seen on the well preserved internal right side (Fig. 3.6). This maxillary palatal flange is well above the level of the tooth row and extends posteriorly onto palatine flange.

As the area below each orbit is not preserved, the posterior limit of the maxilla cannot be seen and it is thus not possible to confirm the maxilla-quadratojugal contact. Lee (1997a) notes the maxilla-quadratojugal contact as a synapomorphy of all pareiasaurs. In SAM-PK-8034 it cannot be confirmed, but is assumed to be present.

The external surface of the maxilla is predominately smooth and unornamented, apart from the maxillary boss and the horizontal groove above the tooth row.

**Septomaxilla**

As in most pareiasaurs, no septomaxilla could be identified. Tsuji *et al.* (2013) suggest that the single report of a septomaxilla in *Anthodon* by Boonstra (1934a)

as a probable misidentification, and contends that the septomaxilla has probably been lost in pareiasaurs.

**Lacrimal** (Figs. 3.1, 3.2, 3.3, 3.8, 3.12, 3.13, 3.16, 3.17)

The lacrimal is a small, curved, vaguely diamond-shaped bone that forms the posterodorsal side of the face. The bone has an anteroventrally curved suture with the maxilla, a posteroventrally short suture with the jugal, an anterodorsal suture with the nasal and a posterodorsal suture with the prefrontal.

Sutural contacts with the nasal and prefrontal are most clearly visible on the internal surface on the left side of the skull (Fig. 3.17). The inner margin of the left orbit shows the sutural contact between the lacrimal and the prefrontal's descending flange (Figs. 3.2, 3.17).

In lateral view, the lacrimals anterior margin forms a small portion of the posterodorsal margin of the external naris, and its posterior margin makes up most of the anterior margin of the orbit (Figs. 3.2, 3.3). A large, distinct boss is present near the centre of the lacrimal and is surrounded by a complex of four smaller bosses or short rugose protuberances close to the main lacrimal boss. The complex as a whole is oriented posterodorsally, with two of the surrounding protuberances located anteroventrally and the other two posterodorsally to the central main lacrimal boss (Fig. 3.16).

The internal surface of the lacrimal is smooth, except for a small indentation that occurs in the middle of the bone, directly underneath the main central boss of the external surface (Fig. 3.17).

**Prefrontal** (Figs. 3.1, 3.2, 3.3, 3.12, 3.13, 3.16, 3.17)

The prefrontal is a large, roughly rectangular bone, located on the anterodorsal edge of the orbit. Most of the bone forms part of the dorsal skull table with only a small portion forming part of the lateral side of the face.

Dorsally it has short transverse sutures with the lacrimal anteriorly and the postfrontal posteriorly, and longer, curved sutures with the nasal anteromedially and the frontal posteromedially (Figs. 3.1, 3.12). Both sides of the internal surfaces of the skull reveal sutures with the nasal and frontal (Fig. 3.13). The left side of the external surface shows that these sutures with the nasal and frontal occur along the medial edge of a circular bowl-shaped depression.

The internal surface along the anterodorsal orbital margin reveals the long, thin, and curved descending flange of the prefrontal which is a wedge shaped ventrally tapering extension (Figs. 3.16, 3.17). It is widest dorsally and narrows ventrally. Laterally, the descending flange of the prefrontal, along the anterior orbital margin is not visible in right lateral view as it is covered by the lacrimal (Fig, 3.3), but is visible in left lateral view in the anterior orbital margin (Figs. 3.2, 3.4, 3.16, 3.17).

The descending flange of the prefrontal reaches the foramen orbitonasale or lateral nasal fenestra at the base of the antorbital buttress (Fig. 3.13). This foramen is located at the confluence of the prefrontal, the lacrimal, the palatine, and the jugal (Fig. 3.13).

The prefrontal bears three small, very distinct, pointed bosses: two longitudinal larger bosses on the anterodorsal orbital border, forming part of the ridge that separates the dorsal skull table from the lateral side of the face; and a third smaller boss located anteromedial to the most anterior orbital boss that nearly reaches the anteromedial edge of the bone (Figs. 3.1, 3.12). A wide, bowl-shaped depression is located medial to the two larger orbital marginal bosses and posterior to the third smaller boss. The medial curved, raised edge of this

depression marks the sutures between the prefrontal and frontal bones and is demarcated by a ring of raised bone on the frontal.

The internal bone surfaces of the prefrontal on both sides are smooth but reveal a circular swelling, demarcated by ridges of raised or slightly shifted bone. The edges of this circular swelling mark the prefrontal-frontal and prefrontal-nasal sutural contacts.

**Postfrontal** (Figs. 3.1, 3.2, 3.3, 3.12, 3.13, 3.14, 3.15)

The postfrontal is a small, curved bone located on the dorsal skull table, forming the central dorsal edge of the orbital margin. In dorsal view, the bone is roughly rectangular. It has a short transverse suture with the prefrontal anteriorly, a longitudinal suture with the fontal anteromedially, a short suture with the parietal posteromedially, and a transverse suture with the postorbital posteriorly (Figs. 3.1, 3.12).

On the external surface the sutures of the left postfrontal with the frontal and prefrontal can be seen (Figs. 3.1, 3.12) and on the internal surface, the sutures of the right postfrontal with all its neighbours are obvious (Fig 3.13). On the left internal surface only the suture with the parietal and postorbital can be clearly seen (Fig 3.15).

In lateral view, the triangular postfrontal is wedged between the prefrontal and postorbital, decreasing in width ventrally with the result that is makes up only a very small portion of the dorsal orbital margin. The suture with the prefrontal occurs anterior to the dorsal midpoint of the orbit, and the suture with the postorbital occurs posterior to the dorsal midpoint of the orbit (Figs. 3.2, 3.3). The postfrontal differs in shape when viewed externally (Fig. 3.12) compared to internally (Fig. 3.13). On the internal surface, the postfrontal is mediolaterally widened, approximately twice as wide as long (Fig 3.13). Conversally, on the

dorsal skull surface, the postfrontal is longitudinally elongated, approximately twice as long as wide (Figs. 3.1, 3.12).

The postfrontal bears a single large, wide and low boss over most of its external surface, which covers the dorsal orbital margin (Figs. 3.1, 3.2, 3.3, 3.12). This boss forms part of the ridge that separates the dorsal skull table from the lateral side of the skull. The postfrontal boss continues medially almost unabated onto the frontal, being confluent with the frontal's large, wide posterolateral boss (Figs. 3.1, 3.12). The postfrontal and frontal are separated by an indistinct, shallow longitudinal trough, which is more easily identified on the left external skull surface. The internal surface of the postfrontal is smooth and featureless.

**Postorbital** (Figs. 3.1, 3.2, 3.3, 3.12, 3.13, 3.14, 3.15, 3.18, 3.19)

The large postorbital forms most of the posterodorsal orbital margin. The bone consists of two roughly equal plates; a horizontally flat dorsal portion forming part of the dorsal skull table, and a vertically orientated lateral portion forming part of the cheeks of the skull.

In dorsal view the bone is roughly pentagonal. It has a short transverse sutural contact with the postfrontal anteriorly and the supratemporal posteriorly, and a longitudinal suture with the parietal medially (Figs.3.1, 3.12, 3.13). In lateral view, it has a vertical suture with the squamosal posteriorly, and a horizontal suture with the jugal ventrally (Figs. 3.1, 3.2). All sutural contacts between the postorbital and its neighbours are clear on the internal surface of the left cheek and dorsal skull table as raised ridges of bone (Fig. 3.15).

On the skull table, along the orbital margin, the postorbital bears two bosses that form part of the junction of the dorsal skull table and the lateral cheek: a medium-sized, wide, poorly defined boss above the posterodorsal orbital margin and a smaller wide, low and indistinct boss lower down on the posterior orbital

margin (Fig. 3.14). These two orbital bosses contribute to a thickened swelling of the posterodorsal orbital margin.

Two parallel raised ridges of bone are present on the posterior portion of the dorsal skull table section of the postorbital (Fig. 3.14). Clear on the left side of the skull, these longitudinally rugose ridges radiate anteriorly from the extremely large supratemporal boss at the back of the skull. Immediately ventral to these two rugose ridges, the postorbital shows a swelling, creating the sharp edge of the cheek (Fig. 3.14). This swelling continues posteriorly onto the squamosal forming a ledge which overlies a very deep horizontal trough (Fig. 3.14). The overhang is larger, and the trough is deeper than it would naturally be as the left cheek is somewhat "tucked in" underneath the dorsal skull table, due to deformation. On the right side, these ridges are not well preserved and only part of the swelling that demarcates the cheek edge is preserved. The internal surface of the postorbital is smooth and featureless.

**Nasal** (Figs. 3.1, 3.2, 3.3, 3.12, 3.13)

The large nasal is roughly rectangular, being longer than wide and located on the anteromedial margin of the dorsal skull table. The bone is slightly convex and the suture along the midline with its contralateral element is visible only on the inner surface (Fig. 3.13).

In dorsal view, the nasal forms the dorsal margin of the external nares and has a long parasagittal suture with the lacrimal laterally. It has a short curved suture with the prefrontal posterolaterally, and a short straight transverse suture with the frontal posteriorly (Figs. 3.1, 3.12). This curved sutural contact with the prefrontals and the straight transverse contact with the frontals are identifiable internally (Fig. 3.13).

Anteriorly, only a very small section of the lateral descending nasal processes are preserved as short extensions forming the dorsal most portion, and only

preserved section, of the internarial bar. These short extensions either side of the midline make up the dorsomedial corner margin of the external naris and are best viewed internally (Fig. 3.13). This small preserved section of the bar is posterodorsally orientated and would maintain its orientation ventrally to meet the broken off anchorage point of the bar on the premaxilla (Figs. 3.1, 3.6). However, the posterodorsally orientation is due to the dorsoventral crushing and slight posterior displacement of the skull, and the bar would likely have been vertically or only slightly posterodorsally oriented in its natural position, producing a blunt snout appearance in lateral view, as recorded in all other *Tapinocephalus* Assemblage Zone pareiasaurs (Lee 1995, Lee 1997a, Jalil and Janvier 2005, Tsuji *et al.* 2013, Turner *et al.* 2015).

In dorsal view, the nasal has a large, prominent, longitudinally elongated, oval boss near the centre of the bone, above the external naris, which converges slightly anteriorly towards the midline. Three smaller elongated protuberances (rugose ridges), radiate from the main central boss to nearly reach the edge of the bone: one laterally and slightly anteriorly oriented emanating from the lateral side, one posteriorly oriented emanating from the posterior side, and one posteromedially oriented emanating from the medial side (Figs. 3.1, 3.12).

On the internal surface, directly below each main nasal boss, is a long, sharp, raised parasagital ridge. This ridge is thickest anteriorly and tapers posteriorly, converging slightly medially towards the midline of the skull, before disappearing into the smooth posterior surface, well before the suture with the frontal is reached (Fig. 3.13).

**Frontal** (Figs. 3.1, 3.2, 3.12, 3.13)

The frontal is a large, roughly rectangular bone, being longer than wide, located on the anterior half of the dorsal skull table. In dorsal view, it meets its contralateral element with a midline sutural contact and has a short straight

transverse suture with the nasal anteriorly. It has a short curved parasagittal suture with the prefrontal anterolaterally and a parasagittal suture with the postfrontal posterolaterally. The bone has a straight transverse suture with the parietal posteriorly, which is identifiable internally on the right side of the skull (Fig. 3.13).

The frontal has a large, low, wide boss posterolaterally which is a continuation of the central boss of the postfrontal (Figs. 3.1, 3.12). In lateral view, this main frontal boss is in line with the vertical centre of the orbit (Fig. 3.2). A separate, smaller boss or tubercle is positioned in the centre of the frontal, located anteromedially to the main frontal boss (Figs. 3.1, 3.12). Rugose radial ridges emanate from the smaller boss at the centre of each frontal and not from the larger posterolateral boss. Anterolaterally, these rugose ridges terminate along the contact with the prefrontal and anteriorly, along the contact with the nasal.

The internal surface of the frontal is smooth apart from a short, sharp and distinct parasagittal ridge (Fig. 3.13). Immediately posterior to this ridge the frontals contact the anterior half of the cylindrical shaped sphenethmoid bone.

**Parietal** (Figs. 3.1, 3.2, 3.3, 3.12, 3.13, 3.14, 3.15)

The parietal is a large approximately square bone which is slightly longer than wide, and is located on the posterior half of the dorsal skull table. It meets its contralateral element with a midline sutural contact, visible on the external surface only. The medial half of the parietal is flat and the lateral half is slightly convex.

The parietal contacts the frontal with a straight transverse suture anteriorly. It has a short suture with the postfrontal anterolaterally, and a longitudinal suture with the postorbital laterally. It has a curved suture with the supratemporal posterolaterally and a straight transverse suture with the postparietal posteriorly (Figs. 3.1, 3.12). Sutural contacts with the supratemporal and postparietal can

only be seen on the inner surfaces of the right side of the dorsal skull table (Fig. 3.13) and on the inner surface of the left cheek (Fig 3.15).

A wide, low and very indistinct boss in the centre of the right parietal is surrounded by a few small circular pits, and indistinct radial rugose ridges. The corresponding area on the left parietal is not preserved (Fig. 3.12) and has been filled in with Pratley Putty (TM) during the cranial reconstruction performed as part of this dissertation.

The pineal foramen (pf) is positioned along the skull midline on the anterior third of the parietals and is enclosed within a slightly raised rim of bone. The foramen is positioned far anteriorly on the parietal, close to the contact with the frontal, yet some distance behind the level of the posterior limit of the orbit. On the dorsal skull surface, the foramen is relatively small (Figs. 3.1, 3.12), but is much larger on the internal skull surface (Fig. 3.13). Externally, it is anteroposteriorly elongated and therefore oval in cross section, consistent with the mediolateral compression of the skull and would have been more circular if undistorted.

On the internal surface, the anterior portion of the parietal has a strong sutural contact with the posterior half of the cylindrical sphenethmoid, and the posterior portion has a contact with the anterior part of the ventral process of the postparietal. Posteriorly, a shallow narrow parietal trough with slightly raised edges on both sides extends from the posterior border of the pineal foramen towards the descending process of the postparietal. This trough is the same width as the pineal foramen but becomes wider posteriorly. Along the anterolateral edges of this trench, the sphenethmoid contacts the ventral surfaces of the parietal with a posterior tapering process (Fig. 3.13).

**Postparietal** (Figs. 3.1, 3.4, 3.5, 3.12, 3.13, 3.14, 3.15)

The postparietal is a large, single, unpaired element. It is a broad and rectangular bone, wider than long, and forms the posteromedial edge the dorsal skull table.

In dorsal view the postparietal has a transverse, but slightly inverted v-shaped suture with the parietals anteriorly, and curved longitudinal sutures with the supratemporals laterally (Figs. 3.1, 3.12). Only a small triangular section of the postparietal is not preserved (Fig. 3.1). The sutures are revealed internally as raised ridges and slightly overlapping bones only on the left side of the skull (Figs. 3.13, 3.15). Sutures were also evident on the sides of the bone fragments before cranial reconstruction, within the small triangular missing section on the left side of the skull, between the postparietal and the left parietal. This section has now been filled in with Pratley Putty (TM) during the cranial reconstruction performed as part of this thesis.

In occipital view, the postparietal is a U-shaped bone, with the middle of the bone positioned at the level of the dorsal skull table and the sides rising sharply laterally towards the supratemporals. On the posterior border of the skull, but somewhat above the posterior edge so as to be placed on the dorsal skull table, a large and distinct oval boss is present on either side, located in the posterolateral corners of the bone (Fig. 3.5). In dorsal view, this boss is present on the posterior border of the skull (Figs. 3.1, 3.12, 3.14). The right boss is broken off near its base (Fig 3.12). In occipital view, the margin of the posterior border of the skull curves downwards to form a thin and sharp edge which slightly overhangs the occiput (Fig. 3.5). This thin edge is slightly swollen to form a small, sharp posteroventrally directed projection, medial to the posterior border boss (Figs. 3.1, 3.5). The inclusion of these posterolateral corner bosses on the postparietal makes the element a very wide and large bone, as is the condition observable in the holotype of *Nochelesaurus* (SAM-PK-6239). The suture between the postparietal and supratemporal extends longitudinally through a slight depression between the postparietal posterior boss and the very large supratemporal boss (Fig 3.14) but can only be observed on the internal skull surface (Fig. 3.15)

In dorsal view, a longitudinally oriented, shallow, wide and very indistinct boss is present on the dorsal skull table on either side of the bone, near its anterolateral corners (Fig. 3.1, 3.12). Medial to both the anterolateral and posterolateral bosses of the postparietal, on either side of the midline is a shallow, narrow, and indistinct longitudinal depression which extends over most of the postparietal to reach the parietal.

On the internal surface, most of the postparietal forms a thickened bar of bone approximately 3 cm wide and 2 cm deep (Fig. 3.13, 3.15). The width of this bar remains consistent as it follows the contour of the posterior edge of the skull. The posterodorsal edge of this bar forms the thin posterior skull margin. This bar continues laterally on both sides of the skull to suture with each supratemporal (Fig. 3.5). Below the level of the thickened bar, the anterior portion of the postparietal is at the general level of the internal skull table.

Internally, along the midline of the skull, a sharp ridge or ventral sagittal process extends a short distance anteriorly from the posterior edge of the postparietal, before developing into a thick triangular ventrally directed process or pillar. This descending process of the postparietal sutures with the dorsal ascending process of the supraocciital (Fig. 3.13).

**Supratemporal** (Figs. 3.1, 3.2, 3.3, 3.4, 3.5, 3.12, 3.13, 3.14, 3.15, 3.18, 3.19, 3.22)

This element has in the past been called a “tabular” by some authors (e.g. Haughton and Boonstra 1929a, Boonstra 1934a). I here consider the large bone on the posterolateral corner of the skull table to be the supratemporal, as maintained by Lee (Lee 1995, 1997a, Lee *et al.* 1997) and Tsuji (Tsuji *et al.* 2013). This bone is large and heavily ornamented, located on the dorsal skull table, and forms the postero-lateral corners of the skull.

In dorsal view the supratemporal has a long, anteroposteriorly oriented suture with the squamosal laterally (Fig. 3.1). Anterolaterally, the supratemporal has a

suture with the postorbital, anteromedially with the parietal, and posteromedially with the postparietal (Fig. 3.12, 3.13, 3.14, 3.15). Sutures between the supratemporal and squamosal are identifiable on the left external skull surface (Fig 3.14). Internally, also on the left of the skull, clear sutures and raised edges of bone are visible showing contacts with the squamosal, postorbital, parietal and postparietal (Fig 3.10). A large section of the posterolateral corner of the right supratemporal is not preserved (Fig. 3.1, 3.3, 3.5).

On the posteromedial corner of the bone, the left supratemporal carries the remnants of a large boss, which is broken off near its base such that its true height cannot be determined (Fig. 3.14). However, it is clear that this boss demarcates the posterolateral corner of the skull and was extremely large and slightly oval in cross section, being transversely slightly wider than its longitudinal length. As with the lateral boss of the postparietal, this boss is located on the dorsal skull table, somewhat above the margin of the posterior border of the skull (Fig. 3.5). The right boss is not preserved as a large section of the right supratemporal is broken off (Fig. 3.1). Two prominent and robust rugose straight ridges extend anteriorly from the boss onto the postorbital (Fig. 3.1), forming a deep trench between these two ridges.

In occipital view, the posterolateral edge of the skull table is thin and slightly overhangs the occiput, from the medial postparietal to the laterally positioned supratemporal (Fig. 3.5).

On the internal surface, the supratemporal forms a thickened bar of bone (about 3 cm wide and 2 cm deep) situated along the posterior edge of the bone. This bar is a continuation from medially positioned postparietal. The left supratemporal shows the bar forming a thick flange, medially directed and vertically oriented, which has a blunt dorsal contact with the distal end of the paroccipital process of the opisthotic (Fig. 3.15) and ventrally a horizontal suture with the squamosal. On the left side of the skull, the inner surface of the supratemporal bar reveals

the horizontal suture between the supratemporal and the squamosal (Fig. 3.15) which is normally covered by the blunt contact with the paroccipital process of the opisthotic. This suture is only visible because the left distal end of the paroccipital process of the opisthotic is detached from the supratemporal-squamosal contact. On the right supratemporal, a large piece of the supratemporal bar is broken off and is attached to the paroccipital process of the opisthotic (Fig. 3.22).

Internally, median to the thickened bar, the supratemporal comprises a large portion of flat smooth featureless bone that is at the general level of the internal skull table (Fig. 3.15).

**Squamosal** (Fig. 3.1, 3.2, 3.3, 3.4, 3.5, 3.12, 3.13, 3.14, 3.15, 3.18, 3.19, 3.22, 3.24, 3.25, 3.26)

The squamosal is a large flat bone, located on the lateral side of the skull. The bone forms the posterodorsal margin of the cheek and has a long and narrow horizontal portion contributing to the dorsal skull table. The external surface is heavily ornamented with deep rugose ridges and surrounding small circular pits. A large triangular section of bone is missing from the anterior portion of the left squamosal, filled with dark grey plaster infill and covered by a small rectangular metal plate (Fig. 3.14).

In lateral view, the squamosal has a long straight horizontal sutural contact with the supratemporal dorsally, which occurs some distance above the ventral edge of the overhanging swelling that separates the dorsal skull table from the lateral cheeks (Fig. 3.14). This thick, cheek edge swelling, is a continuation from the anteriorly positioned postorbital and overlies a deep horizontal trough which dissipates posteriorly. The squamosal therefore forms the posterior part of the lateral cheek from which the postorbital forms the anterior part. Anterodorsally, the squamosal has a posterodorsally oriented vertical sutural contact with the

postorbital, anteroventrally it has a short suture with the jugal, and ventrally a long straight horizontal suture with the quadratojugal (Fig. 3.15).

All sutural contacts between the squamosal and its neighbours are clear on the internal surface of the left cheek as raised ridges of bone, with the suture to the quadratojugal identifiable on the external surface (Fig. 3.15).

In lateral view the squamosal houses two, large, rounded bosses on its posterior edge (Figs. 3.14, 3.18). These two bosses are different in their orientation and shape. The dorsal portion of the bone houses a smaller less distinct boss, which extends dorsally onto the supratemporal. This dorsal squamosal boss is flat, vertically oriented and faces posteriorly. A larger boss is on the central and ventral portion of the squamosal's posterior edge. This boss is oval in cross section and is longer in the vertical plane. On the lateral cheek surface, the top section of this boss extends rurther anteriorly than any of other bosses on the posterior edge of the quadratojugal. In occipital view, this ventral squamosal boss is "splayed" outwards and is best seen on the right of the skull (Fig. 3.5). This orientation is maintained by the most dorsal posterior cheek boss of the quadratojugal. Unlike most of the bones of the skull, the lateral surface of the squamosal does not have a large central boss, or a complex of smaller bosses near the centre of the bone. The lateral surface of the squamosal has straight rugose parallel ridges, emanating in two directions: vertical ridges in the posterior half of the bone that continue ventrally onto the quadratojugal and oblique ridges in the anterior half of the bone that continue anteriorly onto the jugal.

On the posterior edge of the cheek, at the squamosal-quadratojugal contact, is a broad, shallow, weekly developed indentation, referred to a remnant of the otic notch or temporal emargination (Figs. 3.2, 3.3, 3.14, 3.15, 3.18, 3.19).

In occipital view, the posterodorsal margin of the cheek on the squamosal is thin and is a ventral continuation of the posterior skull margin from the supratemporal. This thin edge dissipates between the two posterior squamosal

bosses. Below this, the bone expands greatly in robustness on the squamosal continuing onto the quadratojugal, where it attains a width of approximately three times the width of the posterior cheek margin of the dorsal portion of the squamosal (Fig. 3.5).

On the internal surface, the left squamosal has a medially directed, vertically oriented blunt contact with the distal end of the paroccipital process of the opisthotic (Fig. 3.15). A small piece of the left squamosal is broken off and is attached to the paroccipital process of the opisthotic (Figs. 3.22, 3.24). A large piece of the right squamosal is also broken off and is attached to the paroccipital process of the opisthotic (Fig. 3.22). Below the blunt contact with the opisthotic, the squamosal tapers to a thin vertical medial flange which contacts the lateral margin of the vertical ramus of the quadrate (Fig. 3.15).

**Quadratojugal** (Figs. 3.1, 3.2, 3.3, 3.4, 3.5, 3.14, 3.15, 3.18, 3.19, 3.25, 3.26)

The quadratojugal is a large, flat bone, located posteroventrolaterally on skull. The bone forms the ventral border of the lateral cheek and the ventral part of the posterior margin of the cheek. The lateral external surface is massively ornamented with numerous medium-sized distinct bosses, and small circular pits within deep rugose furrows (Figs. 3.14, 3.18).

In lateral view, the quadratojugal shares a long straight horizontal dorsal suture with the squamosal. Anteriorly, it has a curved suture with the jugal (Figs. 3.14, 3.18). The anterior portions of both quadratojugals are not preserved, making it impossible to determine whether the quadratojugal meets the maxilla (Figs. 3.2, 3.3). Sutural contacts of the quadratojugal with the squamosal and jugal are well exposed on the external and internal surfaces of both cheeks (Figs. 3.14, 3.15, 3.18, 3.19). Externally, the curved contact with the jugal is observed in a long and narrow, deep trench or embayment.

On the lateral side of the cheek, anterior to the posterior cheek margin, the quadratojugal houses a complex of two bosses (Figs. 3.14, 3.18). These occur in a curved arc that is obliquely oriented, following the curvature of the posteroventral edge of the cheek corner. It comprises a small, weakly developed dorsal boss, followed ventrally by a large, longer and curved boss. These two bosses are oval in cross section, are elongated and curved in the direction of the curved arc.

Arrangement of these lateral bosses on the quadratojugal is asymmetrical on either side of the skull. On the right lateral cheek, the arrangement is simple, consisting only of the smaller dorsal boss and the larger ventral curved boss, both of which are very distinct (Figs. 3.3, 3.18). On the left lateral cheek, the smaller dorsal boss is present, but the large ventral boss is much larger, longer and extends anteriorly much further than on the right cheek (Figs. 3.2, 3.14). Above the large, curved, ventral corner boss is a strong, distinct, horizontal rugose ridge emanating forward, and above this rugosity a deep horizontal embayment in which the suture with the jugal occurs, is present. The large, curved, ventral corner boss and the rugose ridge create the appearance of two to three indistinct, posterodorsally orientated, and elongated curved protuberances or rugose ridges creating a general thick swelling of the lower half of the quadratojugal of the left cheek.

The lateral surface of the quadratojugal has rugose parallel ridges, emanating in two directions: vertical rugose ridges located posteriorly emanating down from the lateral surface of the squamosal, and horizontal ridges that reach anteriorly onto the jugal. Small deep circular pits are present between the lateral cheek bosses and rugosity, which are best preserved on the right cheek.

On the posterior edge of the cheek, the quadratojugal houses four very large but low, bulbous bosses (Figs. 3.14, 3.18). The most dorsally located boss is the largest and most bulbous and is splayed posterolaterally, as can be seen in occipital view on the right of the skull (Fig. 3.5). (On the left side of the skull, the

dorsal quadratojugal posterior cheek edge boss appears vertically oriented and facing posteriorly, but this is probably due to distortion and poor preservation). The remaining three ventral bosses are vertically oriented and face posteriorly, on both sides of the skull.

The arrangement of the corner boss on the posterior edge of the quadratojugal is asymmetrical. On the left cheek, the corner or angle boss is very distinct, pointed and "teat" shaped (Figs. 3.2, 3.14). On the right cheek, the corner or angle of the cheek consists of two very close bulbous bosses which are indistinct and almost appear as one large boss. One is ventrally directed and appears to reach anteriorly on the ventral margin of the cheek and the other is posteroventrally directed (Figs. 3.3, 3.18). This right cheek corner double boss arrangement, resulting in the appearance of a boss on the ventral margin of the quadratojugal, is not repeated in any other specimen of *Tapinocephalus* Assemblage Zone pareiasaur studied.

As with the posterior cheek bosses of the squamosal, the cheek bosses of the posterior border of the quadratojugal are best preserved and prepared on the right cheek (Fig. 3.18).

In occipital view, the posterior cheek edge is greatly thickened and is widest dorsally, where several small circular pits are present. As in all pareiasaurs, the quadratojugal is ventolaterally expanded and creates the ventral overhang of the cheek, well past the level of the maxillary tooth row (Fig. 3.5).

Besides the posteroventral corner boss of the cheek, the ventral cheek margin of the quadratojugal does not bear any bosses. However, this ventral cheek margin is not completely straight; but presents a moderate, low, smooth and continuous ventral bulging or convex curvature over the entire length. This ventral cheek bulging is best seen in lateral view (Figs. 3.3, 3.18).

On the dorsal portion of the internal surface of the left quadratojugal the bone tapers to a thin vertical medial flange, which is a continuation of the same

internal flange from the dorsally located squamosal (Fig. 3.15). This quadratojugal medial flange sutures with the lateral margin of the vertical ramus of the quadrate, below the quadrate foramen and is best seen in occpitial view on the right side of the skull (Figs. 3.25, 3.5) Below the quadratojugal flange, the internal surface of the quadratojugal shows a thin horizontal cylindrical ridge which tapers anteriorly (Fig. 3.15). This internal cheek ridge contributes to a cylindrical thickening of the internal ventral cheek margin.

**Jugal** (Figs. 3.1, 3.2, 3.2, 3.4, 3.8, 3.13, 3.14, 3.15, 3.18, 3.19)

The jugal is a flat bone located on the side of the skull. It forms the anteroventral portion of the lateral cheek and the ventral and posteroventral orbital margin. A large section of the left jugal underneath the orbit is missing (Fig. 3.2). The external surface is heavily ornamented with numerous pointed and distinct bosses, and small circular pits within the furrows between deep rugose ridges.

In lateral view, dorsally the bone shares a short straight horizontal suture with the postorbital and posterodorsally a short suture with the squamosal (Figs. 3.2, 3.3). Anterodorsally the jugal has a short suture with the lacrimal, and anteroventrally, a long suture with the maxilla. Posteroventrally it has a long curved suture with the quadratojugal. Laterally, along the orbital margin, the jugal bears a small, wide, low, indistinct boss on the posteroventral orbital margin, above which the horizontal suture between the postorbital and the jugal passes (Fig. 3.3, 3.14).

On the lateral surface, at a level in line with and ahead of the posterior margin of the orbit, the jugal has a complex of two to three small pointed bosses. These bosses are vertically oriented on the left cheek, but oblique on the right (Figs. 3.14, 3.18). Both cheeks are missing sections of the anterior part of the jugal and it is certain that this complex of bosses was obliquely or posterovertically oriented, as in all other *Tapinocephalus* Assemblage Zone pareiasaur specimens

studied. Horizontal and posterodorsal oblique rugose ridges radiate out from these bosses and continue posterodorsally onto the squamosal and horizontally posteriorly onto the quadratojugal. The internal surface of the preserved jugal is smooth and featureless.

### 3.2.2 Palate

**General Comments**

The palate comprises the palatal sections of the premaxilla and maxilla, as well as the vomer, palatine, ectopterygoid, pterygoid, and epipterygoid. The palate forms a flat horizontal plate that is in a plane well above the level of the tooth row or alveolar ridge at the ventral margin of the maxilla. The palatal elements are generally well preserved.

Most of the anteromedial palate (i.e. most of the vomer) is not preserved. The posteromedial section of the palate is preserved on a single large palatal fragment (Fragment F), comprising mostly the pterygoid, but includes small medial portions of the vomers, palatines and epipterygoids. The lateral sections of the palate, i.e. the palatal flanges of the premaxilla and maxilla, and the lateral sections of the palatine and ectopterygoid, are broken off from the single large palatal fragment and are all attached to the premaxilla and maxilla on fragment A.

The palate features three important openings: the very large parallel internal naris or choana separating the lateral maxilla and palatine from the medial premaxilla and vomer, the large oval suborbital vacuity or foramen palatinum posterius between the palatine and ectopterygoid, and the interpterygoid vacuity between the pterygoids and the basisphenoid.

**Vomer** (Figs. 3.1, 3.4, 3.6, 3.20, 3.21)

The vomer is a flat bone forming most of the anterior medial portion of the palate. The central part of the vomer is not preserved, and only small portions of its extreme anterior and the extreme posterior sections are.

Anteriorly, the vomer sutures with the palatal flange of the premaxilla and forms the posterior border of the single medial prepalatal foramen (ppf) (Figs. 3.1, 3.6). Medially, the vomer sutures with its contralateral element along the midline, and laterally it forms the anteromedial border of the choana or internal naris (Fig. 3.6). As the central part of the vomer is not preserved, the shape and structure of the medial borders of the choana or internal naris cannot be determined. The preserved anterior portion of the vomer is somewhat distorted and twisted downwards, but is still in the same plane and level as the preserved premaxillary palatal flange, the maxillary palatal flange and the palatine flange, all being well above the tooth row (Fig. 3.6).

Posteriorly, there are clear sutures of the vomer with the pterygoid medially and the palatine laterally (Figs. 3.20, 3.21). In dorsal view, the posterior section of the vomer has a high narrow median sagittal ridge, which continues posteriorly onto the pterygoid where it widens and becomes more robust (Fig. 3.20).

In ventral view, the posterior vomer, shows two slightly raised, sagittal, lateral ridges (i.e. one either side of the midline). Each ridge carries two parallel rows of small palatal teeth, 1-2 mm in diameter that continue posteriorly onto the pterygoid. The teeth are all broken off at their bases (Fig. 3.21).

**Palatine** (Figs. 3.4, 3.6, 3.9, 3.7, 3.10, 3.11, 3.13, 3.20, 3.21)

The palatine is a long, flat bone forming most of the lateral portion of the anterior half of the palate. Anterolaterally it sutures with the palatal flange of the maxilla, which forms part of the anterolateral margin of the choana**,** with the

palatine forming the lateral (Figs. 3.6, 3.11) and the posterior borders of the choana.

Posteriorly, the palatine sutures with the pterygoid, the vomer medially (Figs. 3.20, 3.21), and the ectopterygoid laterally (Figs. 3.6, 3.9, 3.11). The large, oval and transversely elongated foramen palatinum posterius (fpp) or suborbital vacuity, is located on the suture between the palatine and the ectopterygoid (Fig. 3.6). The palatine-ectopterygoid suture is best seen on the right side of the dorsal surface of the palate (Fig. 3.6). The palatine-pterygoid curved posteromedial sutural contacts are clearly visible on both sides of the dorsal surface of the posterior palate (Fig 3.20).

On the dorsal surface of the palatine, visible on the right side of the skull, the palatine sends up a vertical flange that sutures with the descending flange of the prefrontal, and forms the medial margin of the foramen orbitonasale (for). The vertical palatal flange and the foramen orbitonasale are visible on the ventral surface of the skull table (Fig. 3.13).

The ventral surface of the palatine reveals a longitudinal posteriorly converging ridge, carrying two short parallel rows of small palatal teeth (broken off at their base) which continues posteriorly onto the pterygoid (Fig. 3.21).

**Ectopterygoid** (Figs. 3.6, 3.7, 3.10, 3.11)

The ectopterygoid is a small bone that has a long anteromedial contact with the palatine, a short anterolateral contact with the maxilla, and presumably a posterior suture with the pterygoid, although this is not preserved (Fig. 3.6). Most of the bone is flat and does not show any ridges on either the ventral or dorsal surfaces, or any palatal teeth on the ventral surface.

The middle and posterior portions of each ectopterygoid are not preserved, but the anteromedial and anterolateral portions that suture with the palatine and

the maxilla are preserved, in the same plane and at the same level as the palatal portions of the premaxilla, maxilla and palatine (Figs. 3.6, 3.7, 3.10, 3.11).

**Pterygoid** (Figs. 3.4, 3.5, 3.20, 3.21, 3.25, 3.26, 3.27, 3.28)

The pterygoid is a robust, complex bone, forming the posteromedial part of the palate. The bone is sutured along the midline with its contralateral element and comprises a relatively flat horizontal plate at the level of the palate, and a vertically orientated posterior quadrate ramus.

Anteriorly, it has a transverse suture with the vomer, and laterally a curved suture with the palatine which is easily seen on the dorsal surface of the posteromedial palate (Fig. 3.20). Posteriorly, the pterygoid sutures with the basipterygoid process (btp) of the basisphenoid along the lateral borders of the interpterygoid vacuity (itv) (Fig. 3.20). This basicranial articulation and suture is strong and immobile. Posterolaterally the pterygoid sutures with the quadrate on the quadrate ramus of the pterygoid (Figs. 3.4, 3.5, 3.20, 3.21, 3.25, 3.26).

In ventral view, a large open interpterygoid vacuity is present between the pterygoid and basisphenoid. The anterior and anterolateral borders of the interpterygoid vacuity are formed by the pterygoid, and the posterolateral and posterior border are formed by the basisphenoid, although the posterior border is not visible in ventral view (Fig. 3.21) but is visible in dorsal view (Fig. 3.20). The vacuity is rectangular; the anterior border is long, transverse and slightly curved producing a shallow u-shaped border, the lateral borders are short, longitudinal and slightly concave. The anterior border is lined with a row of small palatal teeth, three to five on each side of the midline, which are broken off at their bases, and are located some distance anterior to the border margin (Fig. 3.4, 3.21).

Along the midline, anterior to the interpterygoid vacuity, is a long deep oval depression which extends about half the length of the pterygoid before rising to

merge with the general level of the pterygoid. This depression houses numerous very small irregularly placed denticles on either side of the midline, and is demarcated laterally on either side by a raised medial sagittal ridge which extends the entire length of the pterygoid. Each medial sagittal ridge contains two parallel rows of small conical palatal teeth (i.e. a median and a lateral row). These palatal teeth of 1-2 mm in diameter are broken off at their bases, and number between 24 to 34 teeth per row. These ridges and palatal teeth continue anteriorly onto the vomer (Fig. 3.21).

Posteriorly, near the anterior border of the interpterygoid vacuity the medial sagittal ridges curve posterolaterally to diverge slightly and only the lateral palatal teeth row extends here, as the median palatal teeth row curves medially towards the midline to outline the anterior border of the interpterygoid vacuity, but some distance anterior to the vacuities border (Fig. 3.21). Another ridge bearing two parallel rows of six to ten palatal teeth each extends anterolaterally from a point near the middle of the pterygoid onto the palatine (Fig. 3.21).

A partial section of the transverse flange of the pterygoid or pterygoid wing (pw) is preserved on both sides and is laterally directed with a slightly ventral inclination projecting it just below the general level of the palate. The flange is very small, and does not reach near to the lateral cheek. The right pterygoid flange is partly covered by an unidentified displaced piece of bone, partially covering the posterolateral border of the flange. The eroded posterior border of the right flange reveals one small palatal tooth, indicating that both eroded sides probably held a row of small teeth, as is present in the other members of middle Permian South African pareiasaurs (Figs. 3.4, 3.21).

From the median base of the transverse flange of the pterygoid, the vertically orientated quadrate ramus of the pterygoid extends posterolaterally to suture with the vertically orientated dorsal ramus of the quadrate (Fig. 3.4) The sutural contacts between the pterygoid and quadrate via the quadrate ramus of the

pterygoid are clearer on the right side, on the posterior and anterior surfaces (Figs. 3.25, 3.26) and the dorsal surfaces of the bones (Fig. 3.20).

The dorsal surface of the pterygoid is well-exposed and the anterior portion shows a high narrow median sagittal ridge, running along the midline, as is a posterior continuation from the vomers. Posteriorly the ridge gradually increases in robustness, width and height and then tapers sharply off to dissipate into the surface of the bone. Either side of the high medial ridge, a separate short and sharp longitudinally crest is present which just reaches onto the basisphenoid (Fig. 3.20).

**Epipterygoid** (Fig. 3.20)

The epipterygoid is a small transversely orientated flat plate of bone. Visible only in dorsal view, it overlies the quadrate ramus of the pterygoid, immediately lateral to the longitudinal crest on the pterygoid, and almost reaches the basipterygoid process of the basisphenoid. More of the bone is preserved on the right of the skull, with only a small piece on the left (Fig. 3.20).

### 3.2.3 Braincase and Occiput

#### General Comments

The braincase comprises elements of the basisphenoid, basioccipital, supraoccipital, exoccipital, sphenethmoid, prootic, opisthotic, and quadrate. These elements are generally well preserved and prepared but are robust, massive and strongly fused, such that most sutural contacts are difficult to discern with certainty. However, the shapes of the bones and their contributions to the different regions of the braincase are identifiable and are described here.

Most of the elements of the braincase are fused on a single large fragment (Fragment G) which has been prepared and is visible in all views. Only the sphenethmoid and a small dorsal part of the supraoccipital are attached to the ventral surface of the skull table, and the anterior portion of the basipterygoid process of the basisphenoid is attached to the palate.

Both paroccipital processes of the opisthotic are preserved, although the left side is crushed and distorted inwards, shortening the transverse horizontal length compared to that of the right. In addition the distal end of the left paroccipital processes of the opisthotic has small pieces of the squamosal and supartemporal still attached. The distal end of the right paroccipital process has a large piece of the ventral section of the supratemporal bar and the squamosal still attached.

The braincase sutures to the skull roof anterodorsally at the supraoccipital and sphenethmoid, and laterally by the paroccipital processes of the opisthotics suturing with the supratemporal and squamosal.

The braincase features three important openings: the large foramen magnum above the occipital condyle; the fenestra ovalis; and the jugular foramen on the lateral sides of the braincase.

**Basisphenoid** (basisphenoid and parasphenoid) (Figs. 3.4, 3.5, 3.20, 3.21, 3.22, 3.23, 3.24)

The basisphenoid is a massive and complex bone forming the floor and ventral part of the lateral walls of the braincase. It sutures anteriorly with the pterygoid (Fig. 3.20), laterally with the prootic (Figs. 3.22, 3.23), and posteriorly with the basioccipital (Fig. 3.23).

At its anterior end, the bone forms the basipterygoid process which is a vertical plate, projecting downwards and outwards, and extending forward to create the posterolateral sides of the interpterygoid vacuity (Fig. 3.20). Here the

basisphenoid has a strong suture with the pterygoid which forms the anterior and the anterolateral borders of the interpterygoid vacuity (Figs. 3.20, 3.21). On the right side of the skull, part of the basipterygoid process is not preserved, and has been filled with Pratley Putty (TM) to join the braincase to the palate (Fig. 3.4). The left side preserves the entire basipterygoid process, forming part of the border of the interpterygoid vacuity, and is attached to the palate. The ventral surface of this process does not carry any detectible tubercle.

In ventral view, the basisphenoid is “hourglass-shaped” with a very narrow “waist” (Appendix A, B, Fig. 3.4). Anteriorly, at the basiscranial articulation of the basisphenoid with the pterygoid on the lateral borders of the interpterygoid vacuity, the basisphenoid is wide. Immediately behind the interpterygoid vacuity, the basisphenoid is very narrow and transversely constricted and pinched (Figs. 3.4, 3.23). However, the displacement of the palate backwards and to the left of its natural position widens the width of the narrowest point of the “waist”. The basisphenoid then widens posteriorly to reach the distal ends of the basal tubera (Figs. 3.4, 3.23**).**

Posteriorly, two long cylindrical posteriorly diverging basal tubera are present on the ventrolateral edges of the basisphenoid, with a deep midline groove in between. The tubera are formed mostly by the basisphenoid, but show a transverse suture with the basioccipital, indicating a small contribution by this element. This suture is readily identifiable within a distinct groove. The basal tubera extend much closer to the posterior edge of the occipital condyle than to the basipterygoid processes (Fig. 3.4).

In lateral view, sutures of the basisphenoids are easily identifiable on the left and right lateral surfaces, as a short horizontal suture with the prootic, as a vertical suture with the opisthotic and as a long horizontal ridge between the basioccipital and basisphenoid (Fig. 3.24). The fenestra ovalis is large, oval and anterodorsally orientated. The prootic-basisphenoid suture extends anteriorly from the middle of the fenestra ovalis. The margin of the fenestra is formed by

the basisphenoid ventrally and anteriorly, and by the prootic anteriorly, dorsally and posteriorly. A small horizontal ledge below the fenestra, stretches backwards and underneath the horizontally curved basisphenoid-basioccipital suture (Fig. 3.24).

A very anteroposteriorly short and wide cultriform process extends anteriorly along the midline from the basisphenoid as a horizontal flat bone, ending as a blunt anterior tip (Figs. 3.22, 3.24). In dorsal view, the projecting anterior cultriform process has a shallow longitudinal groove extending posteriorly (Fig. 3.22). The cultriform process forms the anterior portion of the very thick base of the cavum cranii or braincase**,** which is a longitudinally cylindrical cavity or opening. The very thick floor of the braincase is formed by the basisphenoid, the lateral walls by the basisphenoid ventrally and prootic dorsally, and the roof by the supraoccipital (Fig. 3.22).

**Basioccipital** (Figs. 3.4, 3.5, 3.23, 3.24)

The basioccipital is a medially positioned very robust bone (Fig. 3.23). Anteriorly, it forms a curved transverse suture with the basisphenoid on the basal tubera and dorsally it sutures with the exoccipital.

In occipital view, the basioccipital forms most of the circular occipital condyle, except for small dorsolateral portions which are formed by the exoccipitals. The centre of the posterior surface of the occipital condyle is excavated forming a deep hollow concave pit. Above this pit the sutures between the basioccipital and the exocippital are reasonably clear (Fig. 3.5).

The posterior ends of the basal tubera show only a small contribution by the basioccipital (Figs. 3.4, 3.23). In ventral view, anteriorly, a small, triangular, deep cavity is present along the midline, laterally flanked by the posterior ends of the basal tubera on either side. Just behind the posterior border of this cavity, a short, shallow, indistinct transverse ridge is present, but there is no obvious

round posteroventral projecting, median tubercle, as has been reported for *Pareiasaurus nasicornis* (Lee *et al.* 1997) and *Scutosaurus* (Lee 1995). Posterior to the basal tubera, the basioccipital forms a very short neck that widens to reach the occipital condyle.

In lateral view, the basioccipital sutures with the basisphenoid ventrally. The jugular foramen is located just behind the fenestra ovalis, and slightly lower down. The basioccipital forms the anteroventral, ventral, and the posteroventral margin of the jugular foramen. The suture between the basioccipital and exoccipital extends horizontally posteriorly from the posterodorsal corner of the jugular foramen (Fig 3.24).

**Exoccipital** (Figs. 3.5, 3.22, 3.23, 3.24)

The exoccipital is a small bone forming part of the occipital condyle and the foramen magnum. The bone sutures with the basioccipital ventrally, the opisthotics laterally, and the supraoccipital anteriorly.

In occipital view, the exoccipital forms the extreme dorsolateral portions of the circular occipital condyle (Fig. 3.5). The condyle is nearly circular but is slightly flattened on its dorsal surface, just below the foramen magnum. On the posterior surface of the occipital condyle, the exocipitals present a short curved horizontal suture with the basioccipital, medially curving upwards to contact with its contralateral element along the midline.

The foramen magnum is large and oval and slightly wider than high. Its ventral border is formed by the dorsal margin of the occipital condyle. The lateral borders are formed by the exocipitals and the dorsal border by the supraoccipital (Fig. 3.5).

In dorsal view (Fig 3.22), the exoccipital sutures with the supraoccipital anteromedially, such that the supraoccipital prevents the exoccipital from

meeting its contralateral element on the midline. These sutural contacts are identifiable on the right side. Laterally, the supraoccipital sutures with the opisthotic. This suture is also very clear on the right side.

Lateral to the occipital condyle, the exoccipital sends out a horizontal flat triangular flange which extends along and covers the median ventroposterior, posterior and dorsoposterior surface of the paroccipital process. This lateral flange of the exoccipital is easily identifiable on the right exoccipital in dorsal, ventral and occipital views (Fig 3.5, 3.22, 3.23).

In lateral view, the exoccipital forms the posterodorsal border of the jugular foramen. Behind the jugular foramen, the exoccipital's horizontal suture with the basioccipital ventrally is very clear (Fig 3.24).

**Supraoccipital** (Figs. 3.5, 3.13, 3.22)

The supraoccipital is a short and thick verticaly oriented pillar of bone. It comprises two portions: the ventral portion is horizontally flat, expanded and forms the roof of the braincase or cavum cranii; the dorsal portion consists of a short narrow ascending process or pillar which sutures the braincase to the ventral surface of the median skull roof. In the holotype of *Embrithosaurus*, the supraoccipital is broken and is preserved separately: the ventral flat portion is preserved on the dorsal side of the braincase (Fig. 3.22), and the dorsal short vertical pillar is preserved on the inner surface of the skull table (Fig. 3.13). The dorsal ascending process of the supraoccipital is roughly triangular and is preserved attached to the descending process of the postparietal on the internal surface of the skull table (Fig. 3.13). In occipital view, this process has a strong horizontal suture (Fig. 3.5).

The inner surface of the parietal shows a midline shallow narrow trough just anterior to the descending process of the postparietal (Fig. 3.13). In some other pareisaur specimens such as NHMUK R7782, which Watson (1914b) refers to

*Embrithosaurus* and in many specimens of *Scutosaurus* (Lee 1995), the parietal trough carries a long median anterior projection from the supraoccipital. In the holotype of *Embrithosaurus*, a bone break is present on the anterior face of the descending process of the postparietal, where a long median anterior supraoccipital projection may have been.

The dorsal view of the braincase (Fig. 3.22) shows the horizontally flat ventral portion of the supraoccipital. Anterolaterally the supraoccipital contacts the prootic, laterally it contacts the opisthotic, and posterolaterally the bone has a curved sutural contact with the exoccipital. This ventral portion of the supraoccipital forms the flat horizontal median roof and the dorsal margin of the brain case. The dorsal surface of the suparoccipital shows triangular ridges, converging posteriorly to a tip on the midline, which indicate where the ascending process of the supraoccipital was anchored. A small median crest, the crista supraoccipitalis (cs), extends along the midline, posteriorly from the tip of the triangular ridge, to reach the margin of the foramen magnum (Fig. 3.22). The supraoccipital forms the dorsal margin of the foramen magnum posteriorly, separating the two exoccipitals.

**Prootic** (Figs. 3.4, 3.22, 3.23, 3.24)

The prootic is a curved, robust, and elongated bone, located on the anterior portion of the lateral side of the brain case. In dorsal and ventral view it is positioned lateral to the supraoccipital and medial to the opisthotic (Figs. 3.22, 3.23). The medial wall of the prootic is fully ossified and forms part of the lateral walls of the cavum cranii or braincase.

In lateral view, it shares a horizontal suture with the basisphenoid, and a vertical suture with the opisthotic (Fig. 3.24). The prootic forms the anterior, dorsal and posterior border of the fenestra ovalis and the dorsal part of the lateral walls of the braincase (Fig. 3.24). Behind the fenestra ovalis, the prootic occupies a very

small space, stretching about half way back to the jugular foramen. This small portion of the prootic it is bounded ventrally by the basisphenoid (Fig. 3.24).

**Opisthotic** (Figs. 3.4, 3.5, 3.22, 3.23, 3.24)

The opisthotic is a large and elongated wing-like bone, located on the posterior portion of the lateral side of the braincase. It forms the paroccipital process that laterally sutures the braincase to the skull roof.

The paroccipital process of the opisthotic is a horizontal bar or wing of bone that connects the braincase to the inner sides of the skull roof. In occipital view, the paroccipital process is u-shaped, which proximally starts at the level of the foramen magnum, it then projects laterally horizontally and slightly downwards before curving sharply upwards towards the corner of the inner surface of the skull roof (Fig. 3.5). Laterally the distal end of the paroccipital process sutures with the inner surface of the dorsolateral corner of the skull roof, against the short but strong ventral process or flange from the supratemporal and a medial process or flange of the squamosal (Fig. 3.5).

The left paroccipital process is crushed downwards and inwards, shortening the length of the process compared to the less distorted right side. Large fragments of the supratemporal and squamosal are still attached to the right paroccipital process (Fig. 3.22, 3.24). The left side has a small, flat piece of the squamosal attached and a long, thin piece of the supratemporal attached, with the blunt contact with the rest of the supratemporal visible.

In dorsal view, the opisthotic forms most of the posterior lateral side of the braincase, suturing medially with the supraoccipital (Fig. 3.22). Posteromedially, it has a suture with the exoccipital, and anteriorly a short and very strong suture with the prootic (Fig 3.22). The horizontally oriented bar of the paroccipital process projects posterolaterally from the side of the braincase. Towards the distal ends, the process everts so as to turn the tip to face more dorsally for

reception of the supratemporal and squamosal. This distal dorsal surface is generally flat, but slightly bowl-shaped overall. Posterior to the dorsal articular surface, the paroccipital process presents a small knob-like projection that narrows to end with a vertically pointed distal tip (Fig. 3.22). On the ventral surface of the paroccipital process presents a thin plate-like edge (Fig. 3.23).

In lateral view, the paroccipital process is located above the fenestra ovalis and forms the anterodorsal and dorsal borders of the jugular foramen (Fig. 3.24).

**Quadrate** (Figs. 3.4, 3.5, 3.6, 3.8, 3.10, 3.11, 3.15, 3.25, 3.26, 3.27, 3.28)

The quadrate is a wide and thin curved plate of bone, transversely oriented and located on the inside of the lateral cheeks.

In occipital view, the quadrate consists of a vertical ramus or flange that extends ventrally and laterally from its sutural contacts with the medial flanges of the squamosal and the quadratojugal (Figs. 3.5, 3.25, 3.27). Dorsolaterally, the quadrate sutures with the medial flange of the squamosal, and ventrolaterally with the medial flange of the quadratojugal. On the inner left cheek, a piece of the quadrate is attached to the medial flange of the squamosal (Fig. 3.15). Sutures with the medial flanges of the squamosal and quadratojugal are best observed on the posterior and anterior surfaces of the right quadrate (Figs. 3.25, 3.26). Medially, the quadrate has a reduced suture with the quadrate ramus of the pterygoid. Ventrally, the quadrate articulates with the articular of the lower jaw. Dorsally, the quadrate does not meet the paroccipital process of the opisthotic

At the intersection of the squamosal-quadratojugal-quadrate a large quadrate foramen is present. Observable on only the right side, the foramen is almost completely surrounded by the quadrate, which forms the dorsomedial, medial and ventromedial borders, with the squamosal forming the dorsolateral border

and the quadratojugal the ventolateral border of the foramen (Figs. 3.5, 3.25, 3.26).

The quadrate is highest laterally and decreases in height medially. The ventral half of the quadrate thickens medially, and develops into a strong swelling, which continues into the quadrate ramus of the pterygoid. On the posteromedial facing surface of the quadrate, this swelling creates a horizontal jutting out ledge with a small dorsal flat surface, and an embayment behind it (Figs. 3.25, Fig 3.27). The anterior facing surface of the quadrate is smooth and featureless.

The long and thin mandibular articulations of both quadrates are broken off and are tightly occluded with the lower jaw, obscuring study of the cranio-mandibular joint morphology (Figs. 3.6, 3.8, 3.10, 3.11). In addition, unprepared matrix surrounds the left cranio-mandibular joint, further obscuring study. The ventral articular surfaces of the occluded quadrates cannot be observed directly, but certainly consist of a lateral and medial condyle, separated by a medial groove, as the articulars do show corresponding lateral and medial cotyles for their reception (Fig 3.6). The ventral ends of the quadrates face slightly forward, and are indented.

**Sphenethmoid** (Pleurosphenoid) (Fig. 3.13)

The sphenethmoid is large, cylindrical, dumbbell-shaped bone located on the ventral surface of the median skull table. It is elongated longitudinally, and sutures with its contralateral element along the midline.

The sphenethmoid is attached to the ventral surface of the skull table fragment The bone is distorted: it is dorsoventrally crushed, displaced to the left and with its left element twisted forward (Fig. 3.13).

The two plates of bone are strongly ossified and sutured laterally to the inner skull roof surface either side of the skull midline. Anterodorsally these plates

anchor with the anchor with the internal surface of the frontals, and posterodorsally with the internal surface of the parietals (Fig 3.13). Ventrally the sphenethmoid curves medially to meet with its contralateral element on the midline, forming a cylindrical cavity around the midline inner skull surface

In ventral view, the lateral walls are longitudinally oriented but with a deep concave impression medially, creating a “dumbbell” shape. The four corners of these walls splay outwards laterally as they anchor to the skull roof, increasing the width of the longitudinal ends of the sphenethmoid and contributing to the concave “dumbbell” shape of the element (Fig 3.13).

The lateral borders of the pineal foramen are formed by the posterior median surfaces of the walls of the sphenethmoid (Fig 3.13). The posterior edge of the sphenethmoid contacts the anterior cultriform process of the basisphenoid. The ventral midline edge where the two sphenethmoids meet is sharp and pointed and projects ventrally. A ventrally facing raised oval process is found on the posterior section of the ventral midline edge, at the contact with the basisphenoid.

**Stapes (Columella Auris)**

The stapes is not preserved and, of all pareiasaurs, has been described only in *Scutosaurus* (Lee 1995) and *Arganaceras vacanti* (Jalil and Janvier 2005).

### 3.2.4 Lower Jaw

**General Comments**

The lower jaw comprises the dentary, angular, surangular, articular, prearticular, coronoid, and splenial bones. It is tightly occluded to the skull, with the result that the dorsal portion of the lower jaw and most of the mandibular teeth are

obscured. The lower jaw is well prepared and exposed on the lateral, medial and ventral surfaces, which are smooth and have no ornamentation, except for the ventrally directed boss on the angular.

The left mandible is almost complete except for a large anterior lateral section of the surangular and small anterior section of the medial prearticular which are not preserved and are filled in with white plaster. A small section of the lateral surangular and dentary and the medial coronoid and articular of the right mandible are also not preserved.

The lower jaw comprises mainly sheet-like bones that form internal and external plates covering the meckelian canal between the dentary and splenial, and posteriorly the intra-mandibular cavity between the lateral coronoid and surangular, the medial splenial, prearticular and articular, and the ventral angular. The articular is the only robust, non sheet-like bone and forms the hinge between the lower jaw and the skull.

Previous workers drew sutures between the bones in thin black ink. This study verifies most of these previous interpretations, raised ridges of bone are visible along many of these lines, indicating a slight separation or displacement of the bony elements through distortion. My observations differ from previous interpretations regarding the sutures between the prearticular and the splenial and coronoid bone on the medial surface of the left mandible, as I consider that they pass at a higher level.

Two distortions severely affect the lower jaw: significant twisting of the midline of the jaw to the right resulte in the left ramus appearing shortened and the right appearing much extended posteriorly; mediolateral compression inwards towards the midline produced in the appearance of a pointed snout and lower jaw.

The lower jaw features two important large medial openings: the foramen intermandibularis that extends to the meckelian canal, and the foramen intermandibularis caudalis between the angular, splenial and the prearticular.

**Dentary** (Figs. 3.2, 3.3, 3.6, 3.7, 3.8, 3.9, 3.10, 3.11)

The dentary is the largest bone of the lower jaw and bears all the mandibular teeth on the alveolar ridge. Anteriorly, the dentaries are fused along the midline, forming the dorsal half of the very strong mandibular symphysis, where they create a short but distinctly raised and pointed vertical protuberance. This mandibular midline symphysis swelling continues ventrally onto the splenials (Fig. 3.7).

The dentary forms roughly the anterior two thirds of the lower jaw, and contacts the splenial anteroventrally, the angular ventrally, the surangular posteroventrally, and the coronoid posterodorsally (Figs. 3.8, 3.10). The lateral extent of the dentary is revealed by its slightly raised edges at the contacts with the splenial, angular and surangular. The dentary does not contribute to the ventral surface of the lower jaw (Fig. 3.7).

In medial view, the bone shows a much smaller exposure than in lateral view, being concealed mostly by the splenial and by a thin flat projection from the coronoid below the last three posterior teeth, leaving only the dorsal marginal tooth row and the most anterior part of the dentary visible (Figs. 3.9, 3.11). The medial sutural contacts of the dentary with the coronoid and splenial are best viewed on the less distorted right mandible and are shown by raised ridges of bone (Fig. 3.11). Dorsally, the dentary does not form any part of the lateral rim of the adductor fossa (af) (Figs. 3.6, 3.9, 3.11).

In addition to the alveolar ridge a separate distinct horizontal shelf, the crista dentalis (cd), extends posteriorly from the symphysis and passes just below two

erupting teeth. Posteriorly this shelf coincides with the horizontal sutural contact of the dentary-splenial (Figs. 3.9, 3.11).

Anteriorly a large triangular foramen, the foramen intermandibularis medius (fim) is present and extends to the meckelian canal. This foramen, located above the symphysis, is formed by the splenial ventrally and the dentary dorsally (Figs. 3.6, 3.11). The meckelian canal extends horizontally internally between the enclosing curved sheet-like lateral dentaries and the medial splenials.

On the right lateral side, one of the two expected lateral foramina are visible, the foramen dentofaciale majus (fdm), located on the dentary between the sixth and seventh upper jaw teeth counting from front to back (Fig. 3.10). This foramen leads into the meckelian canal but is not observed on the left lateral side of the mandible, due to the far overhanging occluded upper jaw covering the dorsal portion of the dentary.

**Angular** (Figs. 3.2, 3.3, 3.6, 3.7, 3.8, 3.9, 3.10, 3.11)

The angular is a large anteroposteriorly elongated bone which covers most of the posterior half of the ventral surface of the lower jaw.

In lateral view, the angular makes a long narrow horizontal contribution to the most ventral portion of the mandible where it contacts the splenial anteriorly, the dentary anterodorsally, the surangular dorsally, and the articular posteriorly. The broken off “angular boss” is visible on the anterior half of the angular (Figs. 3.2, 3.3, 3.7, 3.8, 3.9, 3.10, 3.11).

In medial view, the angular has a long suture with the splenial anterodorsally, an equally long suture with the prearticular posterodorsally, and a short suture with the articular posteriorly. At the junction of the splenial, angular and prearticular, the angular forms the posteroventral border of the foramen intermandibularis

caudalis (fic). This large foramen is oval and longitudinally elongated (Figs 3.9, 3.11).

In ventral view, the angular tapers to a point anteriorly, where it wedges between the lateral dentary and medial splenial (Fig. 3.7). On the ventral surface, level and in front of the foramen intermandibularis caudalis, is the remnant of the broken off “angular boss”. These bosses are broken off near their base and are now missing, but were originally complete and present, as can be seen in photographic plates of the lower jaw from Haughton and Boonstra (1930a) (Fig. 1.8) and Boonstra (1934a) (Fig. 1.7). These photographs reveal the boss to be relatively small, slender and narrow, projecting only a short distance considering the size of the skull when compared to other large South African *Tapincocephalus* Assemblage Zone pareiasaur specimens studied. The exposed broken cross sections show the bosses to be longitudinally oval and longer than wide. They are posteroventrally directed, with a distinct swelling midway along their length, distinctly narrowing distally after that, before swelling slightly again to reach a rounded blunt point distally. This gives the impression of a “bovine teat” boss shape, which is remarkably small for the size of the skull, and contrasts with the large square “door knob-like”, the long, thin, conical “horn-like”, and the small low “pyramid-like” shapes of the angular bosses of other South African pareiasaurs, described by Haughton and Boonstra (1930a).

Anterior to the angular boss the jaw is slightly longer than posterior to it.

**Surangular** (Figs. 3.2, 3.3, 3.6, 3.7, 3.8, 3.10, 3.11)

The surangular is a large curved plate of bone covering most of the posterior half of the lateral surface of the lower jaw.

In lateral view, the surangular contacts the dentary anteriorly, with a curved oblique suture, the angular ventrally, with a long horizontal suture, and the articular posteriorly, with a vertical suture (Fig 3.2, 3.3, 3.6, 3.7, 3.8, 3.10).

Dorsally, the extreme anteromedial section of the right surangular, forms a very small part the lateral edge of the posterior portion of the adductor fossa (af) (Fig. 3.6). The small adductor fossa is a bowl like depression just behind the tooth row on the dorsal and medial surface of the lower jaw. It is bounded laterally and anteriorly by the coronoid, posteriorly by the surangular, and medially by the prearticular (Figs. 3.9, 3.11). In dorsal view, on both sides of the lower jaw immediately behind the adductor fossa, is a long, narrow and deep intra-mandibular cavity (imc), which is partially filled with matrix, in which the surangular forms its entire lateral wall (Fig. 3.6).

In dorsal view, the anterior portion of the surangular is convex. Posteriorly it curves concavely outwards as it overlaps the wide articular on the lateral side of the jaw (Fig 3.6) and here it presents a sharp, flat surface of a lateral shelf, that faces dorsolaterally.

**Coronoid** (Figs. 3.3, 3.6, 3.7, 3.9, 3.10, 3.11)

The coronoid is an anteroposteriorly elongated, tin, slender bone located almost entirely on the medial surface of the lower jaw, with only a small portion on the lateral side. In medial view the coronoid contacts the dentary dorsally with a long horizontal suture, the splenial anteriorly with a short vertical suture, and the prearticular ventrally with a long horizontal suture (Figs. 3.7, 3.9, 3.11).

In dorsal view, the right coronoid passes from the medial surface to the lateral surface, immediately behind the most posterior mandibular tooth on the dentary (Fig 3.6). In lateral view, the small exposure of the right coronoid shows that the coronoid process is not well developed, and rises only slightly above the level of the mandibular tooth row (Figs. 3.3, 3.10).

**Prearticular** (Figs. 3.6, 3.7, 3.9, 3.11)

The prearticular is a large sheet-like bone covering most of the posterior part of the medial surface of the mandible. In medial view, the bone contacts the splenial anteriorly, the angular ventrally, covers a large part of the articular posteriorly, and contacts the coronoid dorsally (Figs. 3.6, 3.7, 3.9, 3.11). The prearticular forms the entire dorsal and posterior border of the large, oval foramen intermandibularis caudalis (Figs. 3.9, 3.11).

Dorsally, the prearticular forms the medial margin of the adductor fossa (Fig. 3.6). Just below the fossa, the prearticular has a short, curved, horizontal shelf that forms a prominent horizontal lip, best seen in medial view (Figs. 3.9, 3.11). This small but prominent shelf has been called a “scroll-like” structure by Broom (1924) in his description of *Pareiasaurus strubeni*. The anterior portion of this shelf is preserved on the right (Fig. 11), and the middle portion of this shelf is missing on the left (Fig. 3.9). Dorsally, the prearticular forms a small part of the anteromedial wall of the intra-mandibular cavity (Fig. 3.6).

**Articular** (Figs. 3.3, 3.6, 3.7, 3.8, 3.9, 3.10, 3.11)

The articular is a robust and complex bone, located at the posterior end of the lower jaw and is unlike any of the other elements which are all curved sheets of bone. The articular contributes to the lateral, posterior and medial sides of the posterior portion of the mandible and serves as the jaw hinge.

In lateral view the articular presents a short contact with angular ventrally, and a long vertical contact with the surangular anteriorly (Figs. 3.8, 3.10). In medial view it contacts the angular ventrally, and has a long vertical contact with the prearticular anteriorly (Figs. 3.9, 3.11). Exposure of the articular is substantially greater on the medial surface (behind the prearticular) than on the lateral side where it is almost entirely covered by the surangular.

In dorsal view, the posterior half of the bone is greatly transversely expanded, with the anterior half sending a tapering forward extension clasped between the prearticular medially and the surangular laterally. This strong pointed wedge of the articular forms most of the medial wall of the posterior portion of the intra-mandibular cavity (Fig. 3.6). Posteriorly, the width of the bone accommodates the cranio-mandibular joint in a wide hollow area articularis mandibularis for the reception of the quadrate of the skull. On the left side, this hollowed-out area is partially filled with matrix, is almost horizontal, and faces dorsally and only slightly laterally. On the right, it is significantly deformed, being much narrower and facing dorsolaterally. Much of it is covered and obscured by the articulated quadrates. However, the left side shows that it consists of a lateral and a medial cotyle (Fig. 3.6). The posterior margin of the articular shows a shallow indentation on the rim where an antero-posteriorly oriented medial ridge extends between the two cotyles. Lateral to this shallow indentation, the posterolateral edge of the articular bears a very short, rounded lip or overhang extension, a posterior retroarticular process which according to Haughton and Boonstra (1930) is a wall that limits the extent to which the jaw can be opened.

**Splenial** (Figs. 3.2, 3.3, 3.6, 3.7, 3.8, 3.9, 3.10, 3.11)

The splenial is a large, elongated and curved plate of bone, forming most of the ventral and medial surfaces of the anterior half of the lower jaw.

Anteriorly, it sutures with its contralateral element along the midline, forming the ventral half of the very strong mandibular symphysis which is posteroventrally directed. The symphysis is very distinct, raised and pointed from the ventral surface of the splenial at the midline of the jaw, creating a ventral flange or mentum. Ventrally, there are small swellings on either side of the symphysis (Figs. 3.3, 3.7, 3.9, 3.10).

On the medial surface, the foramen intermandibularis medius , located above the symphysis, is bounded by the splenial ventrally. The splenial forms the ventral floor of the foramen intermandibularis medius (Fig. 3.11). Anteriorly, the splenial has a horizontal suture with the dentary dorsally, just below the distinct crista dentalis or horizontal shelf of the dentary (Figs. 3.9, 3.11). The splenial has two flanges posteriorly: a dorsal flange that projects far below the tooth row and forms a vertical suture with the coronoid, and a ventral flange which is wider, longer, and more robust, and reaches further posteriorly than the dorsal flange (Figs. 3.9, 3.11). The ventral flange is somewhat swollen and thickened, extending posteriorly until it reaches the very large foramen intermandibularis caudalis (fic), where it forms the anterior and anteroventral border. Between the two posteriorly directed flanges, there is a wedge shaped contact with the prearticular.

### 3.2.5 Marginal Dentition

#### General Comments

The premaxilla and maxilla bear all of the upper jaw marginal teeth on their ventral margins and because of tight jaw occlusion only the labial surfaces are exposed. Almost the entire tooth row is exposed, except for some of the posteriormost teeth, which are not preserved.

The dentary carries all of the lower jaw marginal teeth on the alveolar ridge of the dorsal margin. Only the lingual surfaces of the lower jaw teeth are exposed, again due to the occlusion with the upper jaw. On the right ramus almost the entire tooth row is exposed, except for the two or three most anterior teeth, on the left ramus only the two posteriormost teeth are exposed.

In both upper and lower jaws, the teeth occur in a single row, are very close together, and decrease in size posteriorly, with the posteriormost teeth being about two- thirds of the size of the anteriormost. All the marginal teeth are

deeply thecodont and single rooted, as shown by two broken posterior right mandibular teeth.

The crowns are short, stubby, wide and bulbous, and are very slightly longer than wide creating a slightly elongated oval shape. The crowns are leaf-shaped and labio-lingually flattened, thereby broadened and extend outwards along the jaw margin wider than the roots.

**Upper marginal dentition** (Figs. 3.2, 3.3, 3.7, 3.8, 3.10, 3.29, 3.30, 3.31, 3.32, 3.33, 3.34)

Eleven maxillary teeth are exposed on the right maxilla of the upper jaw, however two wide gaps are observed and each gap probably represents the position of a missing tooth. The first is in the position of the first maxillary tooth, immediately behind the third premaxilla tooth; the other is in the position of the sixth maxillary tooth, between the fifth and seventh maxillary tooth (Fig. 3.33, maxillary teeth numbered one and six) making a total of at least 13 maxillary teeth on the right side.

On the left maxilla, 12 maxillary teeth are exposed, however, there is a wide gap (that probably held a missing tooth), where the ninth maxillary tooth would have been positioned, between the eighth and tenth tooth (Fig. 3.31, maxillary tooth numbered nine) making a total of at least 13 maxillary teeth on the left side. Additionally, a maximum of two to three teeth were probably held in the unpreserved missing posterior most sections of each maxilla, resulting in a total of 15-16 maxillary teeth per side.

In addition to the maxillary teeth, there are three premaxillary teeth on each side of the upper jaw, resulting in a total of 18-19 teeth on each side. This is slightly less than, but agrees approximately with the number noted by Lee (1997a) who noted approximately 20 upper jaw teeth. All teeth are orientated vertically and point directly downwards, but are slightly medially oriented towards the palate

by 10-20 degrees from the vertical. However, the posterior half of the right maxillary teeth point inwards towards the palate by about 40 degrees. This is a taphonomic affect caused by the dorsoventral crushing and twisting of the right side of the skull (Fig 3.3).

The crowns of all the premaxillary teeth are damaged and it is not possible to determine the number of cusps (Figs. 3.29, 3.30). However, although their size is larger than the more posterior maxillary teeth, their general morphology and overall shape are identical to the adjacent better preserved maxillary teeth, which each bear nine marginal cusps (Fig. 3.34), suggesting the same number of cusps for the premaxillary teeth. I have observed no evidence to indicate that the cusp numbers differs between premaxillary and maxillary teeth on the holotype of *Embrithosaurus* (SAM-PK-8034). This contradicts Broom who stated that the front teeth of SAM-PK-8034 have "apparently" seven cusps, although he admitted that they are damaged and his assessment is tentative (Broom 1903:127). The majority of the maxillary teeth are well preserved and the number of cusps have been determined accurately through additional preparation of the labial surfaces of the second to tenth teeth (left maxilla) (Figs. 3.31, 3.32), and the labial surfaces of the seventh to eleventh teeth (right maxilla) (Figs. 3.33, 3.34). Nine irregularly arranged (i.e. unevenly spaced) cusps are positioned on the margins of each crown, and the central cusps are arranged differently to those of the lateral cusps (Fig. 3.34). Three central cusps on the distal tip or apex of the crown are set very close together, and are virtually at the same level, except for the central cusp which projects slightly further distally. There are no gaps between the three central cusps, which are followed laterally by a very small gap to the first lateral cusp on either side of the crown, creating the appearance of five central cusps being very close together. Separate from these five central cusps, are two lateral cusps on either side of the crown which have large gaps between each other and the central cusps. The base of the crown is formed laterally by the lowest of these two lateral cusps. Overall the relatively large number of marginal cusps, and the relatively close spacing of the

five central cusps, create the appearance of rounded, broad and wide teeth, in labial view. The distal crown of one tooth overlaps the mesial crown of the adjacent tooth behind it such that the first lateral mesial cusps at the base of each tooth are not exposed (Fig 3.31, 3.32, 3.33, 3.34 – cusp number nine on each tooth). The base of each tooth is narrow and widens distally to accommodate the first lateral cusps. The crowns are oval and vertically elongated. A few teeth with damaged cusps give the false impression of triangular crowns with a broad base at the level of the first lateral cusps, tapering to a point at the apex of the crown at the central cusps.

The maxillary teeth are only slightly elongate and oval, being slightly longer than wide and are evenly swollen or bulbous such that the labial surfaces are strongly, smoothly and evenly convex over their entire width. They bear very fine vertical striations and stripes on the smooth surfaces, but no grooves or ridges (Figs. 3.32, 3.34).

**Lower marginal dentition** (Figs. 3.6, 3.9, 3.11, 3.37, 3.38)

There are 16-17 teeth in the dentary on each side of the lower jaw. On the right medial side, the tooth row has 15 marginal teeth clearly exposed, with some space anteriorly covered by occluded elements of the upper jaw that contain a additional one to two teeth (Figs. 3.6, 3.11). This is in general agreement with Lee (1997a) who noted approximately 18 lower jaw teeth on either side for *Embrithosaurus*. Two erupting replacement teeth are observed far below the alveolar ridge, in line with the sixth and tenth exposed dentary teeth, counting backwards from the front (Figs. 3.6, 3.11). The dorsal surface of the medial side of the right dentary is dorsoventrally crushed and displaced to the right, creating the appearance of forward and outward pointing teeth, but this is a taphonomic effect. The lower jaw teeth would point directly upwards or only slightly outwards in their natural position.

Anteriorly on the left medial side, four teeth are partially exposed (Fig. 3.9). Posteriorly, only the two most posterior teeth are exposed. Because they are small and broken off near their bases (Figs. 3.6), it is impossible to count the number of lower jaw teeth on the left ramus.

Most of the exposed teeth on the right mandible are well preserved and the number of cusps have been determining accurately through additional preparation of the fourth to tenth exposed teeth (Fig. 3.38).

Nine cusps on the margins of the crown are arranged irregularly, but with a slightly different configuration to that of the upper jaw teeth. Three central cusps are set close together on the apex of the crown, virtually on the same plane, but with the central cusp being slightly longer. Three lateral cusps on either side are set apart from the three central cusps, and are all approximately equally spaced from each other, with equally wide gaps between all three (Fig. 3.38).

Also different from the evenly swollen and convex labial surfaces of the maxillary teeth, the lingual surface of the mandibular teeth are swollen and convex only near the base, at the level of the first lateral cusps, and are concave or scooped out or thinner above the swollen base, where the tooth thickness narrows towards the crown. The swollen base creates a triangular horizontal bulge, which is shallow and does not stretch very high (Fig. 3.38). The teeth are therefore labio-lingually flattened and very thin above the triangular horizontal bulge. The distal ends of the cusps are narrow and show shallow grooves or ridges separating neighbouring cusps from each other, that does not reach the bulge . In cusp numbers the lower jaw teeth are the same as the upper jaw, however in arrangement or spacing between cusps, the cusps on the lingual surfaces of the mandibular teeth appear taller and more spread out with wider gaps than the cusps on the labial surfaces of the upper jaw teeth.

The labial surfaces of the lower jaw teeth are not exposed, making it impossible to compare them directly to the labial surfaces of the upper jaw teeth.

**Key to interpretive drawings:**

Sutures in solid lines have been positively identified; those in dotted lines are extrapolated from internal surfaces and the sides of bones. Light grey indicates sides of bones or bone breaks, dark grey indicates foramen or fenestra, black indicates deep cavities such as the orbits. Numbers indicate: marginal cheek bosses; teeth positions counting back from the front; or tooth cusps. Cranial bosses are in bold.

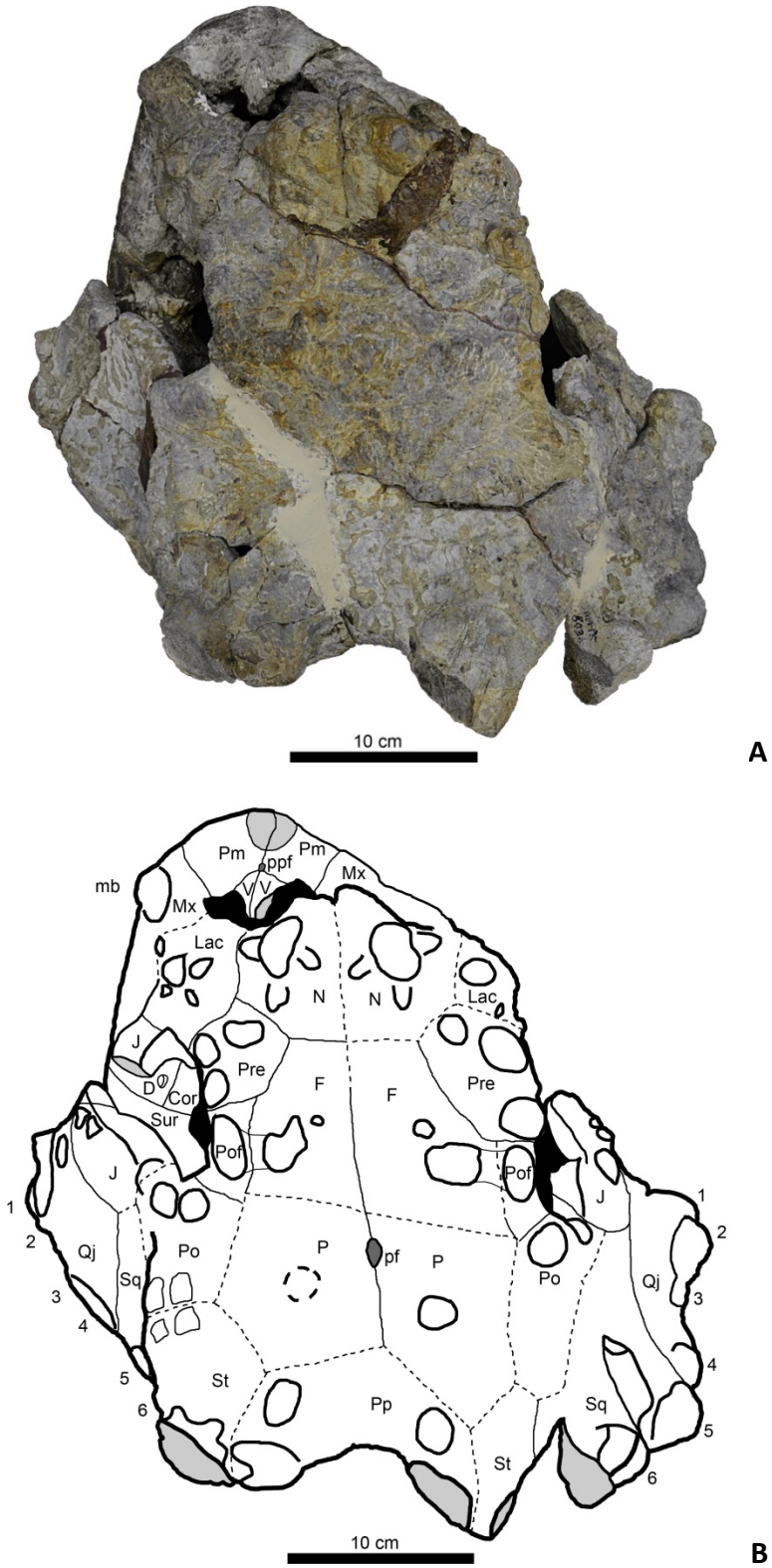


**Figure 3.1:** Photograph (A) and interpretive drawing (B) of the skull of the holotype of *Embrithosaurus schwarzi* (SAM-PK-8034), in dorsal view.




**Figure 3.2:** Photograph (A) and interpretive drawing (B) of the skull of the holotype of *Embrithosaurus schwarzi* (SAM-PK-8034), in left lateral view.

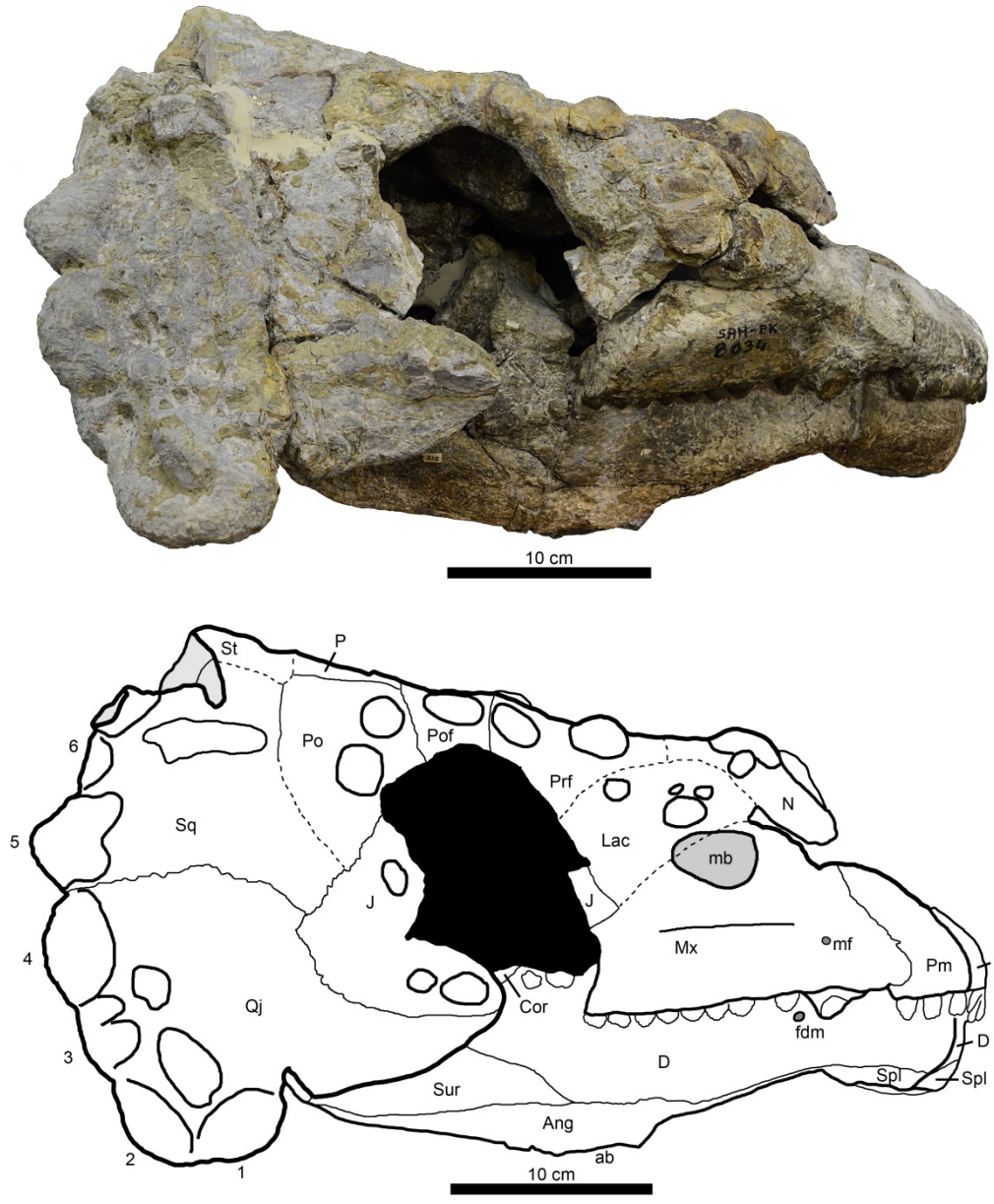


**Figure 3.3:** Photograph (A) and interpretive drawing (B) of the skull of the holotype of *Embrithosaurus schwarzi* (SAM-PK-8034), in right lateral view.

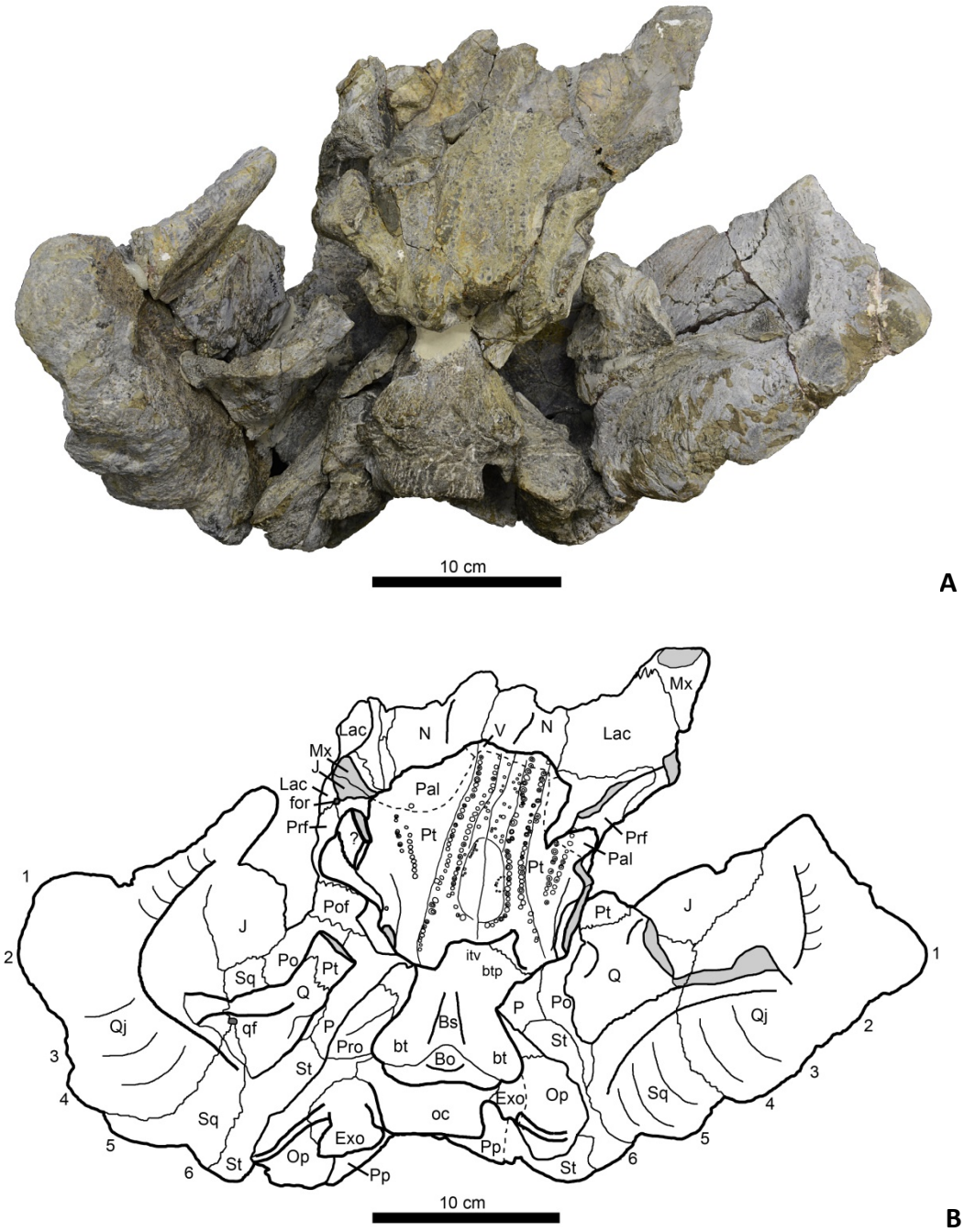


**Figure 3.4:** Photograph (A) and interpretive drawing (B) of the skull of the holotype of *Embrithosaurus schwarzi* (SAM-PK-8034), in ventral view.

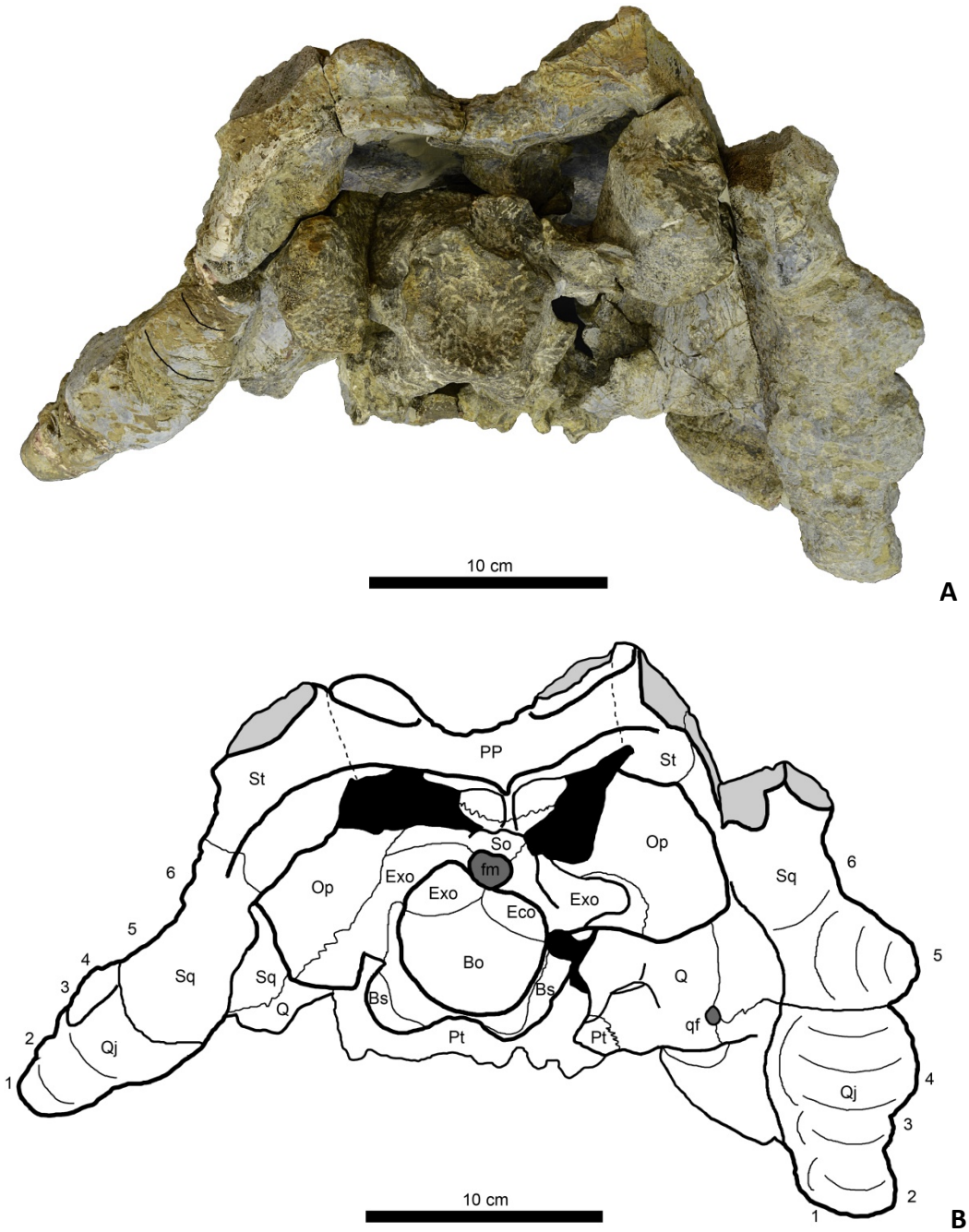


**Figure 3.5:** Photograph (A) and interpretive drawing (B) of the skull of the holotype of *Embrithosaurus schwarzi* (SAM-PK-8034), in occipital view (excluding the lower jaw fragment A).

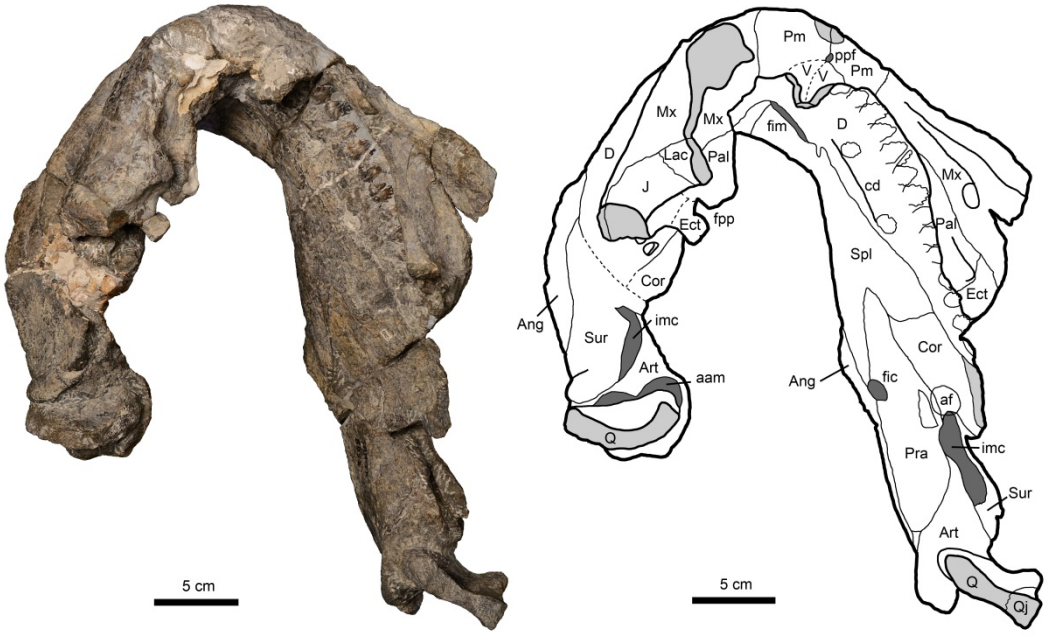


**Figure 3.6:** Photograph (A) and interpretive drawing (B) of the lower jaw and snout (fragment A) of SAM-PK-8034, in dorsal view.

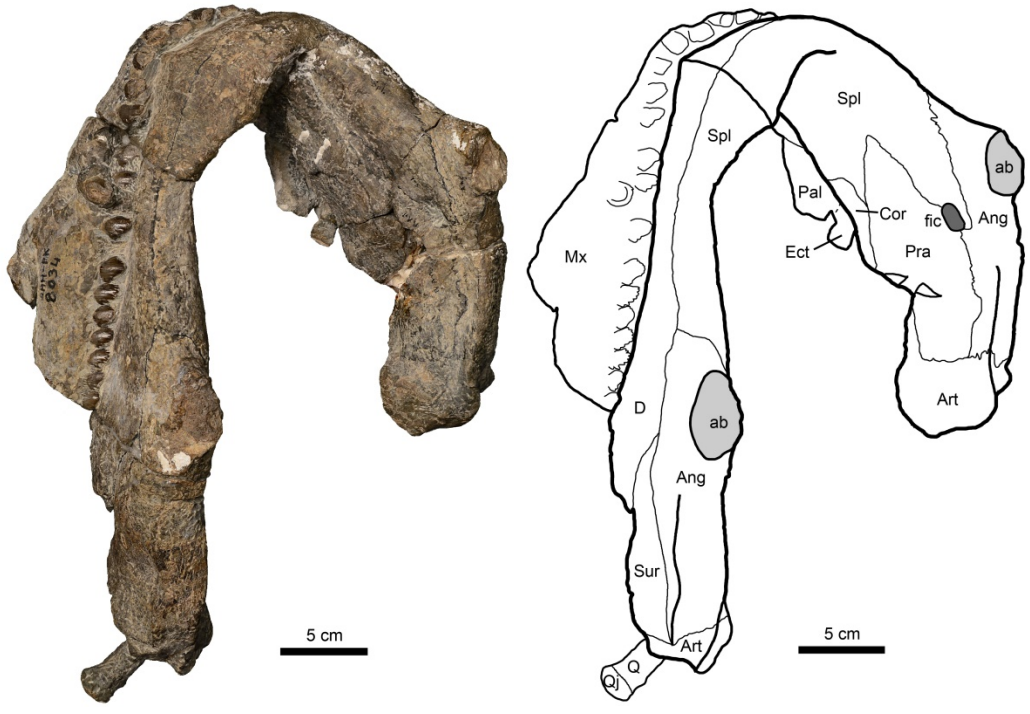


**Figure 3.7:** Photograph (A) and interpretive drawing (B) of the lower jaw and snout (fragment A) of SAM-PK-8034, in ventral view.

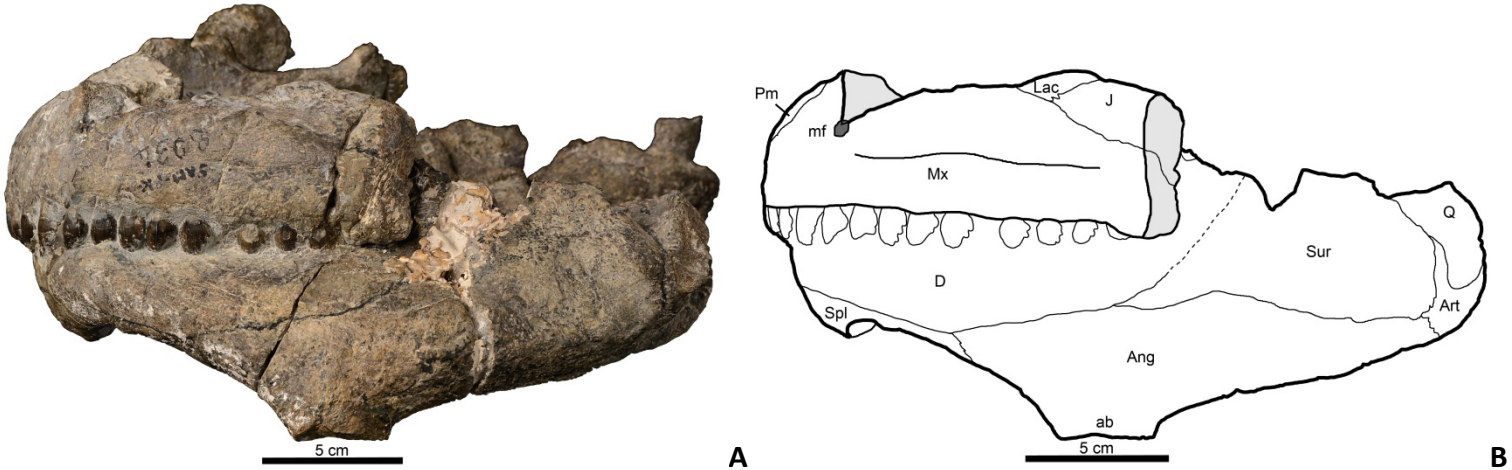


**Figure 3.8:** Photograph (A) and interpretive drawing (B) of the left lower jaw (fragment A) of SAM-PK-8034, in lateral view.

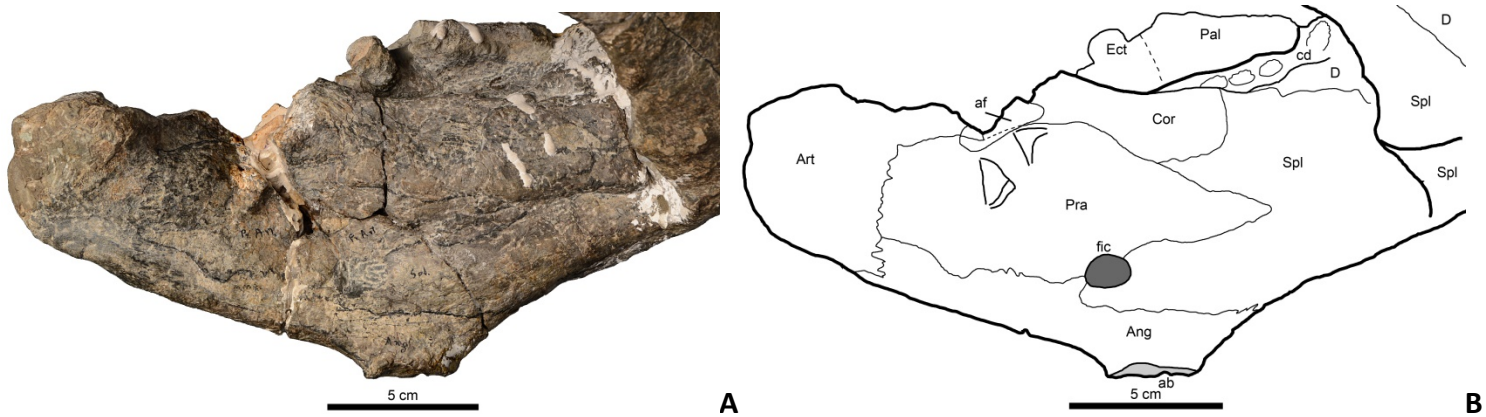


**Figure 3.9:** Photograph (A) and interpretive drawing (B) of the left lower jaw (fragment A) of SAM-PK-8034, in medial view.

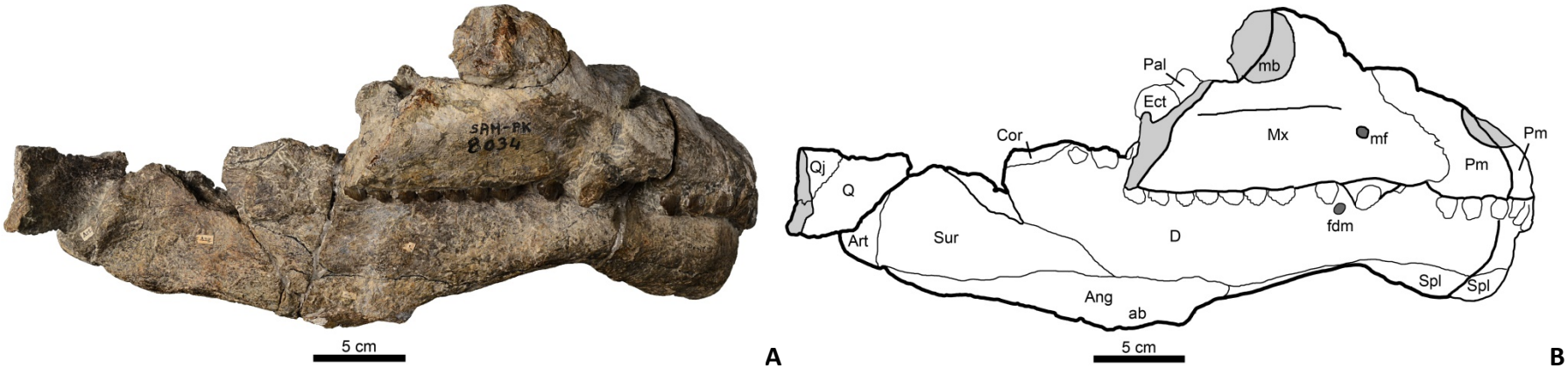


**Figure 3.10:** Photograph (A) and interpretive drawing (B) of the right lower jaw (fragment A) of SAM-PK-8034, in lateral view.

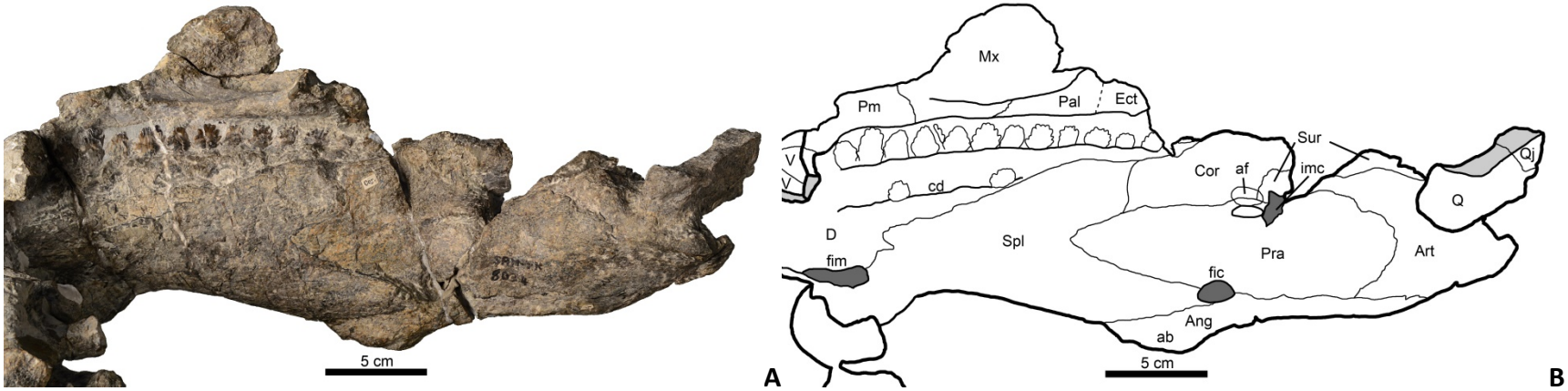


**Figure 3.11:** Photograph (A) and interpretive drawing (B) of the right lower jaw (fragment A) of SAM-PK-8034, in medial view.

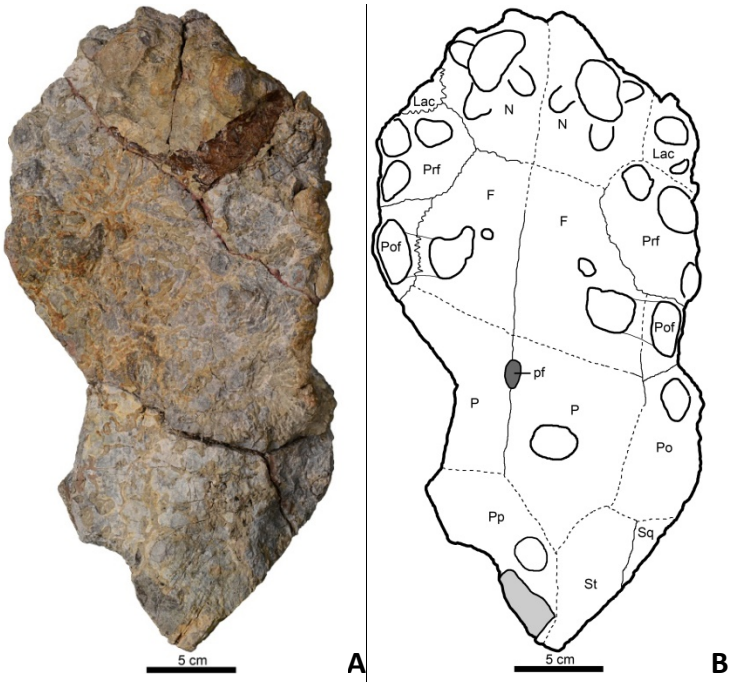


**Figure 3.12:** Photograph (A) and interpretive drawing (B) of the skull table (fragment B) of SAM-PK-8034, in dorsal view. Anterior to the top of the page.

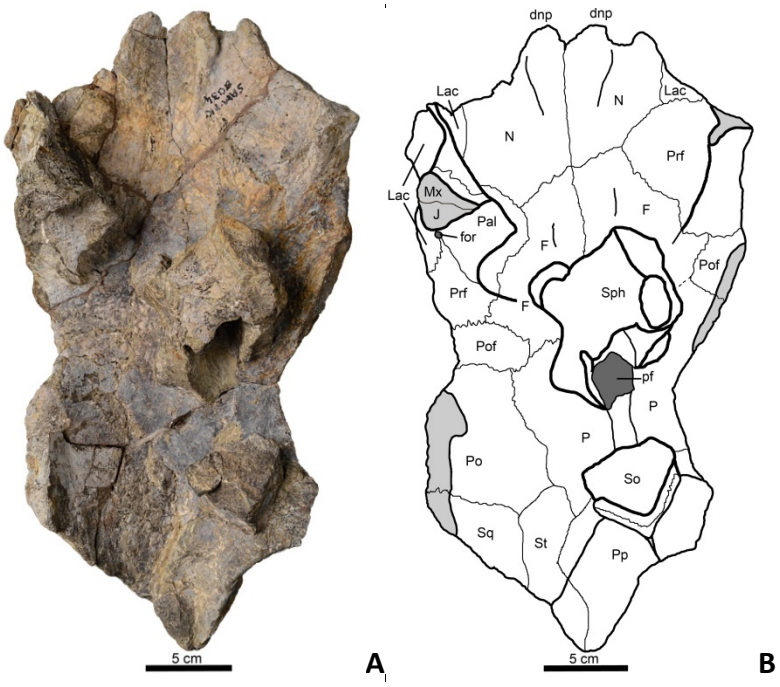


**Figure 3.13:** Photograph (A) and interpretive drawing (B) of the skull table (fragment B) of SAM-PK-8034, in ventral view. Anterior to the top of the page.

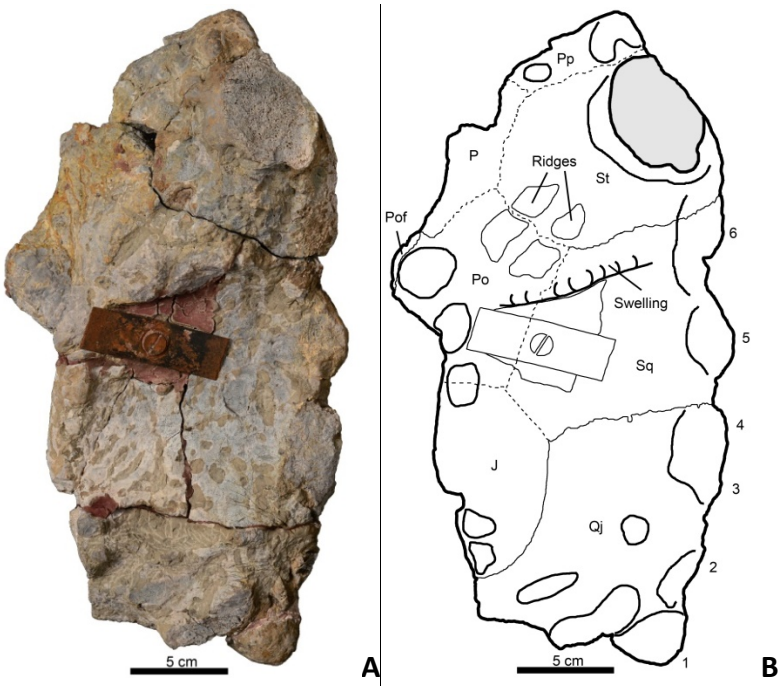


**Figure 3.14:** Photograph (A) and interpretive drawing (B) of the left cheek (fragment C) of SAM-PK-8034, in lateral view, with metal plates, screws and putty shown. Dorsal to the top of the page.

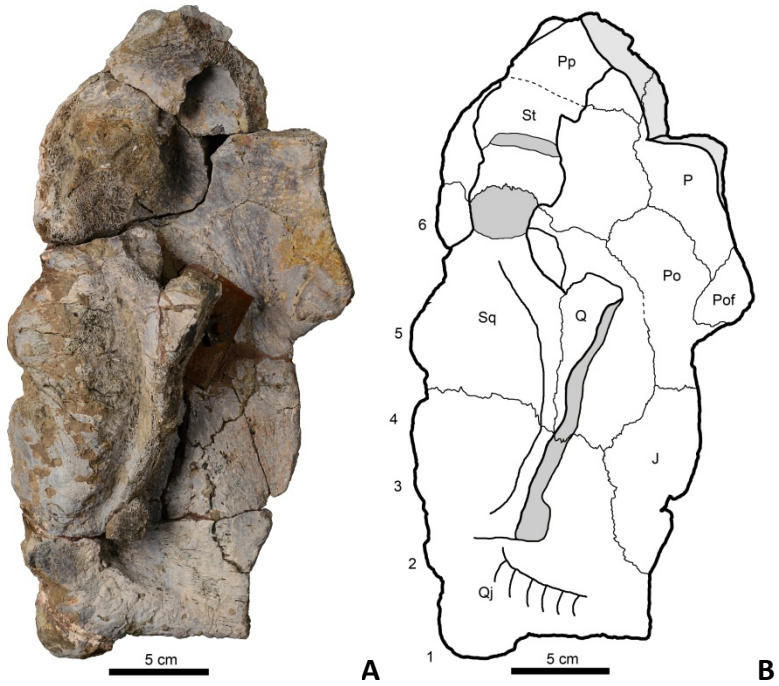


**Figure 3.15:** Photograph (A) and interpretive drawing (B) of the left cheek (fragment C) of SAM-PK-8034, in medial view. Dorsal to the top of the page.

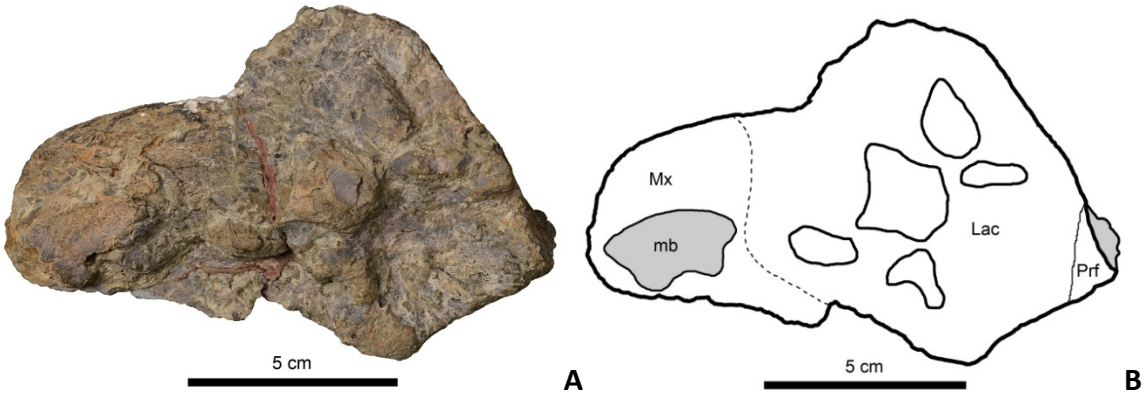


**Figure 3.16:** Photograph (A) and interpretive drawing (B) of the left lacrimal (fragment D) of SAM-PK-8034, in lateral view. Dorsal to the top of the page.

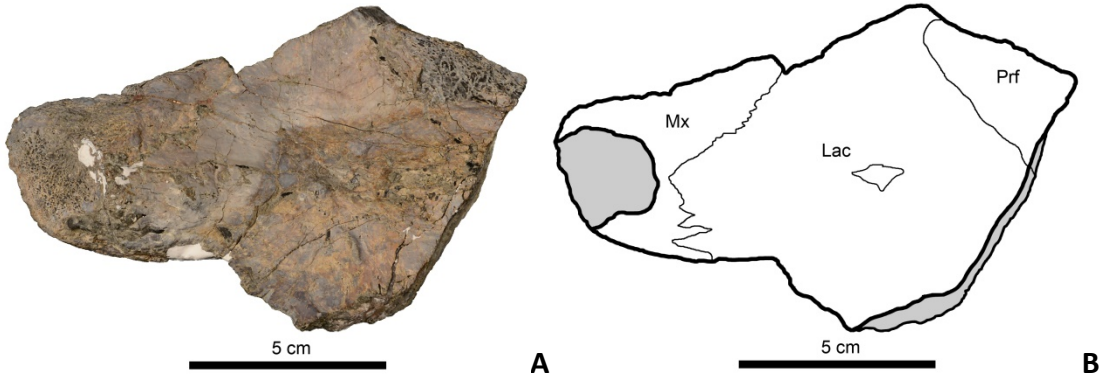


**Figure 3.17:** Photograph (A) and interpretive drawing (B) of the left lacrimal (fragment D) of SAM-PK-8034, in medial view. Dorsal to the bottom of the page.

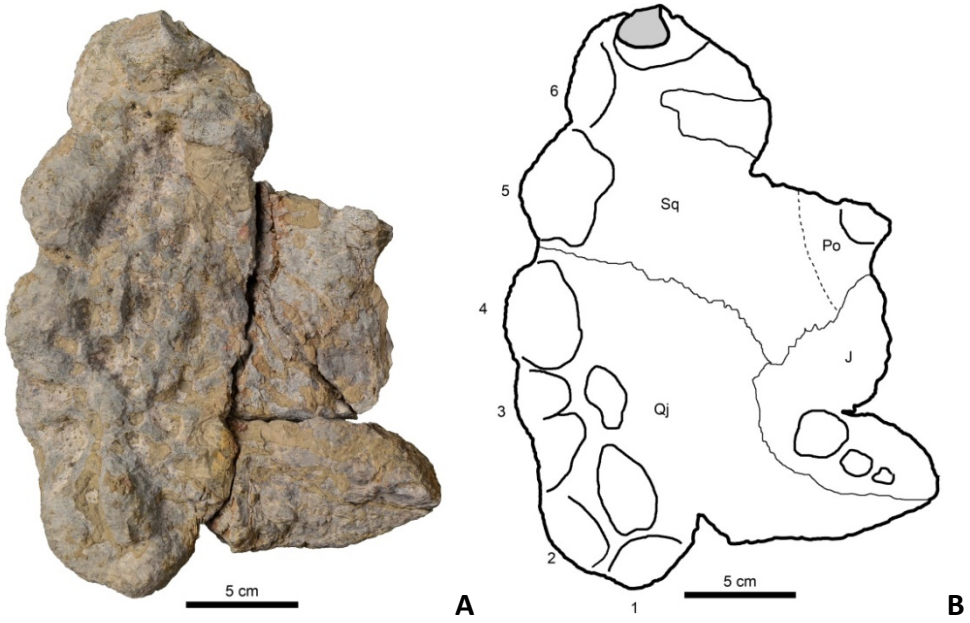


**Figure 3.18:** Photograph (A) and interpretive drawing (B) of the right cheek (fragment E) of SAM-PK-8034, in lateral view. Dorsal to the top of the page.

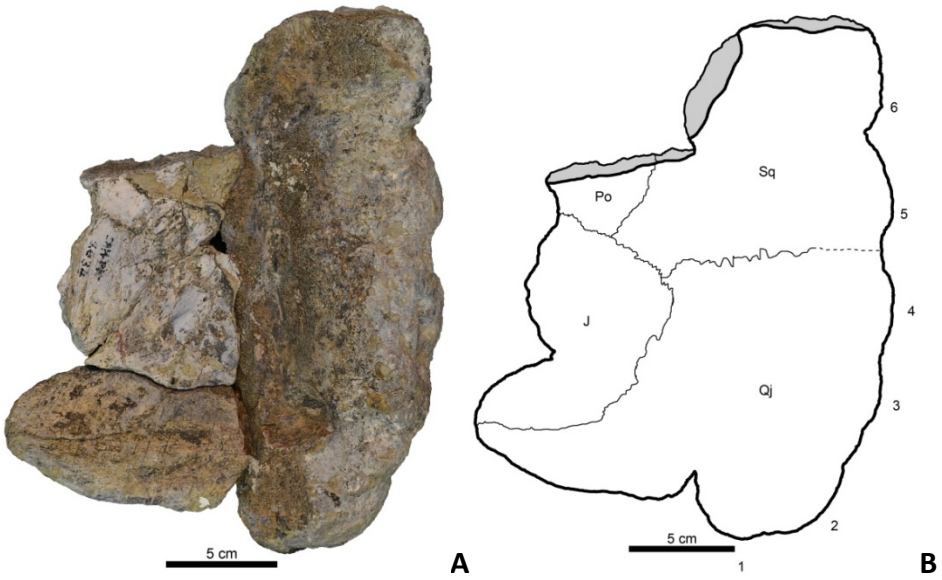


**Figure 3.19:** Photograph (A) and interpretive drawing (B) of the right cheek (fragment E) of SAM-PK-8034, in medial view. Dorsal to the top of the page.

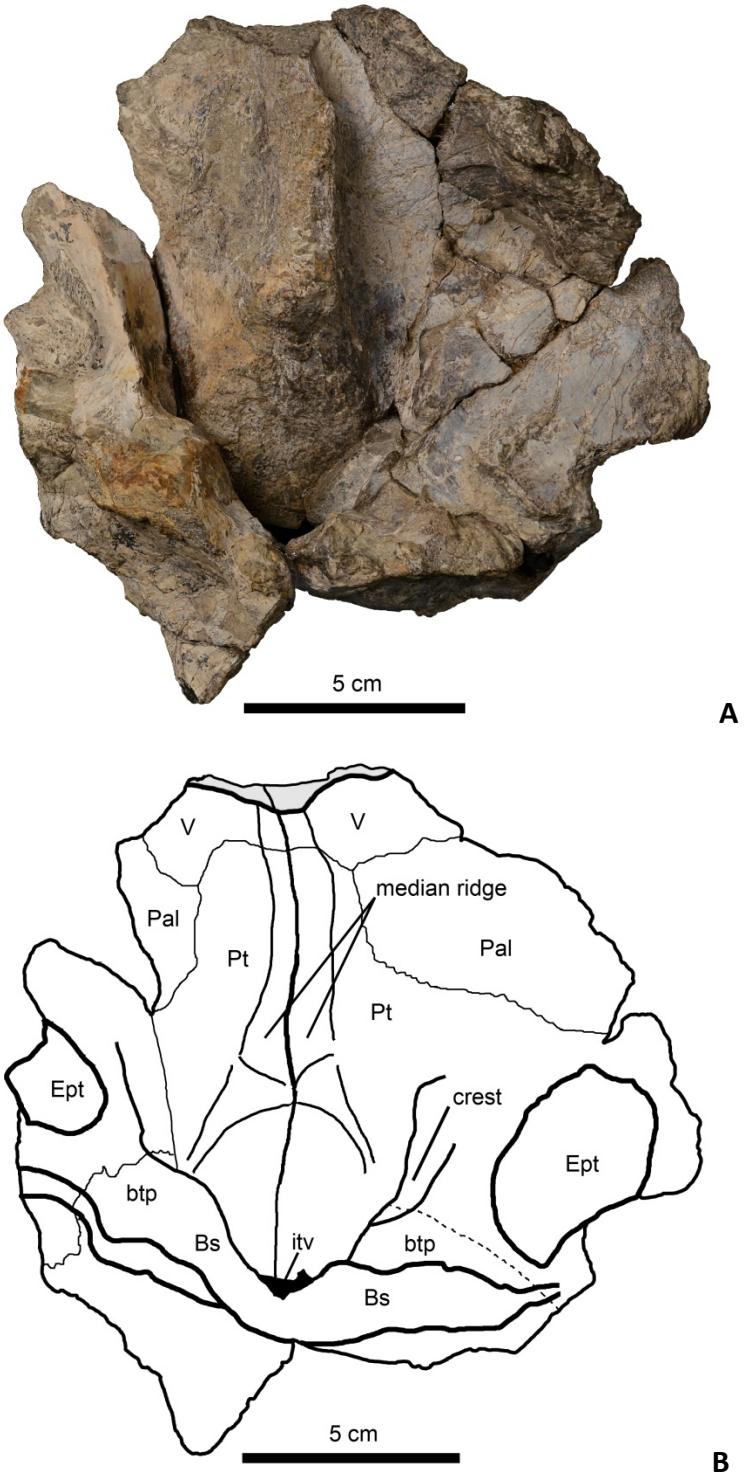


**Figure 3.20:** Photograph (A) and interpretive drawing (B) of the palate (fragment F) of SAM-PK-8034, in dorsal view. Anterior to the top of the page.

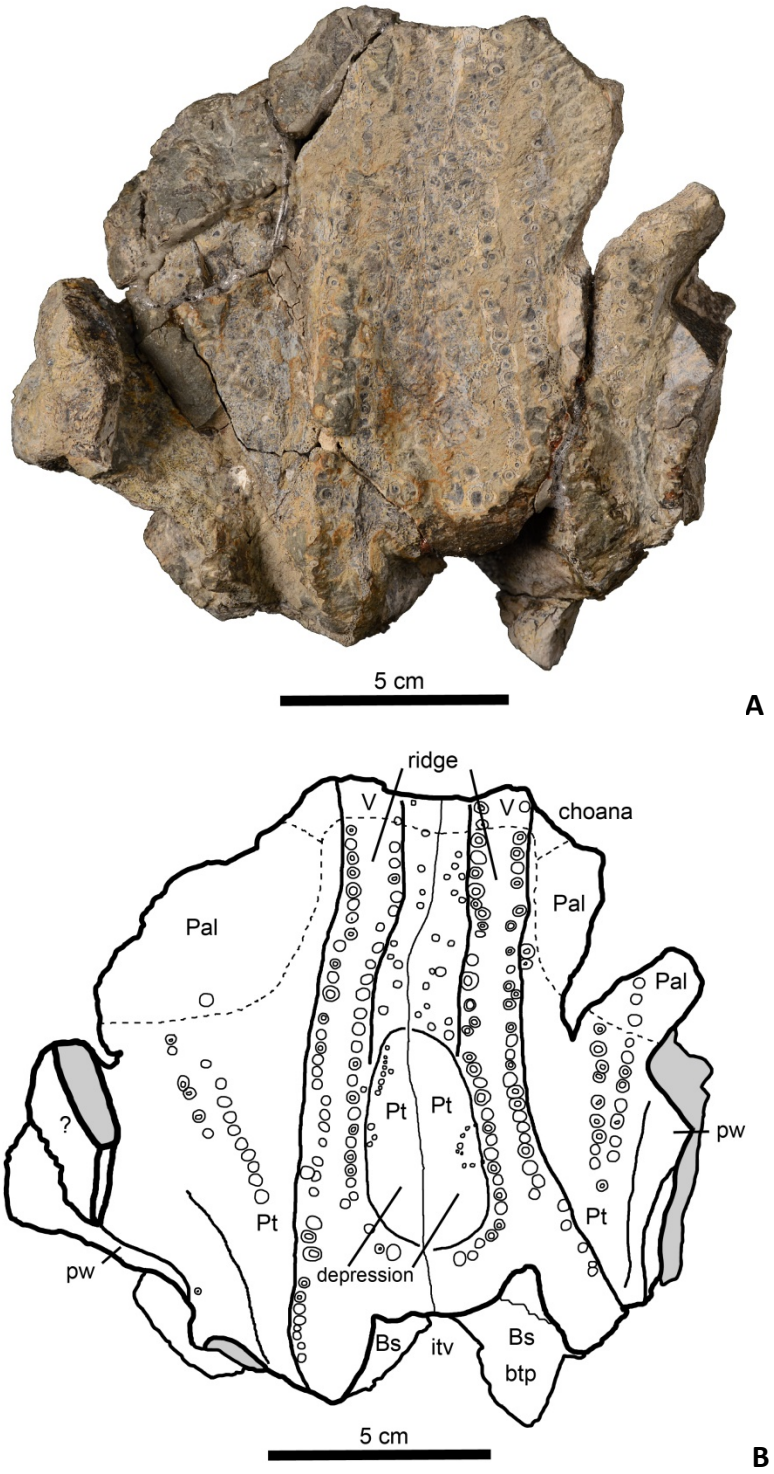


**Figure 3.21:** Photograph (A) and interpretive drawing (B) of the palate (fragment F) of SAM-PK-8034, in ventral view. Anterior to the top of the page.

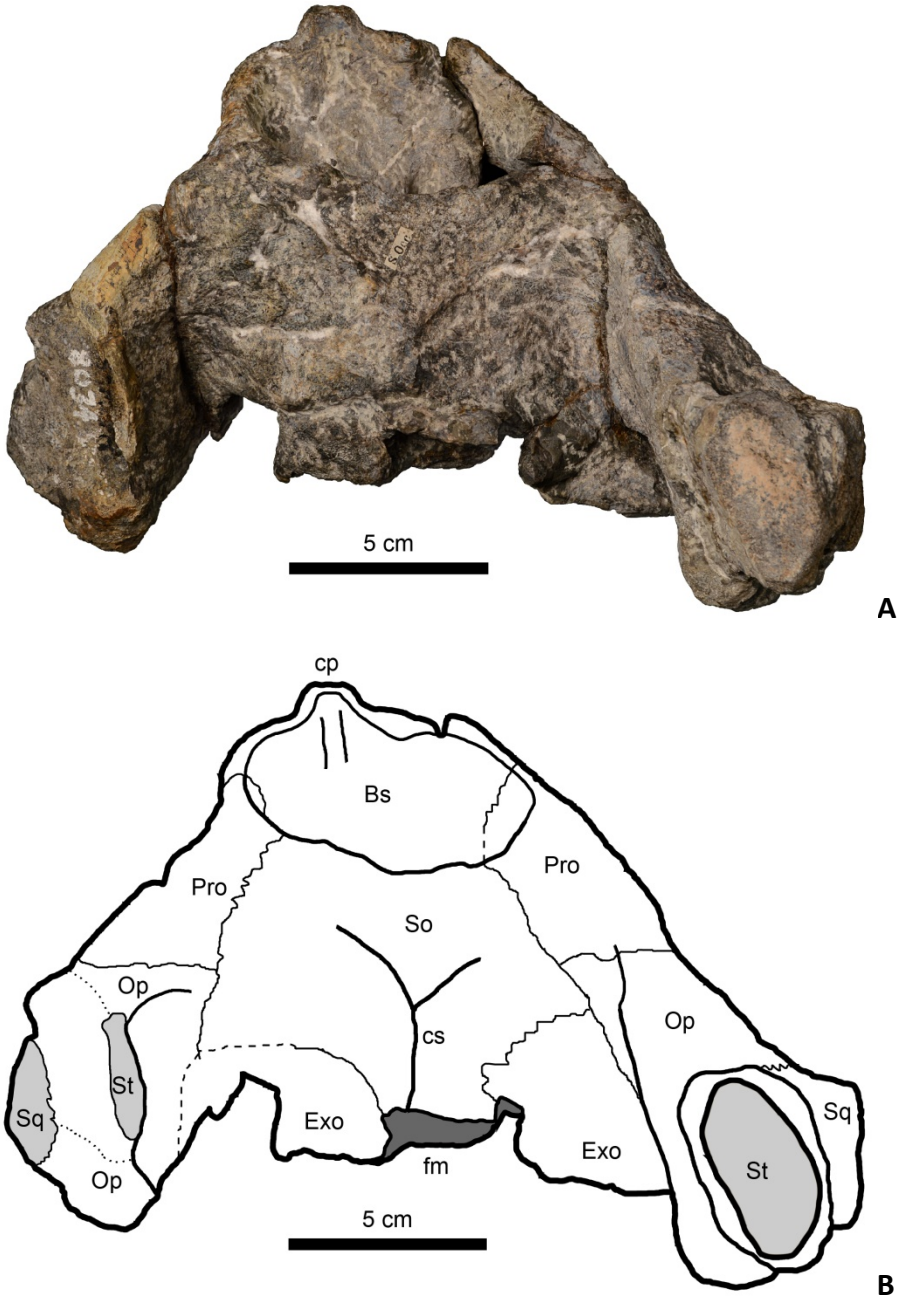


**Figure 3.22:** Photograph (A) and interpretive drawing (B) of the braincase (fragment G) of SAM-PK-8034, in dorsal view. Anterior to the top of the page.

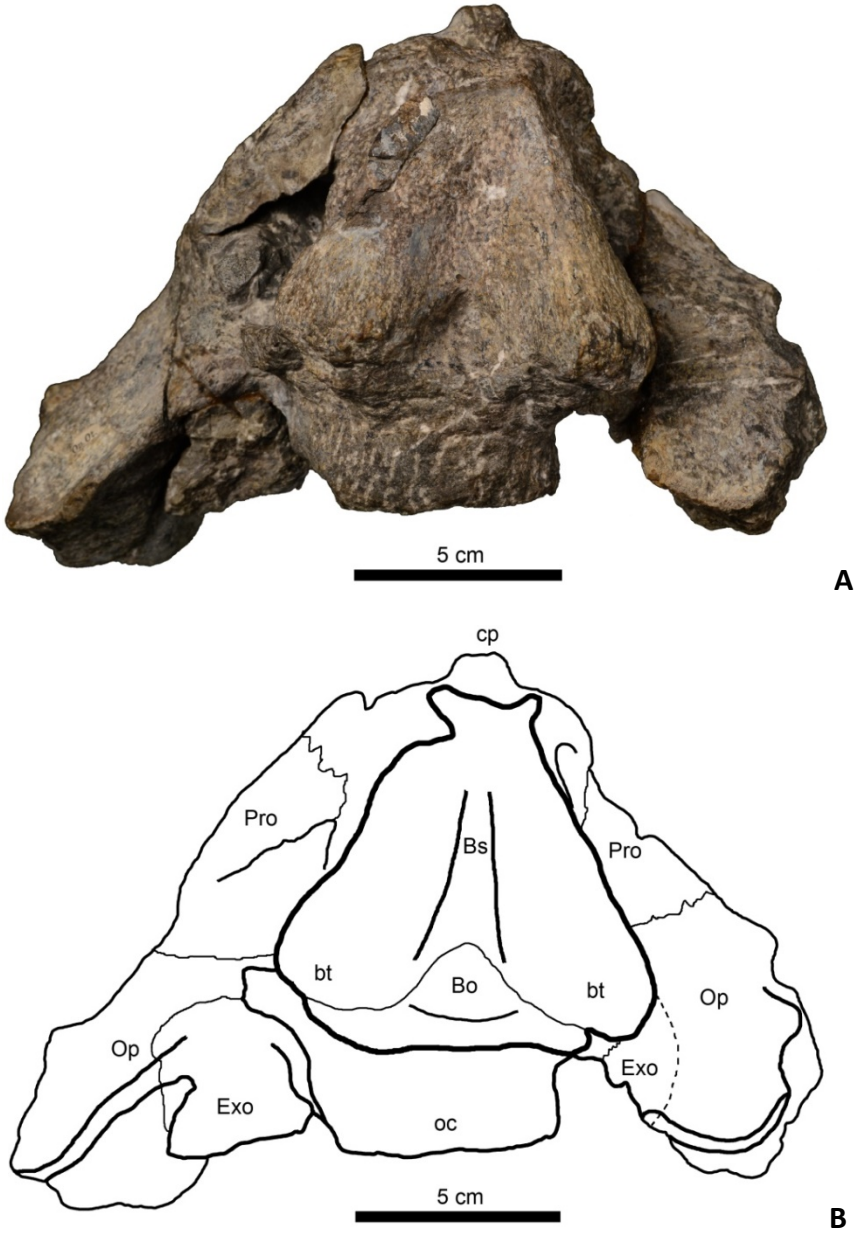


**Figure 3.23:** Photograph (A) and interpretive drawing (B) of the braincase (fragment G) of SAM-PK-8034, in ventral view. Anterior to the top of the page.

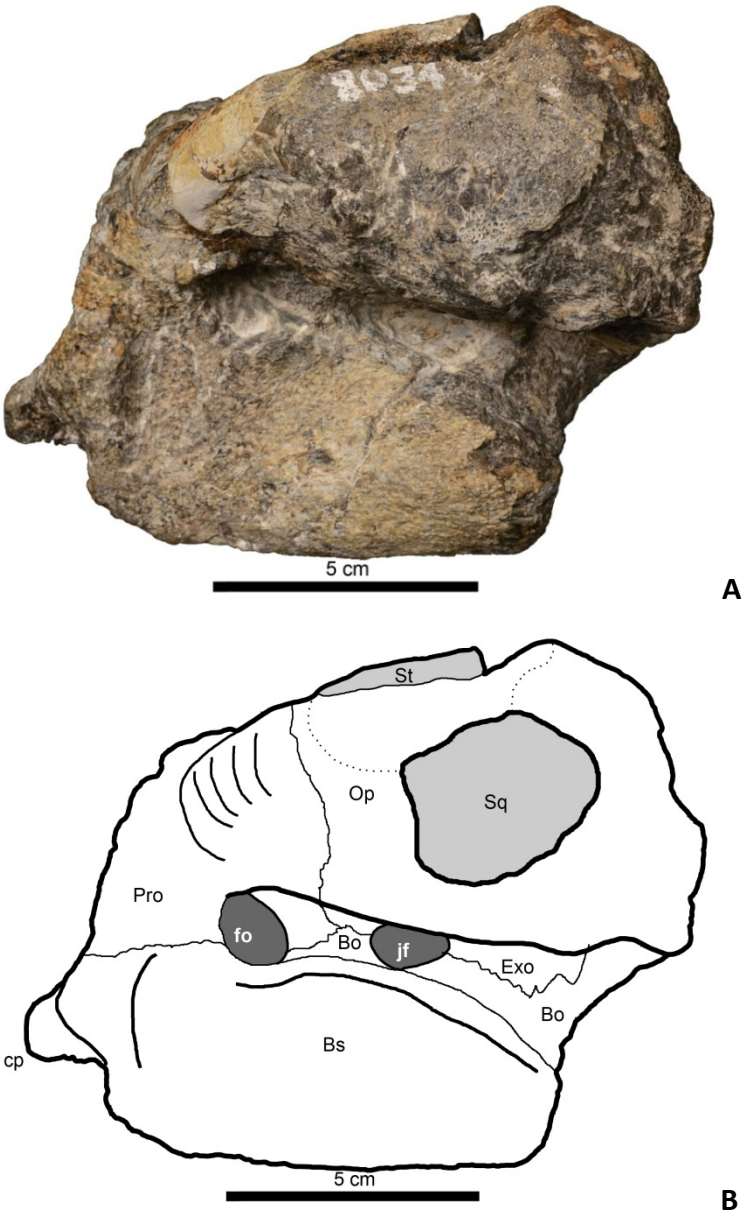


**Figure 3.24:** Photograph (A) and interpretive drawing (B) of the braincase (fragment G) of SAM-PK-8034, in left lateral view. Dorsal to the top of the page.

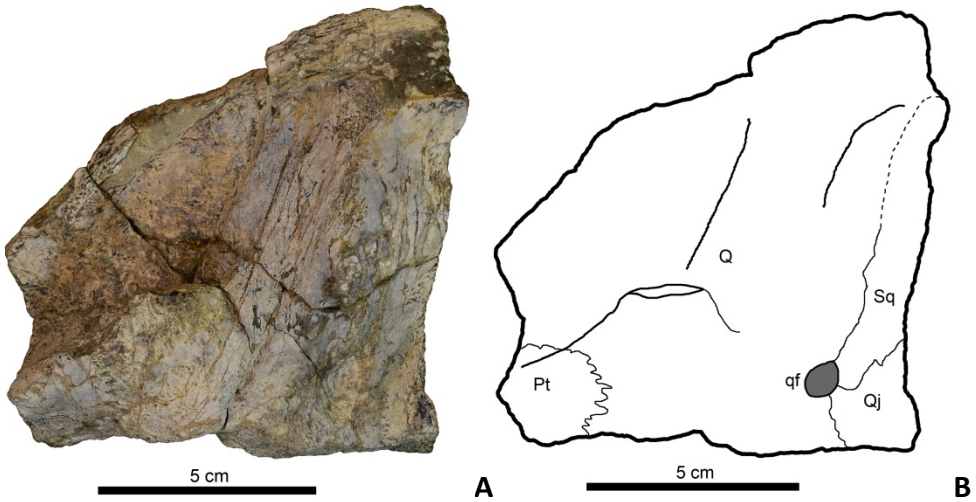


**Figure 3.25:** Photograph (A) and interpretive drawing (B) of the right quadrate (fragment H) of SAM-PK-8034, in occipital view. Dorsal to the top of the page.

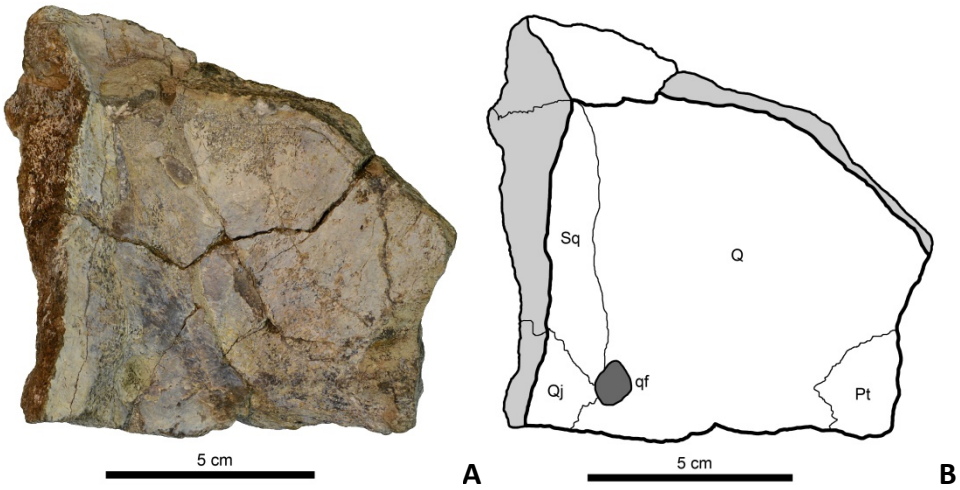


**Figure 3.26:** Photograph (A) and interpretive drawing (B) of the right quadrate (fragment H) of SAM-PK-8034, in anterior view. Dorsal to the top of the page.

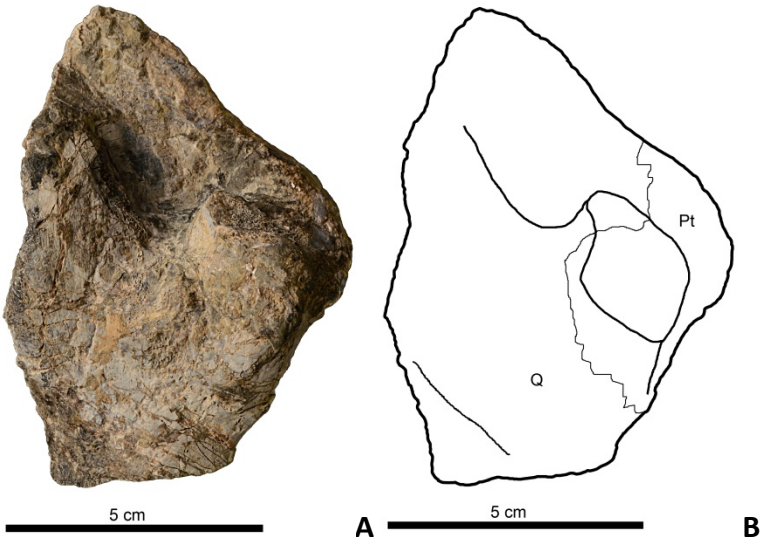


**Figure 3.27:** Photograph (A) and interpretive drawing (B) of the left quadrate (fragment I) of SAM-PK-8034, in occipital view. Dorsal to the top of the page.

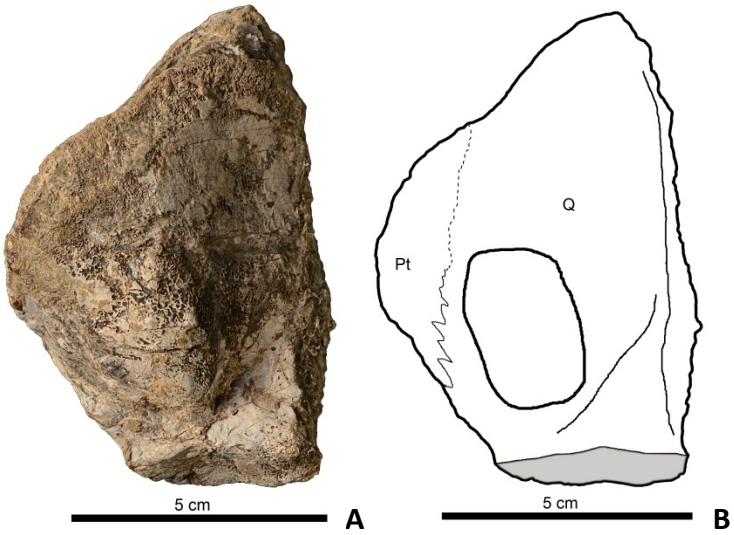


**Figure 3.28:** Photograph (A) and interpretive drawing (B) of the left quadrate (fragment I) of SAM-PK-8034, in anterior view. Dorsal to the top of the page.

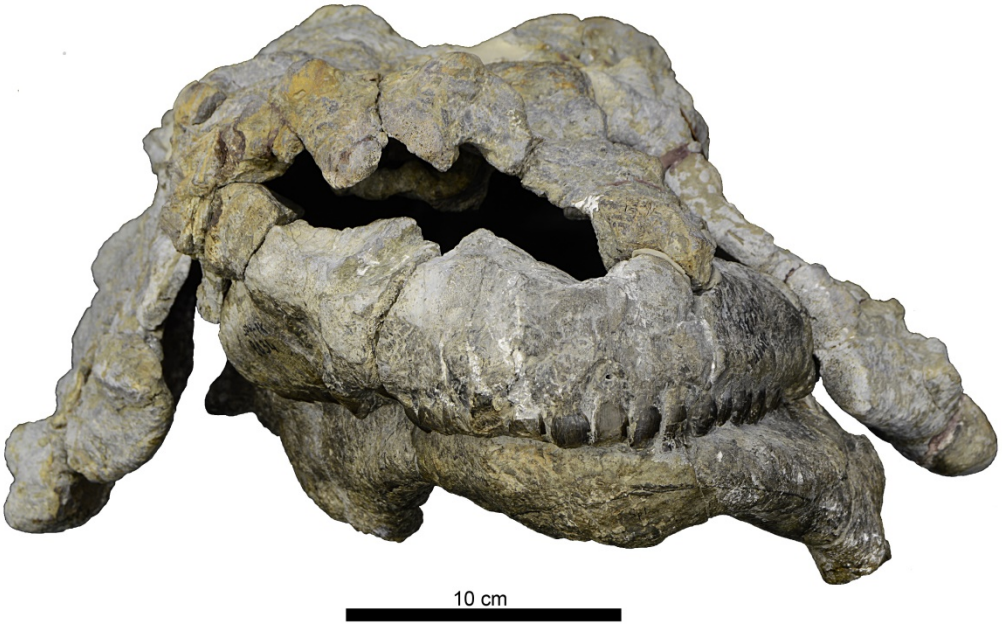


**Figure 3.29:** Photograph of the skull of SAM-PK-8034, in anterior view.




**Figure 3.30:** Photograph of the anterior snout and upper jaw teeth (premaxilla) of SAM-PK-8034, in anterior view. Three damaged premaxillary teeth can be seen either side of the midline.

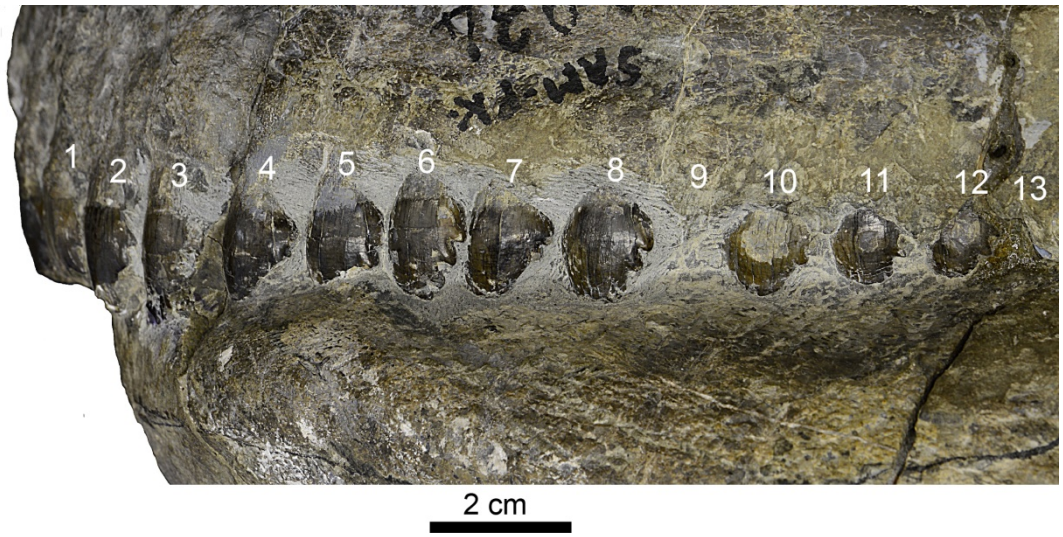


**Figure 3.31:** Photograph of the upper left tooth row of SAM-PK-8034, in left lateral view, showing all thirteen exposed maxillary teeth (numbered 1-13), including the gap where the missing ninth tooth would be.

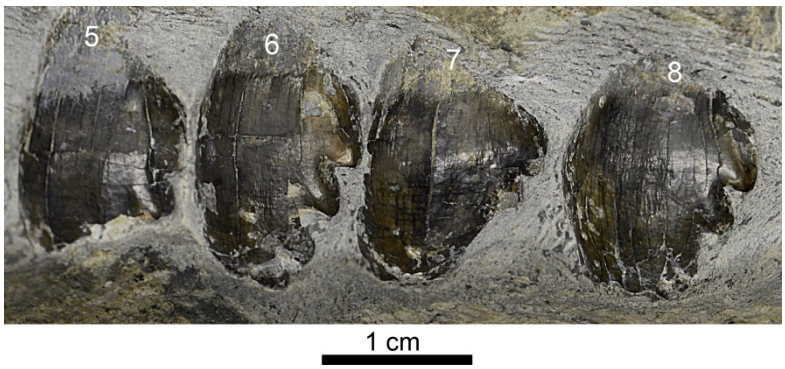


**Figure 3.32:** Photograph of the upper left maxillary teeth of SAM-PK-8034, in lateral view, showing the fifth to eighth teeth. Cusp numbers are not easy to discern due to uncleared matrix and the overlapping nature of the teeth.

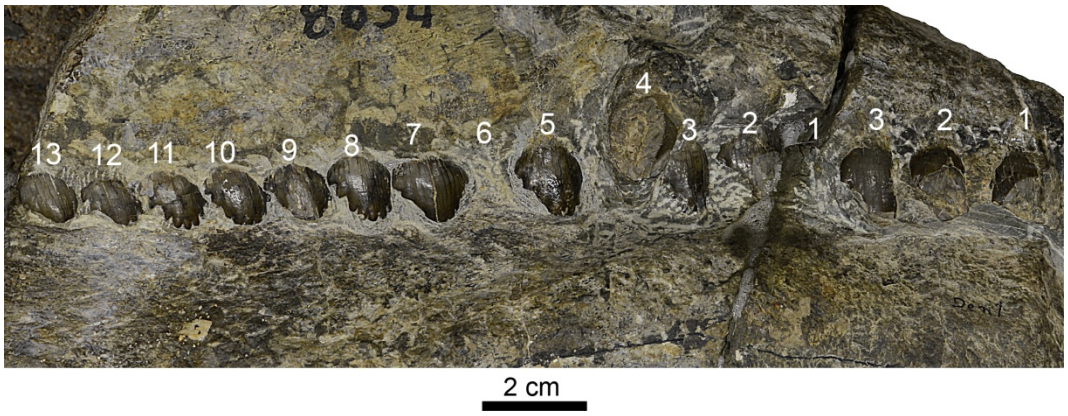


**Figure 3.33:** Photograph of the upper right tooth row of SAM-PK-8034, in lateral view, showing all three exposed premaxillary teeth (numbered 1-3) and all thirteen exposed maxillary teeth (numbered 1-13).

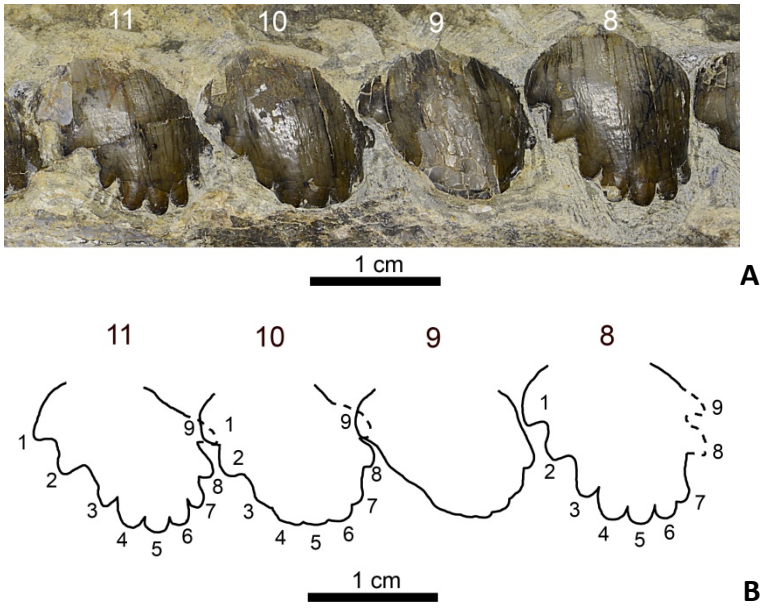


**Figure 3.34:** Photograph (A) and interpretive drawing (B) of the upper right maxillary teeth of SAM-PK-8034, in lateral view, showing the eight to eleventh teeth. Nine cusps are easily identifiable on the eighth, tenth and eleventh teeth.




A

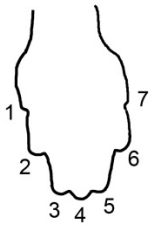


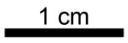


B

**Figure 3.35:** Photograph (A) and interpretive drawing (B) of the right maxillary teeth of NHMUK R1970, in lateral view. Cusps number seven on each tooth. Note the elongated tooth shape, with the three central cusps located at the distal end of the long trident.

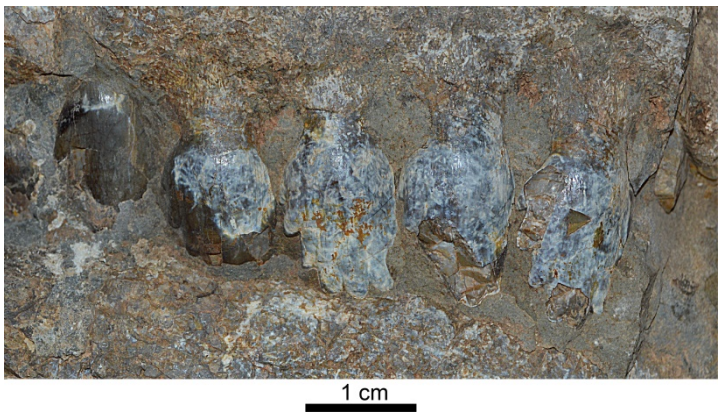


**Figure 3.36:** Photograph of the upper right tooth row of SAM-PK-9098, in lateral view, showing nine cusps on each tooth on wide, short, stubby maxillary teeth, allowing for positive identification as *Embrithosaurus*.

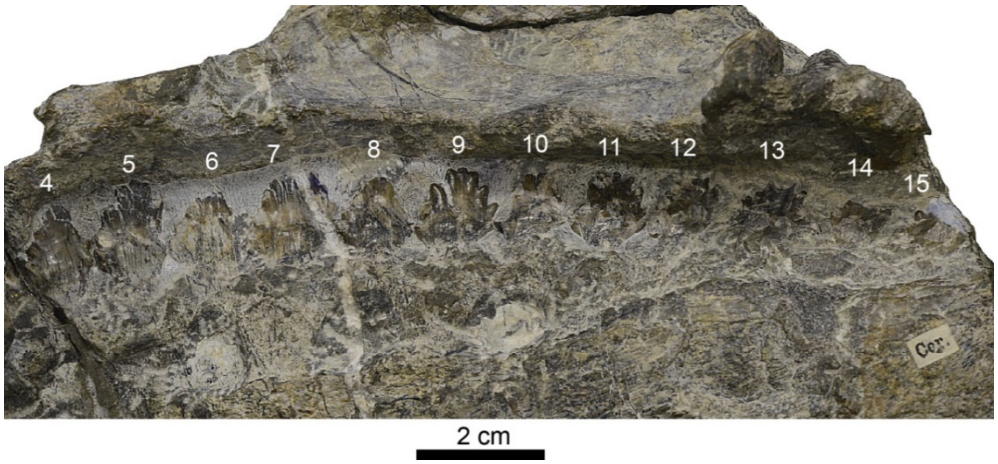


**Figure 3.37:** Photograph of the lower right mandibular tooth row of SAM-PK-8034, in medial view, showing the fourth to fifteenth dentary teeth.

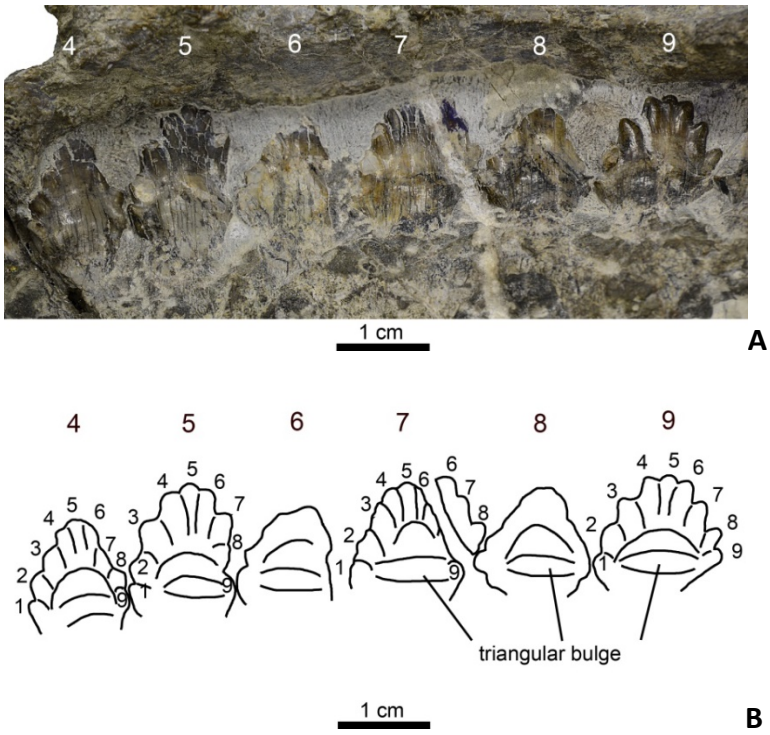


**Figure 3.38:** Photograph (A) and interpretive drawing (B) of the lower right mandibular tooth row of SAM-PK-8034, in medial view, showing the fourth to ninth teeth. Nine cusps are easily identifiable on the fourth, fifth, seventh and nine teeth. Note the triangular bulge.

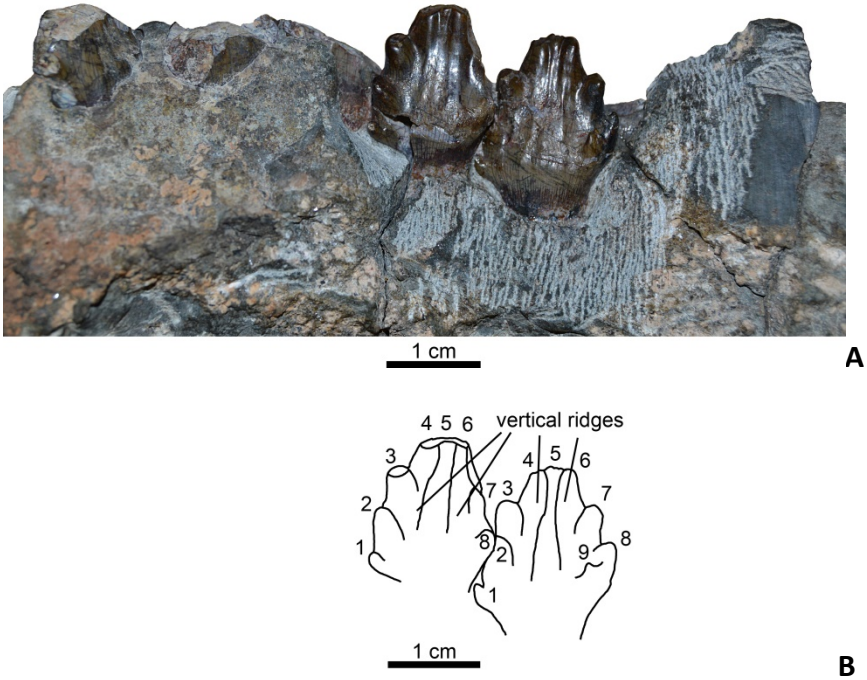


**Figure 3.39:** Photograph (A) and interpretive drawing (B) of lower right mandibular teeth of SAM-PK-6239, in medial view. Note the vertical ridges from cusps four and six, and the non-symmetrically arranged lateral marginal cusps on the anterior margin (cusps one and two) and the posterior margin (cusps eight and nine).

# CHAPTER FOUR: RESULTS: TAXONOMIC REVIEW

## 4.1 Format and introduction

This chapter begins with two tables that show the condition of 14 features that vary among the four pareiasaurs compared: Table 4.1, for dentition, and Table 4.2, for the skull, and are expained in the amended diagnoses of *Embrithosaurus*.

I have accepted the taxonomy proposed by Lee (1995, 1997a), in which four taxa are valid, as my study shows numerous differences in the cranial morphology of the four taxa.

The logical flow of this chapter has been designed as follows for each taxon discussed. First the most recent diagnosis of Lee (1995, 1997a) is presented (an approach also used by Tsuji 2010) consisting of cranial and postcranial autapomorphies, and the cranial and postcranial differences with the other *Tapinocephalus* Assemblage Zone pareiasaurs. Lee's synonym list is also presented.This is followed by my amended diagnosis, consisting of: synonyms, cranial autapomorphies, and the diagnoses containing unique and shared anatomical characters with the other basal species. Although shared anatomical characters with other basal species are not usually included in a diagnosis, they are included here, as these basal species are very similar to each other and can often only be identified through a combination of these shared features. In the amended diagnosis of *Embrithosaurus schwarzi* only, an additional section explains in detail the five dental and nine cranial features noted in Table 4.1 and Table 4.2, even though this creates some repetition of information.

Postcrania were not studied and are not included in my amended diagnosis, and therefore I retain Lee's (1995, 1997a) postcranial autapomorphies and differences compared to the other *Tapinocephalus* Assemblage Zone pareiasaurs

Autapomorphies discussed are unique anatomical features present in only one pareiasaurian taxon, considering all species and not only the basal forms.

Finally, for each taxon, I list and comment on the holotype specimen, the specimens identified by Lee (1995, 1997a) with which I concur, and the specimens that I have identified in this study.

| DENTAL FEATURES | *Embrithosaurus* | *Nochelesaurus* | *B. baini* | *B. seeleyi* |
|---|---|---|---|---|
| 1. Maxillary teeth - cusps | **9** | 7-9 | 7- 9 | **7** |
| 2. Maxillary teeth - shape and central tower cusp arrangement | **Wide, 5 cusp central tower** | Elongated, 3 cusp central tower | Elongated, 3 cusp central tower | Elongated, 3 cusp central tower |
| 3. Mandibular teeth - cusps | **9** | 7-9 | 7-9 | **7** |
| 4. Mandibular teeth – cusp arrangement | Symmetrical mesial and distal marginal cusps | **Non-symmetrical mesial and distal marginal cusps** | Symmetrical mesial and distal marginal cusps | Symmetrical mesial and distal marginal cusps |
| 5. Mandibular teeth - lingual surface features | Low triangular bulge, smooth, without ridges | **High vertical bulge, not smooth, two vertical ridges** | Low triangular bulge, smooth, without ridges | Low triangular bulge, smooth, without ridges |

**Table 4.1:** Dental comparison of South African middle Permian pareiasaurs. Normal text indicates when the feature is shared by more than one species. Bold text indicates when the feature is unique to a particular species in the group.

| CRANIAL FEATURES | *Embrithosaurus* | *Nochelesaurus* | *B. baini* | *B. seeleyi* |
|---|---|---|---|---|
| 6. Maxilla: boss<br><br>AND<br><br>Maxilla: buckling (bending) | Small boss<br><br>Slightly buckling | No boss<br><br>Not buckled | Large boss: High, raised, forming a wide pad<br><br>Sharp buckling | No boss<br><br>Slightly buckled |
| 7. Lacrimal bosses | Relatively distinct | Relatively distinct | **Relatively indistinct** | Relatively distinct |
| 8. Posterior cheek bosses – size and shape | Big, bulbous, somewhat indistinct, wide "teat" shaped corner boss | Horizontal, flat, plate like, posteriorly pointed. Very large, long, "teat" shaped corner boss | Big, bulbous, somewhat indistinct, wide conical corner boss<br>OR<br>Small, round, more distinct. pointed conical corner boss | Small, round, more distinct, conical corner boss |
| 9. Posterior cheek bosses – arrangement pattern (numbers and spacing) | **Corner boss, small boss, tall boss** | Corner boss, small boss, tall boss<br>OR<br>corner boss, two small, bosses, tall boss | Corner boss, small boss, tall boss<br>OR<br>corner boss, two small, bosses, tall boss | Corner boss, small boss, tall boss<br>OR<br>corner boss, two small, bosses, tall boss |
| 10. Quadratojugal lateral surface | Swollen boss complex, curved long bosses or rugosity, horizontal embayment | **Flat surface, curved discrete round bosses** | Swollen boss complex, curved long bosses or rugosity, horizontal embayment | (Poorly preserved) |
| 11. Postparietal shape | Transversely wide, rectangular | Transversely wide, rectangular | **Transversely narrow, square** | **Transversely narrow, square** |
| 12. Cheek size – overhang amount | Large | Large | Small to large | Small |
| 13. Cheek size - angle made below tooth row | Large | Large | Small to large | Small |
| 14. Paroccipital process of opisthotic - size of swollen distal knob | Small to medium | Small to medium | Largest | None, small to medium |

**Table 4.2:** Cranial comparison of South African middle Permian pareiasaurs. Bold text indicates when the feature is unique to a particular species, or is shared by more than one species in the group.

## 4.2 *Embrithosaurus schwarsi* Watson (1914)

### 4.2.1 Diagnosis (Lee 1995, 1997a)

**Synonyms:**

None

**Autapomorphies:**

**Cranial:**

No cranial autapomorphies identified.

**Postcranial:**

*Embrithosaurus schwarzi* is diagnosed with three pelvic autapomorphies:

- A flat, non- everted anterior expansion of the iliac blade. In dorsal view: the anterior expansion of the iliac blade is large and its ventral border is not everted, such that this bone presents a thin edge when viewed dorsally. In all other pareiasaurs, the sacral blade is slightly too greatly everted, presenting a wide lateral surface, when viewed dorsally.
- The iliac blades diverge anteriorly, making an angle of about 40 degrees with the sagittal plane when viewed dorsally, and are not parallel. In all other pareiasaurs, the iliac blades are almost parallel.
- The pelvic symphysis is extremely thick, being almost half as deep as long. In all other pareiasaurs the pelvic symphysis is much thinner.

**Differences compared to other *Tapinocephalus* Assemblage Zone pareiasaur species (Lee 1995, 1997a):**

**Cranial:**

Differentiated from *Bradysaurus* by having more cusps on the teeth (seven to nine cusps per tooth) and larger descending cheek flanges; and

from *Nochelesaurus* by the lack of the distinctive pointed posterior cheek bosses.

**Postcranial:**

Differentiated from from *Bradysaurus* and *Nochelesaurus* by the presence of a narrower femur, and a curved or s-shaped internal trochanter on the femur, not visible in dorsal view. *Embrithosaurus* uniquely possesses distinct small, rounded, central bosses on each osteoderm or scute above the vertebral column, which is of irregular shape, with no ridges radiating out from the centre. *Bradysaurus* and *Nochelesaurus* do not possess bosses on the osteoderms above their vertebral column. *Embrithosaurus* can also be differentiated from *Bradysaurus* in that the torsion in the humerus is only 45 degrees (and not 60 degrees as in *Bradysaurus*).

### 4.2.2 Amended Diagnosis

**Synonyms:**

None

**Autapomorphies:**

**Cranial:**

No unique cranial autapomorphies were identified on the holotype or referred specimens, during this study.

Within the group of *Tapinocephalus* Assemblage Zone species**,** *Embrithosaurus* possesses uniquely shaped wide, short, stubby, and bulbous maxillary teeth, with nine marginal cusps on maxillary and mandibular teeth, cusps arranged more regularly on the maxillary teeth, the presence of only one boss dorsal to the corner boss on the posterior

edge of the quadratojugal, and a small maxillary boss with slight maxillary buckling.

*Embrithosaurus* shares with *Nochelesaurus* a transversely wide and rectangular postparietal and large cheek flanges.

*Embrithosaurus* shares with *B. baini* large, wide, bulbous, indistinct bosses on the posterior edge of the quadratojugal and a swollen boss complex on the lateral surface of the quadratojugal that consists of curved, long bosses with a deep horizontal embayment separating the jugal from the quadratojugal.

**Differences compared to other *Tapinocephalus Assemblage Zone* species:**

**Cranial:**

*Embrithosaurus schwarzi* can be distinguished from the other pareiasaurs of the *Tapinocephalus* Assemblage Zone by the following combination of dental and cranial features.

**Dental features:**

1. *Embrithosaurus schwarzi* can be differentiated from *B. baini*, *B. seeleyi* and *Nochelesaurus* by the presence of nine marginal cusps on all mature and fully erupted maxillary teeth (SAM-PK-8034, SAM-PK-9098), which do not vary in number between different teeth of the same skull. *B. seeleyi* has seven maxillary cusps that do not vary on different teeth (NHMUK 49426). *B. baini* and *Nochelesaurus* share variable, between seven to nine, maxillary teeth cusps. The holotype of *Nochelesaurus* (SAM-PK-6239) has eight to nine cusps on different maxillary teeth. For *B. baini,* seven cusps is the most common condition, but on a referred specimen (SAM-PK-5624) the first left pre-maxillary tooth has nine cusps.
2. *Embrithosaurus schwarzi* possesses unique maxillary teeth which are wide, short, stubby, and bulbous in labial view, due to the more regular

pattern of placement and spacing between the marginal cusps. Three central cusps are located at the apex or distal end of the crown, at the same level, with no gaps between them, followed laterally by a very small gap to the first lateral cusp on either side of the crown, creating the appearance of five central cusps being very close together (SAM-PK-8034, SAM-PK-9098). Two further lateral cusps are present towards the base of the tooth on either side, with large gaps between them, and with the lowest of these cusps located at the base of the crown (Fig. 3.34)**.** In *B. baini, B. seeleyi* and *Nochelesaurus* the maxillary tooth shape in labial view is elongated, tall and narrow, with the three most central cusps being very close together, at the same level, situated at the distal end of the crown on a long, narrow, isolated trident (Fig. 3.38). They also show a much larger gap to the first lateral cusp on either side of the elongated trident, compared to *Embrithosaurus*. Usually *B. baini, B. seeleyi* and *Nochelesaurus* possess only two lateral cusps. Even in the few specimens where *B. baini* and *Nochelesaurus* have nine cusped teeth, the teeth shape are still elongated and narrow with large gaps between all lateral cusps and the central complex.

3. *Embrithosaurus schwarzi* (SAM-PK-8034) can be differentiated from *B. baini*, *B. seeleyi* and *Nochelesaurus* through the presence of nine marginal cusps on all mature and fully erupted mandibular teeth, which do not vary in number between different teeth of the same specimen. *B. seeleyi* has seven mandibular cusps (holotype NHMUK 49426) that do not vary on different teeth. *Bradysaurus. baini* and *Nochelesaurus* possess seven to nine cusps on the mandibular teeth. The holotype of *Nochelesaurus* (SAM-PK-6239) shows eight to nine cusps but a referred specimen (SAM-PK-6240) shows seven on all teeth. For *B. baini*, seven cusps are the most common arrangement, but a referred specimen (SAM-PK-5624) shows eight to nine cusps on several different dentary teeth.

4. In *Embrithosaurus schwarzi*, *B.baini* and *B. seeleyi*, the marginal cusps on each mandibular tooth are arranged symmetrically around the crown, i.e. the spacing between the lateral cusps on the mesial and the distal marginal sides of each tooth crown, are the same (Fig. 3.38). In contrast, *Nochelesaurus* (holotype SAM-PK-6239) has non-symmetrically arranged lateral cusps on either side of the crown. The mesial marginal edge shows a very low basal cusp and the distal marginal edge has no cusps present or a small, vertical, pointed medial cusp (Fig. 3.39).
5. *Embrithosaurus schwarzi, B. baini* and *B. seeleyi* have dentary teeth where the lingual surface is smooth, with a low, horizontal, triangular bulge at the base of the crown. In contrast, *Nochelesaurus* (holotype SAM-PK-6239) has a tall vertical bulge that has two long vertical ridges on either side of the bulge. These ridges extend down from the two lateral cusps of the central three cusp complex (Fig. 3.39).

**Cranial features:**

6. The holotype of *Embrithosaurus schwarzi* (SAM-PK-8034) has a maxilla with a small distinct boss, slightly bucked or bent. *B. baini* has a large boss and sharp buckling, *Nochelesaurus* has no buckling or boss, and *B. seeleyi* has a slight buckling and no maxillary boss.
7. *Embrithosaurus schwarzi, Nochelesaurus* and *B. seeleyi* have lacrimals with relatively distinct bosses. In *B. baini* the large maxillary boss extends onto the lacrimal, covering the anterior half of the bone, a condition which makes the lacrimal's anterior bosses appear less distinct.
8. The holotypes of *Embrithosaurus* (SAM-PK-8034) and *B. baini* (NHMUK R1971) have bosses on the posterior edge of the quadratojugal which are large, wide, low, bulbous and indistinct. The corner boss is wide and "teat" shaped in *Embrithosaurus*, and conical in *B. baini*. In a few specimens of *B. baini* (SAM-PK-9121, SAM-PK-5002, SAM-PK-5624) the posterior quadratojugal bosses are smaller, rounder and more distinct. *B.*

*seeleyi* shows small, round and distinct bosses with a conical corner boss. In *Nochelesaurus* the horizontally oriented and posteriorly directed bosses are flat, plate-like and pointed. In occipital view, they appear flat and wide and plate-like, besides for the corner boss which is "teat" shaped and very large and long (SAM-PK-6239, SAM-PK-6238, SAM–PK-9137, CGP JA 109).

9. *Embrithosaurus schwarzi* shows the following pattern for the bosses on the posterior edge of the cheek on the quadratojugal: a corner boss, a small boss located dorsally to the corner boss with large gaps above and below it, and a highest boss made of two very close almost unabated indistinct bosses, which is vertically elongated, large and bulbous and with each component boss having a rugose emanation forward on the lateral surface of the quadratojugal. Most specimens of *B. baini* (NHMUK R1971, SAM-PK-5624, SAM-PK-5002, SAM-PK-9121)*, B. seeleyi* (NHMUK 49426) and *Nochelesaurus alexanderi* (SAM-PK-6239, SAM-PK- 6240) also follow this boss arrangement. A few specimens of *B. baini* (SAM-PK-12014, SAM-PK-9095), *B. seeleyi* (BP/I/7054, BP/I/7886) and *Nochelesaurus alexanderi* (SAM-PK-6238, SAM-PK-9115, CGP JA 109) show two small bosses with wide gaps above and below, located dorsal to the corner boss.
10. In *Embrithosaurus schwarzi* (SAM-PK-8034, left cheek) and *B. baini* (NHMUK R1971, SAM-PK-5002) two to three indistinct posterodorsally orientated and elongated curved protuberances or rugose lines create a general thick swelling of the lower half quadratojugal, ventral to the suture with the jugal. The suture between the quadratojugal and jugal pass through a deep and distinct embayment which is horizontal, long and thin. A single small curved boss is located posterodorsally to the horizontal embayment. In *Nochelesaurus* (SAM-PK-6239, SAM-PK-6238, SAM-PK-6240) the entire lateral surface is very flat and the lower part of the lateral surface of the quadratojugal is not thickened or swollen, and

has distinct equally sized small bosses occurring in a posterodorsally oriented arc. No deep embayment or is present on the jugal-quadratojugal suture.

11. *Embrithosaurus schwarzi* (SAM-PK-8034) and *Nochelesaurus* (SAM-PK-6239) show a transversely wide and rectangular postparietal in dorsal view. In contrast, *B. baini* (NHMUK R1971, SAM-PK-5002 and the light grey unnumbered specimen from the Council of Geosciences) and *B. seeleyi* (SAM-PK-3718) present transversely narrow and square postparietals.
12. *Embrithosaurus schwarzi* (SAM-PK-8034, 26%) and *Nochelesaurus* (SAM-PK-6239, 28%, SAM-PK-6238, 24%, SAM-PK-6240, 28%) have large cheek flanges that overhang below the tooth row (Appendix A, B). *B. baini* shows variation from small (SAM-PK-5002, 22%) to large (NHMUK R1971, 26%) whereas *B. seeleyi* has the smallest cheek overhangs (NHMUK 49426, 19%) (Appendix A, B).
13. *Embrithosaurus schwarzi* (SAM-PK-8034, 29 degrees) and *Nochelesaurus* (SAM-PK-6239, 33 degrees) have large angles between the ventral border of the cheek and the tooth row margin. *B. baini* shows variation from small (SAM-PK-5002, 22 degrees) to large (NHMUK R1971, 30 degrees) whereas *B. seeleyi* has one of the smallest cheek angles (NHMUK 49426, 20%) (Appendix A, B).
14. *Embrithosaurus schwarzi* (SAM-PK-8034)*, Nochelesaurus* (SAM-PK-6240, SAM-PK-8944), and some specimens of *B. seeleyi* (SAM-PK-3718) have a small-to-medium sized knob-like projection near the distal end of the paroccipital process of the opisthotic. In *B. baini* (NHMUK R1971, SAM-PK-5002, SAM-PK-5624, SAM-PK-9168, SAM-PK-9095) there is a larger and more distinct knob (Appendix A, B).

### 4.2.3 Specimens and Comments

**Holotype Specimen SAM-PK-8034:**

See Chapter 2 –Materials and Methods, 2.1.1 Holotype *Embrithosaurus schwarzi* SAM-PK-8034, for a list of the elements preserved, and Chapter 6 Discussion, 6.1.1 *Embrithosaurus schwarzi* for comments.

**Referred specimens identified as *Embrithosaurus* by Lee (1995, 1997a) and retained:**

**Specimen SAM-PK-K324:**

A partial pelvis identified by Lee (1995, 1997a) as *Embrithosaurus*, this postcranial identification is retained.

**Referred specimens identified during this cranial study:**

**Specimen SAM-PK-9105:**

A large unprepared skull with occluded lower jaw and a partial right foot referred to *B. baini* by Boonstra (1934a). This specimen is tentatively assigned to *Embrithosaurus* by a process of elimination. The teeth are too damaged and unprepared to be accessible. The skull does not have a large maxillary boss or sharp buckling and therefore cannot be assigned to *B. baini*. It does not show the flat pointed posterior cheek bosses of *Nochelesaurus* but has large, bulbous bosses on the posterior edges of the cheeks. The cheek is large and therefore cannot belong to *B. seeleyi*.

**Specimen SAM-PK-9098:**

Several cranial fragments, including a large piece of the right cheek and a large piece of the right maxilla. The basal tubera of the braincase are also preserved. Several vertebrae, part of a humerus, and other fragmentary postcranial elements. This specimen was referred to *Brachypareia rogersi* by Boonstra

(1934a). It shows short and wide maxillary teeth, with nine cusps in the same pattern as the holotype of *Embrithosaurus* SAM-PK-8034 (Fig. 3.36). The posterior bosses of the preserved right cheek are wide and bulbous and therefore only consistent with *Embrithosaurus* and *B. baini*.

**Specimen CGP/1/795 (RMS566):**

A large relatively unprepared skull with partial occluded lower jaw. Numerous unprepared postcranial elements. This specimen has not been published yet. The posterior cheek bosses are all large and bulbous, indistinct and almost smooth, and therefore not a match for *Nochelesaurus*. The cheek is large and therefore not a match to *B. seeleyi*. Since there is no large boss on the maxilla, this specimen cannot belong to *B. baini*. The maxillary teeth are damaged but appear to be wide and not elongated, matching the shape of *Embrithosaurus*.

## 4.3 *Nochelesaurus alexanderi* Haughton and Boonstra (1929)

### 4.3.1 Diagnosis (Lee 1995, 1997a)

**Synonyms:**

- *Dolichopareia angusta* (Haughton and Boonstra 1929a) Holotype Specimen: SAM-PK-6238
- *Brachypareia watsoni* (Haughton and Boonstra 1929a) Holotype Specimen: SAM-PK-6240

**Autapomorphies:**

**Cranial:**

No cranial autapomorphies were identified.

**Postcranial:**

*Nochelesaurus alexanderi* is diagnosed by three postcranial autapomorphies:

- The groove on the internal surface of the scapulocoracoid (leading dorsally from the coracoid foramen) is located anteriorly, very close to the anterior margin of the scapula blade. In all other pareiasaurs, this groove is located medially, i.e. in or near the centre of the scapular blade.
- The presence of a distinct tubercle on the centre of the dorsal surface of the entepicondyle process of the humerus.
- The presence of a flange on the dorsal surface of the femur, projecting distally beyond the postaxial tibial facet.

**Differences compared to other *Tapinocephalus* Assemblage Zone pareiasaur species (Lee 1995, 1997a):**

**Cranial:**

*Nochelesaurus* can be differentiated from *Bradysaurus* and *Embrithosaurus* by having more distinct and pointed bosses on the posterior cheek margin. The descending cheek flanges of *Nochelesaurus* are slightly larger than those of *Bradysaurus*.

**Postcranial:**

*Nochelesaurus* can be differentiated from *Bradysaurus* in that the torsion in the humerus is only 45 degrees (and not 60 degrees as in *Bradysaurus*)

### 4.3.2 Amended Diagnosis

**Synonyms:**

- *Dolichopareia angusta* (Haughton and Boonstra 1929a) Holotype Specimen: SAM-PK-6238
- *Brachypareia watsoni* (Haughton and Boonstra 1929a) Holotype Specimen: SAM-PK-6240

**Autapomorphies:**

**Cranial:**

No unique cranial autapomorphies were identified on the holotype or referred specimens, during this study.

Within the group of *Tapinocephalus* Assemblage Zone species**,** *Nochelesaurus* shows uniquely shaped bosses on the posterior edge of the quadratojugal which are flat, plate-like and pointed, horizontal and posteriorly directed, with a very large, long, "teat" shaped corner boss; mandibular teeth with non-symmetrical arranged mesial and distal marginal cusps; lingual surface of the mandibular teeth with a high vertical bulge demarcated by two vertical ridges; a flat lateral surface of the quadratojugal with curved discrete round bosses; absence of any maxillary boss or maxillary buckling.
*Nochelesaurus* shares with *Embrithosaurus* a transversely wide and rectangular postparietal and large cheek flanges and with *B. baini* seven to nine marginal cusps on all teeth.

### 4.3.3 Specimens and Comments

**Holotype Specimen SAM-PK-6239:**

See Chapter 2 –Materials and Methods, 2.1.3 Holotype *Nochelesaurus alexanderi* SAM-PK-6239, for a list of the elements preserved of this specimen, and Chapter 6 Discussion, 6.1.2 *Nochelesaurus alexanderi* for comments.

**Specimens identified as *Nochelesaurus* by Lee (1995, 1997a) and retained:**

**Specimen SAM-PK-6238:**

Skull consisting of four fragments: a snout, a large right cheek, a small flat dorsal skull table, a large fragment containing most of the palate and braincase. The lower jaw is complete and separate.

This specimen is the holotype of *Dolichoparia angusta* Haughton and Boonstra (1929a). Lee (1995, 1997a) concluded that the original diagnostic features of this taxon are unfounded and that *Dolichoparia angusta* is a junior synonym for *Nochelesaurus alexanderi*, an interpretation with which I agree.

Haughton and Boonstra (1929a) used the approximately equal width between the orbits compared to the width between the bosses of the supratemporal, as diagnostic for *Dolichoparia*. The width between the orbits is actually slightly less than the width between the supratemporal bosses, and as this is the usual condition for these basal pareiasaurs, it is not diagnostic. Haughton and Boonstra (1929a) noted the snout as very pointed for this genus, failing to observe that the skull suffers from severe mediolateral compression, which is readily apparent in the very narrow pineal foramen, the narrow external naris openings, and the exaggerated height of the snout and dorsal skull table caused by vertical stretched deformation. The lower jaw, which is not mediolaterally compressed, appears wider than the compressed deformed skull, as noted by Lee (1995, 1997a).

Lee synonymised *Dolichopareia angusta* with *Nochelesaurus alexanderi* based on fact that the holotype of *Dolichopareia angusta* (SAM-PK-6238) exhibits the anterior location of the scapula groove and the tubercle on the entepicondyle, two of the three postcranial autapomorphies of *Nochelesaurus alexanderi* and that the cranial morphology is consistent with *Nochelesaurus alexanderi*, except for the lack of distinct strong pointed posterior cheek bosses, which Lee attributes to weathering in the specimen.

I also agree with Lee that this skull is not *Embrithosaurus*, as the teeth possess only seven cusps, the skull is not *B. baini* as no large maxillary boss exists and that the skull is not *B seeleyi* as the cheek flanges are far too large. I agree with Lee that the bosses on the posterior cheek edges have likely been affected by weathering and erosion, and are pointed and more like those of *Nochelesurus* if better preserved. The rest of the skull is also severely weathered, eroded and thus appears "smoothed over" in general with indistinct ornamentation. The corner boss on the posterior edge of the cheek is very long, large and "teat" shaped, only consistent with *Nochelesaurus* and *Embrithosaurus*.

**Specimen SAM-PK-6240:**

Small skull and separate lower jaw and fragments of two cervical vertebrae. This specimen is the holotype of *Brachypareia watsoni* Haughton and Boonstra (1929a). Lee (1995, 1997a) found *Brachypareia watsoni* to be a junior synonym of *Nochelesaurus alexanderi*. I concur that the features used by Haughton and Boonstra (1929a) to diagnose *Brachypareia watsoni* are not diagnostic and that this specimen should be referred to *Nochelesaurus alexanderi*. Haughton and Boonstra's (1929a) observations of a supposed larger interorbital width compared to the width between the supratemporal bosses is erroneous. Similarly, the more posterior location of the orbit, the small cheeks, and the pointed snout described by Haughton and Boonstra (1929a) are also unfounded observations as there is nothing unusual or unique about the placement of the orbit, which is normal, the size of the cheeks, which are large, or the morphology of the snout, which is smooth and rounded. The only distinguishing feature present on this juvenile skull is the sharp, pointed, flat, horizontally projecting bosses on the posterior cheek edges which are a good match to *Nochelesurus alexanderi*.

**Referred specimens identified during this cranial study:**

**Specimen SAM-PK-8944:**

Large mediolaterally compressed skull without lower jaw. The right and left radii, ulnae and front feet are supposed to be present, but I could not locate them in the collection. This specimen was referred to *Nochelesaurus alexanderi* by Boonstra (1934a). Although the pointed and flat posterior cheek bosses diagnostic of *Nochelesaurus alexanderi* are weathered and broken off in this specimen, the rest of the skull shows the closest similarities to *Nochelesaurus*. This skull has a wide postparietal and does not possess the characteristic large maxillary boss of *B. baini* or the small maxillary boss of *Embrithosaurus*. The large cheeks and the wide postparietal preclude this specimen form being *B. seeleyi.*

**Specimen SAM-PK-9104:**

Left side of a large skull, without lower jaw, and various unprepared postcranial elements. This specimen was referred to *Bradysaurus baini* by Boonstra (1934a). This skull reveals the diagnostic pointed flat bosses on the posterior cheek edges of the quadratojugal typical of *Nochelesaurus*. It lacks the diagnostic large maxillary boss of *B. baini*, and has only seven cusps on its maxillary teeth and so cannot be *Embrithosaurus*. The cheek is very large and therefore is not *B. seeleyi.*

**Specimen SAM-PK-9115:**

Large skull with occluded lower jaw, both mediolaterally compressed and severely dorsoventrally crushed on the left, near the snout. This specimen was referred to *Bradysaurus seeleyi* by Boonstra (1934a). This severely distorted skull has the flat and pointed posterior cheek bosses, better preserved on the right cheek, which are diagnostic of *Nochelesaurus alexanderi*. Furthermore, the seven cusped maxillary teeth preclude identification as *Embrithosaurus*, the lack of a large maxillary boss indicates it is not a *B. baini*, and the large cheeks preclude identification as *B. seeleyi.*

**Specimen SAM-PK-9137:**

Large skull consisting of numerous cranial fragments that preserves a large wide maxilla and occluded lower jaw, with a large part of the left cheek flange, a large unprepared palatal fragment and a medium sized piece of the dorsal surface of the right supratemporal boss. Numerous postcranial elements. This specimen was referred to *Bradysaurus seeleyi* by Boonstra (1934a) this fragmentary partial skull reveals pointed and flat bosses on the posterior cheek edge of the left quadratojugal which are diagnostic of *Nochelesaurus alexanderi*. The boss located dorsally to the corner boss in particular is extremely thin and pointed. The maxilla is only slightly buckled.

**Specimen SAM-PK-12076:**

Partial skull consisting of five cranial fragments, including a dorsal skull roof fragment and a left cheek fragment. Fragmentary unprepared postcranial elements. This specimen was collected much more recently than most specimens (1957) and has not been listed in taxonomic papers. The left cheek fragment preserves flat and pointed bosses on the posterior cheek edges, characteristic of *Nochelesaurus alexanderi*.

**Specimen CGP JA 109:**

Large, partial and distorted skull with a “glassy” yellow appearance, with very distinct ornamentation, and a partial occluded lower jaw. This unpublished partial skull is severely dorsoventrally crushed and posteriorly distorted. It exhibits large cheeks, discrete lateral bosses on the quadratojugal with no horizontal embayment and no thickening of the lower quadratojugal, very flat pointed posterior cheek bosses, which includes a huge and long “teat” shaped corner boss, all consistent with identification as *Nochelesaurus*.




**Figure 4.1:** Photograph of the skull of the holotype of *Nochelesaurus alexanderi* (SAM-PK-6239), in dorsal view.




**Figure 4.2:** Photograph of the skull of the holotype of *Nochelesaurus alexanderi* (SAM-PK-6239), in ventral view.

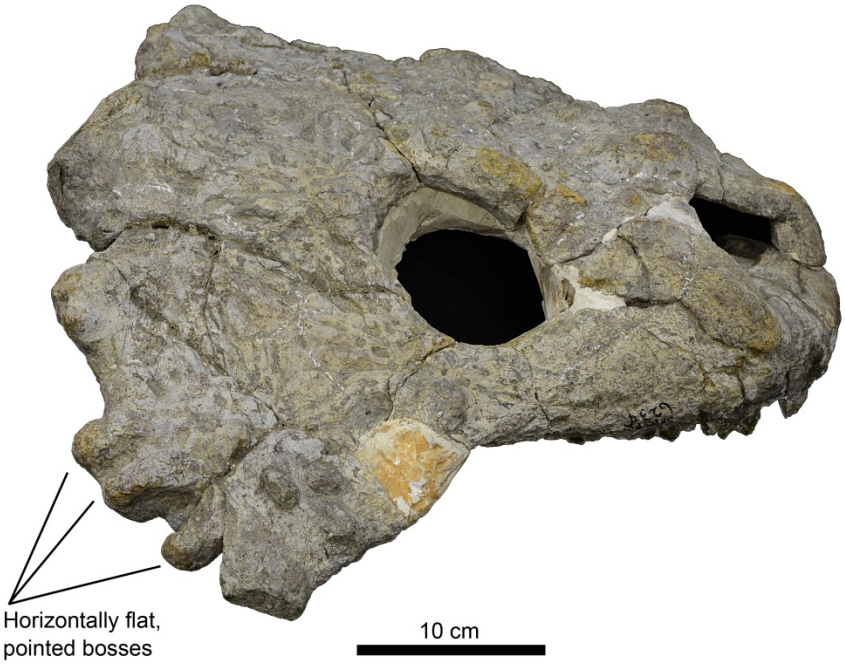


**Figure 4.3:** Photograph of the skull of the holotype of *Nochelesaurus alexanderi* (SAM-PK-6239), in right lateral view.

## 4.4 *Bradysaurus baini* Watson (1914)

### 4.4.1 Diagnosis (Lee 1995, 1997a)

**Synonyms:**

- *Platyoropha broomi* (Haughton and Boonstra 1929a) Holotype Specimen: SAM-PK-5002

**Autapomorphies:**

**Cranial:**

*B. baini* is diagnosed as having three cranial autapomorphies:

- Greatly swollen distal portion of the paroccipital process of the opisthotic.

- Huge, rounded maxillary boss on the maxilla, immediately behind the external naris. In all other pareiasaurs, the maxillary boss is either absent, poorly developed, or takes the form of a small horn.
- The upper jaw teeth point inwards towards the palate. In all other pareiasaurs, except in the late Permian *Pareiasuchus nasicornis*, the teeth of the upper jaw point straight downwards, with little or no palatal inflection.

**Postcranial:**

*Bradysaurus* is diagnosed with one autapomorphy in that the torsion in the humerus is approximately 60 degrees (and not 45 degrees as in *Embrithosaurus*).

**Differences compared to other *Tapinocephalus Assemblage Zone* pareiasaur species (Lee 1995, 1997a):**

**Cranial:**

*Bradysaurus baini* can be differentiated from *Nochelesaurus* through the lack of the distinctive pointed posterior cheek bosses, and can be differentiated from *B. seelei*, and resembles all other pareisaurs, in having large cheek flanges.

**Postcranial:**

*Bradysaurus baini* can be differentiated from *Bradysaurus seelei,* and resembles all other pareisaurs, in having median and lateral pubic processes.

### 4.4.2 Amended Diagnosis

**Synonyms:**

- *Platyoropha broomi* (Haughton and Boonstra 1929a) Holotype Specimen: SAM-PK-5002

**Autapomorphies:**

**Cranial:**

*Bradysaurus baini* is diagnosed by one cranial autapomorphy: The maxilla is sharply buckled (not smooth or rounded) and has a large boss on the lateral surface. This large maxillary boss is elongated, oval, high and raised and forms a wide pad that presents an almost flat surface that faces anterolaterally. This pad is posterodorsally oriented in lateral view. The large maxillary boss covers almost the entire anterolateral surface of the maxilla, behind the external naris, from low down on the maxilla, just above the maxillary foramen, to the top of the bone. This large maxillary boss extends unabated onto the lacrimal, covering the anterior half of the lacrimal and in so doing obscures the lacrimal's anterior bosses, a condition that makes them appear relatively indistinct and low.

Within the group of *Tapinocephalus* Assemblage Zone species**,** *B. baini* has a uniquely large boss on the lateral surface of the maxilla and a sharply buckled or bent maxilla, indistinct anterior bosses on the lacrimal and the largest and the most distinct knob-like projection on the paroccipital process of the opisthotic.

*B. baini* shares with *Embrithosaurus* large, wide, bulbous, indistinct bosses on the posterior edge of the quadratojugal and a swollen boss complex on the lateral surface of the quadratojugal that consists of curved, long bosses or rugosity with a deep horizontal embayment separating the jugal from the quadratojugal.

*Bradysaurus baini* shares with *B. seeleyi* a transversely wide and rectangular postparietal and with *Nochelesaurus* seven to nine marginal cusps on all teeth.

### 4.4.3 Specimens and Comments

**Holotype Specimen NHMUK R1971:**

See Chapter 2 –Materials and Methods, 2.1.5 Holotype *Bradysaurus baini* NHMUK R1971, for a list of the elements preserved of this specimen and Chapter 6 Discussion, 6.1.3 *Bradysaurus baini* for comments.

**Specimens identified as *Bradysaurus baini* by Lee (1995, 1997a) and retained:**

**Specimen SAM-PK-5002:**

Slightly distorted large skull without lower jaw. Parts of left and right scapulo-coracoids, parts of clavicle, part of interclavicle, and parts of left and right humeri. This specimen is the holotype of *Platyoropha broomi* Haughton and Boonstra (1929a). My observations of the specimen agree with Boonstra (1934a) and Lee 1995, 1997a) that this taxon was mistakenly erected based on measurements and proportions of a distorted specimen, and is a junior synonym for *B. baini*. SAM-PK-5002 has the large distinctive maxillary boss and sharply buckled maxilla of *B. baini* together with the horizontal deep embayment on the lateral surface of the quadratojugal with three posterodorsally oriented bosses ventral to the embayment, and the indistinct and low cranial bosses on the lacrimal, prefrontal, frontal, postfrontals and postorbitals.

**Referred specimens identified during this cranial study:**

**Specimen SAM-PK-4350:**

Damaged juvenile skull and occluded lower jaw, some postcranial elements including a well preserved humerus. The posterior dorsal surface is damaged

such that the two large cavities are present. This specimen was referred to *Brachypareia rogersi* by Boonstra (1934a) using general features common to most *Tapincoephalus* Assemblage Zone pareiasaurs. This small skull juvenile skull with clear sutures has massive maxillary bosses and buckling on both maxillae typical of *B. baini.*

**Specimen SAM-PK-5624:**

Finely preserved, slightly dorsoventrally crushed and very well prepared large skull. Almost the entire skull is preserved, except for part of the vomer. This specimen was referred to *Bradysaurus seeleyi* by Boonstra (1934a), this large skull is one of the best preserved and best prepared skulls studied. The left maxilla especially shows the characteristic large maxillary boss and buckling of *B. baini*. The rest of the skull is consistent with the features of *B. baini*, including large cheeks and bulbous medium sized posterior cheek bosses. A premaxillary tooth shows nine marginal cusps including rare distal medial cusps and the dentary teeth show eight to nine cusps.

**Specimen SAM-PK-8933:**

Partial skull consisting of two large cranial pieces, together making up the snout with occluded lower jaw. The dorsal skull roof is not preserved. Numerous postcranial elements. This specimen was assigned to *B. seeleyi* by Haughton and Boonstra (1929a). I assign this fragmentary skull to *B. baini* based on the preserved right maxilla which shows a strong maxillary boss, which continues unabated onto the lacrimal.

**Specimen SAM-PK-9095:**

Small dorsoventrally crushed skull of a juvenile pareiasaur with occluded lower jaw, crudely prepared. This specimen was referred to *Brachypareia rogersi* by Boonstra (1934a) using general features common to most *Tapincoephalus* Assemblage Zone pareiasaurs, and to *B. baini* by Lee (1995, 1997) this small

juvenile skull of a *B. baini* has massively large cheeks, bulbous bosses on the posterior margins of the cheeks, a small sized knob on the parocipital process, and the large distinctive maxillary bosses and buckling on each maxilla.

**Specimen SAM-PK-9121:**

Large dorsoventrally crushed skull. Reconstructed with plaster over the right anterior snout and almost the entire anterior half of the flat dorsal surface, including the dorsal orbital edges. Many lower jaw fragments and a partial clavicle/interclavicle preserved. This specimen was referred to *B. seeleyi* by Boonstra (1934a), this large unprepared and plaster infilled skull preserves the diagnostic large maxillary boss and sharp buckling on its left maxilla as well as three posterodorslly oriented rugose lines and thickened swelling on the lateral surface of the quadratojugal. The cheeks are large, the maxillary teeth are elongated and carry seven cusps each, and the bosses on the posterior edge of the cheek are medium sized.

**Specimen SAM-PK-9168:**

Medium sized skull with occluded lower jaw and numerous postcrania. The snout is reconstructed. This skull was assigned to *B. seeleyi* by Haughton and Boonstra (1929a). This skull has very large cheeks, with the right one showing strong rugose posterodorsolly oriented lines creating a swollen structure on the lower lateral quadratojugal. The maxillary teeth are elongated with seven cusps and a medium sized knob on the paroccipital processes. The posterior cheek bosses are large, low, round and bulbous.

**Specimen SAM-PK-9170:**

Very large and extremely badly preserved and unprepared partial skull, and a partial scapula blade. Only the dorsal surface and left side of the skull is preserved, with an occluded fragmentary lower jaw with several cervical vertebrae. Found in 1929, but not listed in any taxonomic papers, this extremely

badly preserved specimen has the characteristic large maxillary boss and buckling of *B. baini* on its left maxilla.

**Specimen SAM-PK-12014:**

Large unprepared and damaged skull with a partial lower jaw, and no premaxilla preserved. This specimen was collected much more recently than most specimens (1956) and has not been listed in taxonomic papers. The maxilla is sharply buckled and preserves a huge raised maxillary boss with strong rugose lines present. This specimen has the largest maxillary bosses observed of all specimens studied.

**Specimen SAM-PK-12048:**

Fragmentary snout consisting of two large fragments which preserve the right premaxilla, maxilla and occluded lower jaw. A third fragment consists of a portion of the vertebral column with only a few vertebra preserved. This specimen was also collected much more recently than most specimens (1957) and has also not been previously listed in any taxonomic papers. The preserved right maxilla shows a large maxillary boss and buckling characteristic of *B. baini* and elongated seven cusps teeth.

**Specimen SAM-PK-12090:**

Partial skull consisting of several fragments including a very large snout, part of both cheeks, a wide dentary fragment with broken off teeth and several other cranial fragments. This specimen was also collected much more recently than most specimens (1957) and has not been listed in taxonomic papers. The snout fragment preserves a very large and distinctive maxillary boss of a *B. baini*. The maxillary teeth and posterior cheek bosses are also consistent with *B baini.*

**Specimen SAM-PK-12115:**

Very large, partial, unprepared skull completely covered in 1-2 cm thick layer of green calcareous material. This specimen was also collected much more recently than most specimens (1957) and has not been listed in taxonomic papers. Both maxilla preserve large raised maxillary bosses.

**Specimen SAM unnumbered adult:**

Very large skull, that appears to belong to an elderly individual as the cranial ornamentation and bosses are very well developed, with plaster infill in reconstructed parts of the skull. This unnumbered skull has a relatively narrow but clearly distinct and raised long, flat maxillary boss, massive cheeks and large, bulbous bosses on the posterior edge of the cheeks.

**Specimen CGP light grey unnumbered juvenile:**

Complete juvenile skull with occluded lower jaw, pectoral girdle and vertebral column. This specimen is one of the finest preserved and prepared *Tapinocephalus* Assemblage Zone pareiasaurs, with clear sutures. It has the characteristic large maxillary boss and sharp buckling, elongated seven cusp teeth, large cheeks with wide, low bosses on the posterior edges, and a narrow square shaped postparietal bone.

**Specimen CGP dark brown large specimen:**

Complete large skull, occluded lower jaw, pectoral girdle and vertebral column. This specimen is very large and well prepared and shows a large maxillary boss and a large swollen knob on the paroccipital process of the opisthostics. The bosses of the posterior margin of the cheek are relatively small, distinct, and round. The lateral surface of the quadratojugal has two or three thickened rugose curve lines of bosses.

**Specimen BP/I/347:**

Snout fragment and numerous unprepared postcranial elements. This specimen was collected in 1945 and has not been used in taxonomic papers. The preserved snout shows elongated seven cusped teeth and a clear large boss which starts very low down on the maxilla.

**Specimen BP/I/7213:**

Skull consisting of a snout fragment, and a fragment of the left cheek. Numerous postcranial elements. This specimen was collected in 2012 and identified as *Embrithosaurus* by Day (2013) based on the femur, with an s-shaped trochanter, which Lee (1995, 1997a) attributes to this taxon. However, the maxillary teeth exposed have only seven cusps and are elongated, which does not match with *Embrithosaurus*. The bosses on the posterior cheek edges are large and bulbous, which does not match *Nochelesaurus* or *B. seeleyi*, leaving only *B. baini* as the identification, based on a process of elimination. The presence of the maxillary boss cannot be confirmed, as it is mostly eroded away.




**Figure 4.4:** Photograph of the skull of the holotype of *Bradysaurus baini* (NHMUK R1971), in dorsal view.

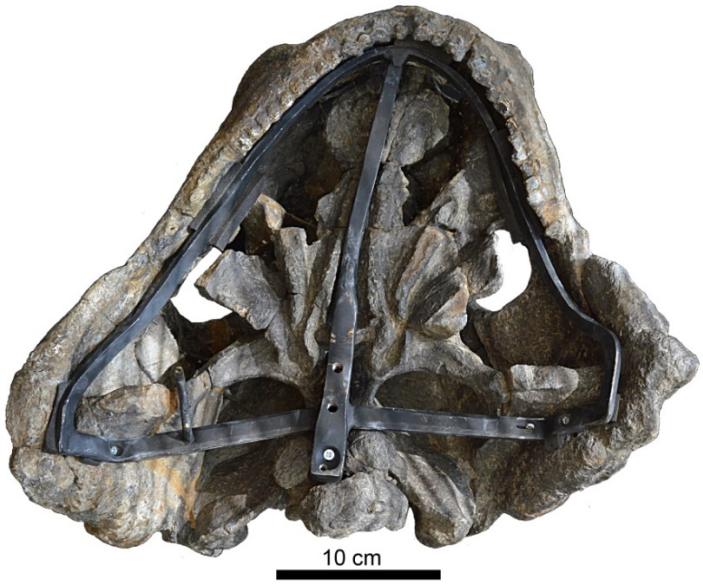


**Figure 4.5:** Photograph of the skull of the holotype of *Bradysaurus baini* (NHMUK R1971), in ventral view.

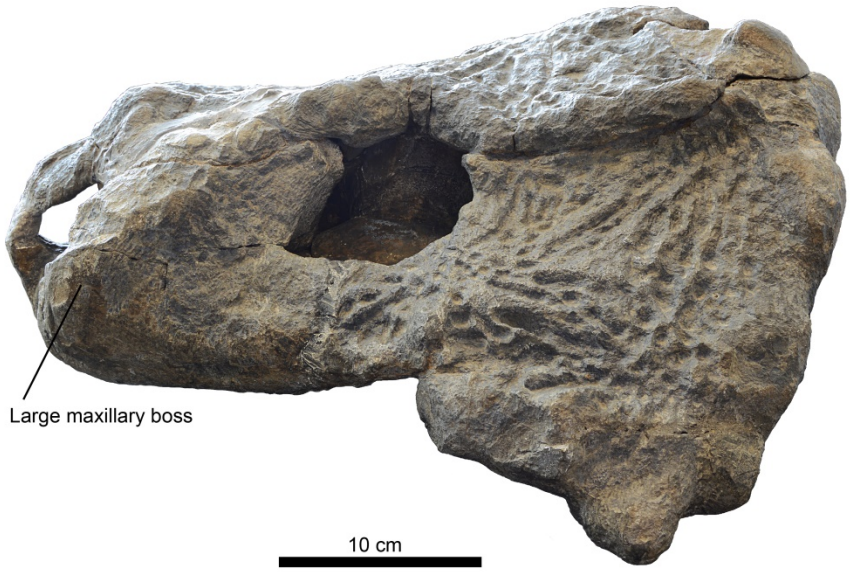


**Figure 4.6:** Photograph of the skull of the holotype of *Bradysaurus baini* (NHMUK R1971), in left lateral view.

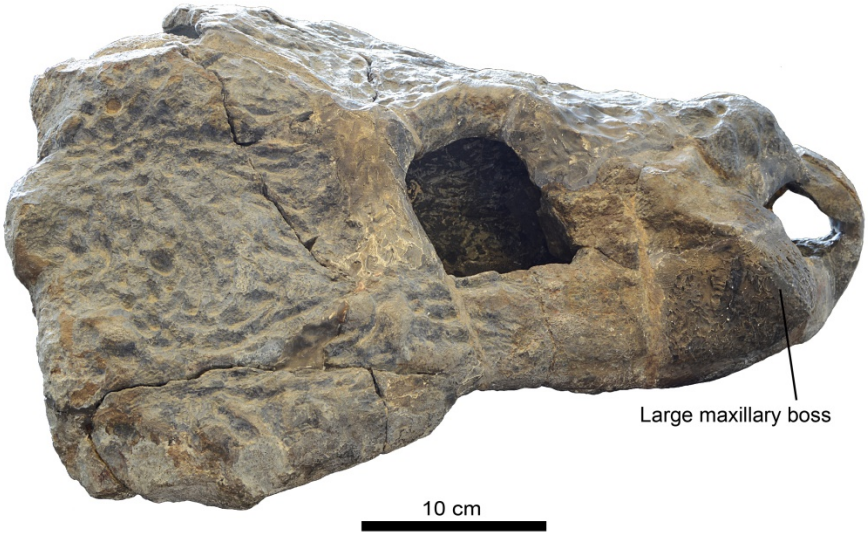


**Figure 4.7:** Photograph of the skull of the holotype of *Bradysaurus baini* (NHMUK R1971), in right lateral view.

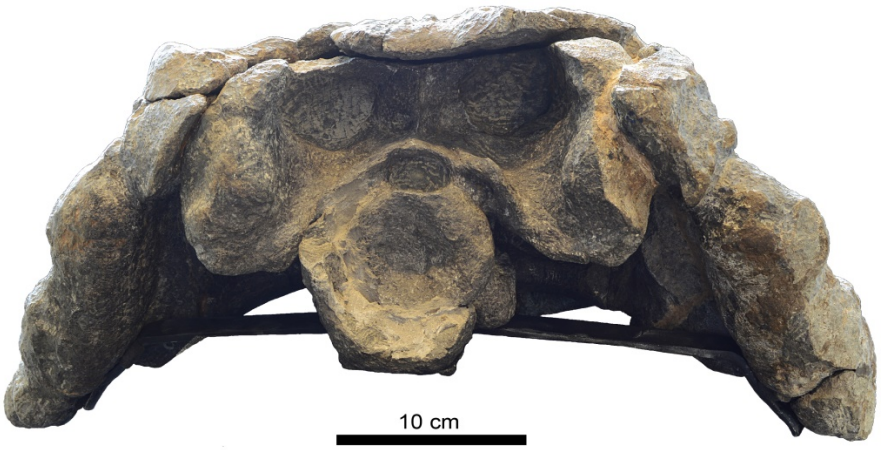


**Figure 4.8:** Photograph of the skull of the holotype of *Bradysaurus baini* (NHMUK R1971), in occipital view.

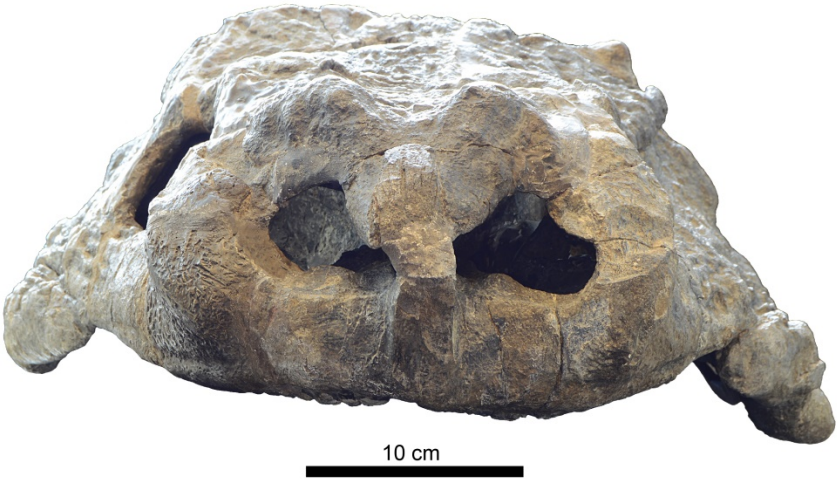


**Figure 4.9:** Photograph of the skull of the holotype of *Bradysaurus baini* (NHMUK R1971), in anterior view.

## 4.5 *Bradysaurus seeleyi* Haughton and Boonstra (1929)

### 4.5.1 Diagnosis (Lee 1995, 1997a)

**Synonyms:**

- *Bradysaurus vanderbyli* (Haughton and Boonstra 1929a) Holotype Specimen SAM-PK-3718

**Autapomorphies:**

**Cranial:**

*Bradysaurus seeleyi* exhibits no obvious cranial or postcranial autapomorphies of its own.

**Postcranial:**

*Bradysaurus* is diagnosed with one autapomorphy in that the torsion in the humerus is approximately 60 degrees (and not 45 degrees as in *Embrithosaurus*).

**Differences compared to other *Tapinocephalus* Assemblage Zone pareiasaur species (Lee 1995, 1997a):**

**Cranial:**

*Bradysaurus seeleyi* can be differentiated from all other pareiasaurs in having very small cheek flanges.

It is differentiated from *B. baini* as it lacks the three cranial autapomorphies of *B. baini*: the distal portion of the paroccipital process of the opisthotic is not greatly swollen, there is no maxillary lump on the maxilla immediately behind the external naris, and the upper jaw teeth point directly downwards and not inwards towards the palate.

**Postcranial:**

*Bradysaurus seeleyi* can be differentiated from all other pareiasaurs in having a continuous pubic rim, rather than the usual median and lateral pubic processes.

### 4.5.2 Amended Diagnosis

**Synonyms:**

- *Bradysaurus vanderbyli* (Haughton and Boonstra 1929a) Holotype Specimen: SAM-PK-3718

**Autapomorphies:**

**Cranial:**

No unique cranial autapomorphies were identified on the holotype or referred specimens, during this study.

Within the group of *Tapinocephalus* Assemblage Zone species**,** *B. seeleyi* has the smallest cheeks of all pareiasaurs in this group, and the absence of a maxillary boss, but has a slight buckling of the maxilla, and seven marginal cusps on all teeth.

*Bradysaurus seeleyi* shares with *B. baini* a transversely narrow and square postparietal and small, round and distinct bosses on the posterior edge of the quadratojugal with some specimens of *B. baini*.

### 4.5.3 Specimens and Comments

**Holotype Specimen NHMUK 49426:**

See Chapter 2 –Materials and Methods, 2.1.7 Holotype *Bradysaurus seeleyi* NHMUK 49426, for a list of the elements preserved of this specimen and Chapter 6 Discussion, 6.1.4 *Bradysaurus seeleyi* for comments.

**Specimens identified as *Bradysaurus seeleyi* by Lee (1995, 1997a) and retained:**

**Specimen SAM-PK-3718:**

Very large and deeply weathered skull, with separate lower jaw. Vertebrae, parts of right and left scapulo-coracoid, parts of right and left humeri, ulnae and radii, and partial left foot. Haughton and Boonstra (1929a) created the species *Bradysaurus vanderbyli* for SAM-PK-3718 based on a very smooth posterior border of the cheek, a narrower interorbital width compared to the width between the supratemporal bosses, and shallow (low, small) cheek. However, as pointed out by Lee (1995, 1997a) the posterior borders of both cheeks are badly damaged, weathered and eroded, consistent with the deep weathering and erosion of the skull in general, and it is not possible to determine the true nature of the posterior cheek bosses. The alleged narrower interorbital width compared to the supratemporal width, are incorrect observations of this specimen. Only the small cheeks are significant features of this specimen. Through a process of elimination, Lee assigned SAM-PK-3718 to *B. seeleyi* and declared *B. vanderbyli* a junior synonym. I retain Lee's assignment of SAM-PK-3718 to *B. seeleyi*, based on its small cheeks and a process of elimination whereby the specimen does not appear to fit with any other species in the group and the fact that Lee observed a smooth pelvic rim, in this specimen.

**Specimen SAM-PK-5012:**

Right side of a skull and occluded lower jaw, numerous postcrania. SAM-PK-5012 was referred to *Brachypareia rogersi* by Haughton and Boonstra (1929a), as the holotype (SAM-PK-8953) consists of only partial postcrania and has no skull. They used similarities of the limb-bones and vertebra to include the two specimens in *B. rogersi*.

Lee declared *Brachypareia rogersi* invalid as the taxon is based on the postcranial remains of a *Pareiasaurus serridens* (SAM-PK-8953) and the skull and postcrania of SAM-PK-5012, a specimen which he assigns to *Bradysaurus seeleyi*.

Lee assigned SAM-PK-5012 to *B. seeleyi*, using a process of elimination, as he did not find the distinguishing maxillary boss of *B. baini* present in the specimen, or the large cheek flanges of *Embrithosaurus* or *Nochelesaurus*, or the distinct pointed posterior cheek bosses of *Nochelesaurus*. I agree with Lee's cranial assement and conclusion for this specimen.

**Referred specimens identified during this cranial study:**

**Specimen CGP/1/810 (RMS1096):**

Small skull. This unpublished unprepared small skull reveals small cheeks, and no maxillary boss, allowing it to be tentatively identified it as *B. seeleyi*. The bosses on the posterior cheek are small and distinct, consistent with *B. seeleyi*.

**Specimen BP/I/297:**

Small skull, mediolaterally compressed, with occluded lower jaw. This unpublished small skull belongs to a juvenile specimen and is mediolaterally compressed and mostly unprepared, the bone is indistinguishable from the matrix. The specimen lacks the large maxillary boss of *B. baini*, and damaged teeth appear to be elongated and therefore inconsistent with *Embrithosaurus*. The posterior cheek bosses are damaged and it has the characteristic small cheeks of *B. seeleyi.*

**Specimen BP/I/4859:**

Small partial skull with some unprepared postcrania. Tentatively referred to *B. seeleyi* based on the presence of a small cheek, this specimen is not *Embrithosaurus* as the maxillary teeth are elongated and seven cusped. It is also not referable to *B. baini* as there is no large maxillary boss, and cannot be assigned to *Nochelesaurus* as the posterior cheek bosses are not flat, but are small, round, distinct.

**Specimen BP/I/7054:**

Small skull, mediolaterally compressed, left side damaged and with an occluded left lower jaw. This unpublished small skull belongs to a juvenile. The skull is mediolaterally compressed, the left side is damaged around the orbit, and the skull is only partially prepared with much matrix remaining. Nevertheless, it is clear that the specimen lacks the large maxillary boss of *B. baini*, and the horizontally flat posterior cheek bosses of *Nochelesaurus*. The cheek is very small and the posterior cheek bosses are consistent with *B. seeleyi*, being small, rounded and distinct.

**Specimen BP/I/7886:**

Skull fragments and postcranial fragments. Tentatively referred to *B. seeleyi*, this skull consists of only a few cranial fragments, including the left quadratojugal cheek, which has very distinct small and rounded bosses on the posterior edge, which are consistent with *B. seeleyi*. The cheek appear to be very small.




**Figure 4.10:** Photograph of the skull of the holotype of *Bradysaurus seeleyi* (NHMUK 49426), in dorsal view.




**Figure 4.11:** Photograph of the skull of the holotype of *Bradysaurus seeleyi* (NHMUK 49426), in ventral view.

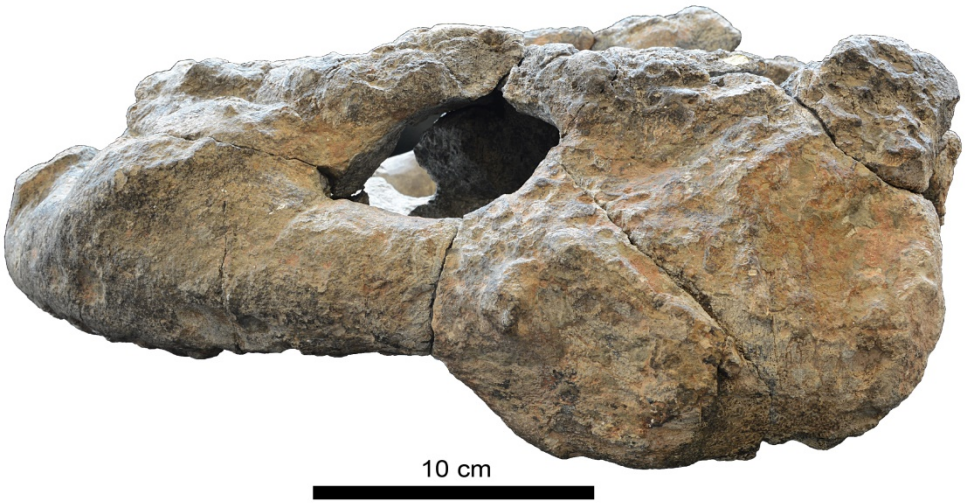


**Figure 4.12:** Photograph of the skull of the holotype of *Bradysaurus seeleyi* (NHMUK 49426), in left lateral view.




**Figure 4.13:** Photograph of the skull of the holotype of *Bradysaurus seeleyi* (NHMUK 49426), in right lateral view.




**Figure 4.14:** Photograph of the skull of the holotype of *Bradysaurus seeleyi* (NHMUK 49426), in occipital view.

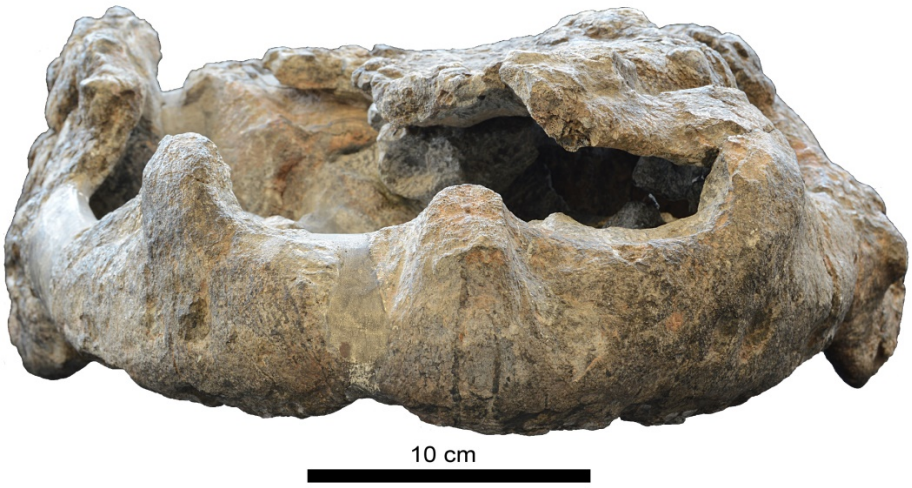


**Figure 4.15:** Photograph of the skull of the holotype of *Bradysaurus seeleyi* (NHMUK 49426), in anterior view.

# CHAPTER FIVE: RESULTS: STRATIGRAPHIC RANGES

## 5.1 Determination of stratigraphic ranges for Abrahamskraal Formation taxa

Day (2013, *et al.* 2015) in his stratigraphic work on the lowermost Beaufort Group, determined the stratigraphic ranges of different tetrapod taxa from the *Tapinocephalus* Assemblage Zone. The majority of *Tapinocephalus* Assemblage Zone pareiasaur specimens were collected prior to 1960, and locality information usually consists of only a farm name, precise Global Positioning Satellite (GPS) latitude and longitude coordinates is only available for recently collected specimens. Nicolas (2007, van der Walt *et al.* 2011), in her creation of the Beaufort Fossil Vertebrate GIS database, assigned a centroid to each farm locality to generate latitude and longitude co-ordinates for historic records with only the farm name noted as the locality. A centroid is latitude and longitude co-ordinates calculated for a central geographic point assigned to a farm. All fossils collected from a particular farm are assigned the latitude and longitude co-ordinates of the centroid. Day (2013) analysed several stratigraphic sections, covering a large sample of the farms of the South Western Karoo and assigned stratigraphic interval ranges to the deposits of each farm, consisting of the height above the base of the Abrahamskraal Formation and the lithostratigraphic members present on each farm. All the pareiasaur specimens studied in this project were recovered west of 24 degrees East longitude, where the Abrahamskraal Formation comprises six lithostratigraphic members (Day 2013).

A large farm may cover a wide stratigraphic interval and include several members. In these few instances more than one member was assigned as the possible stratigraphic provenance of fossils recovered. For more recently collected specimens with precise GPS generated co-ordinates, better constrained stratigraphic ranges were assigned to the fossil recovered.

## 5.2 This study

In the course of this study, only 39 specimens out of 108 cranial pareiasaur specimens (36%) held in museum collections were positively re-identified using my amended diagnosis (Table. 5.1, Appendix D). This low percentage of positive identifications is due to the fragmentary nature, poor preservation and poor state of preparation of the majority of the specimens. For example, the dentition, that provides important diagnostic features, is unprepared in most specimens, including the holotypes. Of the 39 positively re-identified specimens, five lack locality information. One additional specimen, SAM-PK-K324, consisting only of postcranial elements and identified by Lee (1995, 1997a), was also included. I used these 35 specimens with locality information (Appendix C) to produce the new stratigraphic ranges for this study (Fig. 5.1).

| **Institution** | **Specimens studied** | **Specimens Identified** | **Percentage Identified** |
|---|---|---|---|
| NHMUK | 6 | 2 | 33% |
| SAM | 58 | 26 | 45% |
| BPI | 29 | 6 | 21% |
| CGP | 16 | 5 | 31% |
| **TOTAL** | **108** | **39** | **36%** |

**Table 5.1:** Specimen identification per institution, for the 108 cranial pareiasaur specimens recovered from the *Tapinocephalus* Assemblage Zone. Thirty nine specimens (36%) were identifiable to species level. Institutional Abbreviations: **BPI**, Evolutionary Studies Institute, University of the Witwatersrand, Johannesburg (formerly the Bernard Price Institute for Palaeontological Research); **CGP**, Council for Geosciences, Pretoria; **NHMUK**, Natural History Museum of London, United Kingdom; **SAM**, Iziko South African Museum, Cape Town.

The stratigraphic range intervals compiled by Day (2013) for individual farm localities were used to determine the amended stratigraphic ranges for the 35 identified specimens at a species level (Appendix D). Day's (2013) stratigraphic ranges and those resulting from this study are presented and discussed below at a species level.

## 5.3 Stratigraphic ranges of middle Permian pareiasaurs

### 5.3.1 *Bradysaurus* stratigraphic range

Since existing museum catalogues were used by Day for specimen identification of *Bradysaurus,* this genus accounts for the overwhelming majority of pareiasaur specimens stratigraphically charted by Day (2013). The stratigraphic range for 95 specimens of *Bradysaurus* were plotted by Day, who found the stratigraphically lowest occurrence of *Bradysaurus* is for specimen SAM-PK-11940, from the farm Vereniging in the Laingsburg district, which was constrained to a broad interval of 1300-1650 m above the base of the Abrahamskraal Formation. Day assigns this farm to the upper Koornplaats Member.

The stratigraphically highest occurrence of *Bradysaurus* was found on the farm Grootfontein in the Beaufort West district, for specimen SAM-PK-4999, which Day places stratigraphically at the boundary between the Abrahamskraal and Teekloof Formations.

The stratigraphic range of *Bradysaurus* therefore extends from the upper Koornplaats Member to the top of the Karelskraal Member of the Abrahamskraal Formation, covering the upper half of the *Tapinocephalus* Assemblage Zone. Most specimens are found between the mid Swaerskraal and lower Moordenaars Members of the Abrahamskraal Formation (Fig. 5.1).

The stratigraphically lowest and highest specimen occurrences of *Bradysaurus* used by Day (2013), i.e. SAM-PK-11940 and SAM-PK-4999 respectively, were not

positively re-identified as members of that taxon in my study, due to poor preservation and preparation. Eighteen specimens were positively identified in this study as *Bradysaurus baini.* However, two specimens from the Council for Geosciences, and one from the Iziko South African Museum, have no locality or catalogue information, therefore only 15 specimens of *Bradysaurus baini* were used in this study.

The stratigraphically lowest occurrence of *B. baini* are specimens SAM-PK-12048 and BP/I/347 collected on the farms Dwars Rivier in the Laingsburg district and Buffelsvlei in the Beaufort West district respectively, which are not well constrained stratigraphically, but appear to be situated between the upper Koornplaats, Swaerskraal, and lower Moordenaars Members of the Abrahamskraal Formation as determined by Day (2013).

The stratigraphically highest specimen: BP/I/7213, from Witfontein 85, in the Sutherland district, is well constrained to the very top of the Moordenaars Member.

Thus the total stratigraphic range of *B. baini* extends from the upper Koornplaats Member to top of the Moordenaars Member (Fig. 5.1).

Eight cranial specimens of *Bradysaurus seeleyi* were identified in this study.

The stratigraphically lowest occurrence of *B. seeleyi* is found for specimen BP/I/7886 from the farm Blounek, in the Lainsburg district, well constrained to the mid Koornplaats Member of the Abrahamskraal Formation. This is the lowest stratigraphic position for any *Tapinocephalus* Assemblage Zone pareiasaur and is significantly lower than specimen SAM-PK-12048 from Dwars Rivier, used by Day (2013) for *Bradysaurus*, which was not well constrained, and could occur anywhere between the upper Koornplaats to lower Moordenaars Members.

The highest occurrence of *B. seeleyi* is the holotype specimen (NHMUK 49426) from Palmietfontein, in the Beaufort West district, constrained to the upper Karelskraal Member, within 100 m of the top of the Abrahamskraal Formation.

The range of *B. seeleyi* therefore extends from the mid Koornplaats Member upwards to the upper Karelskraal Member (Fig. 5.1).

### 5.3.2 *Embrithosaurus* stratigraphic range

Day considered the existing museum catalogue specimens assigned to *Embrithosaurus* to be spurious as Lee (1995, 1997a) redefined the diagnostic characters for this genus. In his stratigraphic analysis, Day (2013) used the holotype and four of the five specimens referred to *Embrithosaurus* by Lee (1995, 1997a) as one of the specimens (CGP R338) did not have locality information. In addition, Day included a newly recovered specimen, BP/I/7213, from Witfontein 85, in the Sutherland district. This resulted in a Day's use of a total of only six specimens of *Embrithosaurus*.

The stratigraphically lowest occurrences of *Embrithosaurus* are specimens SAM-PK-8034 and SAM-PK-K324 from the farms Hogeveld and Seekoevallei respectively, both in the Beaufort West district. These two localities are constrained to the lower part of the Moordenaars member, being 2150-2250 m above the base of the Abrahamskraal Formation (Day 2013). The stratigraphically highest occurrences of *Embrithosaurus* are specimens NHMUK R7782 from the Hottentotsrivier and BP/I/7213 from Witfontein 85, which Day (2013) considers to be 50-150m below the base of the Poortjie Member. Day therefore considered the stratigraphic range of *Embrithosaurus* to extend from the Moordenaars Member to the lower part of the Karelskraal Member of the Abrahamskraal Formation (Fig. 5.1).

In addition to the holotype (SAM-PK-8034), three cranial specimens were positively identified in this study as *Embrithosaurus*. For one of these specimens (CGP/1/795 RMS566) there is no locality information. A further specimen identified by Lee (1995, 1997a) based on postcrania (SAM-PK-K324) was retained, resulting in four specimens used for the amended stratigraphic range

determination of this study. The relatively low number of specimens identified as *Embrithosaurus* are attributable to the fact that the diagnostic maxillary teeth and cusps are usually not preserved or prepared on the majority of specimens studied.

The straigraphic provenance of the holotype of *Embrithosaurus* (SAM-PK-8034) from Hogeveld is constrained to the lower Moordenaars Member by Day (2013) being 2150-2250 m above the base of the Abrahamskraal Formation, and represents the lowest occurrence of this species.

The highest confirmed stratigraphic occurrence of *Embrithosaurus* is SAM-PK-9105, from Melkboschfontein, constrained to the mid Moordenaars Member. *Embrithosaurus* is therefore restricted to a very narrow stratigraphic range within the Moordenaars Member.

### 5.3.3 *Nochelesaurus* stratigraphic range

Due to changes to the diagnosis of *Nochelesaurus* proposed by Lee (1995, 1997a), Day also considered existing museum identifications to be inaccurate and in his stratigraphic work used only the specimens that were identified as *Nochelesaurus* by Lee (1995, 1997a). These three specimens consist of the holotype (SAM-PK-6239) and two referred specimens (SAM-PK-6238, SAM-PK-6240).

Specimen SAM-PK-6240 is the lowest stratigraphic occurrence of *Nochelesaurus,* from the farm Abrahamskraal in the Prince Albert district, and is stratigraphically not well constrained, covering a large stratigraphic interval between 1700-2100 m above the base of the Abrahamskraal Formation. This corresponds to the entire range of the Swaerskraal Member. The holotype specimen SAM-PK-6239 and referred specimen SAM-PK-6238 were both recovered from Boesmanskop, in the Beaufort West district, and are from the uppermost Karelskraal Member of the Abrahamskraal Formation. *Nochelesaurus* therefore has a stratigraphic range

from the Swaerskraal Member to the uppermost Karelskraal Member of the Abrahamskraal Formation (Fig. 5.1).

In addition to the holotype (SAM-PK-6239), eight cranial specimens were identified as *Nochelesaurus,* although for one of these (CGP JA109) the catalogue and locality information are lost.

The stratigraphic range of *Nochelesaurus* is unchanged from Day (2013) as specimen SAM-PK-6240 is still the lowest and SAM-PK-6239 and SAM-PK-6238 are still the highest specimens, occupying a stratigraphic range from the Swaerskraal Member to the uppermost Karelskraal Member of the Abrahamskraal Formation (Fig. 5.1).

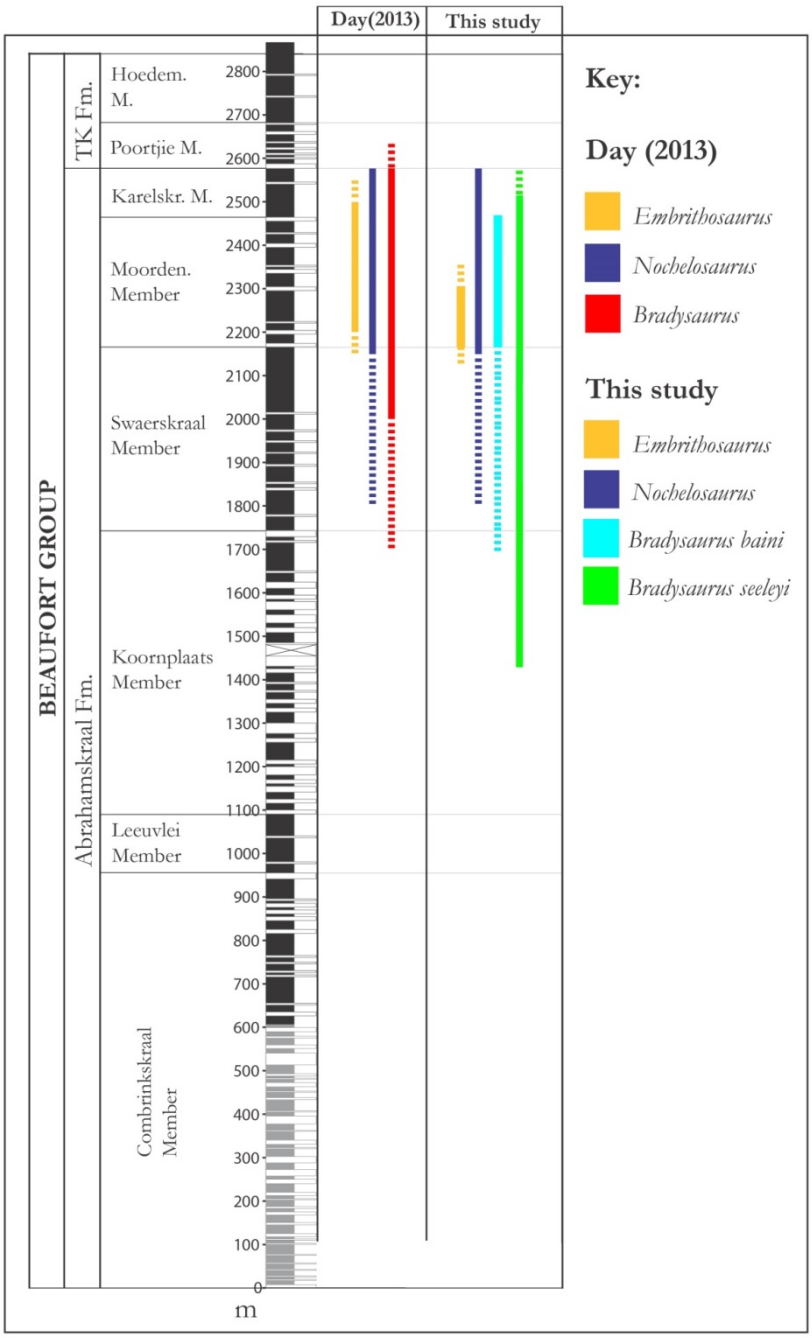


**Figure 5.1:** Composite stratigraphic ranges of pareiasaur genera in the middle Permian Beaufort Group, Day (2013) and this study. Numerals denote meters above the base of the Abrahamskraal Formation. Solid lines indicate well constrained stratigraphic provenances for positively identified specimens of each species. Dotted lines indicate a wide range of possible stratigraphic provenances for positively identified specimens of each species.

# CHAPTER 6 DISCUSSION

Two sections are presented here: a) taxonomic discussion of the valid taxa based on my results compared to previous authors, emphasising new findings and amendments over the latest diagnoses provided by Lee (1995, 1997a), and b) a discussion on the stratigraphic ranges of the valid middle Permian pareiasaurian taxa using positively re-identified specimens, against the most recent compilation of middle Permian tetrapod stratigraphic ranges provided by Day (2013, *et al.* 2015).

## 6.1 Taxonomy

Haughton and Boonstra's (1929a) pareiasaurian classification scheme using cranial differences, recognised the taxonomic challenges presented by the often severely distorted pareiasaurian specimens. They therefore focussed their classification on teeth, with a subdivision using the shape of the dorsal skull table which they considered to be less affected by distortion than the rest of the skull. Their use of the numbers of cusps on the teeth is valid and important, but provided only basic separation of the 12 *Tapincocephalus* Assemblage Zone taxa into two groups: *Embrithosaurus* with nine cusped teeth, and all other 11 taxa with less than nine marginal cusps on their teeth. Their use of the proportions of the dorsal skull table, comparing the width between the orbits to the width between the supratemporal bosses to create three separate conditions, is found to be baseless as was pointed out by Lee (1995, 1997a). The width between the orbits is slightly less than the width between the supratemporal bosses for all basal taxa (Appendix A, B) and thus this character cannot be used for taxonomic differentiation.

Boonstra (1934a) retained all the taxa classified by Haughton and Boonstra (1929a) based on skull shapes and proportions, except for *Platyoropha broomi,* and added several significant morphological cranial features to the diagnosis of

each taxon. Boonstra (1934a) noted the strongly bulged maxilla and lacrimal of *Bradysaurus baini*, the square postparietal of *B. seeleyi,* and the very strong and distinct bosses on the posterior border of the cheek of *Nochelesaurus*. However, Boonstra (1934a) still included many incorrect interpretations in his diagnoses, such as the smooth general cranial ornamentation and the smooth surface of the posterior margin of the cheek of *B. vanderbyli*. The external surface of the holotype skull of *B. vanderbyli* (SAM-PK-3718) is clearly deeply weathered and worn down, as much as one cm deep, smoothing the appearance of the posterior edge of the cheek.

More recently Lee (1995, 1997a) used the presence of anatomical cranial characters to diagnose species, rather than overall skull shape or proportions that are susceptible to distortion or deformation.

The methodology followed in this study is similar to that of Lee (1995, 1997a) in using identification of cranial characters to diagnose species, and differs from the approach adopted by early authors such as Haughton and Boonstra (1929a), who used skull general shapes and proportional differences. An analysis centred on overall skull shape and proportion without taking into account the effects of distortion, would quickly identify two broad skull types: dorsoventrally crushed skulls that are wide, broad and flattened, which are low and have splayed out lateral cheeks and with wide external naris openings on the snout; and mediolaterally compressed skulls that are narrow and high, with cheeks that are more vertically aligned and with external naris openings that are narrow and tall on the snout. Although it is tempting to classify the taxa using these two broad shapes that are easily observable and immediately obvious, it is not the approach used in this study as these two categories are indeed caused by distortion and do not reflect genuine skull shapes. However, a few skull shapes or proportional size differences do appear to be valid and are retained in my diagnoses. These include the strong buckling of the maxilla in *B. baini* (along with the large

maxillary boss) and the relatively small cheek flanges of *B. seeleyi*, even though both of these skull dimensions are susceptible to distortion.

Besides size and shape differences caused by deformation, the lower jaws of all taxa show little variation in specific characters such as foramina, fossae and processes. This lack of variation in characters means that the lower jaws do not appear to have any species consistent diagnostic characters which could be used to distinguish one taxon from another. Only the angular boss of the lower jaw varies significantly in size in many specimens, but appears to follow no consistent pattern that can be reliably used for species identification, as was noted by Haughton and Boonstra (1930a). Differences in the size of the angular boss appear to be related to ontogeny as small specimens always have smaller angular bosses (Lee 1995, 1997a). Since certain large skulls also possess smaller angular bosses, sexual dimorphism may also play a role in causing the variation of this feature.

The number of teeth on the mandible and maxilla are not fixed but range from 17 to 20 in different specimens of the same species. All basal species have teeth numbers that fall within this range, meaning that tooth numbers cannot be used for species diagnosis within the group. Lee (1995, 1997a) notes variation from 18 to 20 teeth in all middle Permian species and that the numbers of teeth are fewer in juvenile specimens. My study confirms the variability and the numbers of teeth in all species as proposed by Lee, and confirms that juvenile specimens have fewer teeth than adults.

According to Lee (1995, 1997a), the more derived late Permian southern African pareiasaurs show different orientations in the rows of palatal teeth and different proportions and placements of the braincase elements compared to the basal species. Accordingly, these features were investigated in my study to identify potential diagnostic differences between the basal pareisaurian species. In the different basal species, the palate and braincase did not reveal any distinguishing features. Features of the palatal teeth, including the numbers of teeth, the

numbers and the orientation of the rows, and the placement of the teeth around the anterior border of the interpterygoid vacuity and on the posterior edge of the pterygoid wing, are similar in all species. The size, proportions and relative placement of the braincase elements, comprising the basisphenoid, basal tubera and occipital condyle, also do not vary between the basal species, as noted by Lee (1995, 1997a).

A challenge in pareiasaurian taxonomy is the genuine, as opposed to taphonomic, asymmetry in many specimens. In particular, the holotype skull of *Embrithosaurus* (SAM-PK-8034) has left and right cheek flanges that are not symmetrical, in two considerations: 1) the shape of the corner or angle boss on the posterior edge of the cheek, and 2) the arrangement of the lateral bosses on the quadratojugal, differ significantly between the left and the right side of the skull. The posterior edge of the left cheek has two very close, almost continious corner bosses that reach onto the ventral surface of the cheek, whereas the right side has a single wide "teat" shaped corner boss. The lateral surface of the right quadratojugal has small, discrete bosses, whereas the left side has larger, longer bosses and more rugose emanations, creating the appearance of two to three indistinct posterodorsally orientated and elongated curved protuberances or rugose lines that create a general thickened swelling of the lower half of the quadratojugal of the left cheek. This lack of bilateral symmetry means that *Embrithosaurus* could be diagnosed differently depending on which side of the cheek of the holotype skull is used. I have used the left quadratojugal when interpreting the bosses of the lateral surface and the corner boss in my diagnoses of *Embrithosaurus*, as the morphology of the left side has been observed more consistently in many specimens of basal pareiasaurs. This is an important finding as currently the morphology of the bosses on the posterior edge of the cheek is used for diagnoses in the Russian pareiasaur *Deltavjatia vjatkensis* which has a uniquely shaped long, rectangular "lozenge" shaped boss on the corner of the cheek (Lee 1995, 1997a, Tsuji 2010) and in *Nochelesaurus*

*alexanderi*, which has uniquely shaped horizontally flat and pointed bosses on the posterior edge of the cheek (Lee 1995, 1997a).

Finally, it must be emphasised that cranial comparision (Table 4.2) shows numerous overlapping features and a lack of cear autapomorphies between the four species. This can be attributed to the excellence of the Karoo fossil record, in which detailed sampling has preserved fossils from an evolving or splitting lineage of animals, making clear species boundaries difficult to establish.

### 6.1.1 *Embrithosaurus schwarzi*

The holotype of *Embrithosaurus schwarzi* (SAM-PK-8034) was described by Broom (1903) as a member of *Pareiasaurus serridens*, although he did not specify details of the similarities. He later admitted this was an error (Broom 1935) after Watson (1914a) noted that the specimen was not at all similar to *P. serridens*. When referring SAM-PK-8034 to *P. serridens* it appears that Broom (1903) misinterpreted the posterior bosses of the corner of the left cheek, which shows two very close unabated, almost indistinguishable bosses that appear to reach anteriorly onto the ventral margin of the cheek. This may have influenced his incorrect referral of the specimen to *P. serridens*, a taxon that has three marginal bosses on the ventral surface of the cheek, located at the corner (angle) of the cheek flange.

The condition of nine cusps on the teeth may also have influenced Brooms (1903) placement of SAM-PK-8034 in *P. serridens,* a taxon which has nine to eleven cusps (Lee 1995, 1997a), as at that time all other known *Tapincephalus* Assemblage Zone pareiasaurs had only seven cusps. Remarking that the skull revealed few distinct cranial sutures, Broom (1903) focused his description on the postcranium and included only a very brief description of the cranial sculpturing, ornamentation and teeth.

In his brief cranial description, Broom (1903) identified many of the prominent cranial bosses, particularly those on the nasal, around the orbital margin, and on the posterior edge of the cheek, but failed to identify the positions and dimensions of most cranial bones and did not specify on which elements the bosses were located. He identified the separation between the lateral cheeks and the flat dorsal skull table as demarcated by a ruguse double ridge that emanates anteriorly from the large supratemporal boss. The numbers and sizes of the cranial bosses and rugose emanations (such as the double ridge) described by Broom (1903) do not distinguish the species and correspond with the situation in most specimens of large *Tapinocephalus* Assemblage Zone pareiasaurs. Broom noted a lack of bilateral symmetry, especially with regards the smaller cranial bosses, protuberances and rugosities.

As explained in the section 1.2 of Chapter one, *Embrithosaurus* has been distinguished from all other *Tapinocephalus* Assemblage Zone pareiasaurs through the presence of up to nine cusps on the maxillary and mandibular teeth. This differs from the much more common arrangement of seven cusps per tooth for all other species from the biozone. Broom (1903) remarked that upper and lower teeth of *Embrithosaurus* have nine cusps per tooth, but added that the upper front teeth may have only seven cusps each. However, as explained in Chapter three, section 3.2.5, the upper front teeth on the premaxilla are all damaged and it is not possible to determine the number of cusps. Conversely, on the maxilla all teeth have nine cusps. The teeth of the right dentary are also well exposed and reveal nine cusps per tooth. Based on the holotype, *Embrithosaurus* thus has nine cusps on all teeth.

Since Broom's 1903 description, most authors have used either a range of seven to nine cusps or only nine cusped teeth as an important distinguishing feature to separate *Embrithosaurus* from the other basal *Tapinocephalus* Assemblage Zone forms (Haughton and Boonstra 1929a, Boonstra 1934a, Boonstra 1969, Kuhn 1969, Lee1995, 1997a). The recognition of nine marginal cusps to identify

specimens of *Embrithosaurus* was inconsistently applied by Boonstra (1934a) who retained specimen NHMUK R7782 even though this specimen possesses only seven marginal cusps of its teeth. Possibly, Boonstra (1934a) merely retained the specimen reference to *Embrithosaurus* assigned by Watson (1914a).

Lee (1995, 1997a) settled on a range of seven to nine cusps. It appears that this may have been done to accommodate two specimens in *Embrithosaurus*: NHMUK R7782 and GSP-CBT-112 based on the presence of the three pelvic autapomorphies. NHMUK R7782 and GSP-CBT-112 both have seven cusps on their teeth visible on the exposed dentary teeth in NHMUK R7782, and the exposed maxillary teeth in GSP-CBT-112.

I only include specimens with nine cusps in E*mbrithosaurus*. My interpretation therefore agrees with the diagnosis of Haughton and Boonstra (1929a), and Boonstra (1934a) who state nine cusps for all teeth as an important diagnostic feature, and differs from Kuhn (1969) and Lee (1995, 1997a) who accepted a range of seven to nine cusps for *Embrithosaurus*. Broom (1935) and Boonstra (1969) did not specify the number of cusps for *Embrithosaurus* in their diagnosis.

More detailed analysis of the teeth has revealed that *Embrithosaurus* possesses maxillary teeth which are uniquely wide, short, stubby, and bulbous. This is because of unique spacing and gaps between the marginal cusps, which are more evenly distributed or regularly spaced than the other species in the group with the result that the three central cusps do not occur on the distal tip of a long, narrow, isolated trident as they do in all other basal taxa. The unique wide maxillary teeth of *Embrithosaurus* are present in at least one published referred specimen (SAM-PK-9098, Fig. 3.35). In contrast the maxillary teeth in NHMUK R7782 and GSP-CBT-112, which have in the past been referred to *Embrithosaurus* (Watson 1914a, Lee 1995, 1997a) are elongated and narrow and do not match the morphology of *Embrithosaurus.*

When Watson (1914b) reassigned the *P. serridens* specimen described by Broom (1903) as the holotype of a new taxon, *Embrithosaurus schwarzi*, he provided

only a brief generic diagnosis and included mostly postcranial features, and only two cranial characteristics; the skull being deep (i.e. large cheek) and narrow (i.e. pointed snout). The skull of the holotype of *Embrithosaurus* does have a large cheek, but this is similar in size to that of *B. baini* and *Nochelesaurus.* The skull of the *Embrithosaurus* holotype is mediolaterally compressed and twisted to the right, creating the appearance of a narrow pointed snout, which was mistakenly considered as diagnostic for *Embrithosaurus* by Haughton and Boonstra (1929a), Boostra (1934a) and most subsequent authors, but correctly pointed out by Lee (1995, 1997a) as a taphonomic artefact.

Haughton and Boonstra's (1929a) use of the nine cusped teeth for *Embrithosaurus* as the most important distinguishing feature for this species is correct. However, their use of the ratio of the interorbital width to the tabular width as a variable feature useful for identification in their scheme, with the interorbital width of *Embrithosaurus* being approximately equal to its tabular width, is unfounded. As noted by Lee (1995, 1997a), and confirmed here, all pareiasaurs from the *Tapinocephlaus* Assemblage Zone, have an interorbital width slightly less than the tabular width (Appendix A, B). The presence of pronounced bosses on the posterior margin of the cheek flange mentioned by Haughton and Boonstra (1929a) are correct, but these large bosses are also present in *B. baini* and are therefore not unique to *Embrithosaurus*.

Boonstra (1934a) provided the most detailed cranial diagnosis for *Embrithosaurus* based on the holotype and specimen NHMUK R7782. However, most of the features he listed are common to most pareiasaurs from the *Tapinocephalus* Assemblage Zone. These include the interorbital width being approximately equal to the tabular width, large bosses on posterior cheek border, ornamentation of pits and rugose ridges, the prominent tabular corner bosses, and the jugal located between the quadratojugal and maxilla. Once again, the erroneous condition of a pointed snout was mentioned. The only truly unique diagnostic feature listed is the presence of nine cusped teeth, which

Boonstra specifically singles out as taxonomically important. The transversely wide postparietal noted is also important as it is shared only with *Nochelesaurus*.

Lee (1995, 1997a) could not identify unique cranial autopomorphies for *Embrithosaurus*. He did however present three pelvic conditions as autapomorphies, all of which had already been identified and discussed by previous authors as important features, although not noted as diagnostic (Watson 1914b, Haughton and Boonstra 1930b). Lee correctly pointed out the lack of large "lump" or boss on the maxilla distinguishing *Embrithosaurus* from *B. baini*. However the holotype of *Embrithosaurus* does have a small distinct maxillary boss. Lee also correctly pointed out the large bulbous posterior cheek bosses that *Embrithosaurus* has in common with *B. baini* and *B. seeleyi,* distinguishing these taxa from *Nochelesaurus* which has uniquely shaped pointier and fatter bosses on the posterior cheeks. The "slightly larger cheek flanges" compared to *B. baini* mentioned by Lee for *Embrithosaurus*, is not relevant as equally sized and even larger cheek flanges are seen in specimens of *Nochelesaurus* and *B. baini.*

In summary it is evident that previously used characters to diagnose *Embrithosaurus* such as seven to nine cusped teeth, a pointed snout, and the interorbital width being approximately equal to the tabular width, are not valid. Thus study has shown that the only diagnostic cranial characters for *Embrithosaurus* are the nine cusps on the teeth, the unique wide shape of the maxillary teeth, the more regular arrangement of the marginal cusps, the presence of only one boss dorsal to the corner boss on the posterior edge of the quadratojugal, and a small maxillary boss with slight maxillary buckling. Other important features that are used for diagnosis include the wide postparietal and the large cheek flanges (shared with *Nochelesaurus*), the large, wide, bulbous, indistinct bosses on the posterior edge of the quadratojugal, and the swollen boss complex on the lateral surface of the quadratojugal (both shared with *B. baini*).

Although the purpose of this study was to provide a detailed cranial description for *Embrithosaurus* and to identify valid defining characters of the genus, this necessitated looking at the defining characters of the other middle Permian pareisaurian taxa. A discussion of these findings are presented below.

### 6.1.2 *Nochelesaurus alexanderi*

The genus *Nochelesaurus* was created by Haughton and Boonstra (1929a) when they reassigned the holotype and only specimen of *Pareiasaurus strubeni* (AMNH FR2232, Broom 1924) to *Nochelesaurus strubeni*. In this new genus they recognised the species *N. alexanderi* (SAM-PK-6239) and *N. strubeni* (AMNH FR2232).

*Nochelesaurus strubeni* (*Pareiasaurus strubeni*) was considered invalid by Lee (1995, 1997a) as he found that the species was mistakenly erected by Broom (1924) using juvenile characteristics, such as fewer teeth, which were not recognised as juvenile features by Broom at the time. Lee found the specimen to be indeterminate because of a lack of preparation (despite the fact that this specimen consists of a very complete skull and skeleton). Even though Lee concluded that *Nochelesaurus* is based on an invalid species (*N. strubeni*) he retained the genus, and nominated the second species (*N. alexanderi*) as the neo-type, a "less disruptive approach" (Lee: 1997a: 248). I concur with Lee's removal of *Nochelesaurus strubeni*, although I have not seen the holotype. The referred specimens (SAM-PK-5019, SAM-PK-5590) used by Haughton and Boonstra (1929a) for this species are unidentifiable due to poor preparation. In addition Boonstra (1934a) referred SAM-PK-1207 and SAM-PK-4253 to *Nochelesaurus strubeni*, both of which are also unidentifiable for the same reason.

Haughton and Boonstra (1929a) identified the genus *Nochelesaurus* as skulls with the interorbital width equal to the tabular width, rather pointed snouts,

deep or large cheeks, massive teeth, and six to eight cusps per tooth. However, in the holotype of *N. alexanderi* (SAM-PK-6239) the interorbital width is actually slightly narrower than the tabular width, and this ratio is shared by all *Tapinocephalus* Assemblage Zone pareiasaurs. The snout is not very pointed. The cheeks are large, but this character is shared with *Embrithosaurus* and *B. baini*. The teeth are large but are within the ranges observed in other large pareisaurid specimens. Amongst these features observed by Haughton and Boonstra (1929a), only the observation of six to eight cusps per tooth are diagnostically significant, as is explained below.

*Nochelesaurus* is defined as possessing six to eight cusps by Haughton and Boonstra (1929a), eight cusps by Boonstra (1934a) and seven cusps by Lee (1995, 1997a). Additional preparation of two mandibular and two maxillary teeth in the holotype (SAM-PK-6239) has revealed eight to nine cusps on the mandibular tooth and at least eight cusps (possibly nine) on the maxillary teeth. In addition, the new preparation of the mandibular teeth on the holotype revealed unique non-symmetrically arranged marginal cusps, with the mesial marginal cusps located much lower down than the distal marginal cusps and with evidence of unique medial marginal cusps (Fig. 3.39).The mandibular teeth of the holotype also show unique vertical ridges not seen in any other referred specimen of *Nochelesaurus* or in any other taxon. The presence of these vertical ridges in the holotype of *Nochelesaurus* is an important distinguishing feature of the taxon. Recent taxonomic work on Chinese pareiasaurs (Benton 2016) has used similar vertical ridges on the lingual surfaces of dentary teeth as significant taxonomic features to distinguish species. Referred specimen, SAM-PK-6240 (identified in this study as *Nochelesaurus* as it has the distinctive horizontally flat, pointed, bosses on the posterior margin of the cheek) has seven cusps on the mandibular teeth, and therefore *Nochelesaurus* has seven to nine cusps on the mandibular and maxillary teeth; the shape of the maxillary teeth is elongated and similar to *B. baini* and *B. seeleyi*, but distinct from those of *Embrithosaurus*.

Amongst the diagnostic characters of Haughton and Boonstra (1929a) for *Nochelesaurus alexanderi* (SAM-PK-6239), is a heavily ornamented skull and "strong" bosses on the posterior border of the cheek. The ornamentation of SAM-PK-6239 appears very distinct, pointed and strong, but this is actually due to the unusually well prepared and well preserved nature of the specimen which enhances the distinctiveness and rugosity of the ornamental bosses and even allows for rare, relatively easy identification of external cranial sutures between the elements. The size and pattern of the cranial ornamentation of SAM-PK-6239 is very similar to most specimens of basal pareiasaurs and is not diagnostic. However the bosses on the posterior margins of the cheeks of *Nochelesaurus alexanderi* (SAM-PK-6239) are "strong" as their long, horizontally plate-like and pointed shape are unique within the basal pareiasaurs, as pointed out by Lee (1995, 1997a).

Boonstra (1934a) mentioned that the holotype for *Nochelesaurus alexanderi* (SAM-PK-6239) carries a unique midline boss at the nasal-frontal suture, which is contributed equally by all four bones. However, he fails to mention this feature in the diagnoses. This feature is present only in the holotype of *Nochelesaurus alexanderi* and is therefore an anomaly. Boonstra's (1934a) observation of a transversely rectangular postparietal is valid but this character is shared with *Embrithosaurus*.

Lee (1995, 1997a) could not identify any unique cranial autopomorphies for *Nochelesaurus*, but he correctly emphasised the distinct and pointed bosses on the posterior cheek edge as the most important diagnostic difference compared to all the other *Tapinocephalus* Assemblage Zone pareiasaurs. He also presented three autapomorphies in the scapulocoracoid, humerus and femur.

*Nochelesaurus* is valid due to the distinctive flat and pointed morphology of the bosses on the posterior edge of the quadratojugal, the lack of any maxillary boss on the snout shared only with *B. seeleyi*, the transversely wide postparietal shared only with *Embrithosaurus*, and the flat surface with more discrete bosses

on the lateral surface of the quadratojugal. Whilst this taxon has similarly shaped elongated maxillary teeth to those of *B. baini* and *B.seeleyi*, important new findings additional to the latest diagnoses of Lee (1995, 1997a) include an increase on the numbers of cusps on the teeth (ranging from seven to nine), the unique non-symmetrical placement of the marginal cusps on the mandibular teeth, and the unique vertical ridges on the lingual surface of the mandibular teeth. However, these additional diagnostic features of the mandibular teeth have not been observed in any referred specimens because of the unprepared nature of the teeth on most specimens.

### 6.1.3 *Bradysaurus baini*

Seeley (1892) described and illustrated NHMUK R1971 from the *Tapinocephalus* Assemblage Zone and named it *Pareiasaurus baini*. He noted mostly postcranial differences compared to the other two large South African pareiasaur species described by that time, i.e. *Pareiasaurus bombidens* and *Pareiasaurus serridens*. Later, Watson (1914b) made NHMUK R1971 the holotype of a new genus, *Bradysaurus*, due to significant morphological differences between all specimens recovered from the *Tapinocephalus* Assemblage Zone and *Pareiasaurus serridens*, recovered from the higher *Cistecephalus* Assemblage Zone (Chapter 1 Introduction).

Cranially, only the condition of a “depressed and rounded” skull was mentioned by Watson (1914b) in his diagnosis of *Bradysaurus baini*, indicating Watson’s observation of dorsoventral compression and a rounded edge between the flat dorsal skull table and the lateral cheeks. My observations show that the skull is only very slightly dorsoventrally crushed, and is not rounded, as it has sharp edges between the dorsal skull table and the lateral cheeks, better observed on the left side. The right side of the skull is slightly posteriorly displaced.

Haughton and Boonstra (1929a) retained *Bradysaurus baini* and expanded Watson's cranial diagnosis to include six cusps per tooth, broad rounded snout, shallow (i.e. small) cheek, interorbital width being much less than the tabular width, and a fairly smooth posterior cheek border. My observations show seven cusps per upper jaw tooth; the cheeks are large and not shallow; the interorbital width is only slightly less than the tabular width; bosses on the posterior cheek borders are large, bulbous, and distinct, especially on the left side, and are not very smooth, which was probably interpreted due to the somewhat indistinct smoother bosses on the right side only; snout is indeed broad and rounded in appearance due to the large maxillary bosses and buckled or bent maxilla.

Boonstra (1934a) correctly noted teeth with seven cusps, the very strongly bulging maxilla and lacrimal, the very strong ridge separating the dorsal and lateral surfaces of the skull and a low tabular boss. The fairly smooth posterior border of the cheek was maintained as an important diagnostic character, although my study shows that this is not the case, and the postparietal was described as transversely wide and rectangular, which is not substantiated by my observations. Only the strongly bulging maxilla and lacrimal are diagnostically significant observations for this taxon.

Lee (1995, 1997a) in his taxonomic reassessment, assigned three cranial autapomorphies to *Bradysaurus baini*: a large "lump" on the maxilla, a distal swollen paroccipital process on the opisthotic and inwards pointing maxillary teeth. Each of these is discussed below.

Boonstra was the first author to note the "very strongly bulged" maxilla and lacrimal of *B. baini* (Boonstra 1934a: 25) as an important diagnostic character. Lee (1995, 1997a) described this character as a large "lump" (i.e. maxillary boss) on the maxilla. This large maxillary boss and sharp buckling or bending of the maxilla is clearly identifiable in many specimens and is retained as an autapomorphy, but is better described as consisting of a large maxillary boss that

extends onto the lacrimal, making the anterior bosses of the lacrimal less distinct, and occurs on a sharply buckled or bent maxilla.

The holotype of *B. baini* and several referred large skulls have a large, knob-like projection near the distal end of the paroccipital process of the opisthotic. However, this knob-like projection (Lee's swollen distal end of the paroccipital process) is not unique to *B. baini* and is found in most specimens, and across all species studied that have the opisthotics preserved and exposed (Appendix A, B). The knob is present in the holotype of *Embrithosaurus* (SAM-PK-8034), but is smaller and less distinct than in the holotype of *B. baini*. The size of this knob in SAM-PK-5002, most certainly a referred specimen of *B. baini*, is identical to the smaller size of the knob in the holotype of *Embrithosaurus* (SAM-PK-8034). The knob, although small, is also seen in NHMUK R7782, which Lee (1995, 1997a) refers to *Embrithosaurus*. A small knob is also present, in SAM-PK-6240, which Lee (1995, 1997a) refers to *Nochelesaurus*, and a large knob is present in SAM-PK-3718, which Lee refers to *B. seeleyi*. This swollen knob-like projection on the distal end of the paroccipital process of the opisthotic, appears to vary primarily with the size of the skull, and is larger in larger specimens, regardless of the species.

Consequently, the knob-like projection on the distal end of the paroccipital process of the opisthotic is removed as an autapomorhpy for *B. baini,* as its presence is not unique to the species. However, its large size is retained as an important character for *B. baini* compared to all other species where it is small to medium in size.

The backwards pointing maxillary teeth autapomorphy, appears to be the result of post mortem distortion. Most of the skulls studied, suffer from varying degrees of distortion, and the maxillary teeth appear to be more effected as almost all skulls studied have inwardly pointed maxillary teeth to differing extents, regardless of the level of distortion of the skull. Different sides of the same skull and even different sections of teeth on the same individual (such as

premaxillary teeth compared to maxillary teeth) are often inwardly distorted to differing degrees, again making it challenging to determine the actual direction the teeth were pointing in life for individual specimens.

Furthermore, inwardly pointing maxillary teeth are found in all species except *Embrithosaurus*. This includes the holotype of *B. baini* (NHMUK R1971), referred specimens of *B. baini* (SAM-PK-5002, SAM-PK-5624), the holotype of *B. seeleyi* (NHMUK 49426), and specimens that Lee refers to *B. seeleyi* (SAM-PK-3718, SAM-PK-5012)*, Nochelesaurus* (SAM-PK-6240) and *Embrithosaurus* (NHMUK R7782, CGP CBT 112). As an example, the undistorted large specimen, SAM-PK-3718, which Lee refers to *B. seeleyi*, clearly has inwards pointing upper jaw teeth. Consequently, it is not possible to verify inwardly pointing maxillary teeth as diagnostic of any particular species. From personal observation, it appears most likely that the maxillary teeth were slightly inwardly pointing in all species in life position, and have been exaggerated through dorsoventral distortion to point more inwards in many specimens.

Currently, only two of the 21 accepted species of pareiasaurs are classified as having inwardly pointed maxillary teeth, i.e. *B. baini* and *Pareiasuchus nasicornis* (Lee 1995, 1997a, *et al.* 1997). It is most probable that the maxillary teeth pointed straight downwards or slightly inwards in all pareiasaur species, due to their inherited common jaw mechanisms. There is no evidence of significantly different jaw mechanics or upper and lower jaw occlusion in *B. baini* or *P. nasicornis*, compared to all other species. Furthermore, the natural orientation of the dentary teeth on all specimens and species studied appears to be slightly outwards, i.e. 10-20 degrees outwards from the vertical. The maxillary teeth likely were directed a similar degree inwards to provide for a sheering surface upon contact with crowns of the mandibular teeth. Therefore, the inwardly pointing maxillary teeth are removed as an autapomorhpy for *B. baini.*

Personal study of a referred specimen of *B. baini* (SAM-PK-5624) has revealed an important new finding of a range of seven to nine marginal tooth cusps and not the reported seven cusps of the latest diagnosis (Lee 1995, 1997a) for *B. baini.*

*Bradysaurus baini* is considered valid because of the distinctive autapomorphy of a large maxillary boss associated with a sharply buckled or bent maxilla. Other important features include the transversely narrow postparietal, the elongated teeth with seven to nine cusped teeth (usually seven), swollen rugose bosses on the lateral surface of the quadratojugal, and the largest knob-like projection on the paroccipital process on the opisthotic.

### 6.1.4 *Bradysaurus seeleyi*

*Pareiasaurus bombidens* was erected by Owens (1876) based on a very imperfect specimen of a fragmentary snout of (NHMUK R1714/43525). Seeley (1888) was the first to describe specimen NHMUK 49426, referring it to *P. bombidens*. He also described and referred specimen NHMUK R1970 to *P. bombidens* in 1892 (Seeley 1892).

Haughton and Boonstra (1929a) did not place Owen's *Pareiasaurus bombidens* in their classification scheme, arguing that the very fragmentary holotype specimen is not good enough to allow for proper diagnosis. Therefore, for the two specimens referred by Seeley to *P. bombidens* (1888, 1892) Haughton and Boonstra (1929a) created the new species *Bradysaurus seeleyi* with NHMUK 49426 the holotype. They noted the well-defined or distinct bosses on the posterior border of the cheek as important and the only feature used to distinguishing this species within the genus. The characteristics defining the genus *Bradysaurus* were: short, broad and rounded snout; shallow (small) cheek; six cusps per tooth; and constricted interorbital width compared to the tabular width. Compared to *B. baini,* only the shallow or small cheek and the relatively

more distinct, smaller bosses on the posterior edge of the cheek, are good diagnostic features.

Later Boonstra (1934a) correctly noted seven cusped teeth, distinct, well-defined bosses on the posterior edge of the cheek, the somewhat bulging maxilla and lacrimal, and the square postparietal but provided diagnostic features with which to positively identify *B. seeleyi.*

Lee (1995, 1997a) agreeing with Haughton and Boonstra (1929a) that the holotype for *P. bombidens* (NHMUK R1714/43525) is based on indeterminate material, declared it *nomen vanum*. My observations of NHMUK R1714/43525 confirm that this fragmentary specimen cannot be distinguished from *Nochelesaurus, B. seeleyi* or *B. baini*. The maxillary teeth of this specimen are elongated and have seven cusps, precluding its identification as *Embrithosaurus*.

Lee retained Haughton and Boonstra's (1929a) *Bradysaurus seeleyi* as valid, noting that the taxon has smaller cheek flanges than any other pareiasaur and that it lacks the three cranial autapomorphies of *B. baini*, i.e. inwards pointing upper jaw teeth, a swollen distal end of the paroccipital process and a large maxillary "lump". NHMUK 49426 does possess significantly smaller cheek flanges than other specimens, and lacks the large maxillary boss and sharp maxillary buckling of *B. baini.* The maxillary teeth of NHMUK-49426 are severely distorted to point inwards, which is probably due to the severe dorsoventral crushing of the skull. It is most likely that in life the maxillary teeth were pointed straight down or slightly inwards. The distal end of the paroccipital process of the opisthotic is much more slender than that of *B.baini*, and has no swelling or knob-like projection compared to the large knob of *B.baini*.

I retain *B. seeleyi* as valid, based on the diagnostic small cheek flanges and only seven cusps per tooth. However, this species has the fewest unique features in the group and, along with the small cheeks and seven cusped teeth, is identified through a combination of characters, which are shared with other species in the group. The lack of a large maxillary boss or sharp buckling is shared with

*Nochelesaurus*, the slight buckling of the maxilla is shared with *Embrithosaurus*, the transversely narrow and square postparietal shared with *B. baini,* and the medium relatively distinct bosses on the posterior edge of the cheeks, shared with certain specimens of *B. baini.*

## 6.2 Stratigraphy

As explained in Chapter 1 Introduction, section 1.3.2, for many years staff and students of the Evolutionary Studies Institute (ESI) have been studying middle Permian biodiversity change in the continental realm based on the fossil record of the Beaufort Group which preserves the most continuous middle Permian fossil record in the continental realm (Rubidge 2005, Nicolas 2007, Van der Walt *et al.* 2011, Day 2013, Rubidge *et al.* 2013, Day *et al*. 2015, Rubidge *et al*. 2016).

This has required taxonomic revisions of all the major tetrapod taxonomic groups which lived in the middle Permian, which has enabled the determination of ranges for all of these different taxa using the Beaufort Fossil Vertebrate GIS database of Karoo fossils tetrapod taxa developed by Nicolas (2007, van der Walt *et al.* 2011), with sector stratigraphic logs of the Abrahamskraal Formation (Day 2013, Day *et al.* 2015).

The pareiasaurs are the only major taxonomic group which have not undergone a recent taxonomic reassessment and many of the identifications in museum catalogues are outdated. Pareisaurs make up about 25% of the middle Permian terrestrial tetrapod fauna of the Karoo (van der Walt 2011, Smith *et al.* 2012). This study is a first attempt to rectify this situation and in the process, re-identifications of specimens in museum collections has been undertaken and their new taxonomic assignments have been updated in the catalogue.

This study has determined stratigraphic ranges for all valid species based on the positive re-identification of 39 cranial specimens using the amended cranial diagnosis (Fig. 5.1).

The stratigraphic range of *Bradysaurus*, previously determined only to genus level by Day (2013*, et al.* 2015) has now been determined for each of *B. baini* and *B. seeleyi.* The stratigraphic range of *B. seeleyi* is significantly extended lower, because of newly discovered specimen (BP/I/7886) from the Koornplaats Member of the Abrahamskraal Formation. *B. seeleyi* is thus the first pareiasaurid to appear.

The stratigraphic range of *Nochelesaurus* remains unchanged in this study, compared to (Day 2013, *et al.* 2015) and along with *B. seeleyi* appear to be the longest lived taxa, surviving until the top of the Karelskraal Member of the Abrahamskraal Formation.

*B. baini* and *Embrithosaurus* show a shorter stratigraphic range compared to the ranges produced by Day (2013, *et al.* 2015) but this is probably due to fewer specimens used in this study, compared to the study of Day (2013, *et al.* 2015).

# CHAPTER 7 CONCLUSION

## 7. 1 Project achievements

In an effort to better understand middle Permian tetrapod biodiversity change in the continental realm, this study has attempted to refine the taxonomy of the pareiasaurids which make up about 25% of the tetrapod fauna of the time, with a view to understand stratigraphic ranges of individual pareiasaurid taxa. The pareiasaurids of the *Tapinocephalus* Assemblage Zone are the oldest and most basal members of this important parareptile lineage which attained Pangean wide distribution in the late Permian.

This study has produced the first detailed cranial description for *Embrithosaurus schwarzi*. The dimensions of most of the preserved cranial elements have been determined and the cranial ornamentation and bosses have been documented in detail in the description and illustrative drawings. *E. schwarzi* is found to be a valid species based on cranial features. It is distinguished from the other very similar basal Southern African pareiasaurs through the morphology of the maxillary teeth, which have nine cusps more evenly arranged, and wider and shorter dimensions than all other basal pareiasaurid species.

The significant changes to the taxonomy of the basal pareiasaurs made by Lee (1995, 1997a), decreasing the 11 original taxa in the group to four, have been confirmed by this study. The holotype skulls of eight of these 11 original taxa (i.e. the six curated in Cape Town and two in London) were studied by personal direct observation. *Nochelesaurus alexanderi, Bradysaurus baini* and *Bradysaurus seeleyi* are found to be valid taxa, based on this cranial reassessment and retaining the postcranial diagnoses supplied by Lee (1995, 1997a).

The cranial diagnoses of all taxa have been amended. The four valid species, which are cranially very similar, can be distinguished in that *Embrithosaurus* has distinctive shaped maxillary teeth and nine cusps on all teeth; *Bradysaurus baini* has a large maxillary boss coupled with a strongly buckled or bent maxilla;

*Nochelesaurus* has distinctive horizontally flat, pointed bosses on the posterior edge of the quadratojugal; and *B. seeleyi* has the smallest cheek flanges. The small cheek flanges of *B. seeleyi* are shared with some specimens of *B. baini* and since *B. seeleyi* shows no further identifiable features, *B. seeleyi* is the least secure taxon. Along with these major differences, each taxon can be identified through a careful analysis of the conditions of the five dental and nine cranial features explained in Chapter 4, Taxonomic Review. The condition of these 14 features is consistent and falls within the ranges defined for all specimens of a particular species.

The methodology followed is this study is similar to Lee (1995, 1997a), and differs from the early authors in the use of specific cranial characters to diagnose and distinguish species, rather than using vague skull shapes and proportions. This study is an attempt to mitigate the effects of interpreting skull shapes and proportions affected by deformation as real morphological differences. This study has shown that most specimens are affected by deformation, which makes the job of analysis very challenging when distinguishing actual morphological features from the effects of distortion.

The study has re-identified 39 cranial specimens from museum collections, and determined updated stratigraphic ranges for the four valid taxa. *Embrithosaurus* occurs in the lower to mid Moordenaars Member; *Nochelesaurus* ranges from the Swaerskraal Member to the uppermost Karelskraal Member; *Bradysaurus baini* from the upper Koornplaats to top of the Moordenaars Member; and *B. seeleyi* ranges the mid Koornplaats Member to the upper Karelskraal Member. *Nochelesaurus* and *B. seeleyi* are present in the uppermost Karelskraal Member of the Abrahamskraal Formation, at the top of the *Tapinocephalus* Assemblage Zone. This has confirmed the occurrence of the basal pareisaurs in the middle to upper *Tapinocephalus* Assemblage Zone, and the extinction of the group by the beginning of the Poortjie Member of the Teekloof Formation (*Pristerognathus* Assemblage Zone). After the straigraphic break of the Poortjie Member a

completely different pareiasaurid fauna is present in the overlying Hoedemaker Member (*Tropidostoma* Assemblage Zone) of the Beaufort Group (van der Walt *et al.* 2011).

## 7.2 Opportunities for future improvements

Although this study has produced the first comprehensive cranial description of *Embrithosaurus* and updated cranial diagnoses for all valid pareiasaurian taxa of the *Tapinocephalus* Assemblage Zone, many opportunities for additional future research have been highlighted as a result of this study.

A comprehensive cranial description for *Nochelesaurus* is lacking, and those of *B. baini* and *B. seeleyi* are brief and were produced in the late 1800's by Seeley (1888, 1892).

Although amended cranial diagnosis for all valid taxa have been produced, further work is still required with regards to understanding important cranial characters. This study removed Lee's (1995, 1997a) autapomorphy of inwardly directed upper jaw teeth from the diagnosis of *B. baini,* proposing that this condition is probably due to distortion. However, the upper jaw morphology needs further study to determine conclusively the actual life condition of the dentition in this species. Distortion, jaw mechanics, upper and lower jaw tooth occlusion and mechanics, tooth wear, the shape of the premaxilla/maxilla (including maxilla overhang over the lower jaw), and the shape of the teeth (straight to curved) need to be investigated in more detail. Similarly, this study also removed Lee's (1995, 1997a) autapomorphy of a swollen distal end of the parocipital process of the opisthotic from the diagnosis of *B. baini*, as this feature is present in all basal pareiasaurian taxa. This size of this feauture is highly variable within each species as there seems to be a lack consistency in the size of the knob-like projection on the distal end of the parocciptial process of the opisthotic and this structure requires further investigation. This is hampered by

the fact the parocciptial process of the opisthotic is not preserved in most specimens and is usually poorly prepared when present. The size of the cheek flange is highly variable in *B. baini,* ranging from small to large. All other species have consistent cheek flange sizes. Therefore the cheek flange size in *B. baini* requires further investigation.

This study identified for the first time two distinct arrangement patterns of the bosses on the posterior edge of the quadratojugal in terms of the number of bosses and their placement or spacing. Both patterns appear to be present in all basal pareiasaurian taxa except for *Embrithosaurus* (Chapter 4, Taxonomic Review) which has only one of the two patterns. These two different patterns could denote sexual dimorphism within each species or could represent species diagnosis. These two boss patterns require more detailed analysis.

This study has also identified the need for a more reliable method to recognise and account for distortion and deformation in a specimen, so as to avoid misinterpretation and diagnoses of cranial features based on taphonomic effects. Distortion affects the interpretation and measurements of the size of the cheeks, which needs to be better quantified than the method used in this study.

Differences were observed but no consistent species diagnostic pattern was found in the arrangement and number of bosses on the frontals, nasals, and postfrontals. The main central boss on the frontal is highly variable in size and distinctiveness, there are lateral and posterior tabs or rugose lines emanating from each main nasal boss, but certain specimens include a medial tab; and the postfrontal appears to vary and has between one to two bosses. Further research may highlight important diagnostic characters related to the bosses and ornamentation of these three cranial elements.

Although the outer surfaces of most maxillary teeth observed are smooth, a few specimens had ridged grooves, but with no consistent pattern for each species. This may be intraspecific variability or conversely may be of diagnostic importance in future studies.

A key finding reported by Lee (1995, 1997a) is that cranial studies alone are not sufficient to produce a robust taxonomic framework for pareiasaurids, as he recognised several diagnostic postcranial characters. Only a brief postcranial description was produced for *Embrithosaurus* by Broom (1903), and no postcranial description has been undertaken for *Nochelesaurus*. The existing brief postcranial descriptions for *B. baini* and *B. seeleyi* were produced in the late 1800's.

Phylogenetic analysis of cranial and postcranial characters were excluded from this exploratory study. The opportunity exists to enhance the current set of cranial and postcranial characters through additional study. A phylogenetic analysis of pareiasaurians needs to be integral to the group, including the younger basal representatives.

Study of the basal pareiasaurs from the *Tapinocephalus* Assemblage Zone has historically been challenging largely because of poor preparation of the specimens. Most material, including the important holotypes, crania and postcrania, and including potentially highly diagnostic dentition, are only partially prepared. The majority of the material was collected prior to the 1930's and was either not prepared or only partially mechanically prepared at the time. It is clear that little or no subsequent preparation has been conducted in recent times using more modern preparation techniques. Many specimens are fragmentary and have been spread amongst a number of boxes, shelves, rooms and locations. This hampers study as most specimens require additional time to locate, move, and reassemble before anatomical studies can be conducted. New preparation of old material, Computer Tomography (CT) scanning, phylogenetic systematics and more accurate stratigraphic information, means that modern researchers can make new contributions towards understanding pareiasaurian taxonomy and biostratigraphy.

## CHAPTER EIGHT: REFERENCES


ABDALA, N. F., KAMMERER, C. F., DAY, M. O., JIRAH, S. and RUBIDGE, B. S. 2014. Adult morphology of the therocephalian *Simorhinella baini* from the middle Permian of South Africa and the taxonomy, geographicand temporal distribution of the Lycosuchidae. *Journal of Palaeontology***, 88,** 1139-1153.

ANGIELCZYK, K. D. and RUBIDGE, B. S. 2013. Skeletal morphology phylogenetic relationships and stratigraphic range of *Eosimops newtoni* Broom 1921, a phlaecephalid dicynodont (Therapsida, Anomodontia) from the middle Permian of South Africa. *Journal of Systematic Palaeontology*, **11 (2)**, 191-231.

BENTON, M. J. 2016. The Chinese pareiasaurs. *Zoological Journal of the Linnean Society*, **177**, 813-853.

BOONSTRA, L. D. 1929a. Pareiasaurian studies. Part 3. On the Pareiasaurian Manus. *Annals of the South African Museum*, **28**, 97-112.

BOONSTRA, L. D. 1929b. Pareiasaurian studies. Part 4. On the Pareiasaurian Pes. *Annals of the South African Museum,* **28**, 113-122.

BOONSTRA, L. D. 1932a. The phylogenesis of the Pareiasauridae: a study in evolution. *South African Journal of Science,* **29**, 480-486.

BOONSTRA, L. D. 1932b. Pareiasaurian studies. Part 7. On the Hind Limb of the Two Little-know Pareiasaurian Genera: Anthodon and Pareiasaurus. *Annals of the South African Museum,* **28**, 429-435.

BOONSTRA, L. D. 1932c. Pareiasaurian studies. Part 8. The Osteology and Myology of the Locomotor Apparatus. B – Fore Limb. *Annals of the South African Museum,* **28**, 437-503.

BOONSTRA, L.D. 1934a. Pareiasaurian studies. Part 9. The cranial osteology. *Annals of the South African Museum*, **31**, 1-38.

BOONSTRA, L. D. 1934b. Pareiasaurian studies. Part 10. The Dermal Armour. *Annals of the South African Museum,* **31**, 39-48.

BOONSTRA, L. D. 1934c. Pareiasaurian studies. Part 11. The Vertebral Column and Ribs. *Annals of the South African Museum,* **31**, 49-66.

BOONSTRA, L. D. 1969. The fauna of the *Tapinocephalus* zone (Beaufort beds of the Karoo). *Annals of the South African Museum,* **56**, 1-73.

BROOM, R. 1903. On an almost perfect skeleton of *Pareiasaurus serridens* Owen. *Annals of the South African Museum*, **4**, 123-138.

BROOM, R. 1912. On a new species of Propappus, and on the Pose of the Pareiasaurian Limbs. *Annals of the South African Museum,* **7**, 323-331.

BROOM, R. 1913. On four new fossil reptiles from the Beaufort Series, South Africa. *Records of the Albany Museum,* **2**, 397-401.

BROOM, R. 1914. Further observations on the South African fossil reptiles. *The American Museum Journal,* **14**, 139-143.

BROOM, R. 1915. Catalogue of types and figured specimens of fossil vertebrates in the American Museum of Natural History. II – Permian, Triassic and Jurassic reptiles of South Africa. *Bulletin American Museum of Natural History,* **25**, 105-164.

BROOM, R. 1916. Pareiasaurian Nomenclature. To the Editors of the Annals and Magazine of natural History. *Annals and Magazine of Natural History,* **17,** 347-348.

BROOM, R. 1924. On some points in the Structure of the Pareiasaurian Skull. *Proceedings of the Zoological Society of London,* **1924**, 499-508.

BROOM, R. 1935. Notes on some species of pareiasarian reptiles. *Annals of the Transvaal Museum,* **18,** 37-51.

CISNEROS, J. C. and ABDALA, F. 2005. Pareiasaurids from the Rio do Rasto formation, southern Brazil: Biostratigraphic implications for Permian faunas of the Parana basin. *Revista Brasileira de Paleontologia*, **8**, 13-24.

DAY, M. O. 2013. middle Permian continental biodiversity changes as reflected in the Beaufort Group of South Africa: a bio-and lithostratigraphic review of the *Eodicynodon, Tapinocephalus,* and *Pristerognathus* Assemblage Zones. Unpublished Ph.D thesis, University of the Witwatersrand, Johannesburg, 1-387.

DAY, M. O., RAMEZANI, J., BOWRING, S. A., SADLER, P. M., ERWIN, D. H., ABDALA, F. and RUBIDGE, B.S. 2015. When and how did the terrestrial mid-Permian mass extinction occur? Evidence from the tetrapod record of the Karoo Basin, South Africa. *Proceedings of the Royal Society of London B,* **282,** 20150834.

GUVEN, S., RUBIDGE, B. S. and ABDALA, F. 2013. Cranial morphology and taxonomy of South African Tapinocephalidae (Therapsida: Dinocephalia): the case of *Avenantia* and *Riebeeckosaurus. Palaeontologia africana*, **48**, 24-33.

HAUGHTON, S. H. 1929. Pareiasaurian studies. Part 2. Notes on some Pareiasaurian Brain-Cases, *Annals of the South African Museum*, **28**, 88-96.

HAUGHTON, S. H. and BOONSTRA, L. D. 1929a. Pareiasaurian studies. Part I. An attempt at a classification of the Pareiasauria based on skull features. *Annals of the South African Museum*, **28**, 79-87.

HAUGHTON, S. H. and BOONSTRA, L. D. 1930a. Pareiasaurian studies. Part 5. On the Pareiasaurian Mandible. *Annals of the South African Museum,* **28**, 261-288.

HAUGHTON, S. H. and BOONSTRA, L. D. 1930b. Pareiasaurian studies. Part 6. The Osteology and Myology of the Locomotor Apparatus. A – Hind Limb. *Annals of the South African Museum,* **28**, 296-366.

HAUGHTON, S. H. and BRINK, A. S. 1954. A bibliographic list of reptilian from the Karroo Beds of Africa. *Annals of the South African Museum,* **28**, 1-171.

JALIL, N.-E. and JANVIER, P. 2005. Les pareiasaures (Amniota, Parareptilia) du Permien superieur du Bassin d'Argana, Maroc. *Geodiversitas*, **27(1)**, 35-132.

KITCHING, J.W. 1995. Biostratigraphy of the *Dicynodon* Assemblage Zone. In: Rubidge, B.S. (ed.). Biostratigraphy of the Beaufort Group (Karoo Supergroup), Biostratigraphic Series 1. *South African Committee for Stratigraphy*, Pretoria, 29-34.

KAMMERER, C. F. 2011. Systematics of the Anteosauria (Therapsida: Dincocephalia). *Journal of Systematic Palaeontology*, **9:2**, 261-304.

KAMMERER, C. F., SMITH, R. M., DAY, M. O. and RUBIDGE, B. S. 2015. New information on the morphology and stratigraphic range of the mid-Permian gorgonopsian *Eriphostoma microdon* Broom, 1911. *Papers in Palaeontology,* **1 (2),** 201-221.

KEYSER, A. W. and SMITH, R. H. M. 1977. Vertebrate biozonation of the Beaufort Group with special reference to the Western Karoo Basin. *Annals Geological, Survey South Africa*, **12**, 1-36.

KUHN, O. 1969. *Cotylosaria. Handbuch der Palaoherpetologie, Teil 6.* Stuttgart: Gustav Fischer Verlag.

LEE, M. S. Y. 1993. The origin of the turtle body plan: bridging a famous morphological gap, *Science*, **261**, 1716-1720.

LEE, M. S. Y. 1995. Evolutionary morphology of pareisaurs. Unpublished Ph.D thesis, University of Cambridge, Cambridge, 1-392.

LEE, M. S. Y. 1997a .A taxonomic revision of pareiasaurian reptiles: implications for Permian terrestrial palaeoecology. *Modern Geology*, **21**, 231-298.

LEE, M. S. Y. 1997b. Pareiasaur phylogeny and the origin of turtles. *Zoological Journal of the Linnean Society*, **120**, 197-280.

LEE, M. S. Y., GOW, C. E. and KITCHING, J. W. 1997. Anatomy and the relationships of the pareiasaur P*areiasuchus nasicornis* from the upper Permian of Zambia. *Palaeontology*, **40(2)**, 307-335.

LYDEKKER, R. 1890. Catalogue of the Fossil Reptilia and Amphibia in the British Museum. Part 4. London, British Museum (Natural History).

NEWTON, E. T. 1893. On some new reptiles from the Elgin sandstones. *Philosophical Transactions of the Royal Society of London B*, **184,** 431-503.

NICOLAS, M. V. M 2007. Tetrapod biodiversity through the Permo-Triassic Beaufort Group (Karoo Supergroup) of South Africa. Unpublished Ph.D thesis, University of the Witwatersrand, Johannesburg, 1-356.

OWEN, R. 1856. Report on the reptilian fossils of South Africa. Part 3. On parts of the skeleton of the trunk of the *Dicynodon tigriceps*. *Trans. Geol. Soc. Ser.* 2, **7**, 241-247.

OWEN, R. 1862. On the dicynodont Reptilia, with a description of some fossil remains brought by H.R.H. Prince Alfred from South Africa, November 1860. *Philosophical Transactions of the Royal Society of London B,* **152**, 455-467.

OWEN, R. 1876. Descriptive and Illustrated Catalogue of the Fossil Reptilia of South Africa in the Collection of the British Museum. London, British Museum (Natural History).

RUBIDGE, B. S. 1987. South Africa's oldest land-living reptiles from the Ecca-Beaufort transition in the southern karoo. *South African Journal of Science,* **83**, 165-166.

RUBIDGE, B. S. and VAN DEN HEEVER, J. A. 1997. Morphology and systematic position of the dinocephalian *Styracocephalus. Lethaia*, **30**, 157-168.

RUBIDGE, B. S. 2005. Re-uniting lost continents – Fossil reptiles from the ancient Karoo and their wanderlust. *South African Journal of Geology*, **108 (3),** 135-172.

RUBIDGE, B. S., ERWIN, D. H., RAMEZANI, J., BOWRING, S. A. and DE KLERK, W. J. 2013. High-precision temporal calibration of late Permian vertebrate biostratigraphy: U-Pb zircon constraints from the Karoo Supergoup, South Africa. *Geology*, **41**, 363-366.

RUBIDGE, B. S., DAY, M. O., BARBOLINI, N., HANCOX, P. J., CHOINIERE, J., BAMFORD, M. K., VIGLIETTI, P. A., and JIRAH, S. 2016. Advances in nonmarine Karoo biostratigraphy: Significance for understanding basin development. In: Linol, B. and de Wit, M. (Eds.), Origin and Evolution of the Cape Mountains and Karoo Basin, Springer International Publishing, 141–149.

SEELEY, H.G. 1888. Researches on the structure, organisation, and classification of the fossil Reptilia. II. On *Pareiasaurus bombidens* (Owen), and the significance of its affinities to amphibians, reptiles and mammals*. Philosophical Transactions of the Royal Society of London B,* **179**, 59-109.

SEELEY, H.G. 1892. Researches on the structure, organisation, and classification of the fossil Reptilia. VII. Further observations on *Pareiasaurus. Philosophical Transactions of the Royal Society of London B,* **183**, 311-370.

SIDOR, C. A., BLACKBURN, D. C. and GABO, B. 2003. The vertebrate fauna of the Upper Permian of Niger –II, Preliminary description of a new pareiasaur. *Palaeontologia africana*, **39:** 45-52.

SMITH, R. M. H. and BOTHA-BRINK, J., 2014. Anatomy of a mass extinction: Sedimentological and taphonomic: evidence for drought-induced die-offs at the Permo-Triassic boundary in the main Karoo Basin, South Africa. *Palaeogeography, Palaeoclimatology, Palaeoecology*, **396**, 99-118.

SMITH, R. M. H. and KEYSER, A. W. 1995a. Biostratigraphy of the *Tapinocephalus* Assemblage Zone. In: Rubidge, B.S. (ed.). Biostratigraphy of the Beaufort Group

(Karoo Supergroup), Biostratigraphic Series 1. *South African Committee for Stratigraphy*, Pretoria, 8-12.

SMITH, R. M. H. and KEYSER, A. W. 1995b. Biostratigraphy of the *Pristerognathus* Assemblage Zone. In: Rubidge, B.S. (ed.). Biostratigraphy of the Beaufort Group (Karoo Supergroup), Biostratigraphic Series 1. *South African Committee for Stratigraphy*, Pretoria, 13-17.

SMITH, R. M. H. and KEYSER, A. W. 1995c. Biostratigraphy of the *Tropidostoma* Assemblage Zone. In: Rubidge, B.S. (ed.). Biostratigraphy of the Beaufort Group (Karoo Supergroup), Biostratigraphic Series 1. *South African Committee for Stratigraphy*, Pretoria, 18-22.

SMITH, R. M. H. and KEYSER, A. W. 1995d. Biostratigraphy of the *Cistecephalus* Assemblage Zone. In: Rubidge, B.S. (ed.). Biostratigraphy of the Beaufort Group (Karoo Supergroup), Biostratigraphic Series 1. *South African Committee for Stratigraphy*, Pretoria, 23-28.

TSUJI, L. A., and MULLER, J. 2009. Assembling the history of the Parareptilia: phylogeny, diversification, and a new definition of the clade. *Wiley-VCHMuseum fur naturkunde Fossil Record*, **12(1)**, 71-81.

TSUJI, L. A. 2010. Evolution, Morphology and Paleobiology of the Pareiasauria and their Relatives (Amniota: Parareptilia). Unpublished Ph.D thesis, Humboldt-University of Berlin, Berlin, 1-188.

TSUJI, L. A., SIDOR, C. A., SEBASTIEN STEYER, J., SMITH, R. M. H., TABOR, N. J. and IDE, O. 2013. The vertebrate fauna of the Upper Permian of Niger –VII. Cranial anaomy and relationships of *Bunostegos akokanenis* (Pareiasauria). *Journal of Vertebrate Palaeontology*, **33(4)**, 747-763.

TURNER, M. L., TSUJI, L. A., IDE, O. and SIDOR, C. A. 2015. The vertebrate fauna of the Upper Permian of Niger –IX. The appendicular skeleton of *Bunostegos*

*akokanenis* (Parareptilia: Pareiasauria). *Journal of Vertebrate Palaeontology*, **35(6)**, e994746.

VAN DER WALT, M., DAY, M., RUBIDGE, B., COOPER, A. K., and NETTERBER, I. 2011. A new GIS-based biozone map of the Beaufort Group (Karoo Supergroup), South Africa. *Palaeontologia africana*, **45**, 1-5.

VON MEYER, H. 1857. Beiträge zur näheren Kenntnis fossiler Reptilien. *Neues Jahrbuch für Mineralogie, Geologie, Paläontologie,* **1857**, 103-104.

WATSON, D. M. S. 1914a. On the skull of a pareiasarian (sic) reptile, and on the relationships of that type. *Proceedings of the Zoological Society of London,* **1914**, 155-180.

WATSON, D. M. S. 1914b. On the nomenclature of pareiasaurs. *Annals of the Magazine of Natural History,* **14**, 98-102.

# CHAPTER NINE: APPENDICES

## 9.1 Appendix A

List of measurements (1-33) and ratios (34-39) taken on the four holotype skulls: SAM-PK-8034 *Embrithosaurus schwarzi*, SAM-PK-6239 *Nochelesaurus alexanderi*, NHMUK R1971 *Bradysaurus baini*, and NHMUK 49426 *B. seeleyi.*

1. Basal midline skull length (midline length): Posterior suture of premaxilla to posterior margin of postparietal.
2. Basal lateral skull length (supratemporal length): Posterior suture of premaxilla to posterior edge of supratemporal.
3. middle dorsal anterior length (midline): Anterior border of pineal foramen to posterior suture of premaxilla.
4. Pineal foramen length (midline): Anterior border of pineal foramen to posterior border of pineal foramen.
5. middle dorsal posterior length (midline): Posterior border of pineal foreman to posterior margin of post parietal.
6. Pineal foramen width: Width between lateral borders of pineal foramen.
7. Snout length: Anterior border of orbits to posterior suture of premaxilla.
8. Orbital length: Anterior border of orbit to posterior border of orbit.
9. Cheek length: Posterior border of orbit to posterior edge of supratemporal.
10. Postparietal length (midline): Maximum length of postparietal.
11. Postparietal width (midline): Maximum width of postparietal.
12. Interorbital width (midline): Width of skull between dorsal orbital borders.
13. Supratemporal width (midline): Width of skull between tops of supratemporal bosses.

14. Snout width over maxilla (dorsal view): Maximum width of snout over maxilla.
15. Snout width over lacrimal (dorsal view): Maximum Width of snout over lacrimal.
16. Snout height (lateral view): Maximum height of snout from ventral tooth row to dorsal skull table, immediately behind nasal bosses.
17. Maximum height of skull/ height of cheek (lateral view): Vertical height from top of supratemporal boss to bottom of corner/angle cheek boss tip, along the bone.
18. Maximum height of cheek overhang (lateral view): Vertical height of cheek overhang: from ventral tooth row to corner/angle cheek boss tip, along the bone.
19. Occipital condyle width (occipital view): Width of occipital condyle.
20. Occiput height (occipital view): Base of occipital condyle to skull roof, over the midline.
21. Maximum width of skull (occipital view): Width of skull across widest point of the cheeks/quadratojugal, across the cheek corner/angle boss.
22. Distal paroccipital process height (occipital view): Distally, maximum vertical height, of paroccipital process.
23. Distal paroccipital process width (occipital view): Distally, maximum horizontal width from skull midline to distal edge of paroccipital process.
24. Distal paroccipital process knob like projection (occipital view): Vertical height of knob.
25. Distal paroccipital process knob like projection (occipital view): Horizontal width of knob.
26. Distal paroccipital process knob like projection (dorsal view): Posterior length of knob that juts out.
27. Maximum width of palate (ventral view): Width between medial borders of posterior most maxillary teeth.

28. Max length of palate length (ventral view): Posterior border of prepalatal foramen to anterior border of interpterygoid vacuity, along the midline.
29. Anterior basisphenoid width (ventral view): At most posterior point of articulation of the basisphenoid with the pterygoid on the lateral borders of the interpterygoid vacuity.
30. Narrowest basisphenoid width (ventral view): Narrowest width at the "waist" of the basisphenoid.
31. Posterior basisphenoid width (ventral view): At distal ends of the basal tubera.
32. Basal tubera to occipital condyle (ventral view): Midline length from basal tubera posterior edge to posterior edge of the occipital condyle.
33. Basal tubera to basipterygoid process (ventral view): Length from basal tubera posterior edge to the basipterygoid processes, at the most posterior point of articulation of the basisphenoid with the pterygoid on the lateral borders of the interpterygoid vacuity.
34. Skull Ratio: Interorbital width to supratemporal bosses width.
35. Skull Ratio: Snout width over maxilla to snout height over maxilla.
36. Skull Ratio: Snout width over lacrimal to snout height over lacrimal.
37. Skull Ratio: Size of cheek: Vertical cheek overhang, to entire vertical height of cheek.
38. Skull Ratio: Size of cheek angle below tooth row in degrees: tooth row to quadratojugal corner boss tip.
39. Skull Ratio: Basisphenoid: narrowest point of waist to widest posterior width.

## 9.2 Appendix B

Table of distances (in mm) of the different measurements and ratios presented in Appendix A, for the four holotype skulls: SAM-PK-8034 *Embrithosaurus schwarzi*, SAM-PK-6239 *Nochelesaurus alexanderi*, NHMUK R1971 *Bradysaurus baini*, and NHMUK 49426 *B. seeleyi.*

| No | SAM-PK-8034 | | | SAM-PK-6239 | | | NHMUK R1971 | | | NHMUK R49426 | | |
|---|---|---|---|---|---|---|---|---|---|---|---|---|
| | Midline | Left | Right | Midline | Left | Right | Midline | Left | Right | Midline | Left | Right |
| 1 | 315 | | | 363 | | | 370 | | | 300 | | |
| 2 | | 350 | 360 | | | 403 | | 405 | 434 | | 335 | 340 |
| 3 | 202 | | | 246 | | | 231 | | | 200 | | |
| 4 | 14 | | | 14 | | | 22 | | | 10 | | |
| 5 | 99 | | | 103 | | | 117 | | | 90 | | |
| 6 | 8 | | | 13 | | | 18 | | | 8? | | |
| 7 | 93,5 | 91 | 96 | | | 118 | 117,5 | 103 | 132 | 86 | 83 | 89 |
| 8 | 95 | 94 | 96 | | | 91 | 95,5 | 94 | 97 | 90,5 | 90 | 91 |
| 9 | 166,5 | 165 | 168 | | | 194 | 206,5 | 208 | 205 | 161 | 162 | 160 |
| 10 | 46 | | | 47 | | | | | | | | |
| 11 | 125 | | | 130 | | | | | | | | |
| 12 | 189 | | | 201 | | | 195 | | | 190 | | |
| 13 | 200 | | | 215 | | | 216 | | | 210 | | |
| 14 | 240 | | | | | | 250 | | | 200 | | |
| 15 | 220 | | | | | | 250 | | | 200 | | |
| 16 | 140 | | | | | | 145 | | | 110 | | |
| 17 | 270 | 260 | 280 | | | 290 | 280 | 280 | 280 | 210 | 205 | 215 |
| 18 | 70 | 60 | 80 | | | 80 | 73 | 78 | 68 | 40 | 45 | 35 |
| 19 | 66 | | | n/a | | | 75 | | | 53 | | |
| 20 | 125 | | | n/a | | | 149 | | | 93 | | |
| 21 | 445 | | | | | | 510 | | | 390 | | |
| 22 | 65 | 64 | 66 | n/a | | | 75 | 76 | 74 | 48,5 | 44 | 53 |
| 23 | 99 | 98 | 100 | n/a | | | 115 | 113 | 117 | 118,5 | 120 | 117 |
| 24 | 39,5 | 42 | 37 | n/a | | | 53 | 57 | 49 | | | |
| 25 | 33 | 30 | 36 | n/a | | | 38,5 | 40 | 37 | | | |
| 26 | 18,5 | 20 | 17 | n/a | | | 27,5 | 28 | 27 | | | |
| 27 | 200 | | | | | | 300 | | | 260 | | |
| 28 | | | | n/a | | | 240 | | | 201 | | |
| 29 | 69 | | | n/a | | | 72 | | | 73 | | |
| 30 | 54 | | | n/a | | | 54 | | | 46 | | |
| 31 | 88 | | | n/a | | | 91 | | | 80 | | |
| 32 | 32 | | | n/a | | | 27 | | | 20 | | |
| 33 | 67 | | | n/a | | | 80 | | | 83 | | |
| 34 | 0,95 | | | 0,93 | | | 0,90 | | | 0,90 | | |
| 35 | 1,71 | | | | | | 1,72 | | | 1,82 | | |
| 36 | 1,57 | | | | | | 1,72 | | | 1,82 | | |
| 37 | 0,26 | | | | | 0,28 | 0,26 | | | 0,19 | | |
| 38 | 29 | 24 | 34 | | | 33 | 30 | 35 | 25 | 20 | 22 | 18 |
| 39 | 0,61 | | | | | | 0,59 | | | 0,58 | | |

## 9.3 Appendix C

Table of 108 South African middle Permian cranial pareiasaur specimens studied, showing the original species identifications and the identifications of this study.

| | | | Original ID | | | This study | | |
|---|---|---|---|---|---|---|---|---|
| | **Specimen** | **Description** | **Genus** | **Species** | **Identifier** | **Genus** | **Species** | **Identifier** |
| 1 | NHMUK R1971 | Holotype skull and skeleton | *Pareiasaurus* | *baini* | Seeley 1892 | *Bradysaurus* | *baini* | M Van den Brandt |
| 2 | NHMUK 49426 | Partial skull and postcrania | *Pareiasaurus* | *bombidens* | Seeley 1888 | *Bradysaurus* | *seeleyi* | M Van den Brandt |
| 3 | NHMUK R1714 (43525) | Holotype partial snout, some vertebrae | *Pareiasaurus* | *bombidens* | Owen 1876 | Not identified - inconclusive | | |
| 4 | NHMUK R1970 | Partial skull and postcrania | *Pareiasaurus* | *bombidens* | Seeley 1892 | Not identified - inconclusive | | |
| 5 | NHMUK R1996 | Holotype upper jaw & dentary fragments | *Pareiasaurus* | *russouwi* | Seeley 1892 | Not identified - not found | | |
| 6 | NHMUK R7782 | Partial skull | *Embrithosaurus* | *schwarzi* | Watson 1914 | Not identified - inconclusive | | |
| 7 | SAM-PK-3718 | Holotype skull and postcrania | *Bradysaurus* | *vanderbyli* | Haughton & Boonstra 1929 | *Bradysaurus* | *seeleyi* | M Van den Brandt |
| 8 | SAM-PK-4350 | Skull and postcrania | *Brachypareia* | *rogersi* | Boonstra 1934 | *Bradysaurus* | *baini* | M Van den Brandt |
| 9 | SAM-PK-5002 | Holotype skull and postcrania | *Platyoropha* | *broomi* | Haughton & Boonstra 1929 | *Bradysaurus* | *baini* | M Van den Brandt |
| 10 | SAM-PK-5012 | Partial skull and postcrania | *Brachypareia* | *rogersi* | Haughton & Boonstra 1929 | *Bradysaurus* | *seeleyi* | M Van den Brandt |
| 11 | SAM-PK-5624 | Skull | *Bradysaurus* | *seeleyi* | Boonstra 1934 | *Bradysaurus* | *baini* | M Van den Brandt |
| 12 | SAM-PK-6238 | Holotype partial skull | *Dolichopareia* | *angusta* | Haughton & Boonstra 1929 | *Nochelesaurus* | *alexanderi* | M Van den Brandt |
| 13 | SAM-PK-6239 | Holotype skull and postcrania | *Nochelesaurus* | *alexanderi* | Haughton & Boonstra 1929 | *Nochelesaurus* | *alexanderi* | M Van den Brandt |
| 14 | SAM-PK-6240 | Holotype skull | *Brachypareia* | *watsoni* | Haughton & Boonstra 1929 | *Nochelesaurus* | *alexanderi* | M Van den Brandt |
| 15 | SAM-PK-8034 | Holotype skull and postcrania | *Pareiasaurus* | *serridens* | Broom 1903 | *Embrithosaurus* | *schwarzi* | M Van den Brandt |
| 16 | SAM-PK-8933 | Partial skull and postcrania | *Bradysaurus* | *seeleyi* | Haughton & Boonstra 1929 | *Bradysaurus* | *baini* | M Van den Brandt |
| 17 | SAM-PK-8944 | Partial skull and postcrania | *Nochelesaurus* | *alexanderi* | Boonstra 1934 | *Nochelesaurus* | *alexanderi* | M Van den Brandt |
| 18 | SAM-PK-9095 | Skull | *Brachypareia* | *rogersi* | Boonstra 1934 | *Bradysaurus* | *baini* | M Van den Brandt |
| 19 | SAM-PK-9098 | Partial skull and postcrania | *Brachypareia* | *rogersi* | Boonstra 1934 | *Embrithosaurus* | *schwarzi* | M Van den Brandt |
| 20 | SAM-PK-9104 | Partial skull and postcrania | *Bradysaurus* | *baini* | Boonstra 1934 | *Nochelesaurus* | *alexanderi* | M Van den Brandt |
| 21 | SAM-PK-9105 | Skull and postcrania | *Bradysaurus* | *baini* | Boonstra 1934 | *Embrithosaurus* | *schwarzi* | M Van den Brandt |
| 22 | SAM-PK-9115 | Skull | *Bradysaurus* | *seeleyi* | Boonstra 1934 | *Nochelesaurus* | *alexanderi* | M Van den Brandt |
| 23 | SAM-PK-9121 | Partial skull and postcrania | *Bradysaurus* | *seeleyi* | Boonstra 1934 | *Bradysaurus* | *baini* | M Van den Brandt |
| 24 | SAM-PK-9137 | Partial skull and postcrania | *Bradysaurus* | *seeleyi* | Boonstra 1934 | *Nochelesaurus* | *alexanderi* | M Van den Brandt |
| 25 | SAM-PK-9168 | Skull and postcrania | *Bradysaurus* | *seeleyi* | Haughton & Boonstra 1929 | *Bradysaurus* | *baini* | M Van den Brandt |
| 26 | SAM-PK-9170 | Partial skull | *Bradysaurus* | *baini* | SAM catlogue | *Bradysaurus* | *baini* | M Van den Brandt |
| 27 | unnumbered adult | Skull | | | Specimen unnumbered | *Bradysaurus* | *baini* | M Van den Brandt |
| 28 | SAM-PK-12014 | Partial skull | *Bradysaurus* | *sp.* | SAM catlogue | *Bradysaurus* | *baini* | M Van den Brandt |
| 29 | SAM-PK-12048 | Partial skull and postcrania | *Bradysaurus* | *sp.* | SAM catlogue | *Bradysaurus* | *baini* | M Van den Brandt |
| 30 | SAM-PK-12076 | Partial skull and postcrania | *Bradysaurus* | *sp.* | SAM catlogue | *Nochelesaurus* | *alexanderi* | M Van den Brandt |
| 31 | SAM-PK-12090 | Partial skull | *Bradysaurus* | *sp.* | SAM catlogue | *Bradysaurus* | *baini* | M Van den Brandt |
| 32 | SAM-PK-12115 | Partial skull | *Bradysaurus* | *sp.* | SAM catlogue | *Bradysaurus* | *baini* | M Van den Brandt |
| 33 | SAM-PK-1204 | Partial skull and postcrania | *Bradysaurus* | *baini* | Boonstra 1932 | Not identified - inconclusive | | |

| | | | Original ID | | | This study | | |
|---|---|---|---|---|---|---|---|---|
| | **Specimen** | **Description** | **Genus** | **Species** | **Identifier** | **Genus** | **Species** | **Identifier** |
| 34 | SAM-PK-1207 | Partial skull | *Nochelesaurus* | *strubeni* | Boonstra 1934 | Not identified - unprepared | | |
| 35 | SAM-PK-1208 | Skull | *Bradysaurus* | *baini* | SAM catlogue | Not identified - unprepared | | |
| 36 | SAM-PK-3030 | Partial skull | *Brachypareia* | *watsoni* | Haughton & Boonstra 1930 | Not identified - unprepared | | |
| 37 | SAM-PK-3434 | Partial skull | *Bradysaurus* | *sp.* | SAM catlogue | Not identified - unprepared | | |
| 38 | SAM-PK-4345 | Partial skull | *Koalemasauus* | *acutirostris* | Boonstra 1934 | Not identified - unprepared | | |
| 39 | SAM-PK-4346 | Partial skull and postcrania | *Bradysaurus* | *seeleyi* | Boonstra 1929 | Not identified - unprepared | | |
| 40 | SAM-PK-4347 | Partial skull | *Bradysaurus* | *baini* | Haughton & Boonstra 1929 | Not identified - unprepared | | |
| 41 | SAM-PK-4352 | Partial skull and postcrania | *Nochelesaurus* | *strubeni* | Boonstra 1934 | Not identified - unprepared | | |
| 42 | SAM-PK-4999 | Partial skull and postcrania | *Bradysaurus* | *baini* | Haughton & Boonstra 1929 | Not identified - unprepared | | |
| 43 | SAM-PK-5000 | Partial skull and postcrania | *Bradysaurus* | *baini* | Boonstra 1934 | Not identified - unprepared | | |
| 44 | SAM-PK-5008 | Partial skull | *Bradysaurus* | *sp.* | SAM catlogue | Not identified - unprepared | | |
| 45 | SAM-PK-5019 | Partial skull | *Nochelesaurus* | *strubeni* | Haughton & Boonstra 1929 | Not identified - unprepared | | |
| 46 | SAM-PK-5127 | Partial skull and postcrania | *Bradysaurus* | *baini* | Haughton & Boonstra 1929 | Not identified - unprepared | | |
| 47 | SAM-PK-6535 | Partial skull and postcrania | *Dolichopareia* | *angusta* | Haughton & Boonstra 1930 | Not identified - unprepared | | |
| 48 | SAM-PK-8941 | Skull and postcrania | *Bradysaurus* | *vanderbyli* | Haughton & Boonstra 1929 | Not identified - unprepared | | |
| 49 | SAM-PK-9001 | Partial skull and postcrania | *Bradysaurus* | *baini* | Boonstra 1934 | Not identified - unprepared | | |
| 50 | SAM-PK-9114 | Partial skull | *Brachypareia* | *watsoni* | Haughton & Boonstra 1930 | Not identified - unprepared | | |
| 51 | SAM-PK-9118 | Partial skull | *Brachypareia* | *watsoni* | Haughton & Boonstra 1930 | Not identified - unprepared | | |
| 52 | SAM-PK-11940 | Partial skull | *Brachypareia* | *rogersi* | SAM catlogue | Not identified - unprepared | | |
| 53 | SAM-PK-12015 | Partial skull | *Bradysaurus* | *sp.* | SAM catlogue | Not identified - unprepared | | |
| 54 | SAM-PK-12068 | Partial skull | *Bradysaurus* | *sp.* | SAM catlogue | Not identified - unprepared | | |
| 55 | SAM-PK-12071 | Partial skull | *Bradysaurus* | *sp.* | SAM catlogue | Not identified - unprepared | | |
| 56 | SAM-PK-12072 | Partial skull | *Bradysaurus* | *sp.* | SAM catlogue | Not identified - unprepared | | |
| 57 | SAM-PK-12116 | Partial skull | *Bradysaurus* | *sp.* | SAM catlogue | Not identified - unprepared | | |
| 58 | SAM-PK-12128 | Partial skull | *Bradysaurus* | *sp.* | SAM catlogue | Not identified - unprepared | | |
| 59 | SAM-PK-12140 | Partial skull | *Bradysaurus* | *sp.* | SAM catlogue | Not identified - unprepared | | |
| 60 | SAM-PK-12216 | Skull | *Bradysaurus* | *sp.* | SAM catlogue | Not identified - unprepared | | |
| 61 | SAM-PK-12231 | Partial skull | *Bradysaurus* | *sp.* | SAM catlogue | Not identified - unprepared | | |
| 62 | SAM-PK-K196 | Partial skull | *Bradysaurus* | *sp.* | SAM catlogue | Not identified - unprepared | | |
| 63 | SAM-PK-K197 | Partial skull | *Bradysaurus* | *sp.* | SAM catlogue | Not identified - unprepared | | |
| 64 | SAM-PK-K7665 | Partial skull | *Bradysaurus* | *sp.* | SAM catlogue | Not identified - unprepared | | |
| 65 | BP/I/297 | Skull | *Bradysaurus* | *sp.* | ESI catlogue | *Bradysaurus* | *seeleyi* | M Van den Brandt |
| 66 | BP/I/347 | Partial skull and postcrania | *Pareiasaurus* | *sp.* | ESI catlogue | *Bradysaurus* | *baini* | M Van den Brandt |
| 67 | BP/I/4859 | Partial skull and postcrania | *Bradysaurus* | *sp.* | ESI catlogue | *Bradysaurus* | *seeleyi* | M Van den Brandt |
| 68 | BP/I/7054 | Skull | *Pareiasaurus* | *sp.* | ESI catlogue | *Bradysaurus* | *seeleyi* | M Van den Brandt |
| 69 | BP/I/7213 | Partial skull and postcrania | *Pareiasaurus* | *sp.* | ESI catlogue | *Bradysaurus* | *baini* | M Van den Brandt |
| 70 | BP/I/7886 | Partial skull and postcrania | | | No ID on ESI catalogue | *Bradysaurus* | *seeleyi* | M Van den Brandt |
| 71 | BP/I/1574 | Partial skull and postcrania | *Pareiasaurus* | *sp.* | ESI catlogue | Not identified - unprepared | | |

| | | | Original ID | | | This study | | |
|---|---|---|---|---|---|---|---|---|
| | Specimen | Description | Genus | Species | Identifier | Genus | Species | Identifier |
| 72 | BP/I/1577 | Partial skull | *Pareiasaurus* | *sp.* | ESI catlogue | Not identified - unprepared | | |
| 73 | BP/I/1578 | Partial skull | *Pareiasaurus* | *sp.* | ESI catlogue | Not identified - unprepared | | |
| 74 | BP/I/1772 | Partial skull | *Pareiasaurus* | *sp.* | ESI catlogue | Not identified - unprepared | | |
| 75 | BP/I/1777 | Partial skull | *Pareiasaurus* | *sp.* | ESI catlogue | Not identified - unprepared | | |
| 76 | BP/I/1782 | Partial skull | *Pareiasaurus* | *sp.* | ESI catlogue | Not identified - unprepared | | |
| 77 | BP/I/2233 | Partial skull | *Pareiasaurus* | *sp.* | ESI catlogue | Not identified - unprepared | | |
| 78 | BP/I/4848 | Skull | *Bradysaurus* | *sp.* | ESI catlogue | Not identified - unprepared | | |
| 79 | BP/I/4855 | Partial skull | *Bradysaurus* | *sp.* | ESI catlogue | Not identified - unprepared | | |
| 80 | BP/I/5414 | Partial skull | *Bradysaurus* | *sp.* | ESI catlogue | Not identified - unprepared | | |
| 81 | BP/I/5418 | Partial skull | *Bradysaurus* | *sp.* | ESI catlogue | Not identified - unprepared | | |
| 82 | BP/I/5435 | Partial skull | *Bradysaurus* | *sp.* | ESI catlogue | Not identified - unprepared | | |
| 83 | BP/I/6870 | Partial skull | | | No ID on ESI catalogue | Not identified - unprepared | | |
| 84 | BP/I/6976 | Partial skull | | | No ID on ESI catalogue | Not identified - unprepared | | |
| 85 | BP/I/7036 | Partial skull | | | No ID on ESI catalogue | Not identified - unprepared | | |
| 86 | BP/I/7037 | Partial skull | | | No ID on ESI catalogue | Not identified - unprepared | | |
| 87 | BP/I/7082 | Partial skull | | | No ID on ESI catalogue | Not identified - unprepared | | |
| 88 | BP/I/7165 | Partial skull and postcrania | *Pareiasaurus* | *sp.* | ESI catlogue | Not identified - unprepared | | |
| 89 | BP/I/7242 | Partial skull | | | No ID on ESI catalogue | Not identified - unprepared | | |
| 90 | BP/I/7252 | Partial skull and postcrania | *Pareiasaurus* | *sp.* | ESI catlogue | Not identified - unprepared | | |
| 91 | BP/I/7266 | Partial skull | | | No ID on ESI catalogue | Not identified - unprepared | | |
| 92 | BP/I/7276 | Partial skull | | | No ID on ESI catalogue | Not identified - unprepared | | |
| 93 | BP/I/7870 | Partial skull and postcrania | | | No ID on ESI catalogue | Not identified - unprepared | | |
| 94 | CGP dark brown large specimen | | | | Specimen unnumbered | *Bradysaurus* | *baini* | M Van den Brandt |
| 95 | CGP Light grey unnumbered juvenile | | | | Specimen unnumbered | *Bradysaurus* | *baini* | M Van den Brandt |
| 96 | CGP/1/795 (RMS566) | Skull and postcrania | | | CGP catlogue card lost | *Embrithosaurus* | *schwarzi* | M Van den Brandt |
| 97 | CGP/1/810 (RMS1096) | Skull | *Pareiasaurus* | *sp.* | CGP catlogue | *Bradysaurus* | *seeleyi* | M Van den Brandt |
| 98 | CGP JA 109 | | | | CGP catlogue card lost | *Nochelesaurus* | *alexanderi* | M Van den Brandt |
| 99 | 113/CGP/1/811 | Partial skull | | | CGP catlogue card lost | Not identified - unprepared | | |
| 100 | CGP CBT 112 | Skull and postcrania | *Pareiasaurus* | *serridens* | CGP catlogue | Not identified - inconclusive | | |
| 101 | CGP R338 | Partial skull | | | CGP catlogue card lost | Not identified - unprepared | | |
| 102 | CGP/1/820 (RMS1304) | Partial skull | *Pareiasaurus* | *serridens* | CGP catlogue | Not identified - unprepared | | |
| 103 | CGP/1/866 (RMS565) | Skull | *Pareiasaurus* | *sp.* | CGP catlogue | Not identified - inconclusive | | |
| 104 | JP56 (CGP/1/847) | Partial skull | *Bradysaurus* | *sp.* | CGP catlogue | Not identified - unprepared | | |
| 105 | RMS 1095 | Skull and postcrania | *Bradysaurus* | *sp.* | Skull not found | | | |
| 106 | RMS1258 | Partial skull | *Pareiasaurus* | *sp.* | CGP catlogue | Not identified - unprepared | | |
| 107 | RMS1296 | Skull | *Pareiasaurus* | *sp.* | CGP catlogue | Not identified - unprepared | | |
| 108 | S260 | Skull | *Bradysaurus* | *sp.* | CGP catlogue | Not identified - not found | | |

## 9.4 Appendix D

Table of the 35 specimens identified during this study to species level, with the stratigraphic range intervals compiled by Day (2013) for individual farm localities.

| Count | Collection Number | Higher Taxon | Family or Clade | Genus | Species | Source of ID | Locality (Farm and District) | Member Range |
|---|---|---|---|---|---|---|---|---|
| 1 | SAM-PK-012048 | Parareptilia | Pareiasauria | *Bradysaurus* | *baini* | M Van den Brandt | Dwars Rivier 14, Laingsburg | upper Koornp to lower Moord |
| 2 | NHMUK R1971 | Parareptilia | Pareiasauria | *Bradysaurus* | *baini* | Holotype | Die Bad 286, Beaufort West | lower to mid Moord |
| 3 | SAM-PK-009095 | Parareptilia | Pareiasauria | *Bradysaurus* | *baini* | M Van den Brandt | Veldmans River 9, Prince Albert | mid Moord |
| 4 | SAM-PK-004350 | Parareptilia | Pareiasauria | *Bradysaurus* | *baini* | M Van den Brandt | Leeurivier, Rietfontein 306, Beaufort West | mid to upper Moord |
| 5 | SAM-PK-005624 | Parareptilia | Pareiasauria | *Bradysaurus* | *baini* | M Van den Brandt | Grootkruidfontein, Kruitfontein 33, Prince Albert | mid Moord |
| 6 | SAM-PK-012090 | Parareptilia | Pareiasauria | *Bradysaurus* | *baini* | M Van den Brandt | Die Vlei, Blaaw Draay 3, Prince Albert | mid Moord |
| 7 | SAM-PK-012115 | Parareptilia | Pareiasauria | *Bradysaurus* | *baini* | M Van den Brandt | Palmietfontein, Kruidfontein 33, Prince Albert | mid Moord |
| 8 | SAM-PK-009121 | Parareptilia | Pareiasauria | *Bradysaurus* | *baini* | M Van den Brandt | Voelfontein, Vogelfontein 1, Prince Albert | lower Moord |
| 9 | SAM-PK-009168 | Parareptilia | Pareiasauria | *Bradysaurus* | *baini* | M Van den Brandt | Knoffelfontein, Van der Byls Kraal 265, Beaufort West | mid Moord |
| 10 | SAM-PK-009170 | Parareptilia | Pareiasauria | *Bradysaurus* | *baini* | M Van den Brandt | Melkboschfontein, Melkbosch Fontein 75, Prince Albert | mid Moord |
| 11 | SAM-PK-008933 | Parareptilia | Pareiasauria | *Bradysaurus* | *baini* | M Van den Brandt | Leeuwfontein, Leeufontein 273, Beaufort West | upper Swaersk. to lower Moord. |
| 12 | SAM-PK-012014 | Parareptilia | Pareiasauria | *Bradysaurus* | *baini* | M Van den Brandt | Rietfontein 269, Beaufort West | lower Moord |
| 13 | BP/1/347 | Parareptilia | Pareiasauria | *Bradysaurus* | *baini* | M Van den Brandt | Buffelsvlei, Buffels Valley 268, Beaufort West | upper Koornp to lower Moord |
| 14 | SAM-PK-005002 | Parareptilia | Pareiasauria | *Bradysaurus* | *baini* | Lee, 1997, M Van den Brandt | Voelfontein, Vogelfontein 1, Prince Albert | lower Moord |
| 15 | BP/1/7213 | Parareptilia | Pareiasauria | *Bradysaurus* | *baini* | M Van den Brandt | Witfontein 85, Sutherland | lower part of the Karelskraal |
| 16 | RMS1096 OR CGP/1/810 | Parareptilia | Pareiasauria | *Bradysaurus* | *seeleyi* | M Van den Brandt | Antjesfontein 14, Prince Albert | lower to mid Moord |
| 17 | BP/1/297 | Parareptilia | Pareiasauria | *Bradysaurus* | *seeleyi* | M Van den Brandt | Kleinwaterval, Spreeuw Fontein 26, Prince Albert | upper Abrahamskraal fm |
| 18 | BP/1/4859 | Parareptilia | Pareiasauria | *Bradysaurus* | *seeleyi* | M Van den Brandt | Riethoek 28, Laingsburg | lower Moord |
| 19 | BP/1/7886 | Parareptilia | Pareiasauria | *Bradysaurus* | *seeleyi* | M Van den Brandt | Blounek, Koornplaats 41, Lainsburg | mid koornplaats |
| 20 | NHMUK R49426 | Parareptilia | Pareiasauria | *Bradysaurus* | *seeleyi* | Holotype | Palmietfontein 229, Beaufort West | upper Karelskraal mem |
| 21 | SAM-PK-003718 | Parareptilia | Pareiasauria | *Bradysaurus* | *seeleyi* | Lee, 1997, M Van den Brandt | Abrahamskraal, Prince Albert | Moord |
| 22 | SAM-PK-005012 | Parareptilia | Pareiasauria | *Bradysaurus* | *seeleyi* | Lee, 1997, M Van den Brandt | Abrahamskraal, Prince Albert | Moord |
| 23 | BP/1/7054 | Parareptilia | Pareiasauria | *Bradysaurus* | *seeleyi* | M Van den Brandt | Rietfontein 269, Beaufort West | lower Moord |
| 24 | SAM-PK-008034 | Parareptilia | Pareiasauria | *Embrithosaurus* | *schwarzi* | Holotype | Hoogeveld lot A, near Knoflock's fontein, Van der Byl's Kraal, Beaufort West | upper Swaersk. to lower Moord. |
| 25 | SAM-PK-009098 | Parareptilia | Pareiasauria | *Embrithosaurus* | *schwarzi* | M Van den Brandt | Knoffelfontein, Van der Byls Kraal 265, Beaufort West | lower Moord |
| 26 | SAM-PK-009105 | Parareptilia | Pareiasauria | *Embrithosaurus* | *schwarzi* | M Van den Brandt | Melkboschfontein, Melkbosch Fontein 75, Prince Albert | mid Moord |
| 27 | SAM-PK-K324 | Parareptilia | Pareiasauria | *Embrithosaurus* | *schwarzi* | Lee, 1997 | Zeekoeivlei, Zeekoevalley 282, Beaufort West | lower Moord |
| 28 | SAM-PK-006238 | Parareptilia | Pareiasauria | *Nochelosaurus* | *alexanderi* | Lee, 1997, M Van den Brandt | Boesmanskop, Bushman's Kop 302, Beaufort West | upper Moord to upper Karelsk. |
| 29 | SAM-PK-006239 | Parareptilia | Pareiasauria | *Nochelosaurus* | *alexanderi* | Holotype | Boesmanskop, Bushman's Kop 302, Beaufort West | upper Moord to upper Karelsk. |
| 30 | SAM-PK-006240 | Parareptilia | Pareiasauria | *Nochelosaurus* | *alexanderi* | Lee, 1997, M Van den Brandt | Abrahamskraal, Prince Albert | Moord + acould be all of Swaersk. |
| 31 | SAM-PK-008944 | Parareptilia | Pareiasauria | *Nochelosaurus* | *alexanderi* | M Van den Brandt | Klein Koedoeskop 310, Beaufort West | mid Moord |
| 32 | SAM-PK-009104 | Parareptilia | Pareiasauria | *Nochelosaurus* | *alexanderi* | M Van den Brandt | Melkboschfontein, Melkbosch Fontein 75, Prince Albert | mid Moord |
| 33 | SAM-PK-009137 | Parareptilia | Pareiasauria | *Nochelosaurus* | *alexanderi* | M Van den Brandt | Voelfontein, Vogelfontein 1, Prince Albert | lower Moord |
| 34 | SAM-PK-009115 | Parareptilia | Pareiasauria | *Nochelosaurus* | *alexanderi* | M Van den Brandt | Voelfontein, Vogelfontein 1, Prince Albert | lower Moord |
| 35 | SAM-PK-012076 | Parareptilia | Pareiasauria | *Nochelosaurus* | *alexanderi* | M Van den Brandt | Varsfontein 254, Beaufort West | upper Swaersk. to lower Moord. |